

NATURAL CHOLINESTERASE INHIBITORS FROM *MYRISTICA*
CINNAMOMEA KING

SITI MARIAM BINTI ABDUL WAHAB

FACULTY OF SCIENCE
UNIVERSITY OF MALAYA
KUALA LUMPUR

2016

**NATURAL CHOLINESTERASE INHIBITORS FROM *MYRISTICA*
CINNAMOMEA KING**

SITI MARIAM BINTI ABDUL WAHAB

**DESSERTATION SUBMITTED IN FULFILMENT OF THE
REQUIREMENTS FOR THE DEGREE MASTER OF SCIENCE**

**DEPARTMENT OF CHEMISTRY
FACULTY OF SCIENCE
UNIVERSITY OF MALAYA
KUALA LUMPUR**

2016

ORIGINAL LITERARY WORK DECLARATION

Name of Candidate: Siti Mariam Binti Abdul Wahab

Registration/Matric No: SGR 140044

Name of Degree: Master of Science (MSc.)

Title of Project Paper/Research Report/Dissertation/Thesis ("this Work"):

Natural Cholinesterase Inhibitors from *Myristica cinnamomea* King

Field of Study: Organic Chemistry

I do solemnly and sincerely declare that:

- (1) I am the sole author/writer of this Work;
- (2) This Work is original;
- (3) Any use of any work in which copyright exists was done by way of fair dealing and for permitted purposes and any excerpt or extract from, or reference to or reproduction of any copyright work has been disclosed expressly and sufficiently and the title of the Work and its authorship have been acknowledged in this Work;
- (4) I do not have any actual knowledge nor do I ought reasonably to know that the making of this work constitutes an infringement of any copyright work;
- (5) I hereby assign all and every rights in the copyright to this Work to the University of Malaya ("UM"), who henceforth shall be owner of the copyright in this Work and that any reproduction or use in any form or by any means whatsoever is prohibited without the written consent of UM having been first had and obtained;
- (6) I am fully aware that if in the course of making this Work I have infringed any copyright whether intentionally or otherwise, I may be subject to legal action or any other action as may be determined by UM.

Candidate's Signature

Date 27 December 2016

Subscribed and solemnly declared before,

Witness's Signature

Date 27 December 2016

Name:

Designation:

ABSTRACT

A new acylphenol, malabaricone E (**72**) together with the known malabaricones A-C (**1-3**), maingayones A and B (**4** and **5**) and maingayic acid B (**69**) were isolated from the ethyl acetate extract of the fruits of *Myristica cinnamomea* King. Their structures were determined by 1D and 2D NMR techniques and LCMS-IT-TOF analysis. Compounds **2** (1.84 ± 0.19 and 1.76 ± 0.21 μM , respectively) and **3** (1.94 ± 0.27 and 2.80 ± 0.49 μM , respectively) were identified as dual inhibitors, with almost equal acetylcholinesterase enzyme (AChE) and butyrylcholinesterase enzyme (BChE) inhibiting potentials. The Lineweaver-Burk plots of compounds **2** and **3** indicated that they were mixed-mode inhibitors. Based on the molecular docking studies, compounds **2** and **3** interacted with the peripheral anionic site (PAS), the catalytic triad and the oxyanion hole of the AChE. As for the BChE, while compound **2** interacted with the PAS, the catalytic triad and the oxyanion hole, compound **3** only interacted with the catalytic triad and the oxyanion hole.

ABSTRAK

Asilfenol baru, malabaricone E (**72**) bersama sebatian yang telah diketahui; malabaricone A-C (**1-3**), maingayone A dan B (**4** dan **5**) dan asid maingayic B (**69**) telah dipencilkan daripada ekstrak etil asetat buah *Myristica cinnamomea* King. Struktur semua sebatian tersebut telah ditentukan melalui teknik 1D dan 2D NMR dan analisis LCMS-IT-TOF. Sebatian **2** (1.84 ± 0.19 dan 1.76 ± 0.21 μM , masing-masing) dan **3** (1.94 ± 0.27 dan 2.80 ± 0.49 μM , masing-masing) telah dikenalpasti sebagai penghalang *dual*, dengan keupayaan menghalang enzim asetilkolinesterase (AChE) dan butrilkolinesterase (BChE) yang hampir sama. Plot *Lineweaver-burk* bagi sebatian **2** dan **3** menunjukkan yang sebatian tersebut merupakan penghalang mod campuran. Berdasarkan kajian dok molekul, sebatian **2** dan **3** berinteraksi dengan tapak periferan anionik (PAS), pemangkin *triad* dan lubang oxyanion AChE. Bagi BChE, sebatian **2** berinteraksi dengan PAS, pemangkin *triad* dan lubang oxyanion manakala sebatian **3** hanya berinteraksi dengan pemangkin *triad* dan lubang oxyanion.

ACKNOWLEDGEMENTS

Firstly, I would like to express my greatest appreciation to my supervisor, Professor Dr. Khalijah Awang, and co-supervisor, Dr. Yasodha Sivasothy, for their advice, guidance and encouragement throughout the course of this study.

Next, I would like to acknowledge the Dean of the Institute of Postgraduate Studies (IPS) for giving me the opportunity to pursue my postgraduate studies in UM.

A special thanks to the Dean of the Faculty of Science and the Head of the Department of Chemistry for providing me with the assistance and facilities which ensured the success of my research.

I would also like to thank IPS for awarding me with the University of Malaya Fellowship Scheme (SBUM) which covered my allowances and tuition fees.

My sincere thanks also goes to Associate Professor Dr. Jamaludin Mohamad, Dr. Liew Sook Yee and Mr. Abdulwali Ablat for their valuable guidance and assistance in conducting the cholinesterase enzymes inhibition assay. Without them, this study would not be complete.

I am also very grateful to the Herbarium staffs, Mr. Din, Mr. Teo and Mr. Rafly, for helping with the collection of the plant material, the identification of it and with the preparation of its voucher specimen. I would also like to forward my appreciation to the technical staffs of the Department of Chemistry in particular Mr. Fateh, Mr. Zakaria, Ms. Norzalida, Mr. Mohamad Akasha and Mrs. Lela for their technical assistance.

I would also like to thank my fellow lab mates for their cooperation and moral support throughout this project.

Last but not least, I would like to convey my deepest gratitude to my beloved family members for their love, support and encouragement throughout my MSc research.

University of Malaya

TABLE OF CONTENTS

	Page
ABSTRACT	ii
ACKNOWLEDGEMENT	iv
LIST OF FIGURES	ix
LIST OF SCHEMES	xii
LIST OF TABLES	xii
LIST OF SYMBOLS AND ABBREVIATIONS	xiv
CHAPTER 1: INTRODUCTION	
1.1 General Introduction	1
1.2 Problem Statement	4
1.3 Research Objectives	4
CHAPTER 2: LITERATURE REVIEW	
2.1 The Myristicaceae	6
2.1.1 Geographical Distribution and Botanical Aspects	6
2.1.2 Classification of the Myristicaceae	8
2.1.3 Traditional Uses	9
2.2 The Genus <i>Myristica</i>	10
2.2.1 Geographical Distribution and Botanical Aspects	10
2.2.2 Phytochemical Composition	11
2.2.2.1 Acylphenols and Dimeric Acylphenols	11
2.2.2.1.1 Biosynthesis of Acylphenols	14
2.2.2.2 Flavans, Lignans and Neolignans	15
2.2.3 <i>Myristica cinnamomea</i> King	27

CHAPTER 3: RESULTS AND DISCUSSION

3.1 Secondary Metabolites Isolated from the Fruits of <i>M. cinnamomea</i>	29
3.1.1 Compound 1: Malabaricone A	30
3.1.2 Compound 2: Malabaricone B	40
3.1.3 Compound 3: Malabaricone C	50
3.1.4 Compound 72: Malabaricone E	60
3.1.5 Compound 4: Maingayone A	71
3.1.6 Compound 5: Maingayone B	82
3.1.7 Compound 69: Maingayic acid B	92
3.2 Comparison between the secondary metabolites isolated from the fruits of <i>M. cinnamomea</i> in the current and previous investigations	101
3.3 Cholinesterase inhibitory activities	101

CHAPTER 4: CONCLUSION 116

CHAPTER 5: EXPERIMENTAL

5.1 Plant Material	118
5.2 Chemicals and Reagents	118
5.2.1 Preparation of Detecting Reagent	120
5.3 Isolation and Purification of the Secondary Metabolites from the Fruits of <i>M. cinnamomea</i>	120
5.3.1 Extraction Procedure	120
5.3.2 Separation Techniques	121
5.3.2.1 Thin Layer Chromatography (TLC)	121
5.3.2.2 Column Chromatography (CC)	121
5.3.2.3 Preparative Thin Layer Chromatography (Prep-TLC)	121

5.3.3 Isolation and Purification of Compounds 1-5, 69 and 72 from the Ethyl Acetate Extract	122
5.4 Characterization of Compounds 1-5, 69 and 72	126
5.4.1 Infrared Spectroscopy (IR)	126
5.4.2 Nuclear Magnetic Resonance Spectroscopy (NMR)	126
5.4.3 Liquid Chromatography Mass Spectrometry-Ion Trap- Time of Flight (LCMS- IT-TOF)	126
5.4.4 Ultra-Violet Spectroscopy (UV)	126
5.4.5 Optical Rotation	127
5.5 Cholinesterase Inhibitory Assay	127
5.6 Enzyme Kinetics and Mode of Inhibition	128
5.7 Molecular Docking	128
5.8 Physical Data of the Isolated Compounds	129
REFERENCES	132
APPENDICES	139

LIST OF FIGURES

Figure 2.1: The leaves (left) and the fruits (right) of <i>Myristica cinnamomea</i> King.....	27
Figure 2.2: Voucher specimen of <i>Myristica cinnamomea</i> King.....	27
Figure 3.1: Structure of compound 1	30
Figure 3.2: Mass spectrum of compound 1	33
Figure 3.3: ¹³ C NMR (a) and DEPT-135 (b) spectra of compound 1	34
Figure 3.4: IR spectrum of compound 1	35
Figure 3.5: ¹ H NMR spectrum of compound 1	36
Figure 3.6: Selected COSY correlations of compound 1	37
Figure 3.7: Selected HMBC correlations of compound 1	38
Figure 3.8: HSQC correlations of compound 1	39
Figure 3.9: Structure of compound 2	40
Figure 3.10: Mass spectrum of compound 2	43
Figure 3.11: IR spectrum of compound 2	44
Figure 3.12: ¹ H NMR spectrum of compound 2	45
Figure 3.13: ¹³ C NMR (a) and DEPT-135 (b) spectra of compound 2	46
Figure 3.14: Selected COSY correlations of compound 2	47
Figure 3.15: HSQC correlations of compound 2	48
Figure 3.16: Selected HMBC correlations of compound 2	49
Figure 3.17: Structure of compound 3	50
Figure 3.18: Mass spectrum of compound 3	53
Figure 3.19: IR spectrum of compound 3	54
Figure 3.20: ¹ H NMR spectrum of compound 3	55
Figure 3.21: ¹³ C NMR (a) and DEPT-135 (b) spectra of compound 3	56
Figure 3.22: Selected COSY correlations of compound 3	57
Figure 3.23: HSQC correlations of compound 3	58

Figure 3.24: Selected HMBC correlations of compound 3	59
Figure 3.25: Structure of compound 72	60
Figure 3.26: Mass spectrum of compound 72	63
Figure 3.27: IR spectrum of compound 72	64
Figure 3.28: ¹ H NMR spectrum of compound 72	65
Figure 3.29: ¹³ C NMR (a) and DEPT-135 (b) spectra of compound 72	66
Figure 3.30: Selected COSY correlations of compound 72	67
Figure 3.31: HSQC correlations of compound 72	68
Figure 3.32: Selected HMBC correlations of compound 72	69
Figure 3.33: Structure of compound 4	71
Figure 3.34: Mass spectrum of compound 4	75
Figure 3.35: ¹³ C NMR (a) and DEPT-135 (b) spectra of compound 4	76
Figure 3.36: IR spectrum of compound 4	77
Figure 3.37: ¹ H NMR spectrum of compound 4	78
Figure 3.38: Selected COSY correlations of compound 4	79
Figure 3.39: Selected HMBC correlations of compound 4	80
Figure 3.40: HSQC correlations of compound 4	81
Figure 3.41: Structure of compound 5	82
Figure 3.42: Mass spectrum of compound 5	85
Figure 3.43: IR spectrum of compound 5	86
Figure 3.44: ¹ H NMR spectrum of compound 5	87
Figure 3.45: (a) ¹³ C NMR and (b) DEPT 135 spectra of compound 5	88
Figure 3.46: Selected COSY correlations of compound 5	89
Figure 3.47: Selected HMBC correlations of compound 5	90
Figure 3.48: HSQC correlations of compound 5	91
Figure 3.49: Structure of compound 69	92
Figure 3.50: Mass spectrum of compound 69	94

Figure 3.51: ^{13}C NMR (a) and DEPT-135 (b) spectra of compound 69	95
Figure 3.52: IR spectrum of compound 69	96
Figure 3.53: ^1H NMR spectrum of compound 69	97
Figure 3.54: Selected HMBC correlations of compound 69	98
Figure 3.55: Selected COSY correlations of compound 69	99
Figure 3.56: HSQC correlations of compound 69	100
Figure 3.57: Structures of compounds 1-5 , 69 and 72	105
Figure 3.58: Lineweaver-Burk plots of cholinesterase inhibition activities of compounds 2 and 3	109
Figure 3.59: Secondary plot of Lineweaver-Burk plots of compounds 2 and 3	110
Figure 3.60: (A) View of compounds 2 (up), 3 (middle) and physostigmine at the binding site of AChE (protein structures are represented by solid ribbon format). (B) Simplified view of compounds 2 (up), 3 (middle) and physostigmine interacting with surrounding amino acid residues which are shown in stick format. The hydrogen bond interaction of the ligands (compounds) with the amino acid residues are shown in green dotted lines.....	113
Figure 3.61: (A) View of compounds 2 (up), 3 (middle) and physostigmine at the binding site of BChE (protein structures are represented by solid ribbon format). (B) Simplified view of compounds 2 (up), 3 (middle) and physostigmine interacting with surrounding amino acid residues which are shown in stick format. The hydrogen bond interaction of the ligands (compounds) with the amino acid residues are shown in green dotted lines.....	114
Figure 3.62: Structure of physostigmine (reference standard).....	115

LIST OF SCHEMES

Scheme 2.1: Classification of the Myristicaceae.....	8
Scheme 2.2: Biosynthetic pathway for the formation of acylphenols.....	14
Scheme 3.1: Proposed biosynthetic pathway for the formation of compound 72	70
Scheme 5.1: Extraction procedure of the fruits of <i>M. cinnamomea</i>	120
Scheme 5.2: Isolation and purification of compounds from the ethyl acetate extract of the fruits of <i>M. cinnamomea</i>	125

LIST OF TABLES

Table 2.1: Summary of the chemical constituents isolated from the genus <i>Myristica</i> and their biological activities.....	15
Table 3.1: ¹ H NMR and ¹³ C NMR spectroscopic assignments of compound 1 in methanol- <i>d</i> ₄	32
Table 3.2: ¹ H NMR and ¹³ C NMR spectroscopic assignments of compound 2 in methanol- <i>d</i> ₄	42
Table 3.3: ¹ H NMR and ¹³ C NMR spectroscopic assignments of compound 3 in methanol- <i>d</i> ₄	52
Table 3.4: ¹ H NMR and ¹³ C NMR spectroscopic assignments of compound 72 in methanol- <i>d</i> ₄	62
Table 3.5: ¹ H NMR and ¹³ C NMR spectroscopic assignments of compound 4 in methanol- <i>d</i> ₄	74
Table 3.6: ¹ H NMR and ¹³ C NMR spectroscopic assignments of compound 5 in methanol- <i>d</i> ₄	84
Table 3.7: ¹ H NMR and ¹³ C NMR spectroscopic assignments of compound 69 in methanol- <i>d</i> ₄	93

Table 3.8: Cholinesterase inhibition activities of compounds 1-5 , 69 , 72 and physostigmine.....	104
Table 3.9: Binding interaction data for compounds 2 , 3 and physostigmine with amino acid residues of <i>TcAChE</i> and <i>hBChE</i>	111

University of Malaya

LIST OF SYMBOLS AND ABBREVIATIONS

α	Alpha
λ	Lambda
μ	Micro
δ	Chemical Shift
<i>s</i>	Singlet
<i>d</i>	Doublet
<i>dd</i>	Doublet of Doublet
<i>m</i>	Multiplet
<i>t</i>	Triplet
<i>p</i>	Pentate
$^1\text{H NMR}$	Proton Nuclear Magnetic Resonance
$^{13}\text{C NMR}$	Carbon-13 Nuclear Magnetic Resonance
IC_{50}	Concentration Needed for Inhibition of 50% Activity
<i>g</i>	Gram
<i>mg</i>	Milligram
<i>mL</i>	Millilitre
<i>m/z</i>	Mass to Charge Ratio
<i>nm</i>	Nanometre
<i>J</i>	Coupling Constant
<i>Hz</i>	Hertz
<i>ppm</i>	Parts Per Million
<i>COSY</i>	Correlation Spectroscopy
<i>DEPT</i>	Distortionless Enhancement by Polarization Transfer
<i>HMBC</i>	Heteronuclear Multiple Bond Correlation
<i>HSQC</i>	Heteronuclear Single Quantum Coherence
<i>IR</i>	Infrared Spectroscopy
<i>NMR</i>	Nuclear Magnetic Resonance

PTLC	Preparative Thin Layer Chromatography
TLC	Thin Layer Chromatography
UV	Ultraviolet Spectroscopy
LCMS-IT-TOF	Liquid Chromatography Mass Spectrometry-Ion Trap- Time of Flight
AChE	Acetylcholinesterase Enzyme
BChE	Butyrylcholinesterase Enzyme
K_i	Inhibition Constant
ADT	AutoDockTools
PAS	Peripheral Anionic Site
AD	Alzheimer Disease

University of Malaya

CHAPTER 1

INTRODUCTION

1.1 General Introduction

Nature has been an attractive source of new therapeutic candidate compounds since a tremendous chemical diversity is found in the multitude of species of plants, animals, marine organisms and microorganisms (Hazalin et al., 2012). Plus, nowadays, the preference for natural and biological products in protecting the human body from diseases has become increasingly popular rather than those of synthetic origin which have undesirable side effects. The plant kingdom with a remarkable diversity in producing natural compounds has attained a special interest in the field of medicinal research to treat human diseases (Ebrahimabadi et al., 2010).

Plants living in the tropical environment have to develop and survive under continuous and intense competition for nutrients and resources. At the same time, the plants also have to develop an array of chemical defences to protect them from viral diseases, fungal pathogens, insects and other predators. Thus, tropical plants are perhaps the most valuable source of new bioactive chemical entities due to their biodiversity coupled with the chemical diversity found within each species (Rahmani, 2003).

With over 15,000 plant species, the Malaysian tropical rainforest offers valuable compounds of starting points for the development of new drugs (Hazalin et al., 2012; Gurib-fakim, 2006). One of the diseases which should regain our concern today is the Alzheimer's disease.

Alzheimer's disease (AD) was described for the first time in 1906 by the German neuropathologist, Alois Alzheimer, when performing a histopathological study of the brain of his patient who was suffering from dementia (Tran & Duong, 2015). He discovered the presence of two types of lesions in the brain, senile plaque and neurofibrillary tangle.

The brain is made up of neurons and they are interconnected to form a network. These connections known as synapses, transmit information from one neuron to another. Ten to fifteen years before the appearance of the AD symptoms, the two main lesions will form in the brain. Senile plaques, composing of amyloid-beta protein, will impair synapses. Thus, the signals cannot pass between the neurons. On the other hand, neurofibrillary tangles which consist of Tau protein will kill the neurons by preventing the normal transport of food and energy around the neurons.

The progression of the neurofibrillary tangles in the brain corresponds with the symptoms of AD, which begins with memory problems, followed by language problems, recognition and capacity to perform gestures (Liang et al., 2015). Therefore, the presence of the two lesions is required to develop AD.

AD is an irreversible disease. It exhibits progressive brain disorder that slowly destroys the memory and thinking skills, hence, eventually decreasing the ability to carry out the simplest tasks (Puri et al., 2015; Liang et al., 2015). This disease affects people worldwide, and the prevalence is increasing as the population ages (Boada et al., 2014). AD is also one of the most common dementia among the elderly (Logue et al., 2014). Dementia is a general term for memory loss and other intellectual abilities serious enough

to interfere with daily life. Thirty-six million people worldwide have been estimated to be living with dementia in 2010, primarily AD (Boada et al., 2014).

AD is currently ranked as the sixth leading cause of death in the United States, but recent estimates indicate that the disorder may rank third, just behind heart disease and cancer, as a cause of death for older people (Burnham et al., 2015). Although decades of research have focused on understanding AD's pathology and progression, there is still a great lack of clinical treatments for those who suffer from it (Burnham et al., 2015). Currently, cholinesterase enzyme (ChE) inhibition represents the most efficacious treatment approach for AD. Two types of ChE have been characterized in the vertebrate tissues; acetylcholinesterase enzyme (AChE) and butyrylcholinesterase enzyme (BChE) (Awang et al., 2010).

University of Malaya

1.2 Problem Statement

Evidence has shown that the secondary metabolites of *Myristica fragrans* Houtt. (nutmeg) are memory enhancers (Cao et al., 2013). Since there are many *Myristica* plants in the forest that has not been studied yet, it is possible that these plants be investigated for their potential as memory enhancer. For this particular study, *M. cinnamomea* King will be the subject of study. *M. cinnamomea*, is closely related to *M. fragrans*, therefore there is a strong possibility that the secondary metabolites of *M. cinnamomea* could inhibit the AChE and BChE which in turn could prevent AD (Cao et al., 2013). The genus *Myristica* is known to be a rich source of acylphenols (Pham et al, 2000). The significant AChE inhibitory activity of acylphenols isolated from the fruits of *M. crassa* with IC_{50} values of 9.4 ± 1.6 and 11.7 ± 2.5 μ M, has made it worthy to investigate the fruits of *M. cinnamomea* in search of potential AD inhibitors (Maia et al., 2008). Preliminary screening of the ethyl acetate extract (at 100 μ g/ mL) of the fruits of *M. cinnamomea* has proven it to be a potential inhibitor of the AChE (95.93 ± 7.86 %) and BChE (70.00 ± 13.17 %).

1.3 Research Objectives

From the view of the above arguments (Section 1.2), the principal objectives of the present MSc work were as follows:

1. To isolate and purify the secondary metabolites from the ethyl acetate extract of the fruits of *M. cinnamomea* using chromatographic techniques such as column chromatography (CC) and preparative thin layer chromatography (prep-TLC).

2. To characterize the above mentioned secondary metabolites using spectroscopic techniques such as 1D NMR (^1H , ^{13}C , DEPT-135), 2D NMR (^1H - ^1H COSY, ^1H - ^{13}C HSQC, ^1H - ^{13}C HMBC), FTIR, LCMS-IT-TOF and UV-Vis spectroscopy.
3. To screen the inhibitory activities of the above mentioned secondary metabolites against the acetylcholinesterase (AChE) and butyrylcholinesterase (BChE) enzymes in order to identify the compound(s) which were responsible in giving rise to the strong AChE and BChE inhibitory activities of the ethyl acetate extract.
4. To carry out kinetic and molecular docking studies on the compound(s) that actively inhibited the AChE and BChE, in order to determine their mode of inhibition (competitive, non-competitive or mixed-type) and to investigate the site at which the active compound(s) bind to the enzymes.

CHAPTER 2

LITERATURE REVIEW

2.1 The Myristicaceae

2.1.1 Geographical Distribution and Botanical Aspects

The Myristicaceae is a pantropical family of trees distributed in the Tropical Rain forests mainly at lowlands throughout the tropics and centred in Malaysia. This family can be found in Central and South America, Africa, Madagascar, India and Asia. The family consists of 21 genera and at least 500 species (Janovec et al., 2004; Doyle et al., 2008). The important genera in the Myristicaceae are *Myristica*, *Horsfieldia*, *Knema* and *Virola* (Beaman, 2002). The Myristicaceae belongs to the Magnoliales order, morphologically considered one of the most primitive of the Angiosperms (flowering plants) (Juan, 2000).

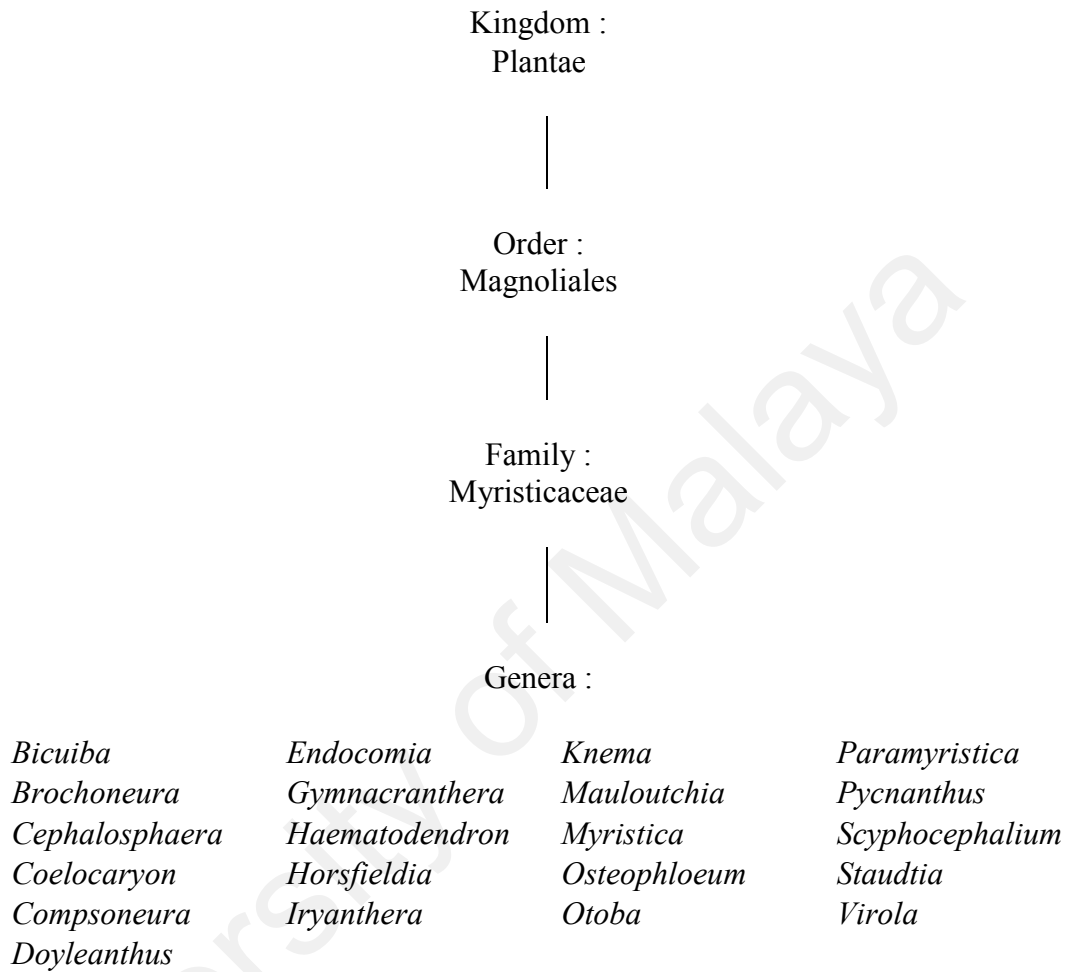
Floristic and ecological studies have revealed that the Myristicaceae rank among the top five to ten most common and important tree families throughout the majority of the lowland moist tropical forests of the world, whereby the family has a significant ecological importance (Janovec et al., 2004; Doyle et al., 2008). Fruits of the Myristicaceae, particularly the lipid-rich aril surrounding the seeds in some species, are important as food for the birds and the mammals of the tropical forests. Numerous species are valued by humans as sources of food, medicine, narcotics and timber, including *M. fragrans* Houtt., the source of nutmeg and mace, spices of commerce.

The trees are small, medium or large, often with buttresses or stilt roots. The outer bark is smooth, scaly or fissured, brown or black in colour while, the inner bark is fibrous and

reddish brown. The wood is soft, white in colour and darkens to red upon exposure especially around the vessels. The twigs are usually reddish or greyish-brown, the old parts being striate while the young parts are smooth or scaly. The leaves are alternate, generally long, leathery, dark shiny green above and sometimes hairy or scaly.

Inflorescences are branching panicles or thick short woody knobs which are amongst or behind the leaves, with the male and female inflorescences usually on different trees whereby the male trees are usually larger and more branched. The flowers are mostly tiny, perianth usually 3-lobed, yellow, cream, white, pink or red in colour, often hairy outside and sometimes sweetly scented. The ovary is one-celled with a single, basal ovule. The fruits are round to oblong usually longer than broad, pointed, yellow or red upon ripening, sometimes hairy, have a thick fleshy wall, ultimately splitting into two halves to expose the single large hard seed (nutmeg), covered in pink or red waxy flesh. Their seeds contain hard, fatty, endosperm divided up by brown lines ("Subclass MAGNOLIIDAE Takhtajan 1966", 2012).

2.1.2 Classification of the Myristicaceae



Scheme 2.1: Classification of the Myristicaceae.

2.1.3 Traditional Uses

Several genera such as *Myristica*, *Virola*, *Iryanthera*, *Knema* and *Pycnanthus* have been extensively used in traditional medicine. Traditional uses of *M. fragrans* (nutmeg) include the treatment of rheumatism, cholera, psychosis, stomach cramps, nausea, diarrhea, flatulence and anxiety in addition to its use as an aphrodisiac and an abortifacient (Barceloux, 2009). The genus *Virola* is typically found in the tropical forests, mainly in the Amazon. *Virola oleifera* is one of the few species existing in the Atlantic forest in the southern region of Brazil and this species has been popularly used due to its wound healing, anti-inflammatory and anti-rheumatic properties (Sartorelli et al., 1997).

The leaves of *Iryanthera juruensis* Warb. are crushed and used by the Amazon Indians to heal infected wounds and cuts. The latex from its bark is mixed with warm water for treating stomach infections (Silva et al., 2001). The genus *Knema* is distributed in tropical Africa, Asia and Australia, and is used in traditional medicine. In Thailand, the stem bark of *Knema furfuracea* Warb. is traditionally employed in the treatment of sores and pimples (Zahir et al., 1993).

Pycnanthus angolensis (Welw.) Warb. is a tree that grows in the West and Central Africa and has the common name 'African nutmeg'. Traditional healers have used its leaves, twigs, seed fat and bark exudate to treat oral thrush, fungal skin infections and shingles while its ground stem bark has been used as a mixture with *Piper guineense* Shumach. and water to produce a paste that is applied topically to treat headaches, body aches and chest pains (Fort et al., 2000). There are folklore claims that this species is also used in the treatment of leprosy (Kuate et al., 2011).

2.2 The Genus *Myristica*

2.2.1 Geographical Distribution and Botanical Aspects

Myristica is a genus comprising 120 species. They are distributed in South Asia, from west Polynesia, Oceania, eastern India to the Philippines (Zhang et al., 2014). The trees are of various sizes, reaching up to about 120 feet in height, with buttresses or stilt roots. The bark is black or brown in colour and the twigs are openly striate when old. The leaves are variously hairy or glaucous below. The inflorescences are branching or axillary panicles, males usually exceeding females. The flowers are flask or bell-shaped, white or pale yellow in colour. The fruits are usually large, with a thick wall and firm flesh. The endosperm contains oil and starch ("Subclass MAGNOLIIDAE Takhtajan 1966", 2012).

By far, the most important species in this genus is *M. fragrans*, a native of the Moluccas, or Spice Islands, in the Indonesian Archipelago (Adjene et al., 2010). The seeds of *M. fragrans* are the source of nutmeg and mace. Besides having a commercial importance as spices which is used in sweet and savoury cooking and also in a variety of drinks, nutmeg is also recognized as a medicine in traditional Chinese medicine and in international natural medicine since at least the seventh century (Van Gils et al., 1994). Nutmeg is also prescribed for medicinal purposes in Asia, including Malaysia to treat many diseases such as rheumatism, muscle spasm, decreased appetite and diarrhea (Nguyen et al., 2010). The chemistry of *M. fragrans* has been extensively explored due to its versatile biological activities and also due to the fact that it is easily available. The secondary metabolites of *M. fragrans* have been reported to exhibit analgesic, anti-inflammatory, antioxidant, anti-carcinogenic, antiplatelet aggregation, psychoactive, antidepressant-like, antifungal, memory enhancing and antidiarrheal activities (Cao et al., 2013).

2.2.2 Phytochemical Composition

The genus *Myristica* has been reported to yield various types of biologically and pharmacologically active compounds inclusive of acylphenols, dimeric acylphenols, flavans, lignans and neolignans.

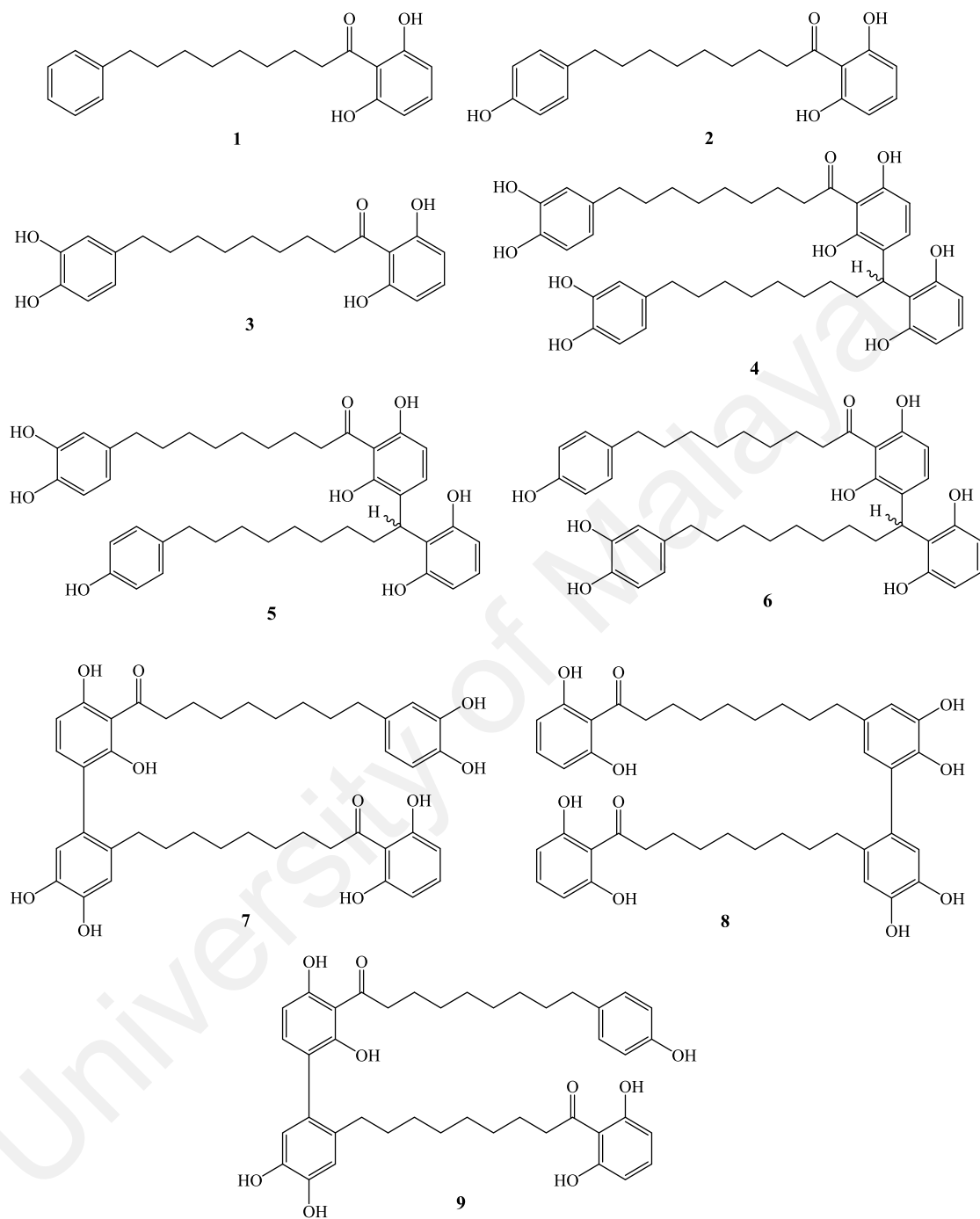
2.2.2.1 Acylphenols and Dimeric Acylphenols

Malabaricones A-C (**1-3**), maingayones A-C (**4-6**) and giganteones A-C (**7-9**) are the common acylphenols and dimeric acylphenols isolated from this genus. Compound **1** from *M. malabarica* Lam. has been reported to exhibit strong cytotoxicity against three leukemic (IC_{50} 12.70 ± 0.10 - 18.10 ± 0.95 $\mu\text{g/mL}$) and three solid tumor (IC_{50} 28.10 ± 0.58 - 55.26 ± 5.90 $\mu\text{g/mL}$) cell lines (Maity et al., 2009). Compound **2**, isolated from the methanol extract of the dried fruit rind of *M. malabarica*, revealed effective healing property against the indomethacin-induced gastric ulceration whereby it reduced the ulcer indices by 60.3% ($P < 0.01$) when introduced to ulcerated mice (Maity et al., 2012). Compound **3** from the seeds of *M. fragrans* showed strong inhibitory activity towards the LPS-induced NO production and it also inhibited the inductions of COX-2 and iNOS mRNA in macrophage RAW264.7 cells with an IC_{50} value of 2.3 μM (Cuong et al., 2011).

Compounds **1-4** which were isolated from the ethyl acetate extract of the fruits of *M. maingayi* Hk. f. were reported to show significant cytotoxicity against human tumoral KB cells with IC_{50} values of 153, 9, 11 and 26 μM , respectively and these compounds also exhibited moderate activity against *Plasmodium falciparum* with IC_{50} values of 98, > 292, 56 and > 143 μM , respectively (Pham et al., 2000). Acetylcholinesterase inhibitory

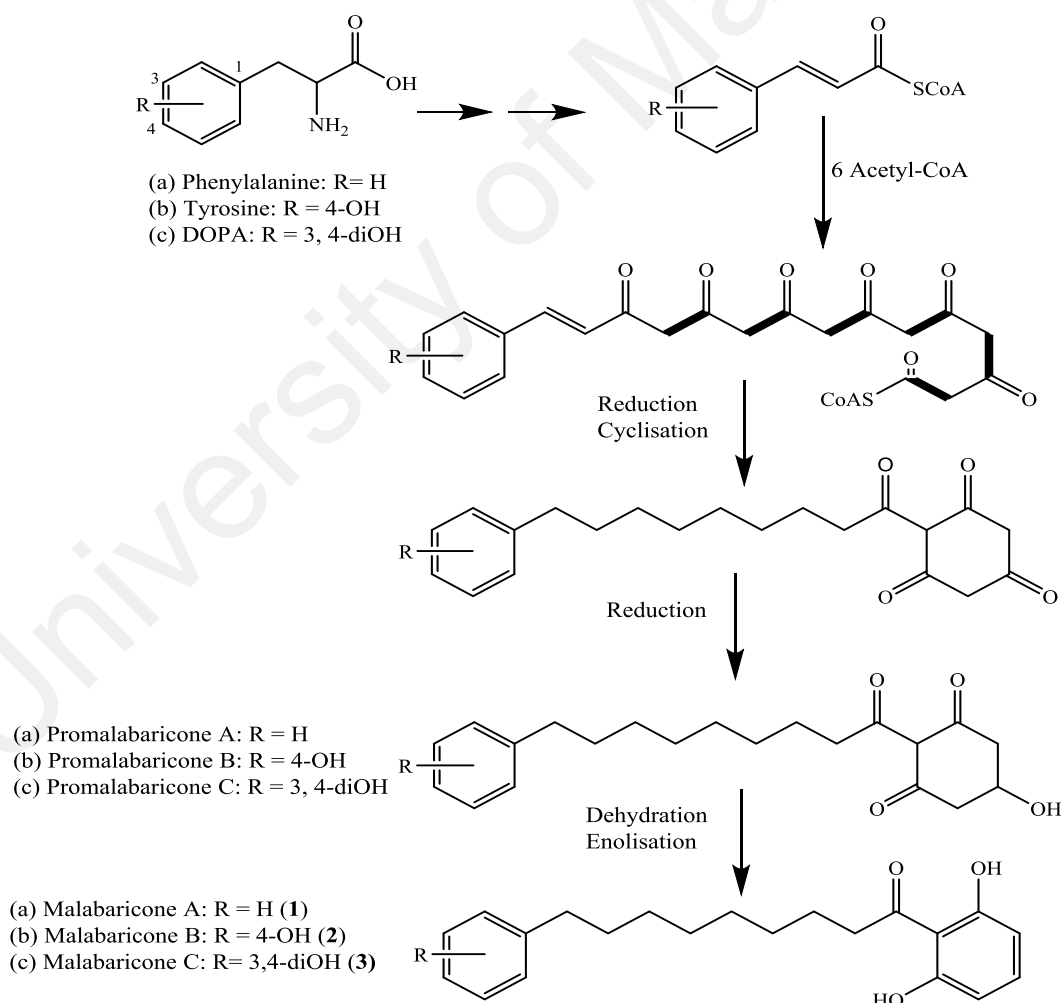
activity was observed for compounds **2**, **3**, **5**, **6**, **7** and **9** which were isolated from the ethyl acetate and methanol extracts of the leaves and the fruits of *M. crassa* King. Compounds **2** (IC_{50} 9.4 ± 1.6 μ M) and **3** (IC_{50} 11.7 ± 2.5 μ M) strongly inhibited the acetylcholinesterase enzyme (Maia et al., 2008). Compounds **7** and **8** from the ethyl acetate extract of the fruits of *M. gigantea* King exhibited *in vitro* cytotoxic activity against human nasopharynx KB cells with IC_{50} values of 11.4 and 1.8 μ g/mL respectively, with the latter being more potent (Pham et al., 2002).

University of Malaya



2.2.2.1.1 Biosynthesis of Acylphenols

The biosynthesis of promalabaricones presumably results from the elongation of a cinnamoyl type precursor, originating from amino acids such as phenylalanine and its hydroxy-derivatives (tyrosine or DOPA) with six acetate (malonate) units, followed by the reduction of the first three acetate units and the cyclisation of the last three acetate units into a triketonic cyclohexane ring according to the phloroglucinol type cyclisation. Subsequently, the reduction of the *para*-carbonyl group into an alcohol yielded the promalabaricones following which the dehydration of the ring hydroxyl led to the formation of the malabaricones (Scheme 2.2) (Pham et al., 2000).



Scheme 2.2: Biosynthetic pathway for the formation of acylphenols

2.2.2.2 Flavans, Lignans and Neolignans

Apart from bioactive acylphenols and dimeric acylphenols, bioactive lignans, neolignans and flavans were also isolated from the genus *Myristica* as summarized in Table 2.1 below.

Table 2.1: Summary of the chemical constituents isolated from the genus *Myristica* and their biological activities

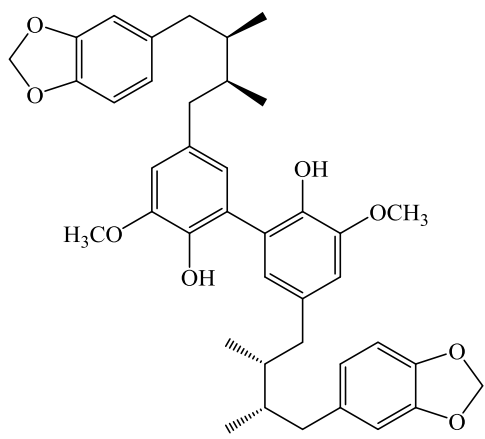
Species	Part of plant investigated and site of collection	Compounds	Biological activity
<i>M. argentea</i> Warb.	Mace; Indonesia (Filleur et al., 2002)	Argenteane (10) <i>Meso</i> -dihydroguaiaretic acid (11) <i>Erythro</i> -austrobailignan-6 (12) Myristargenol-A (13) Licarin-A (14) Licarin-B (15) Machilin-C (16)	-
	Mace; Indonesia (Calliste et al., 2010)	Argenteane (10) <i>Meso</i> -dihydroguaiaretic acid (11) <i>Erythro</i> -austrobailignan-6 (12)	Antioxidant properties, lipid peroxidation inhibitor and DPPH free radical scavenging capacities
<i>M. cagayanesis</i> Merr.	Seeds; Taiwan (Kuo et al., 1989)	Malabaricone A (1) Otobain (17) Otobanone (18) Cagayanin (19) Cagayanone (20)	-
<i>M. ceylanica</i> A. DC.	Bark; Sri Lanka (Herath & Padmasiri., 1999)	Malabaricone A (1) Malabaricone B (2) Demetyldactyloidin (21)	-

<i>M. cinnamomea</i> King	Fruits; Thailand (Sawadjoon et al., 2002)	Myristinins A-F (22-27) Hinokinin (28) Dodecanoylphloroglucinol (29) 1-(2,4,6-trihydroxyphenyl)- 9-phenylnonan-1-one (30)	Anti-fungal agents and COX-2 inhibitors
	Bark; Malaysia (Chong et al., 2011)	Malabaricone C (3)	Anti-quorum sensing agent against <i>Pseudomonas</i> <i>aeruginosa</i> PAO1
	Bark;, Malaysia (Sivasothy et al., 2016 a & b)	Giganteone A (7) Giganteone D (31) Cinnamomeone A (32)	α -glucosidase inhibitors and anti- quorum sensing agent against <i>Escherichia coli</i> biosensors
<i>M. crassa</i> King	Leaves and fruits; Malaysia (Maia et al., 2008)	Malabaricone B (2) Malabaricone C (3) Maingayone B (5) Maingayone C (6) Giganteone A (7) Giganteone C (9)	Acetylcholinesterase inhibitory activity
<i>M. dactyloides</i> Gaertn.	Root bark; Sri Lanka (Herath & Priyadarshani, 1996 & 1997)	Rel.(8 <i>S</i> ,8' <i>S</i>)-bis(3,4- methylenedioxy)-8,8'- neolignan (33) Malabaricanol-A (34) Rel-(8 <i>S</i> , 8' <i>S</i>)dimethyl- (7 <i>S</i> ,7' <i>S</i>)-bis(4-hydroxy-3- methoxyphenyl)tetrahydrofuran (35) Nordihydroguaiaretic acid (36) Rel-(8 <i>R</i> ,8' <i>S</i>)-4-hydroxy-3- methoxy-3',4'- methylenedioxy-8.8'- neolignan (37) Rel-(8 <i>R</i> ,8' <i>S</i>)-3,4-dimethoxy- 3',4'-methylenedioxy- 8.8'- neolignan (38)	-

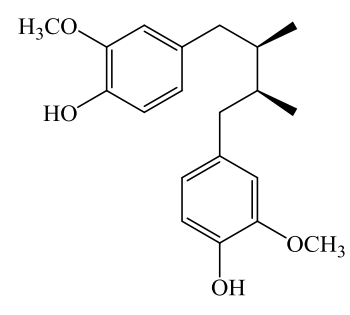
		<p>Rel-(8<i>R</i>,8'<i>R</i>)-4-hydroxy-3-methoxy-3',4'-methylenedioxy-8.8'-neolignan (39)</p> <p>Rel-(8<i>R</i>,8'<i>R</i>)-3,4-dimethoxy-3',4'-methylenedioxy-8.8'-neolignan (40)</p> <p>1-(2,6-dihydroxyphenyl)-9-(4-hydroxy-3-methoxyphenyl)nonan-1-one (41)</p> <p>Malabaricone A (1)</p>	
	<p>Root bark; Sri Lanka (Herath et al., 1998)</p>	Dactyloidin (42)	-
<i>M. fragrans</i> Houtt.	<p>Seeds (Cuong et al., 2011)</p>	Malabaricone C (3)	<p>Strong inhibitory activity towards the LPS-induced NO production and inhibited the inductions of COX-2 and iNOS mRNA in macrophage RAW264.7 cells</p>
	<p>Dried semen; Republic of Korea (Nguyen et al., 2010)</p>	<p>Tetrahydrofuroguaiacin B (43)</p> <p>Saucernetindiol (44)</p> <p>Verrucosin (45)</p> <p>Nectandrin B (46)</p> <p>Nectandrin A (47)</p> <p>Fragransin C₁ (48)</p> <p>Galbacin (49)</p>	<p>AMP-activated protein kinase (AMPK) activators and anti-obesity activity</p>
	<p>Seeds; Hanoi, Vietnam (Min et al., 2011)</p>	<p>(8<i>R</i>,8'<i>S</i>)-7-(3,4-methylenedioxyphenyl)-8-methyl-8'-hydroxymethyl-7'-(3',4'-methylenedioxyphenyl)-butanol (50)</p> <p>(8<i>R</i>,8'<i>S</i>)-7'-(3',4'-methylenedioxyphenyl)-8,8'-dimethyl-7-(3,4-dihydroxyphenyl)-butane (51)</p>	<p>NO production inhibitor in macrophage RAW264.7 cells</p>

		<p><i>Meso</i>-monomethyldihydroguaiaretic acid (52)</p> <p>(+)-guaiacin (53)</p> <p>(7<i>S</i>,8'<i>R</i>,7'<i>R</i>)-4,4'-dihydroxy-3,3'-dimethoxy-7',9'-epoxylignan (54)</p> <p>7-(4-hydroxy-3-methoxyphenyl)-7-(3,4-methylenedioxyphenyl)-8,8-lignan-7-methylether (55)</p>	
	Seeds (Kang et al., 2013)	<i>Erythro</i> -(7 <i>S</i> ,8 <i>R</i>)-7-acetoxy-3,4,3',5'-tetramethoxy-8-O-4'-neolignan (56)	Anti-platelet activity
	Seeds; Indonesia (Cao et al., 2015)	<p>Myrifralignan A (57)</p> <p>Myrifralignan B (58)</p> <p>Myrifralignan C (59)</p> <p>Myrifralignan D (60)</p> <p>Myrifralignan E (61)</p> <p>(7<i>S</i>,8<i>R</i>)-2-(4-allyl-2,6-dimethoxy-phenoxy)-1-(3,4,5-trimethoxyphenyl)-propan-1-ol (62)</p> <p>Myrislignan (63)</p> <p>(7<i>R</i>,8<i>S</i>)-2-(4-propenyl-2-methoxyphenoxy)-1-(3,4,5-trimethoxyphenyl)-propan-1-ol (64)</p> <p>(7<i>S</i>,8<i>R</i>)-2-(4-allyl-2,6-dimethoxyphenoxy)-1-(4-hydroxy-3,5-dimethoxyphenyl)-propan-1-ol (65)</p> <p>Machilin D (66)</p>	NO production inhibitor in macrophage RAW264.7 cells
<i>M. gigantea</i> King	Fruits; Malaysia (Pham et al., 2002)	<p>Malabaricone A (1)</p> <p>Malabaricone B (2)</p> <p>Malabaricone C (3)</p> <p>Maingayone A (4)</p> <p>Giganteone A (7)</p>	<i>In vitro</i> cytotoxic activity against human nasopharynx KB cells

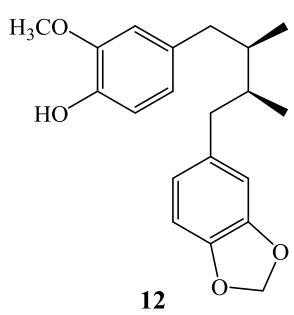
		Giganteone B (8) Promalabaricone C (67) Prepromalabaricone B (68)	
<i>M. maingayi</i> Hk. f.	Fruits (Pham et al., 2000)	Malabaricone A (1) Malabaricone B (2) Malabaricone C (3) Maingayone A (4) Promalabaricone C (67) Maingayic acid B (69) Maingayic acid C (70) Promalabaricone B (71)	Significant cytotoxicity against human tumoral KB cells and moderate activity against <i>Plasmodium falciparum</i>
<i>M. malabarica</i> Lam.	Fruits (Maity et al., 2009)	Malabaricone B (2)	Effective healing property against the indomethacin- induced gastric ulceration
	Fruits (Maity et al., 2012)	Malabaricone C (3)	Anti-inflammatory agent



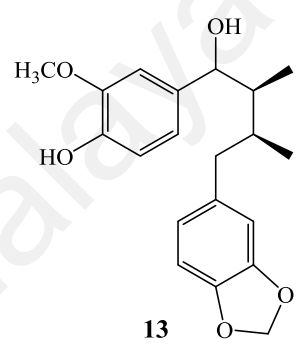
10



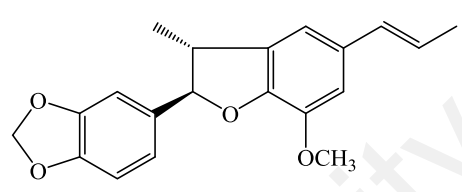
11



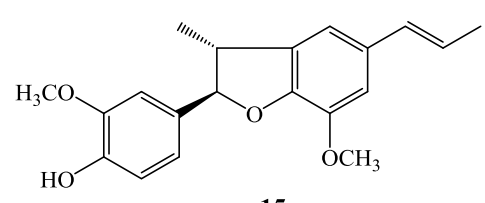
12



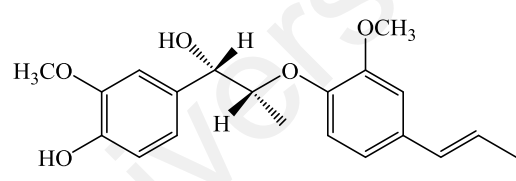
13



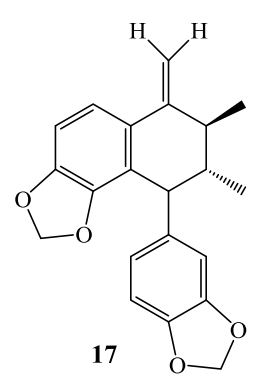
14



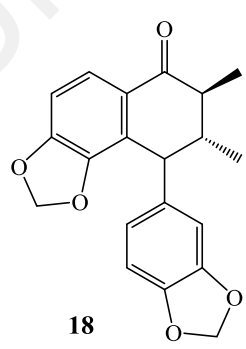
15



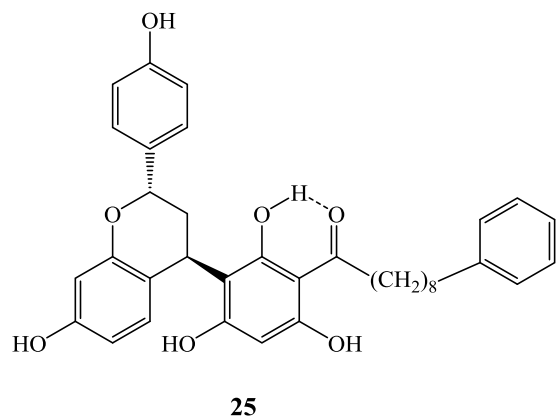
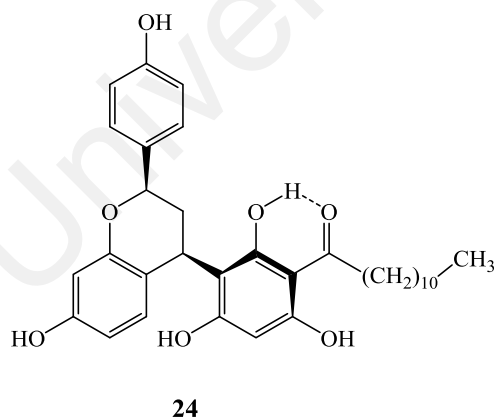
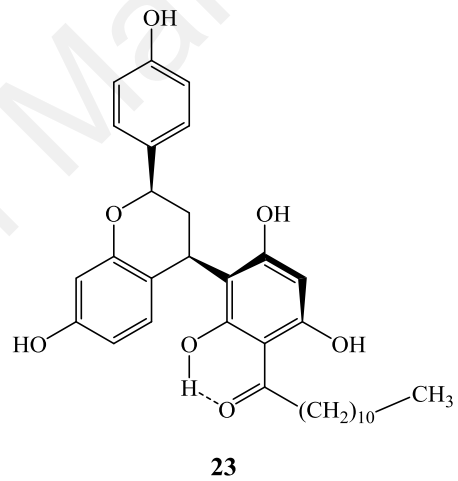
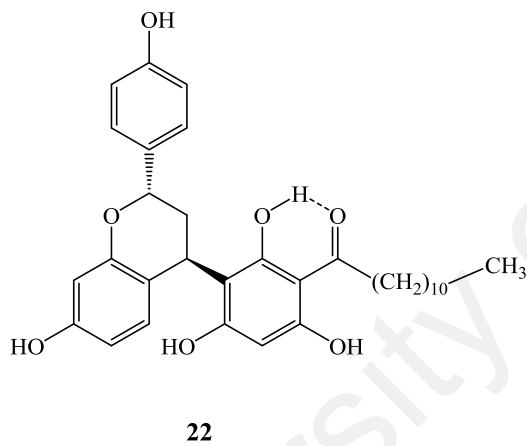
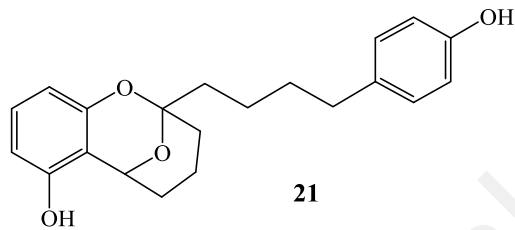
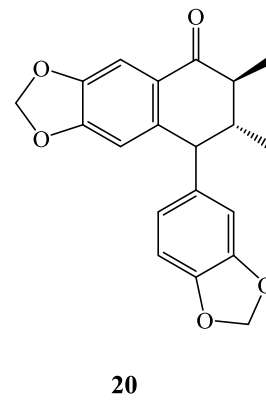
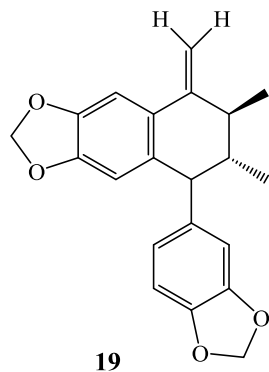
16

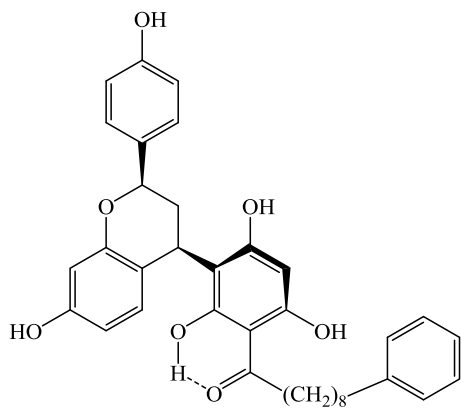


17

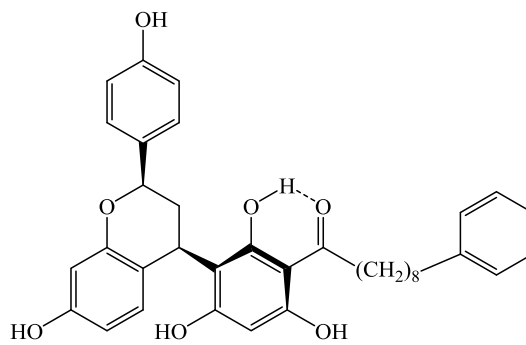


18

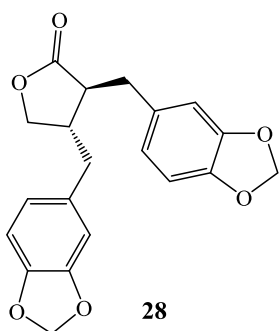




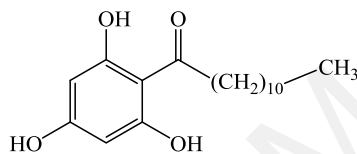
26



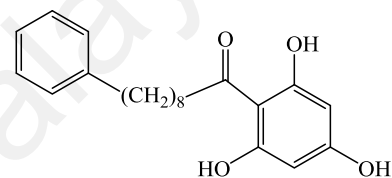
27



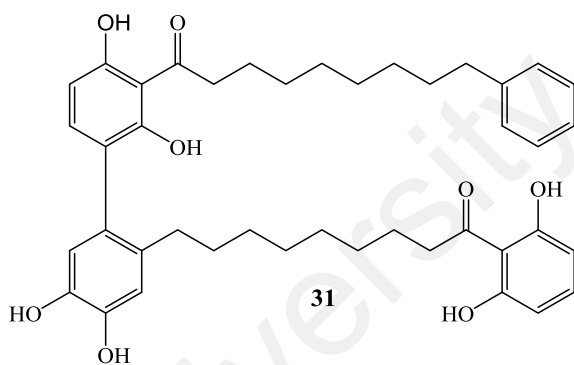
28



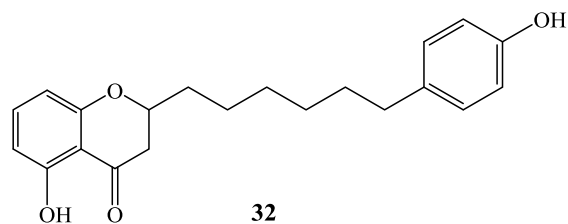
29



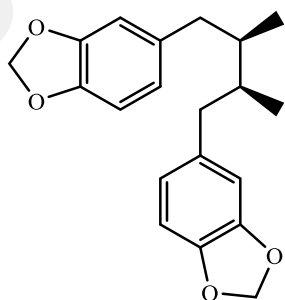
30



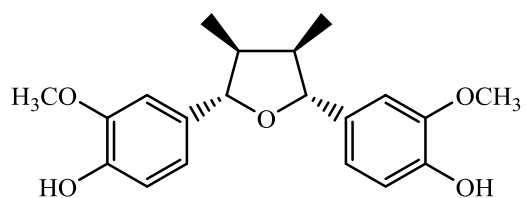
31



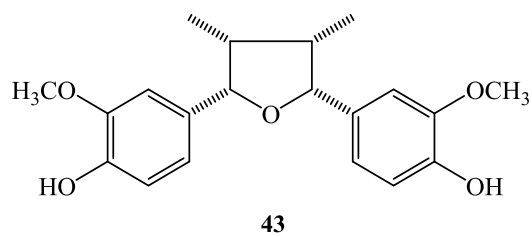
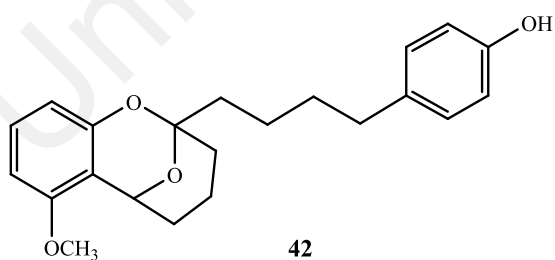
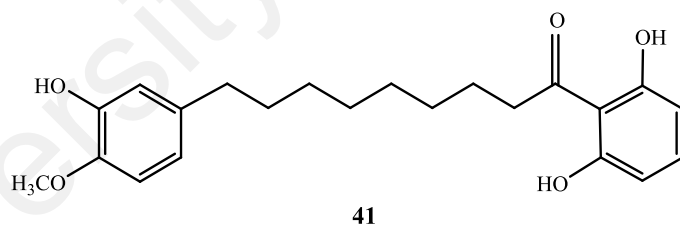
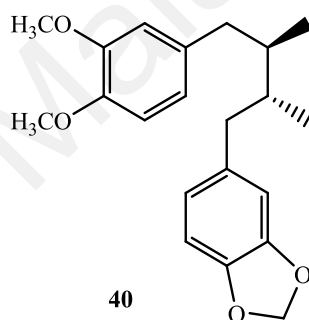
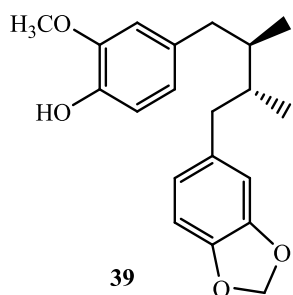
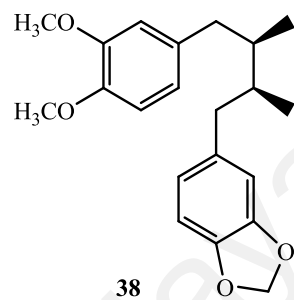
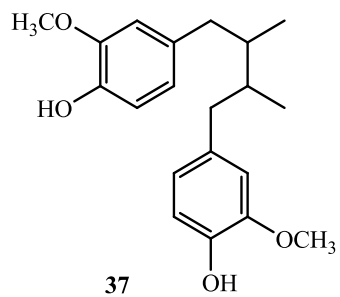
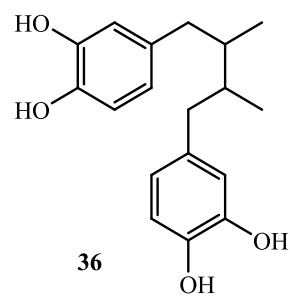
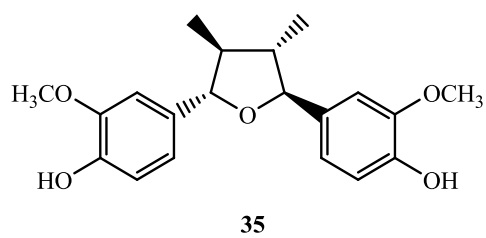
32

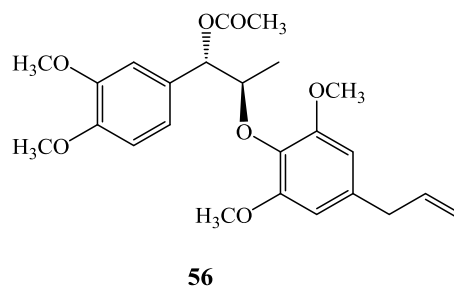
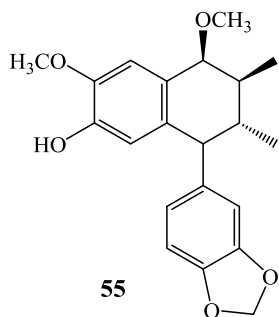
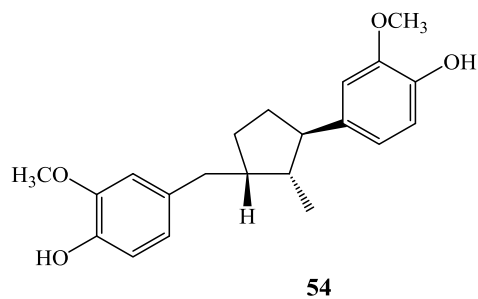
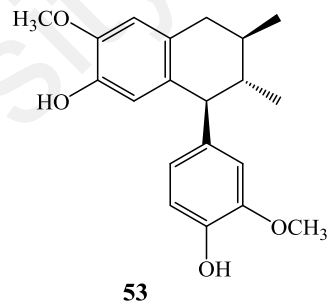
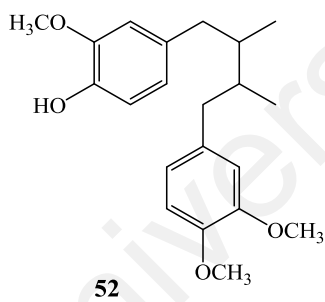
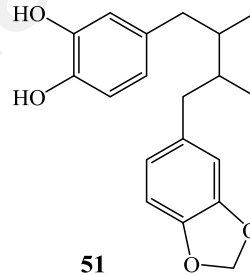
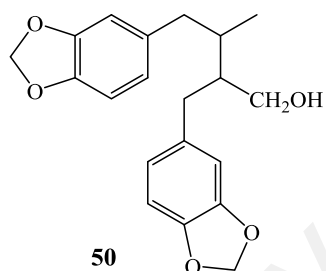
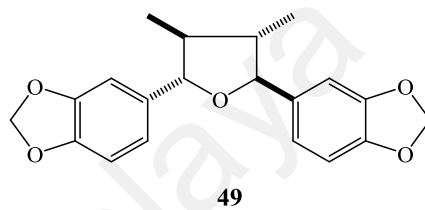
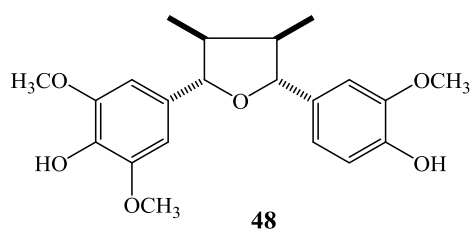
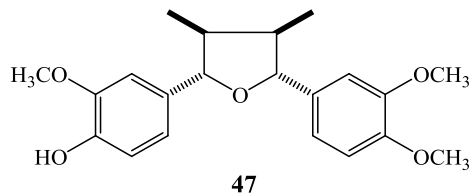
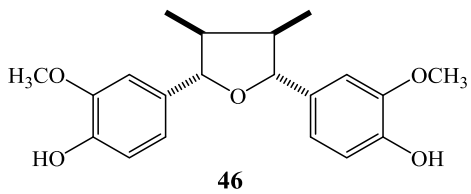
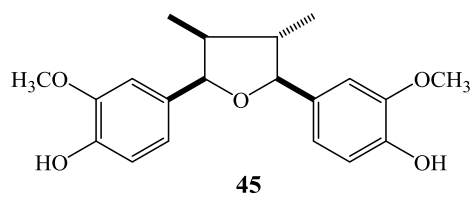
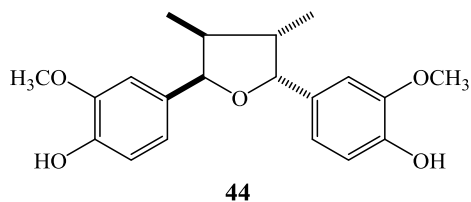


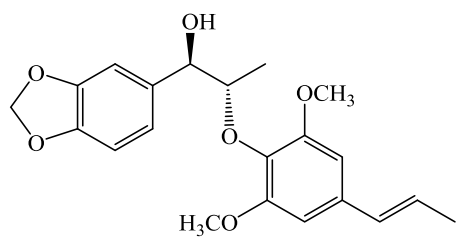
33



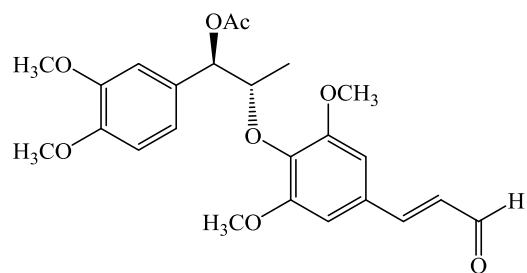
34



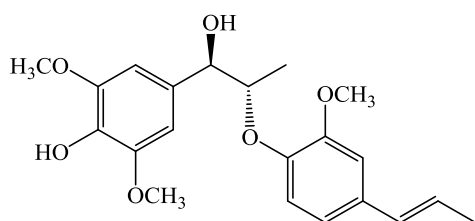




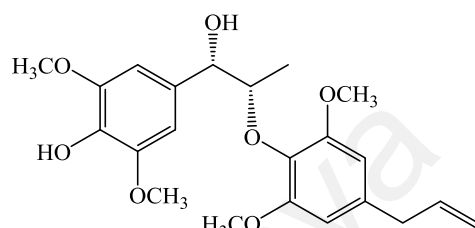
57



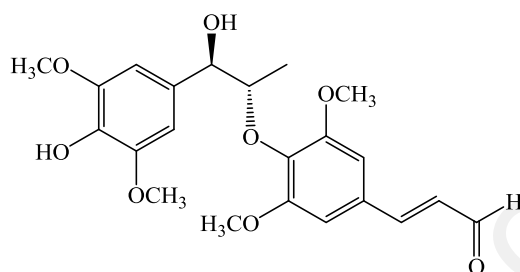
58



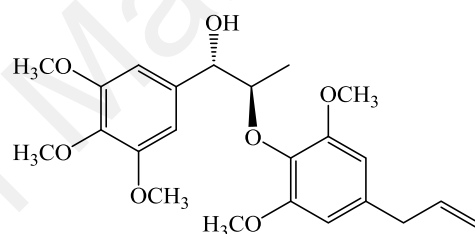
59



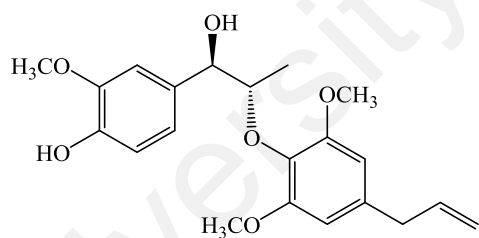
60



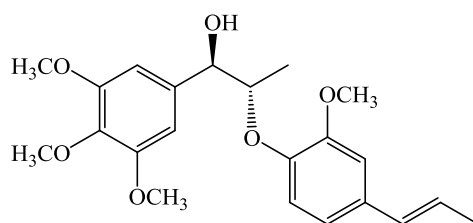
61



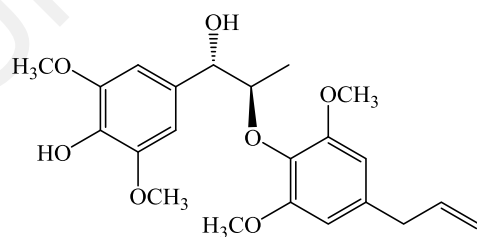
62



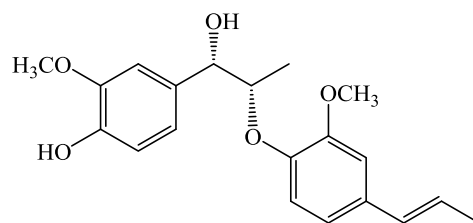
63



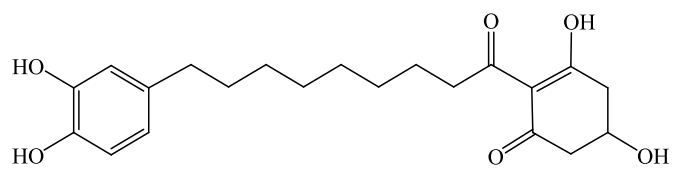
64



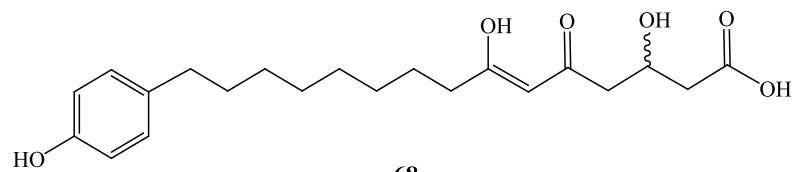
65



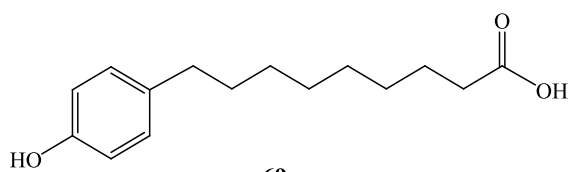
66



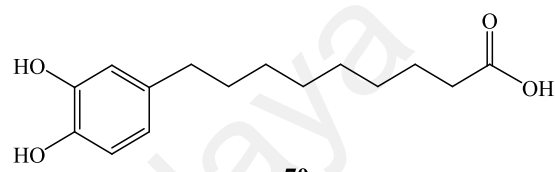
67



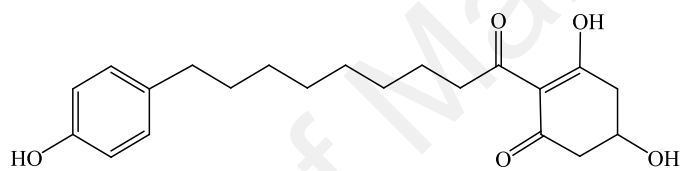
68



69



70



71

University of Malaysia

2.2.3 *Myristica cinnamomea* King

Myristica cinnamomea King (Figures 2.1-2.2) commonly known as cinnamon nutmeg, is distributed in the Malayan Peninsula, Singapore, Borneo and the Philippines. Locally, it is referred to as ‘pala bukit’ whose arils and seeds have a spicy odour resembling those of *M. fragrans*, a nutmeg tree (‘pala’). *M. cinnamomea* is a tree 15 m in height and 45 cm in diameter. Its outer bark is dark brown, rugose with fine grid cracks while the inner bark is pale brown. The leaves are oblong to oblanceolate, bright green above and pale silvery brown below. The fruit is yellow and globose to broadly globular-oblong. Its seeds are red and used as spices (Seidemann, 2005).



Figure 2.1: The leaves (left) and the fruits (right) of *Myristica cinnamomea* King



Figure 2.2: Voucher specimen of *Myristica cinnamomea* King

Previous phytochemical investigation of *M. cinnamomea* revealed the presence of compounds which have been proven to exhibit broad pharmacological activities. The dichloromethane extract of the fruits of *M. cinnamomea* yielded myristinins A-F (**22-27**), hinokinin (**28**), dodecanoylphloroglucinol (**29**) and 1-(2,4,6-trihydroxyphenyl)-9-phenylnonan-1-one (**30**). These compounds were reported to exhibit antifungal activity against *Candida albicans* with IC₅₀ values ranging from 5.9 to 8.8 µg/mL and were also found to inhibit the cyclooxygenase-2 (COX-2) enzyme (Sawadjoon et al., 2002). The methanol extract of the bark on the other hand afforded malabaricone C (**3**), an anti-quorum sensing agent (Chong et al., 2011). Recently, two alpha glucosidase inhibitors; giganteone D (**31**) (IC₅₀ 5.05 µM) and cinnamomeone A (**32**) (IC₅₀ 358.80 µM) were identified in the hexane extract of its bark (Sivasothy et al., 2016a). The same group of researchers also reported giganteone A (**7**) from the ethyl acetate extract of the bark to be an anti-quorum sensing agent against *Escherichia coli* biosensors (Sivasothy et al., 2016b).

CHAPTER 3

RESULTS & DISCUSSION

3.1 Secondary Metabolites Isolated from the Fruits of *M. cinnamomea*

The ethyl acetate extract of the dried fruits of *M. cinnamomea* was fractionated by a combination of chromatographic procedures to yield four acylphenols; malabaricone A (**1**), malabaricone B (**2**), malabaricone C (**3**) and malabaricone E (**72**), along with two dimeric acylphenols; maingayone A (**4**) and maingayone B (**5**) and an acid, maingayic acid B (**69**). Their structures were elucidated on the basis of 1D and 2D NMR techniques and LCMS-IT-TOF analysis. Compounds **1-3** were the major metabolites while the remaining constituents were obtained in smaller amounts. The acetylcholinesterase enzyme (AChE) and butyrylcholinesterase enzyme (BChE) inhibiting potentials of compounds **1-5**, **69** and **72** were evaluated. Kinetic and molecular docking studies were carried out on the compound(s) which actively inhibited each enzyme in order to determine their mode of inhibition (competitive, non-competitive or mixed-type) and to investigate the site at which the active compound(s) bind to the enzymes.

3.1.1 Compound 1: Malabaricone A

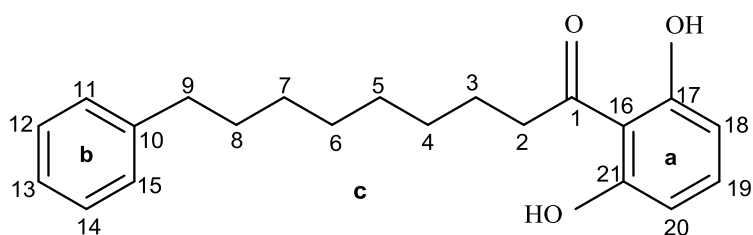


Figure 3.1: Structure of compound 1

Compound 1 (Figure 3.1) was isolated as an optically inactive light yellow amorphous powder. The positive LCMS-IT-TOF analysis (Figure 3.2) which exhibited two pseudo-molecular ions; $[M + H]^+$ at m/z 327.1953 (calcd. for $C_{21}H_{27}O_3$ 327.1955) and $[M + Na]^+$ at m/z 349.1774 (calcd. for $C_{21}H_{26}O_3Na$ 349.1774), enabled a molecular formula of $C_{21}H_{26}O_3$ to be proposed, consistent with 9 degrees of unsaturation. The combined analysis of the ^{13}C NMR (Table 3.1, Figure 3.3a) and DEPT-135 spectra (Figure 3.3b) confirmed the presence of twenty one carbon resonances comprising one carbonyl, twelve aromatic and eight methylene carbons. The UV spectrum exhibited characteristic absorption peaks of an acylphenol moiety at λ_{max} 214, 269 and 342 nm (Pham et al., 2000). The IR spectrum (Figure 3.4) revealed absorption bands due to hydroxyl (ν_{max} 3271 cm^{-1}), methylene (ν_{max} 2920 and 2851 cm^{-1}), conjugated carbonyl (ν_{max} 1628 cm^{-1}) and aromatic (ν_{max} 1589 and 1511 cm^{-1}) functional groups (Pham et al., 2000).

The 1H NMR (Table 3.1, Figure 3.5) and COSY NMR spectra (Figure 3.6) of compound 1 exhibited the typical spin system for a 1, 2, 3-trisubstituted symmetrical aromatic ring (ring a) with a three-proton system forming a triplet at δ_H 7.21 (H-19; δ_C 136.9, C-19) and two doublets at δ_H 6.34 (H-18 & H-20; δ_C 108.5, C-18 & C-20), each with a vicinal mutual coupling of 8.0 Hz (Zahir et al., 1993). The homonuclear couplings between H-18/H-19 and H-19/H-20 (Figure 3.6) in addition to the pertinent long range correlations of H-18/C-

16, C-20, C-21; H-20/C-16, C-17, C-18 and H-19/C-17, C-21 as deduced from the HMBC spectrum (Figure 3.7), further confirmed the structure of ring a (Pham et al., 2000). Ring b on the other hand was a mono-substituted aromatic ring with its signals resonating at δ_{H} 7.12-7.23 (*m*, H-11 to H-15; δ_{C} 126.7-129.5, C-11 to C-15). The two quaternary aromatic carbons at δ_{C} 163.5 (C-17 & C-21) suggested that they were oxygenated (Pham et al., 2000). The signals in the upfield region of the ^1H NMR and ^{13}C NMR spectra of compound **1** were those of the *n*-octyl chain (*c*-chain). The chemical shift of the methylene protons at δ_{H} 3.10 (*t*, $J = 8.0$ Hz, H-2; δ_{C} 45.9, C-2) implied that they were vicinal to the carbonyl carbon at δ_{C} 209.8 (C-1) (Pham et al., 2000). The HMBC cross peaks between C-1 with the methylene protons of H-2 and with those of the aromatic protons of H-18 and H-20 ($^4J_{\text{W}}$ -coupling), unambiguously linked one side of the *n*-octyl chain to C-16 (δ_{C} 111.5) of ring a (Figure 3.7) (Pham et al., 2000). The H-9/C-10, C-11, C-15, H-11/C-9 and H-15/C-9 heteronuclear correlations as inferred from the HMBC experiment confirmed the connectivity of the other end of the *n*-octyl chain to ring b at δ_{C} 144.1 (C-10) (Figure 3.7) (Pham et al., 2000).

The complete assignments of the ^1H NMR and ^{13}C NMR spectroscopic data of compound **1** were achieved with the aid of the COSY, HMBC and HSQC experiments (Figures 3.6-3.8). All of the above mentioned NMR spectroscopic data of compound **1** revealed a striking resemblance to those of malabaricone A. Comparison of the spectroscopic data of compound **1** with those reported in the literature confirmed that compound **1** was malabaricone A, an acylphenol which is ubiquitous in the genus *Myristica* (Pham et al., 2000).

Table 3.1: ^1H NMR and ^{13}C NMR spectroscopic assignments of compound **1** in methanol- d_4

Position	δ_{H} (ppm)		δ_{C} (ppm)	
	Experimental	Literature (Pham et al., 2000)	Experimental	Literature (Pham et al., 2000)
1	-	-	209.8	208.5
2	3.10 (<i>t</i> , $J = 8.0$ Hz)	3.15 (<i>t</i> , $J = 7.5$ Hz)	45.9	44.7
3	1.66 (<i>brt</i> , $J = 8.0$ Hz)	1.71 (<i>p</i> , $J = 7.5$ Hz)	25.9	24.4
4	1.33 ^a (<i>brs</i>)	1.33 (<i>brs</i>)	30.7 ^b	29.3
5	1.33 ^a (<i>brs</i>)	1.33 (<i>brs</i>)	30.6 ^b	29.3
6	1.33 ^a (<i>brs</i>)	1.33 (<i>brs</i>)	30.6 ^b	29.3
7	1.33 ^a (<i>brs</i>)	1.33 (<i>brs</i>)	30.4 ^b	29.1
8	1.58 (<i>brt</i> , $J = 8.0$ Hz)	1.61 (<i>p</i> , $J = 7.5$ Hz)	32.9	31.4
9	2.58 (<i>t</i> , $J = 8.0$ Hz)	2.60 (<i>t</i> , $J = 7.5$ Hz)	37.1	35.9
10	-	-	144.1	142.9
11	7.17 (<i>m</i>)	7.17 (<i>m</i>)	129.5	128.3
12	7.23 (<i>m</i>)	7.26 (<i>m</i>)	129.4	128.1
13	7.12 (<i>m</i>)	7.17 (<i>m</i>)	126.7	125.5
14	7.23 (<i>m</i>)	7.26 (<i>m</i>)	129.4	128.1
15	7.17 (<i>m</i>)	7.17 (<i>m</i>)	129.5	128.3
16	-	-	111.5	110.0
17	-	-	163.5	161.3
18	6.34 (<i>d</i> , $J = 8.0$ Hz)	6.40 (<i>d</i> , $J = 8.3$ Hz)	108.5	108.2
19	7.21 (<i>t</i> , $J = 8.0$ Hz)	7.26 (<i>m</i>)	136.9	135.9
20	6.34 (<i>d</i> , $J = 8.0$ Hz)	6.40 (<i>d</i> , $J = 8.3$ Hz)	108.5	108.2
21	-	-	163.5	161.3

^aOverlapping signals

^bChemical shifts are interchangeable

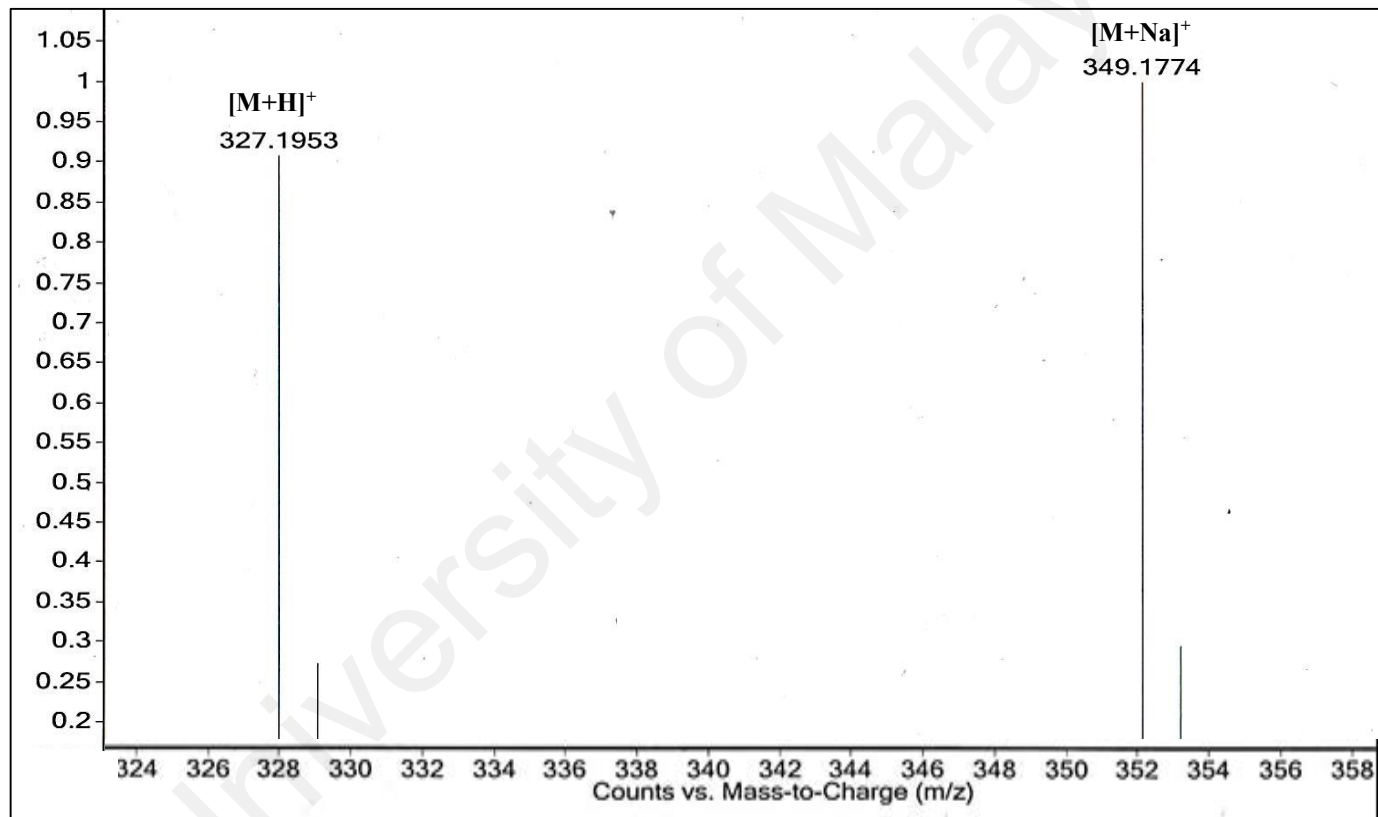
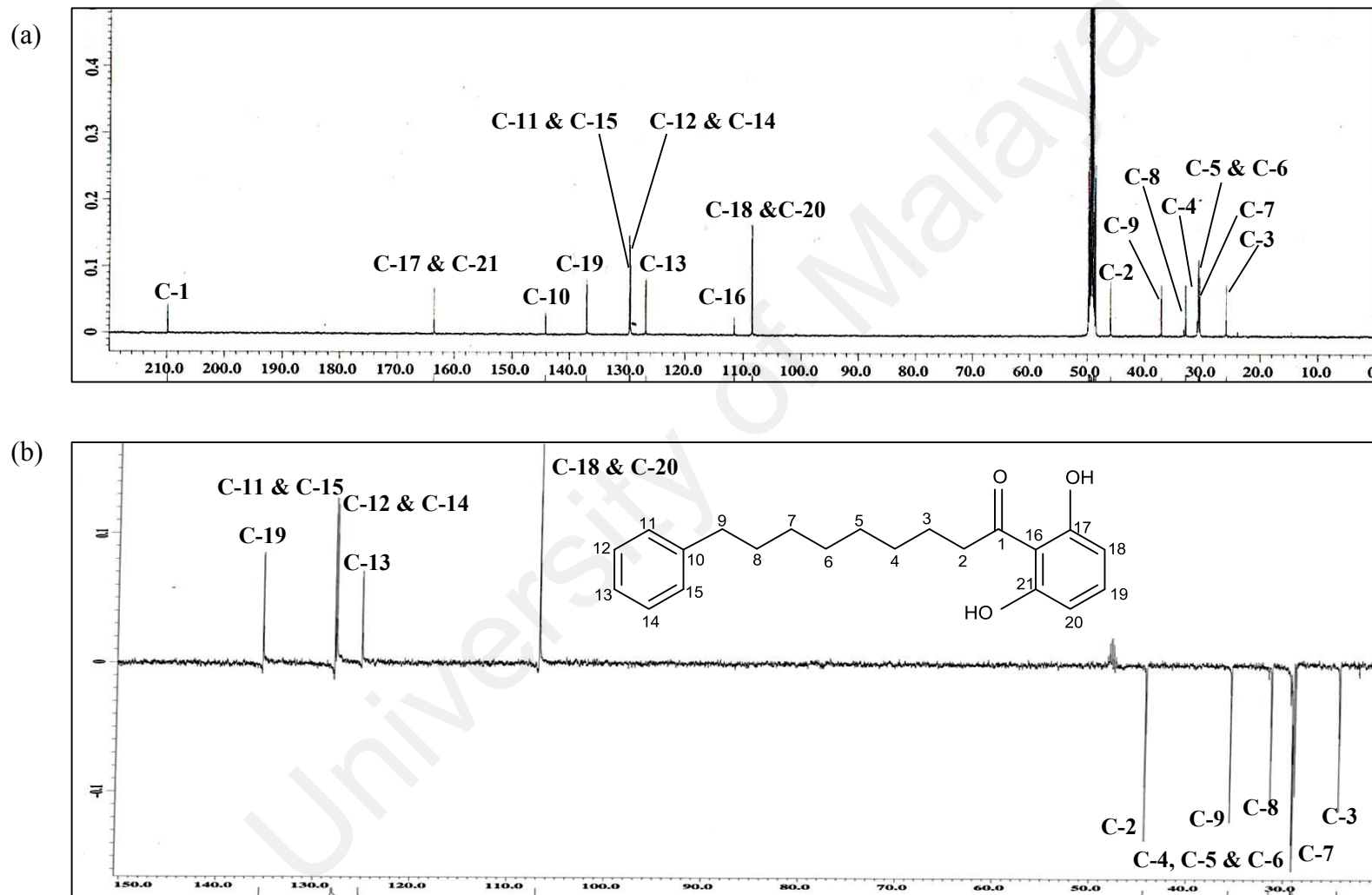


Figure 3.2: Mass spectrum of compound 1



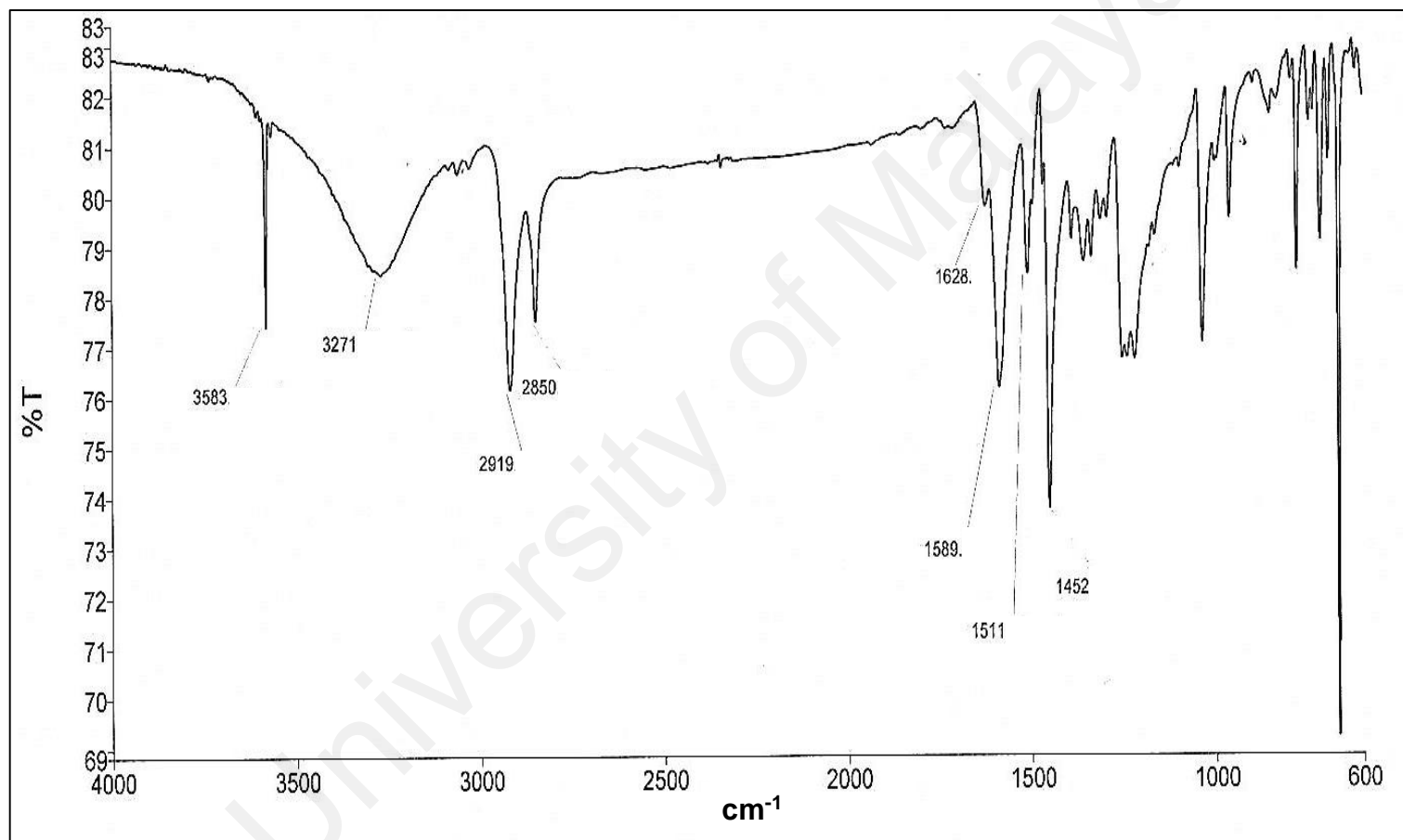


Figure 3.4: IR spectrum of compound 1

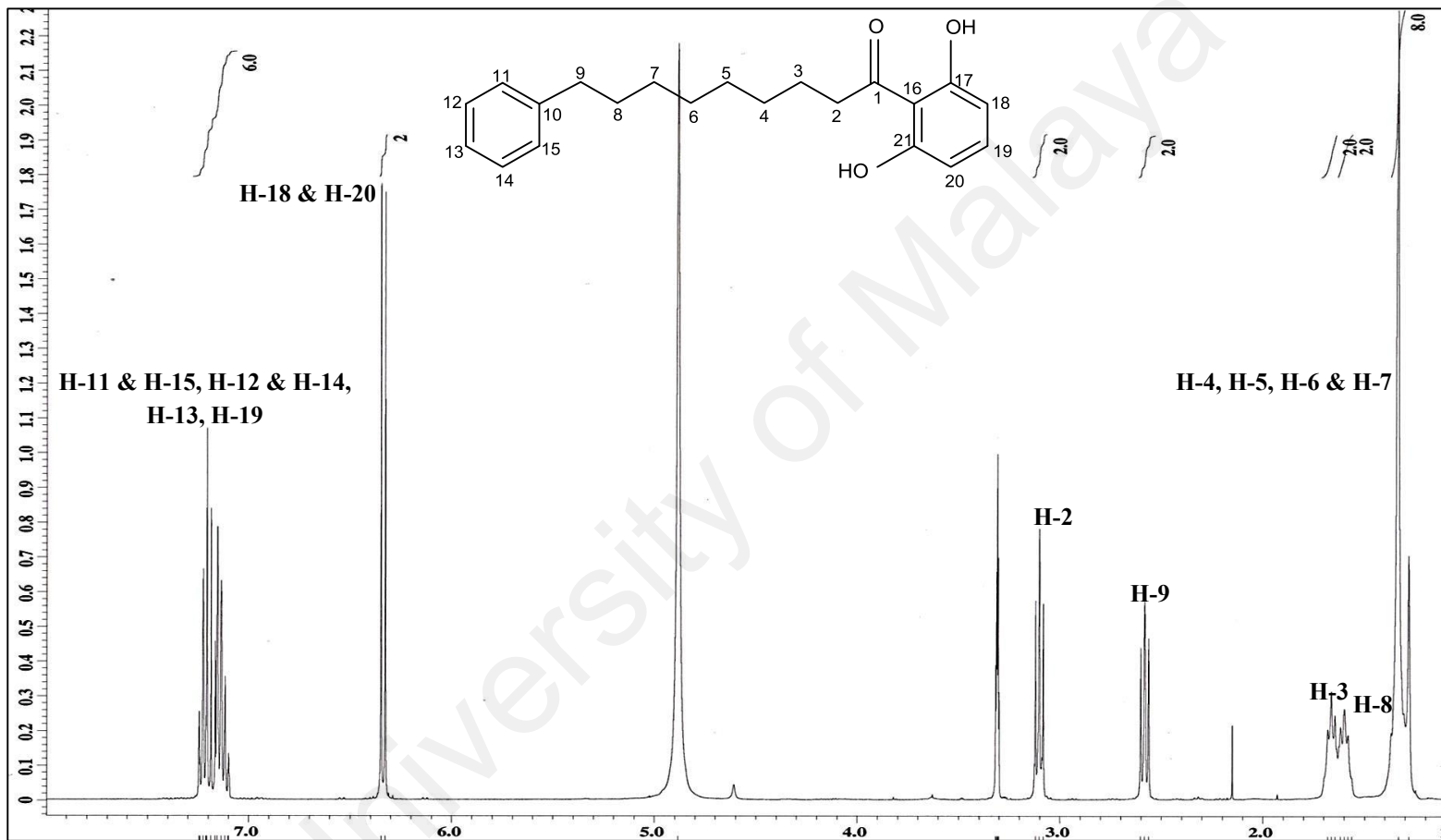


Figure 3.5: ¹H NMR spectrum of compound 1

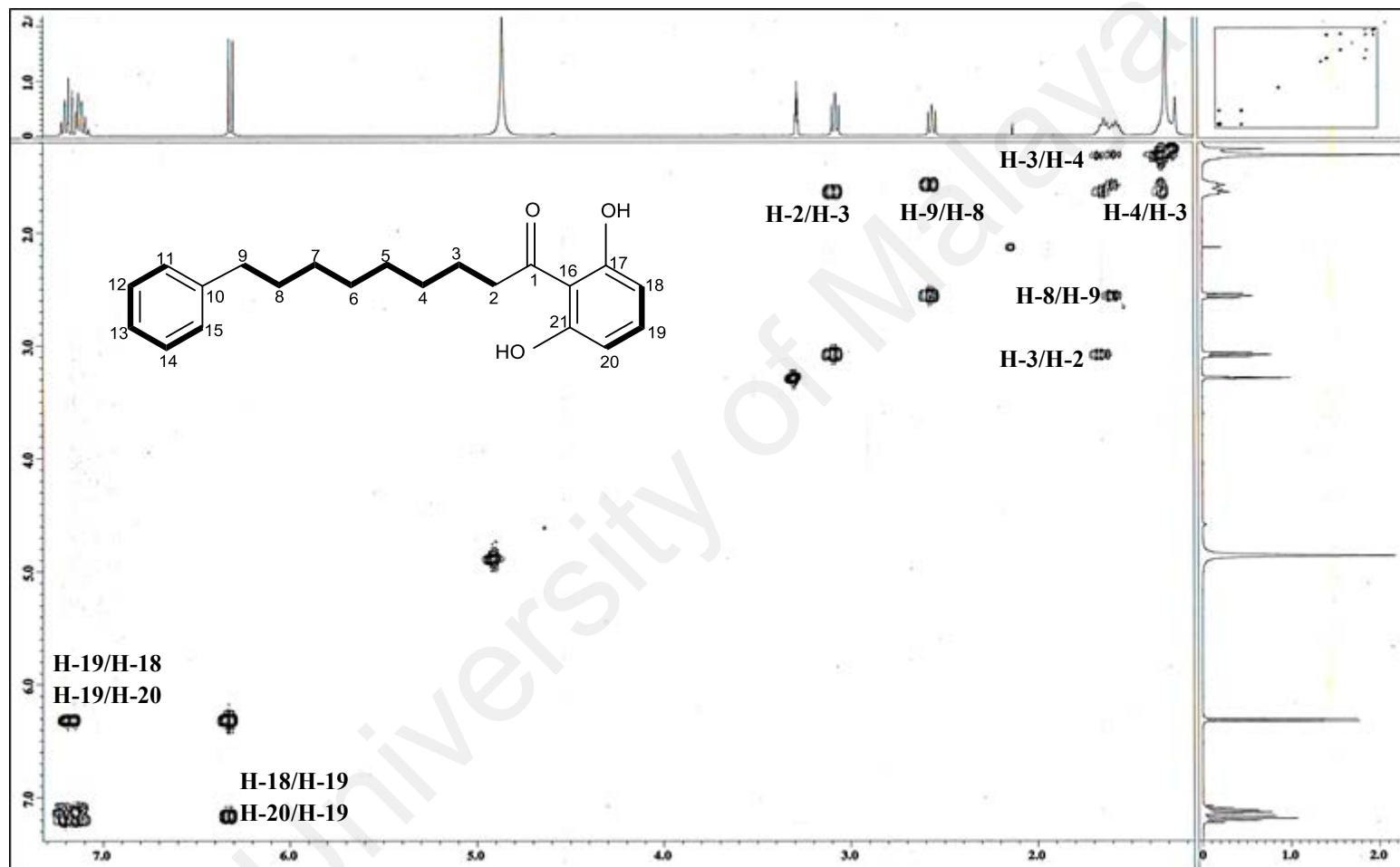


Figure 3.6: Selected COSY correlations of compound 1

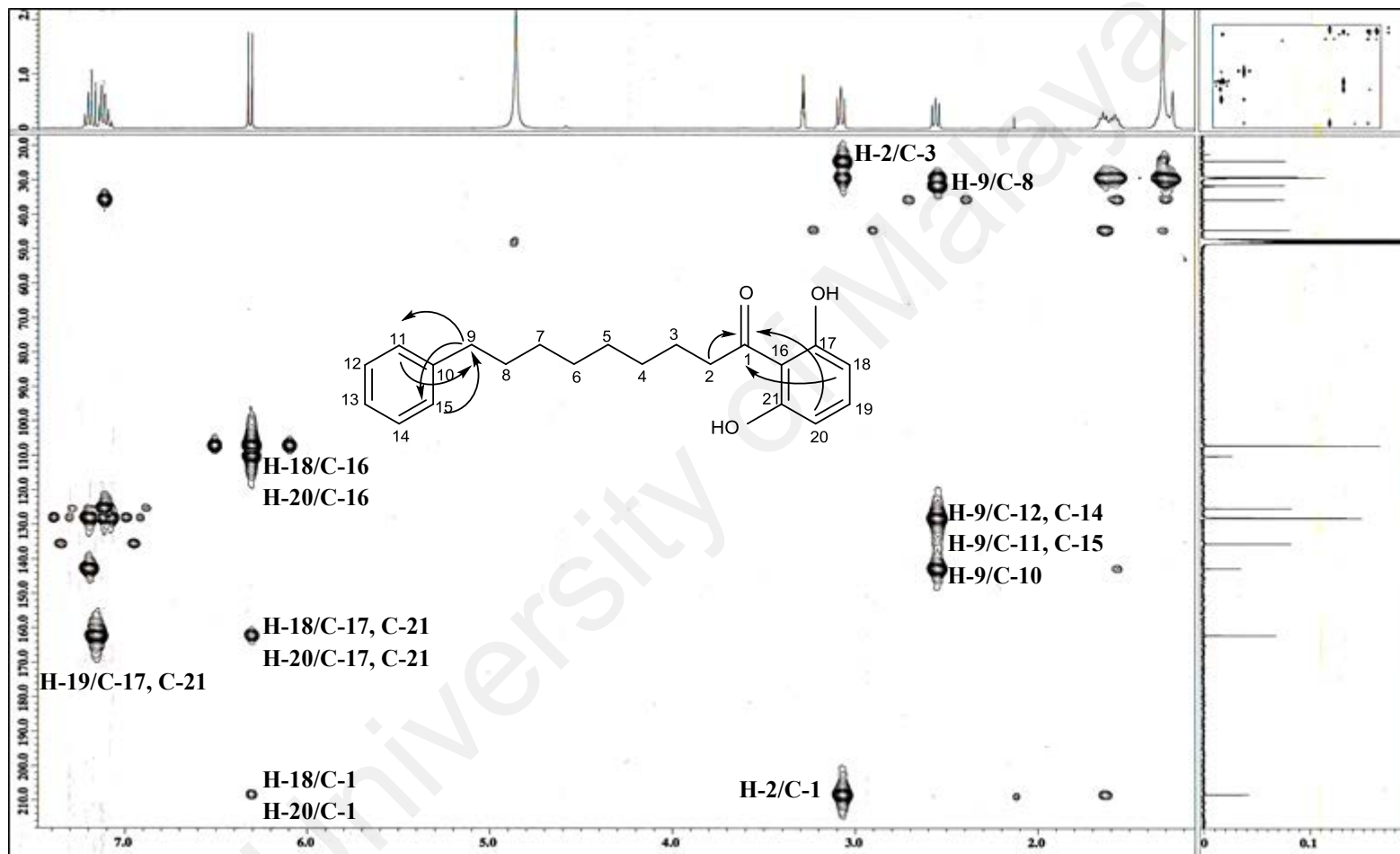


Figure 3.7: Selected HMBC correlations of compound 1

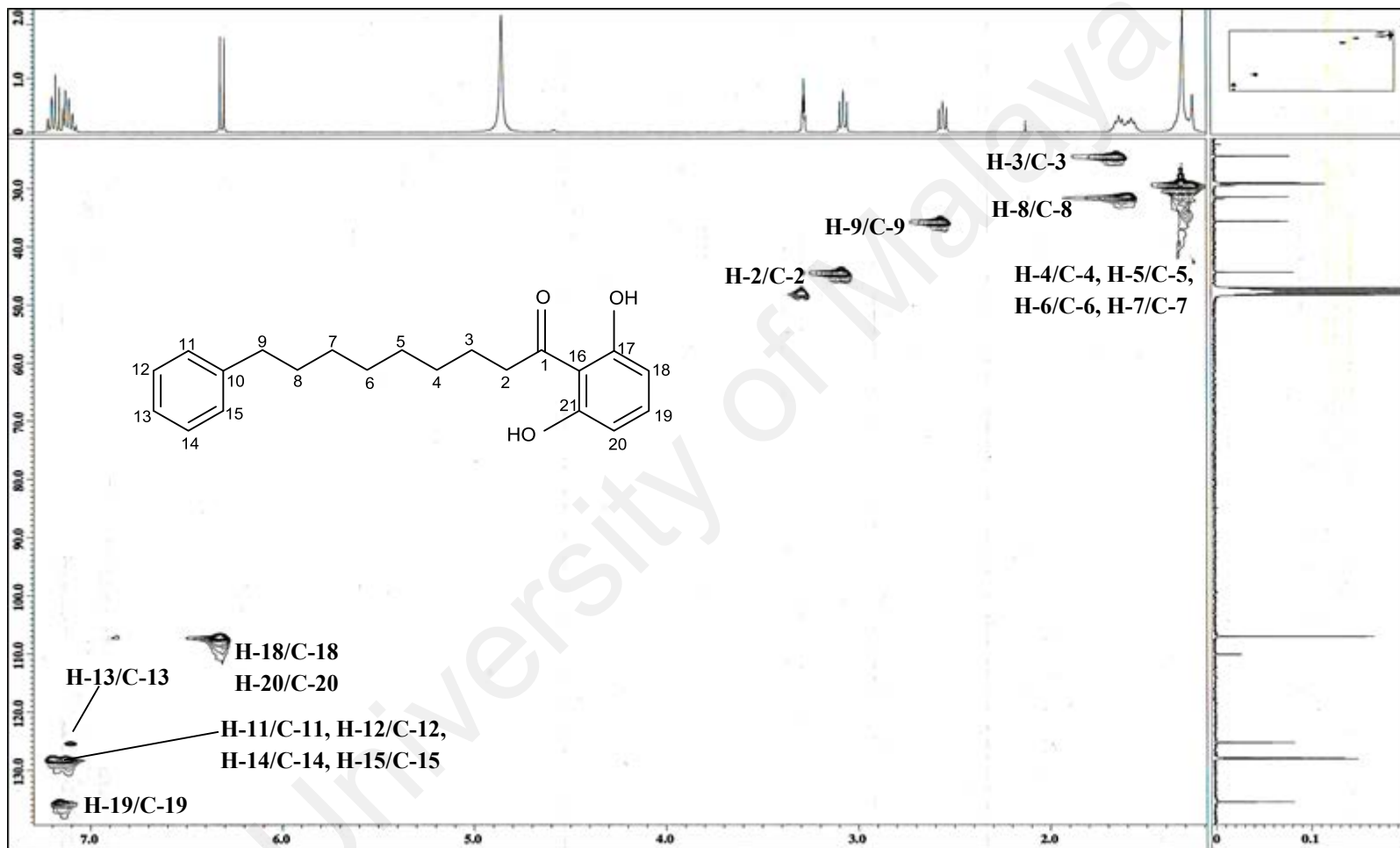


Figure 3.8: HSQC correlations of compound 1

3.1.2 Compound 2: Malabaricone B

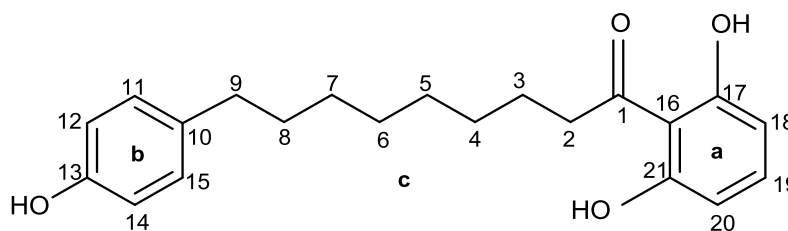


Figure 3.9: Structure of compound **2**

Compound **2** (Figure 3.9), isolated as an optically inactive yellow amorphous powder, was assigned the molecular formula $C_{21}H_{26}O_4$ with 9 degrees of unsaturation as deduced from its positive LCMS-IT-TOF analysis (Figure 3.10) $\{[M + H]^+, m/z 343.1898$ (calcd. for $C_{21}H_{27}O_4$ 343.1904) and $[M + Na]^+, m/z 365.1717$ (calcd. for $C_{21}H_{26}O_4Na$ 365.1723) $\}$.

The IR (Figure 3.11), 1H NMR (Table 3.2, Figure 3.12) and ^{13}C NMR (Table 3.2, Figure 3.13a) spectroscopic data of compound **2** were comparable to those of compound **1**, hence suggesting the possibility of compound **2** being an acylphenol which was structurally related to compound **1** (Figure 3.1). There was however a significant difference between ring **b** of compound **2** upon comparison with that of compound **1**. Unlike the latter whose ring **b** was a mono-substituted aromatic ring, the corresponding substructure in compound **2** was a 1,4-disubstituted aromatic ring with a pair of characteristic AA'BB' doublets [δ_H 6.96 ($J = 8.0$ Hz, H-11 & H-15; δ_C 130.4, C-11 & C-15) and δ_H 6.67 ($J = 8.0$ Hz, H-12 & H-14; δ_C 116.1, C-12 & C-14)]. The 30 ppm downfield shift in the resonance of the C-13 signal (δ_C 156.3) with respect to the corresponding atom in compound **1** (δ_C 126.7, Table 3.1) confirmed that it was oxygenated.

The complete assignments of the 1H NMR and ^{13}C NMR spectroscopic data of compound **2** were achieved with the aid of the COSY, HSQC and HMBC experiments (Figures 3.14-

3.16). All of the above mentioned NMR spectroscopic data of compound **2** revealed a striking resemblance to those of malabaricone B and upon comparison with literature, compound **2** was identified as malabaricone B, an acylphenol which is ubiquitous in the genus *Myristica* (Pham et al., 2000; Maia et al., 2008).

University of Malaya

Table 3.2: ^1H NMR and ^{13}C NMR spectroscopic assignments of compound **2** in methanol- d_4

Position	δ_{H} (ppm)		δ_{C} (ppm)	
	Experimental	Literature (Maia et al., 2008)	Experimental	Literature (Maia et al., 2008)
1	-	-	209.8	209.7
2	3.10 (<i>t</i> , $J = 8.0$ Hz)	3.11 (<i>t</i> , $J = 7.4$ Hz)	45.9	44.7
3	1.66 (<i>p</i> , $J = 8.0$ Hz)	1.67 (<i>p</i> , $J = 7.4$ Hz)	25.9	25.8
4	1.31 ^a (<i>brs</i>)	1.35 (<i>brs</i>)	30.7 ^b	30.3
5	1.31 ^a (<i>brs</i>)	1.35 (<i>brs</i>)	30.6 ^b	30.5
6	1.31 ^a (<i>brs</i>)	1.35 (<i>brs</i>)	30.4 ^b	30.5
7	1.31 ^a (<i>brs</i>)	1.35 (<i>brs</i>)	30.4 ^b	30.6
8	1.56 (<i>p</i> , $J = 8.0$ Hz)	1.55 (<i>p</i> , $J = 7.4$ Hz)	33.2	33.0
9	2.47 (<i>t</i> , $J = 8.0$ Hz)	2.49 (<i>t</i> , $J = 7.4$ Hz)	36.2	36.1
10	-	-	135.0	131.0
11	6.96 (<i>d</i> , $J = 8.0$ Hz)	6.97 (<i>d</i> , $J = 8.4$ Hz)	130.4	130.3
12	6.67 (<i>d</i> , $J = 8.0$ Hz)	6.69 (<i>d</i> , $J = 8.4$ Hz)	116.1	116.0
13	-	-	156.3	156.2
14	6.67 (<i>d</i> , $J = 8.0$ Hz)	6.69 (<i>d</i> , $J = 8.4$ Hz)	116.1	116.0
15	6.96 (<i>d</i> , $J = 8.0$ Hz)	6.97 (<i>d</i> , $J = 8.4$ Hz)	130.4	130.3
16	-	-	111.5	111.5
17	-	-	163.5	163.4
18	6.33 (<i>d</i> , $J = 8.0$ Hz)	6.35 (<i>d</i> , $J = 8.2$ Hz)	108.5	108.4
19	7.17 (<i>t</i> , $J = 8.0$ Hz)	7.19 (<i>t</i> , $J = 8.2$ Hz)	137.0	136.9
20	6.33 (<i>d</i> , $J = 8.0$ Hz)	6.35 (<i>d</i> , $J = 8.2$ Hz)	108.5	108.4
21	-	-	163.5	163.4

^aOverlapping signals

^bChemical shifts are interchangeable

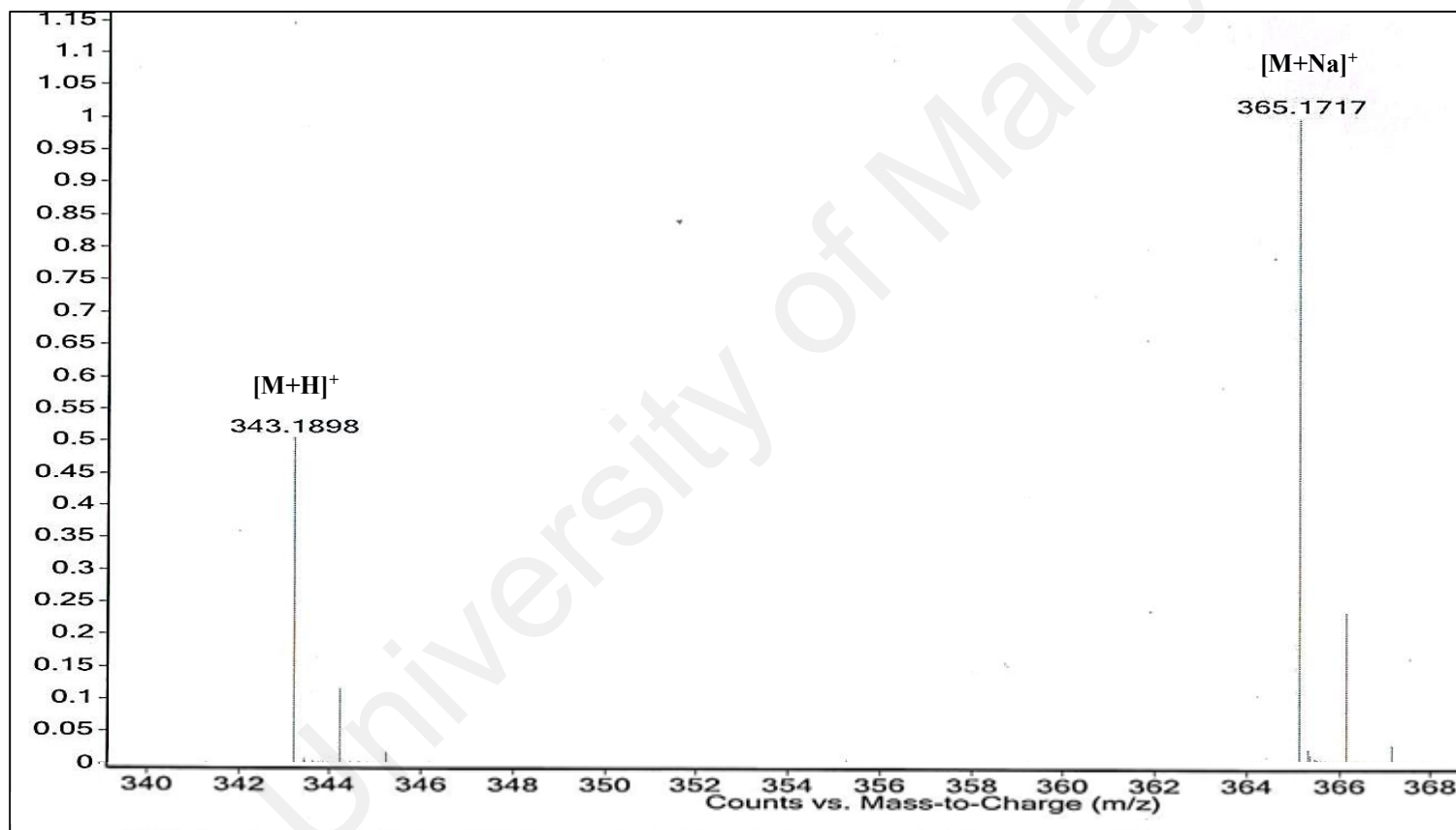


Figure 3.10: Mass spectrum of compound 2

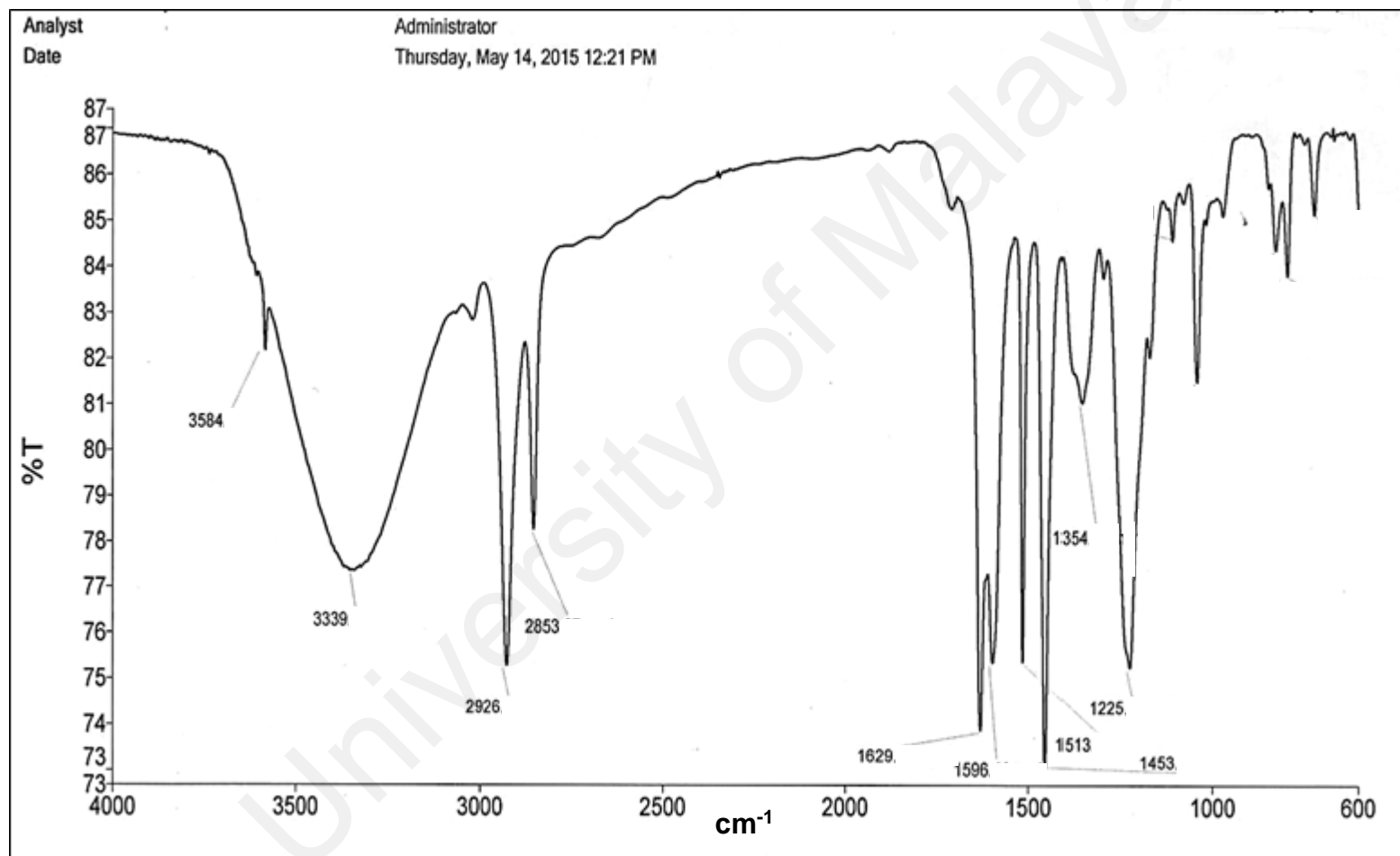


Figure 3.11: IR spectrum of compound 2

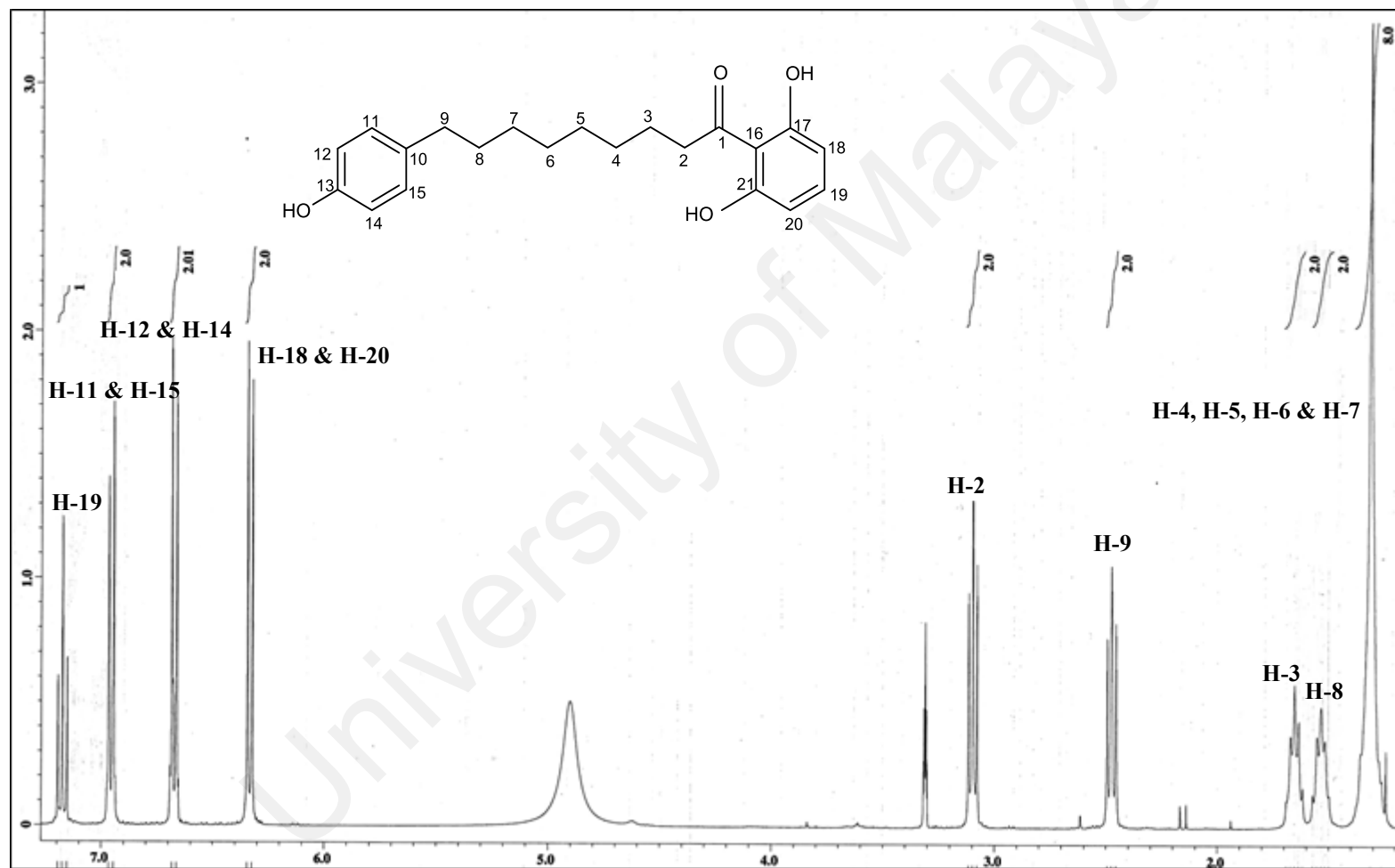


Figure 3.12: ¹H NMR spectrum of compound 2

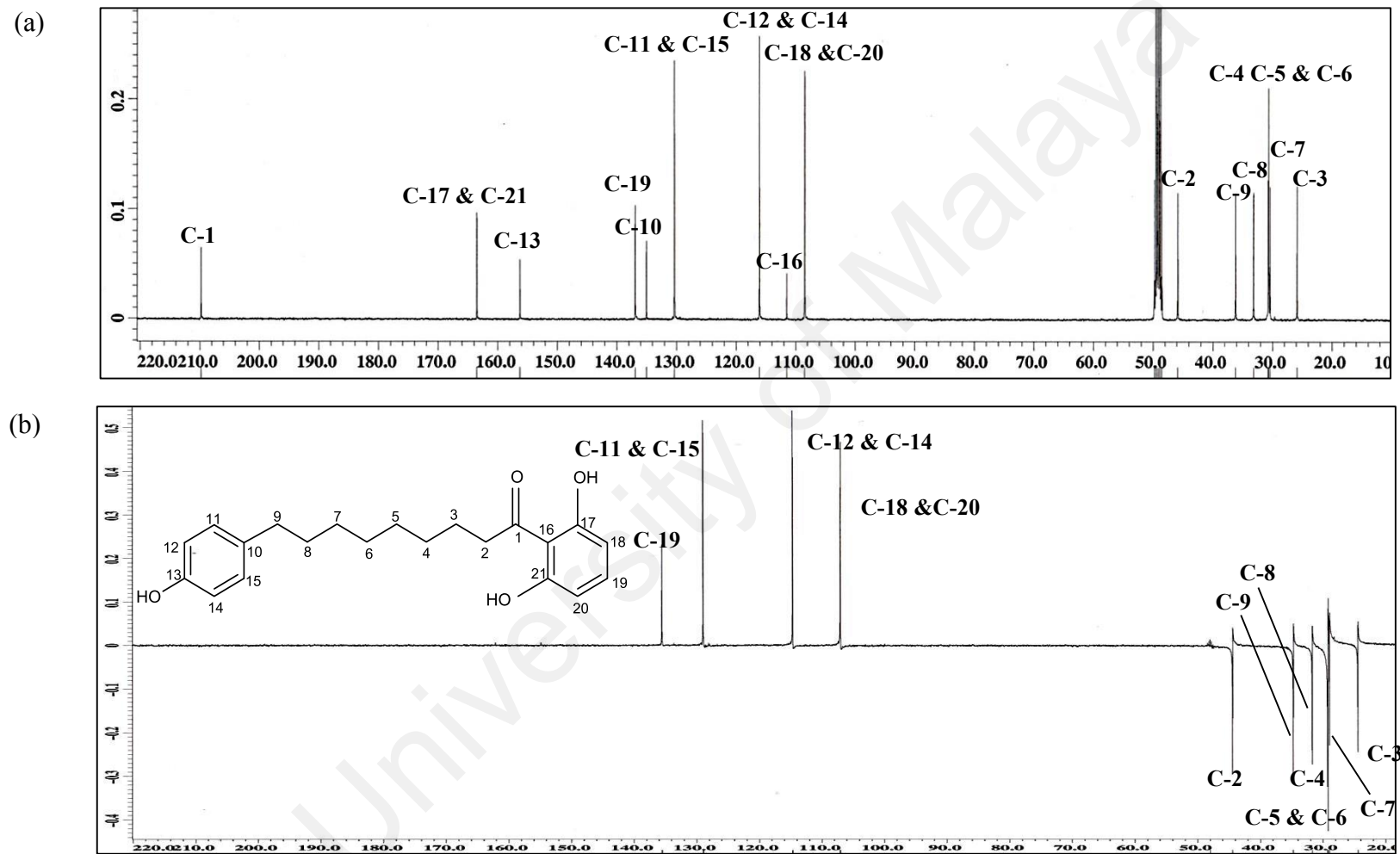


Figure 3.13: ^{13}C NMR (a) and DEPT-135 (b) spectra of compound 2

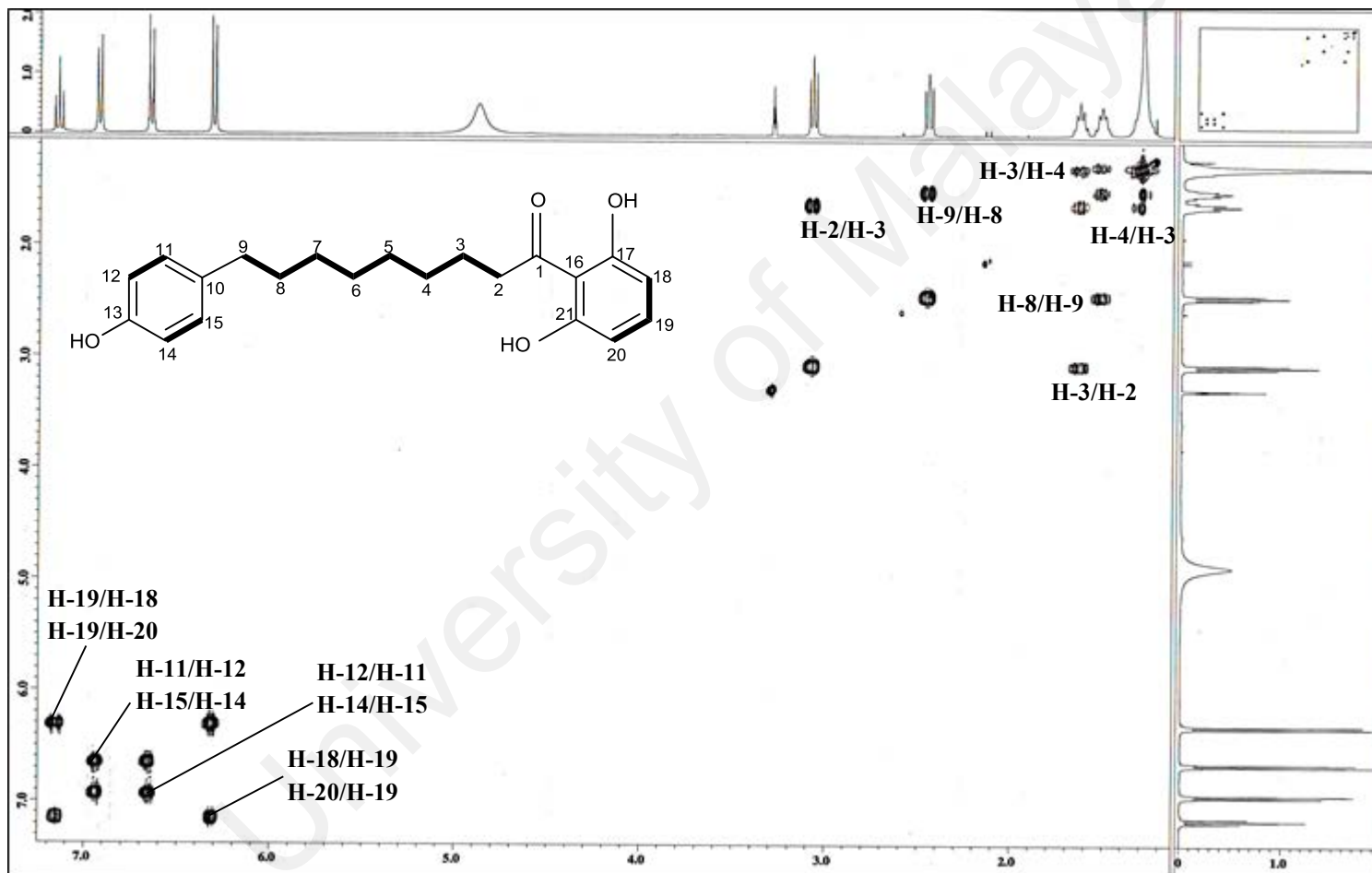


Figure 3.14: Selected COSY correlations of compound 2

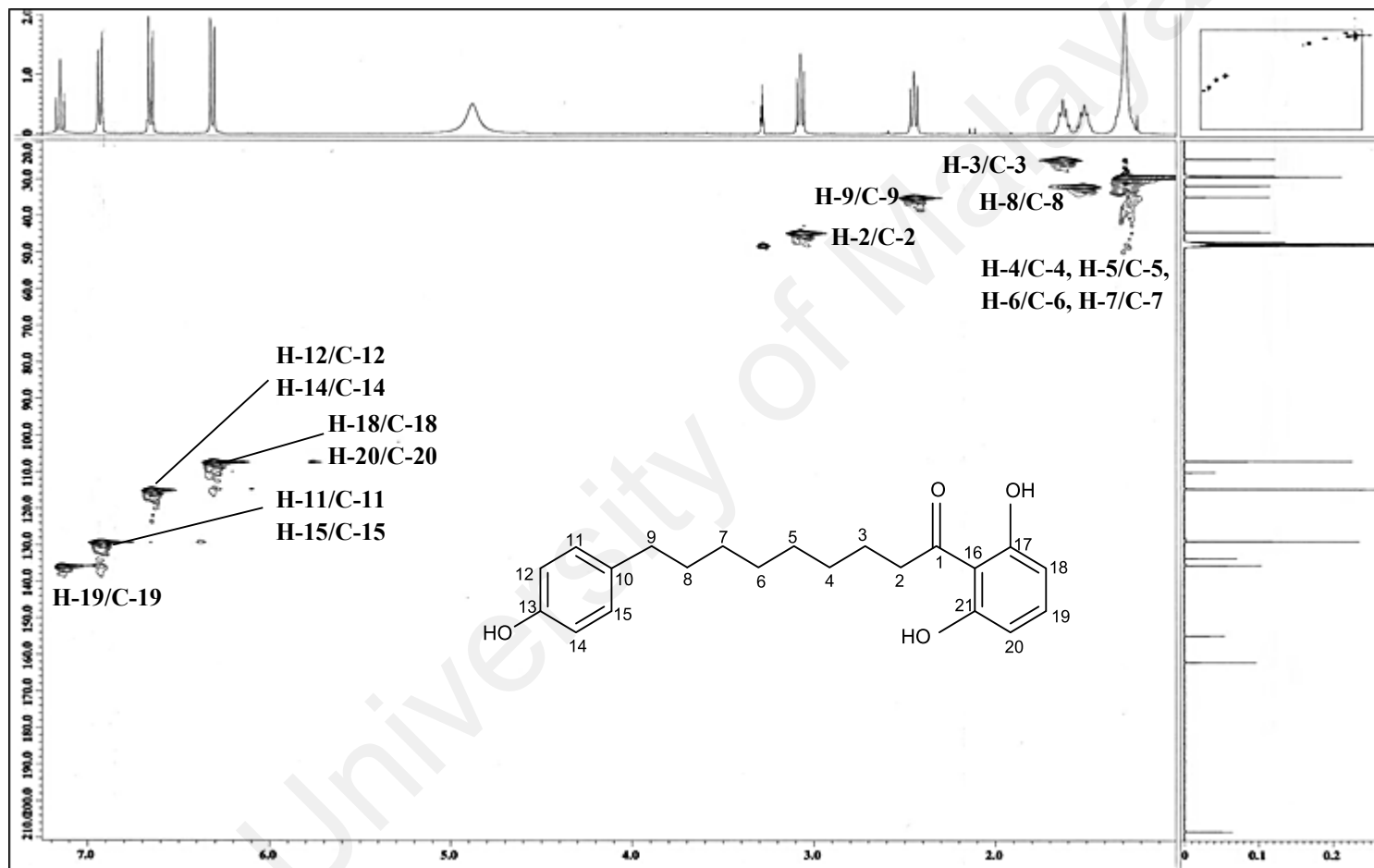


Figure 3.15: HSQC correlations of compound 2

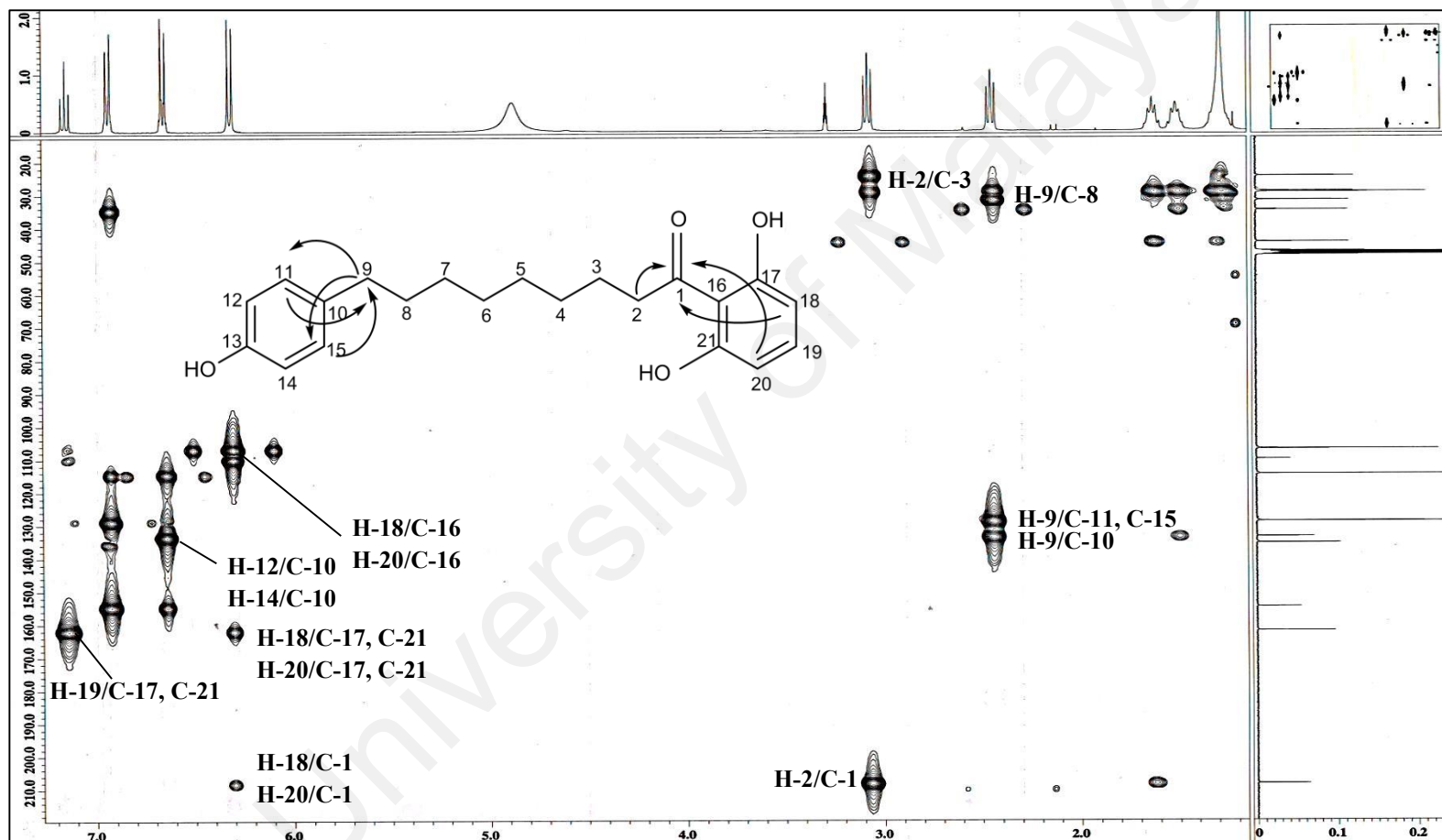


Figure 3.16: Selected HMBC correlations of compound 2

3.1.3 Compound 3: Malabaricone C

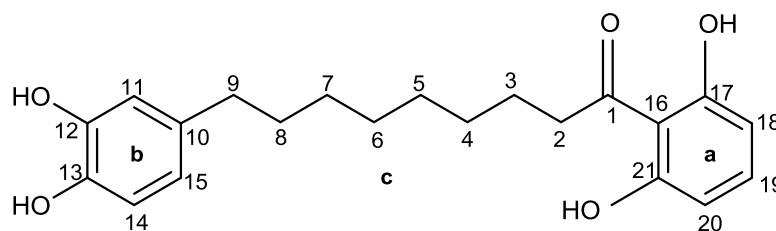


Figure 3.17: Structure of compound 3

Compound 3 (Figure 3.17) was isolated as an optically inactive yellow amorphous powder. It was assigned a molecular formula of $C_{21}H_{26}O_5$ as deduced from its positive LCMS-IT-TOF analysis (Figure 3.18) $\{[M + H]^+, m/z\ 359.1860\}$ (calcd. for $C_{21}H_{27}O_5$ 359.1853)}, corresponding to 9 degrees of unsaturation. The IR (Figure 3.19), 1H NMR (Table 3.3, Figure 3.20) and ^{13}C NMR (Table 3.3, Figure 3.21a) spectra of compound 3 were almost identical to those of compounds 1 and 2, thus supporting the fact that compound 3 was indeed an acylphenol with a structure closely resembling compounds 1 and 2. Nevertheless, there was a significant difference between ring b of compound 3 upon comparison with those of compounds 1 and 2. In contrary to the latter two compounds whose ring b was a mono-substituted aromatic ring and a 1, 4-disubstituted aromatic ring, respectively, the corresponding substructure of compound 3 was a 1, 3, 4-trisubstituted aromatic ring with a characteristic ABX spin system [δ_H 6.46 (*dd*, $J = 8.0$, 1.8 Hz, H-15; δ_C 120.8, C-15), δ_H 6.60 (*d*, $J = 1.8$ Hz, H-11; δ_C 116.6, C-11) and δ_H 6.65 (*d*, $J = 8.0$ Hz, H-14; δ_C 116.3, C-14)], with C-12 (δ_C 146.1) and C-13 (δ_C 144.1) bearing hydroxyl groups.

The complete assignments of the 1H NMR and ^{13}C NMR spectroscopic data of compound 3 were achieved with the aid of the COSY, HSQC and HMBC experiments (Figures 3.22-3.24). All of the above mentioned NMR spectroscopic data of compound 3 revealed a

striking resemblance to those of malabaricone C and upon comparison with literature, compound **3** was confirmed to be malabaricone C, an acylphenol which is ubiquitous in the genus *Myristica* (Pham et al., 2000; Maia et al., 2008).

University of Malaya

Table 3.3: ^1H NMR and ^{13}C NMR spectroscopic assignments of compound **3** in methanol- d_4

Position	δ_{H} (ppm)		δ_{C} (ppm)	
	Experimental	Literature (Maia et al., 2008)	Experimental	Literature (Maia et al., 2008)
1	-	-	209.8	209.7
2	3.10 (<i>t</i> , $J = 8.0$ Hz)	3.12 (<i>t</i> , $J = 7.4$ Hz)	45.9	45.8
3	1.65 (<i>p</i> , $J = 8.0$ Hz)	1.67 (<i>p</i> , $J = 7.4$ Hz)	25.9	25.8
4	1.31 ^a (<i>brs</i>)	1.36 (<i>brs</i>)	30.7 ^b	30.5
5	1.31 ^a (<i>brs</i>)	1.36 (<i>brs</i>)	30.5 ^b	30.6
6	1.31 ^a (<i>brs</i>)	1.36 (<i>brs</i>)	30.5 ^b	30.6
7	1.31 ^a (<i>brs</i>)	1.36 (<i>brs</i>)	30.4 ^b	30.3
8	1.53 (<i>brt</i> , $J = 8.0$ Hz)	1.56 (<i>m</i>)	33.1	32.9
9	2.43 (<i>t</i> , $J = 8.0$ Hz)	2.45 (<i>t</i> , $J = 8.0$ Hz)	36.4	36.3
10	-	-	136.0	135.8
11	6.60 (<i>d</i> , $J = 1.8$ Hz)	6.62 (<i>d</i> , $J = 2.0$ Hz)	116.6	116.6
12	-	-	146.1	146.0
13	-	-	144.1	144.0
14	6.65 (<i>d</i> , $J = 8.0$ Hz)	6.67 (<i>d</i> , $J = 8.0$ Hz)	116.3	116.2
15	6.46 (<i>dd</i> , $J = 8.0, 1.8$ Hz)	6.48 (<i>dd</i> , $J = 8.0, 2.0$ Hz)	120.8	120.7
16	-	-	111.5	111.5
17	-	-	163.5	163.4
18	6.33 (<i>d</i> , $J = 8.0$ Hz)	6.35 (<i>d</i> , $J = 8.0$ Hz)	108.5	108.4
19	7.17 (<i>t</i> , $J = 8.0$ Hz)	7.20 (<i>t</i> , $J = 8.0$ Hz)	137.0	136.8
20	6.33 (<i>d</i> , $J = 8.0$ Hz)	6.35 (<i>d</i> , $J = 8.0$ Hz)	108.5	108.4
21	-	-	163.5	163.4

^a Overlapping signals

^b Chemical shifts are interchangeable

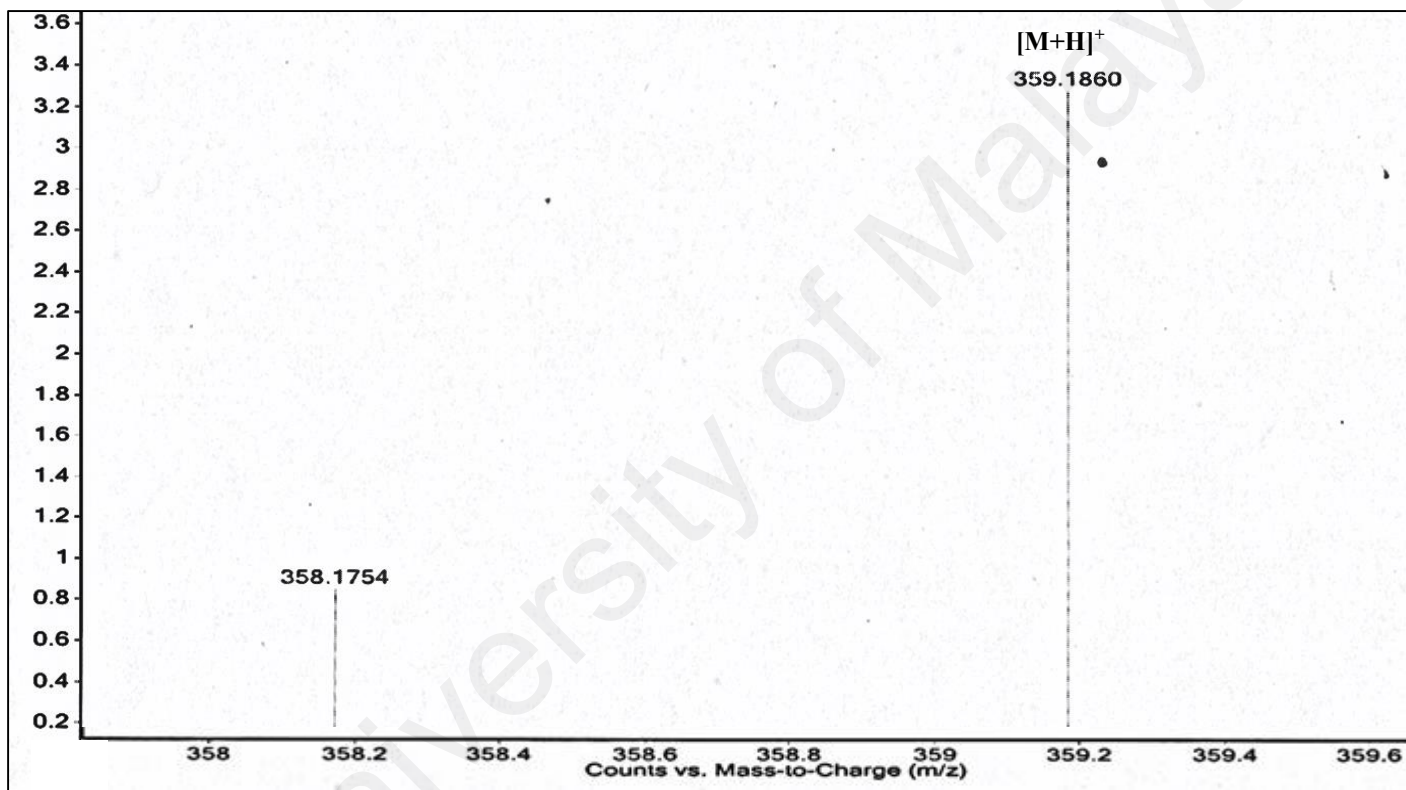


Figure 3.18: Mass spectrum of compound 3

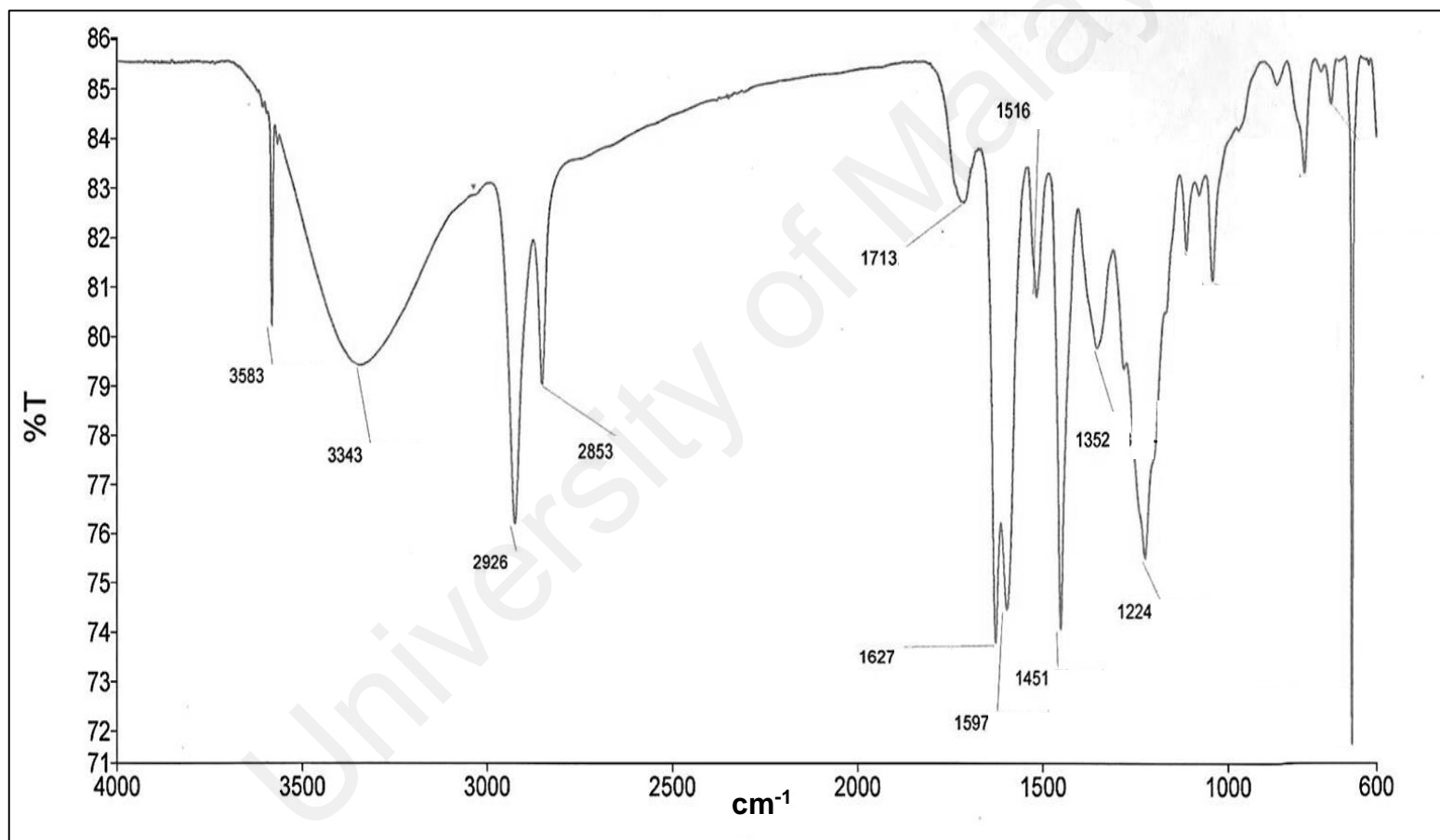


Figure 3.19: IR spectrum of compound 3

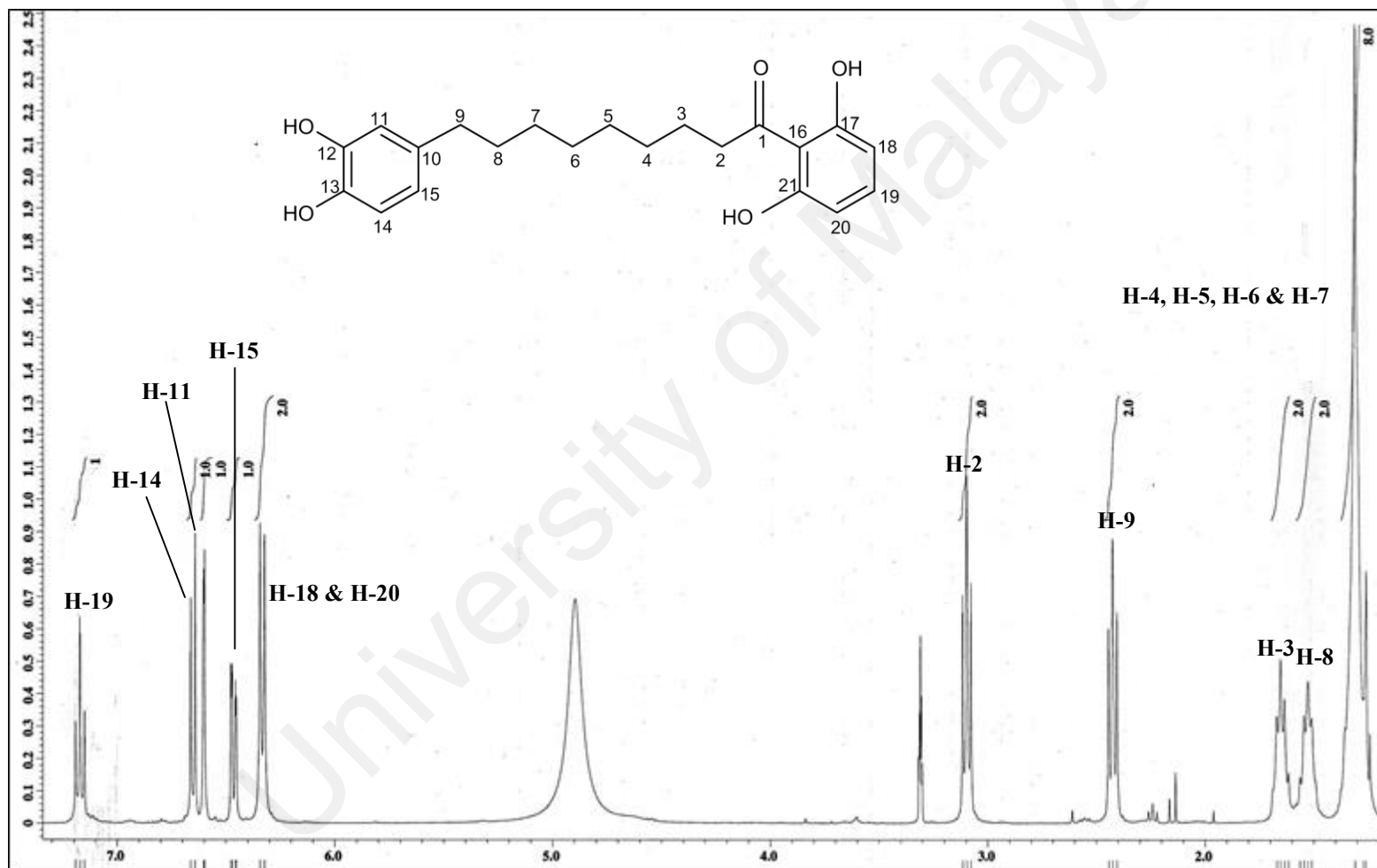


Figure 3.20: ¹H NMR spectrum of compound 3

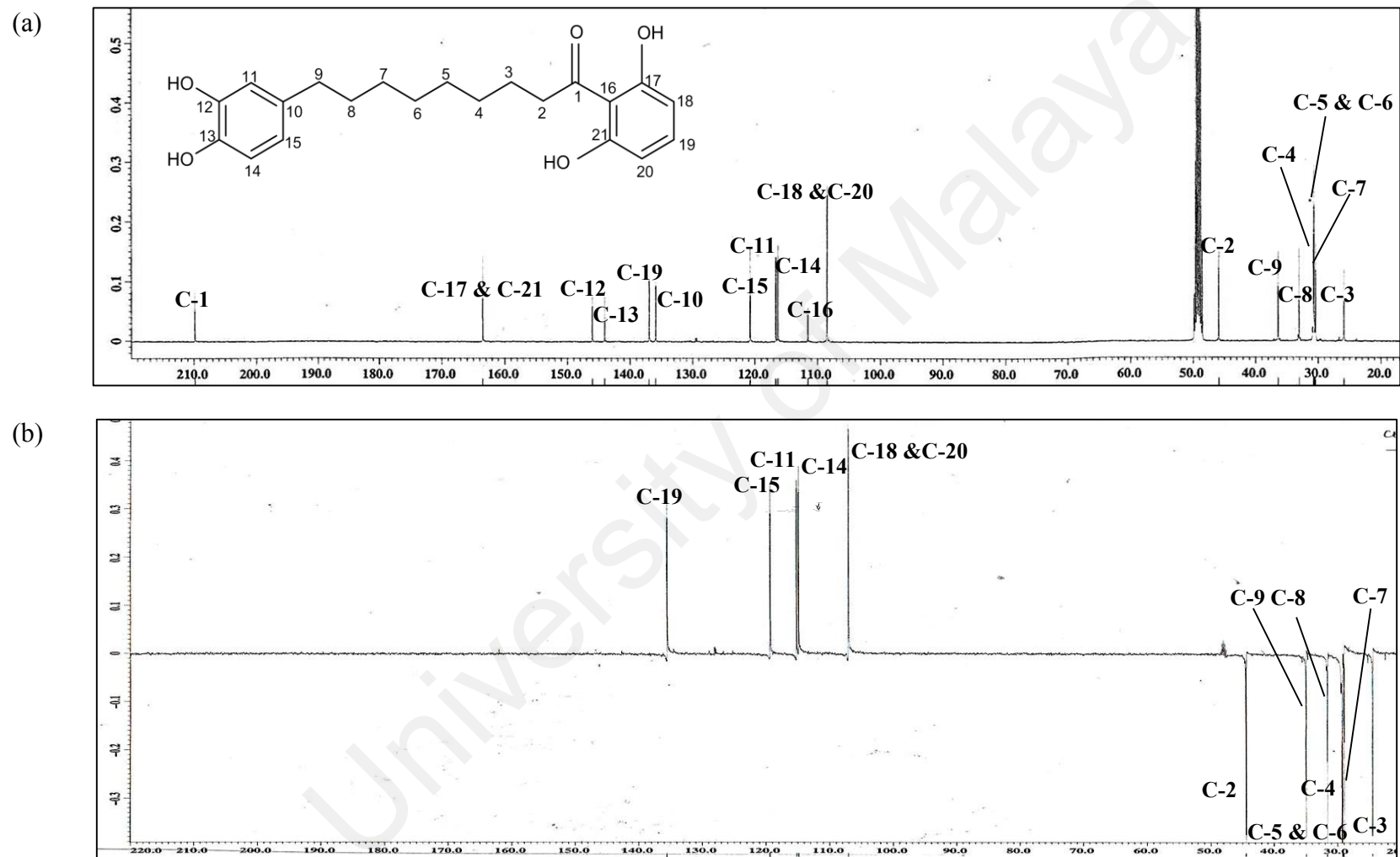


Figure 3.21: ^{13}C NMR (a) and DEPT-135 (b) spectra of compound **3**

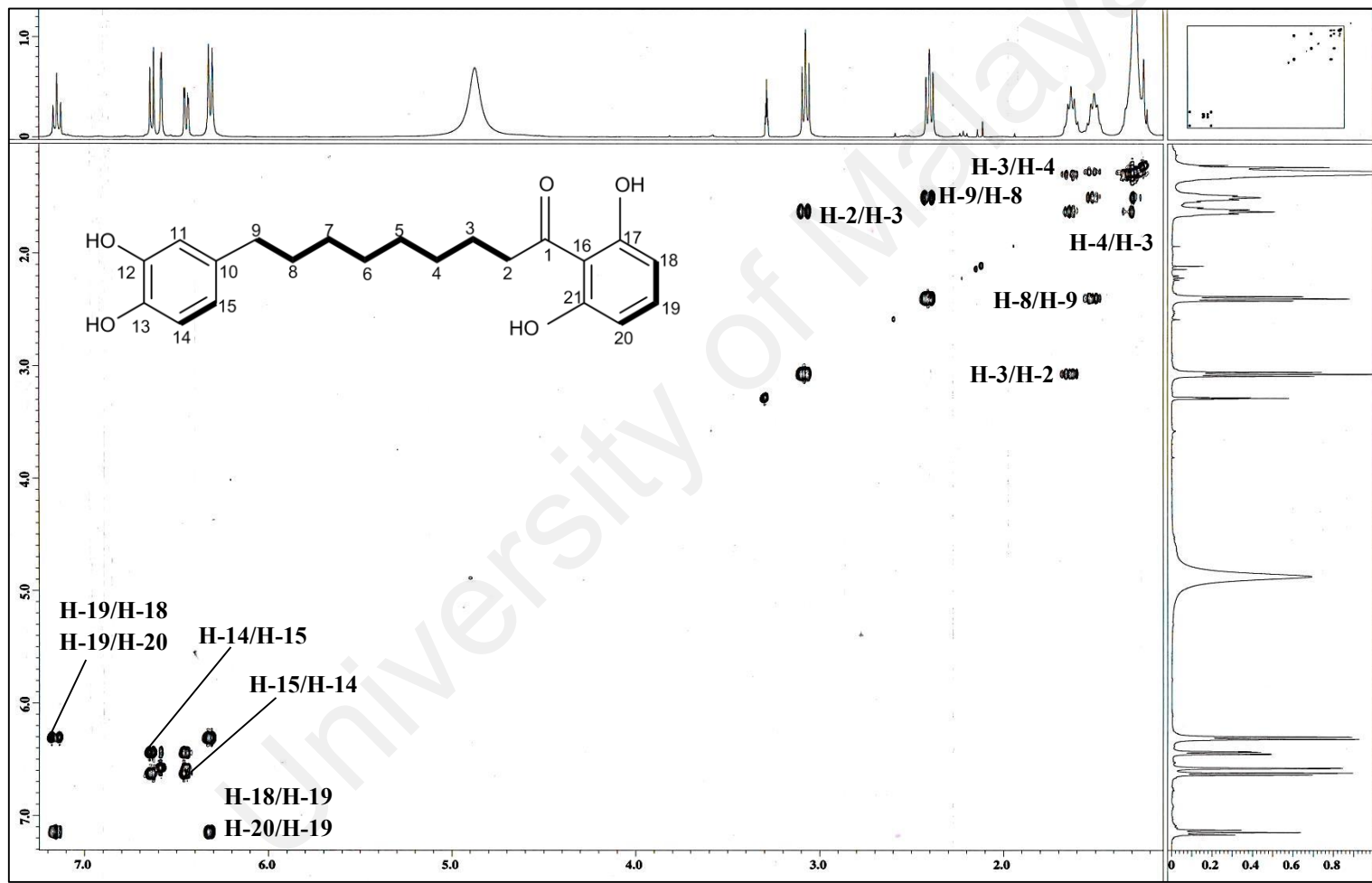


Figure 3.22: Selected COSY correlations of compound 3

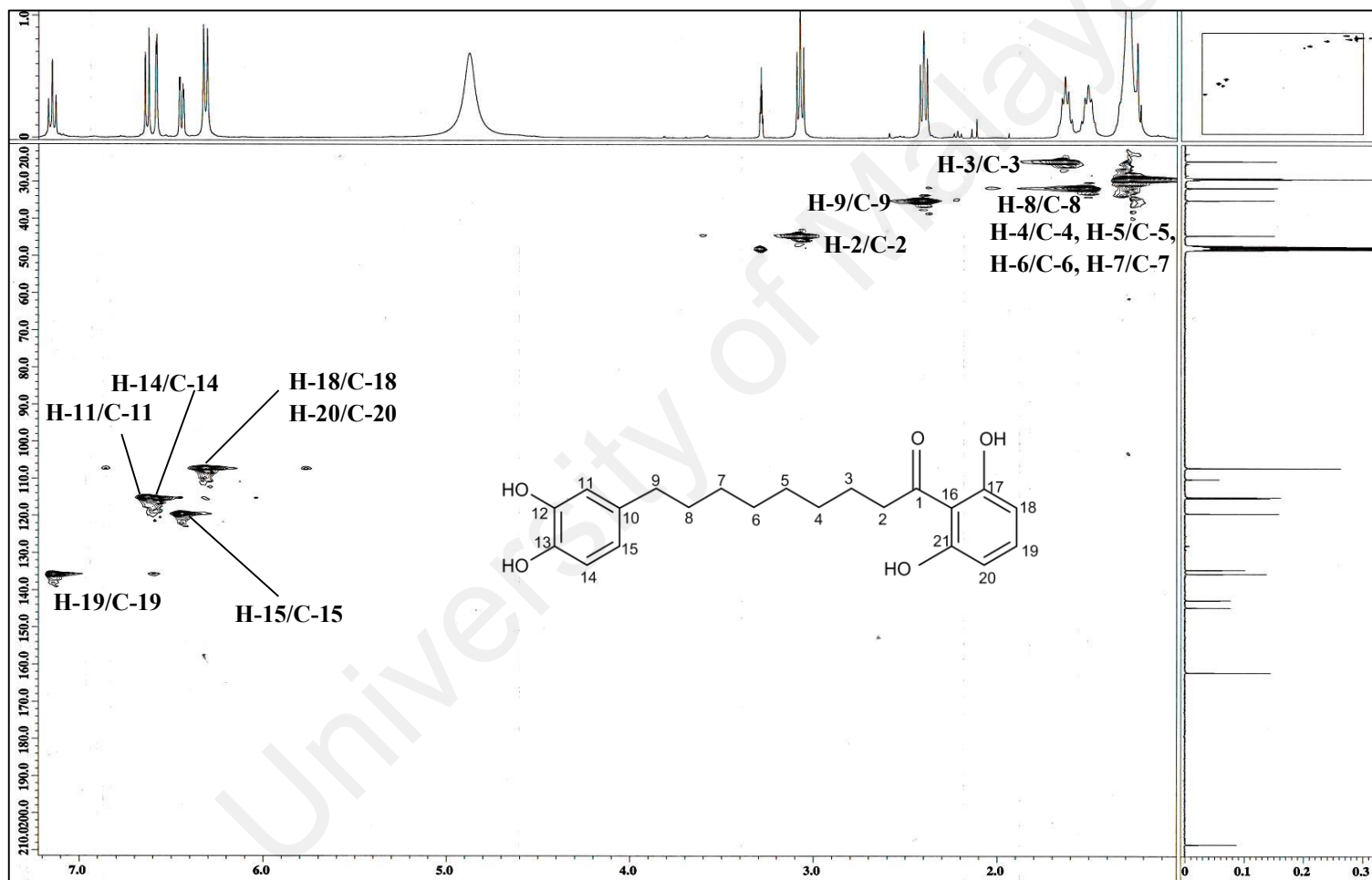


Figure 3.23: HSQC correlations of compound 3

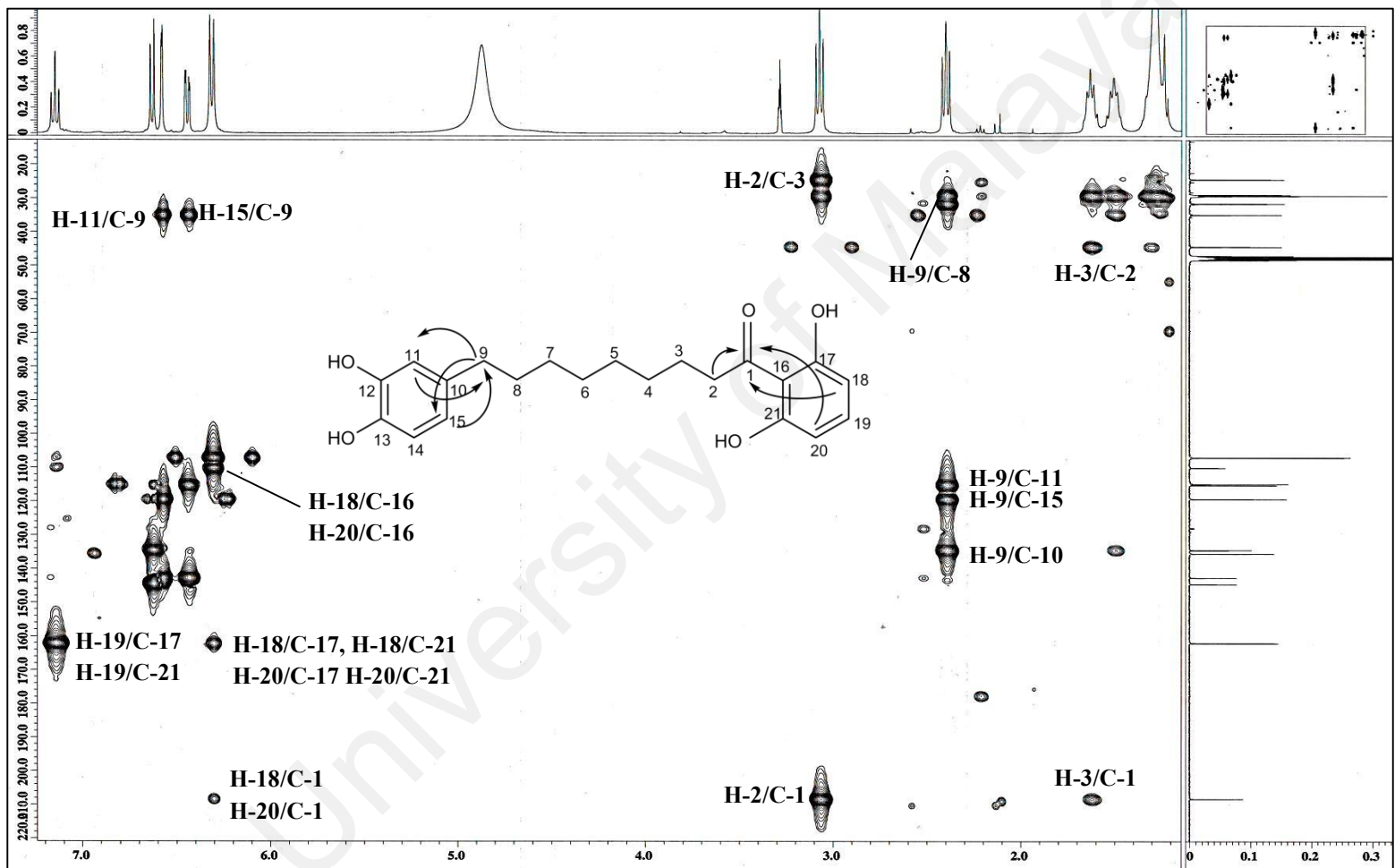


Figure 3.24: Selected HMBC correlations of compound 3

3.1.4 Compound 72: Malabaricone E

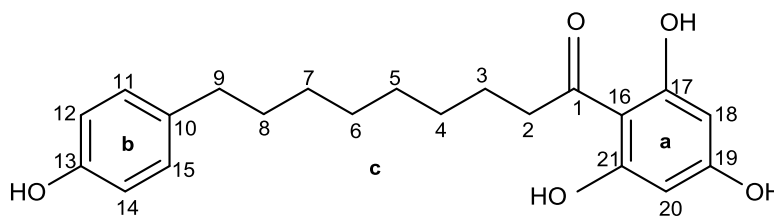


Figure 3.25: Structure of compound 72

Compound **72** (Figure 3.25) was obtained as an optically inactive pale yellow amorphous powder. Its molecular formula was established as $C_{21}H_{26}O_5$ by LCMS-IT-TOF analysis (Figure 3.26) $\{[M + Na]^+, m/z 381.1675 \text{ (calcd. for } C_{21}H_{26}O_5Na \text{ 381.1672)}\}$. The IR (Figure 3.27), 1H NMR (Table 3.4, Figure 3.28) and ^{13}C NMR (Table 3.4, Figure 3.29a) spectra of compound **72** were almost superimposable with those of compound **2** with the only difference being in its ring a which was a 1, 2, 3, 5-tetrasubstituted symmetrical aromatic ring with a two proton system forming a singlet at δ_H 5.80 (H-18 & H-20; δ_C 95.8, C-18 & C-20) instead of a 1, 2, 3-trisubstituted symmetrical aromatic ring as in compound **2**. The absence of the H-18/H-19 and H-19/H-20 homonuclear couplings in addition to the large downfield shift (~ 30 ppm) in the carbon resonance of C-19 (δ_C 166.5) upon comparison to the corresponding atom in compound **2** (δ_C 137.0, Table 3.2) provided evidence that C-19 was oxygenated.

The complete assignments of the 1H NMR and ^{13}C NMR spectroscopic data of compound **72** were achieved with the aid of the COSY, HSQC and HMBC experiments (Figures 3.30-3.32). Compound **72** was established as 1-(2, 4, 6-trihydroxyphenyl)-9-(4-hydroxyphenyl)-nonanone or trivially named as malabaricone E, a new acylphenol since a survey of literature indicated that this compound has never before been isolated from a plant (Abdul Wahab et al., 2016).

The biosynthetic pathway for the formation of malabaricone E (**72**) presumably resulted from the elongation of a cinnamoyl type precursor, originating from a molecule of tyrosine by six acetate (malonate) units to form **I**. Reduction of the first three acetate units and the cyclisation of the last three acetate units of **I** into a triketonic cyclohexane ring according to the phloroglucinol type cyclisation generated **II** following which the enolisation of the ketones in the ring led to the formation of malabaricone E (Scheme 3.1) (Abdul Wahab et al., 2016; Pham et al., 2000).

University of Malaya

Table 3.4: ^1H NMR and ^{13}C NMR spectroscopic assignments of compound **72** in methanol- d_4 (Abdul Wahab et al., 2016)

Position	δ_{H} (ppm)	δ_{C} (ppm)
1	-	207.6
2	3.02 (<i>t</i> , $J = 8.0$ Hz)	44.9
3	1.64 (<i>p</i> , $J = 8.0$ Hz)	26.3
4	1.33 ^a (<i>brs</i>)	30.9 ^b
5	1.33 ^a (<i>brs</i>)	30.6 ^b
6	1.33 ^a (<i>brs</i>)	30.6 ^b
7	1.33 ^a (<i>brs</i>)	30.4 ^b
8	1.55 (<i>brt</i> , $J = 8.0$ Hz)	33.2
9	2.50 (<i>t</i> , $J = 8.0$ Hz)	36.2
10	-	135.0
11	6.97 (<i>d</i> , $J = 8.0$ Hz)	130.3
12	6.67 (<i>d</i> , $J = 8.0$ Hz)	116.1
13	-	156.3
14	6.67 (<i>d</i> , $J = 8.0$ Hz)	116.1
15	6.97 (<i>d</i> , $J = 8.0$ Hz)	130.3
16	-	105.0
17	-	165.9
18	5.80 (<i>s</i>)	95.8
19	-	166.5
20	5.80 (<i>s</i>)	95.8
21	-	165.9

^a Overlapping signals

^b Chemical shifts are interchangeable

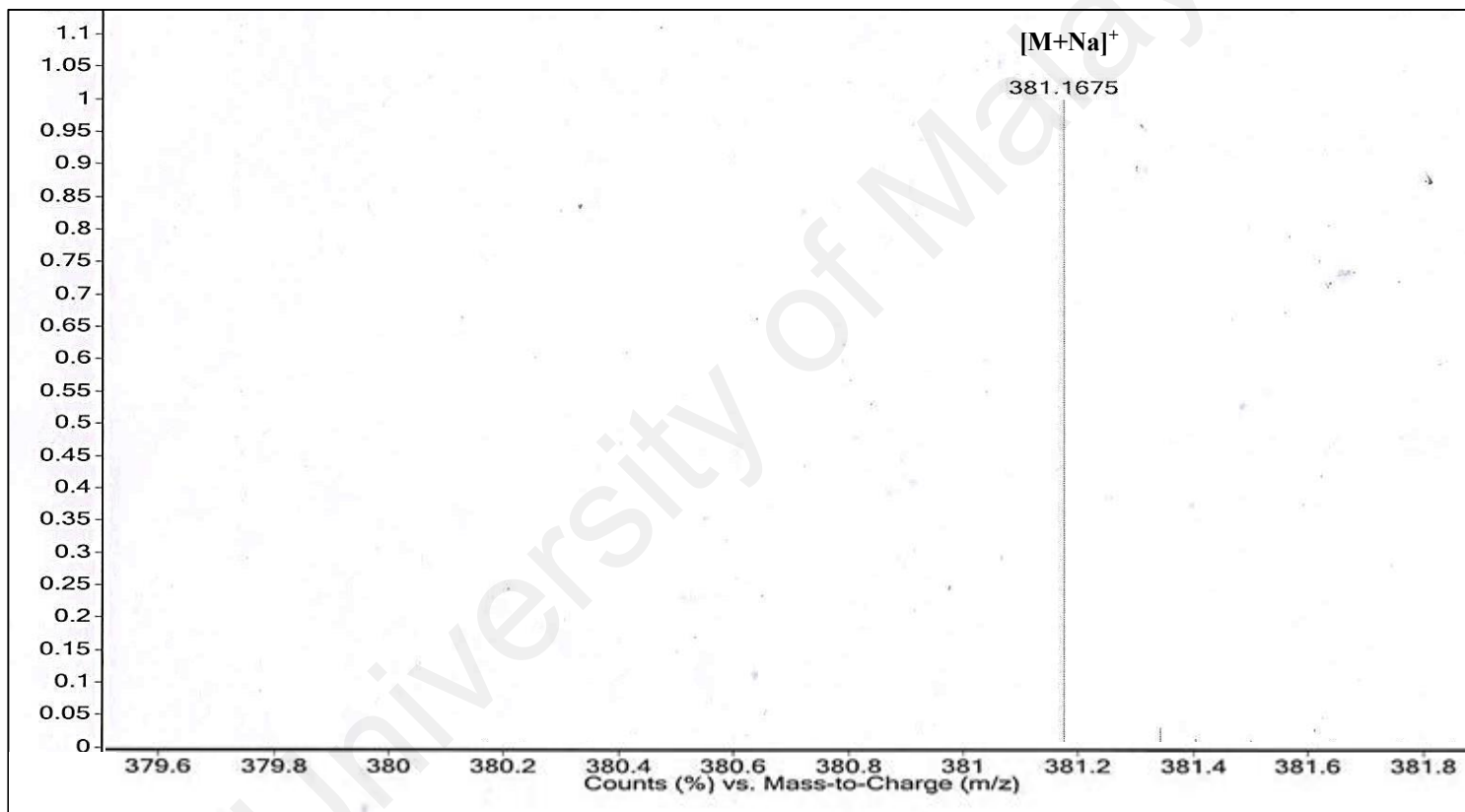


Figure 3.26: Mass spectrum of compound 72

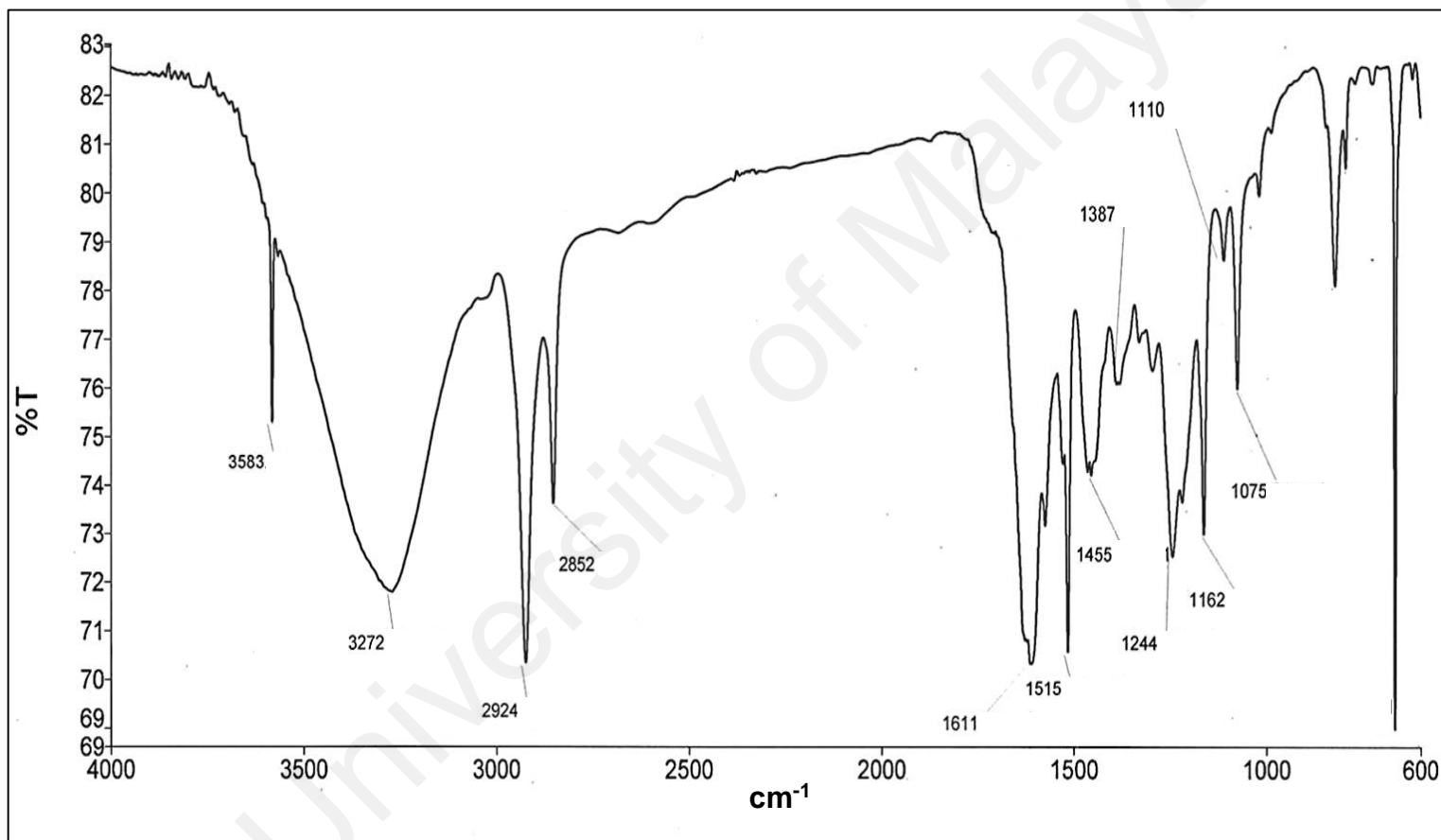


Figure 3.27: IR spectrum of compound 72

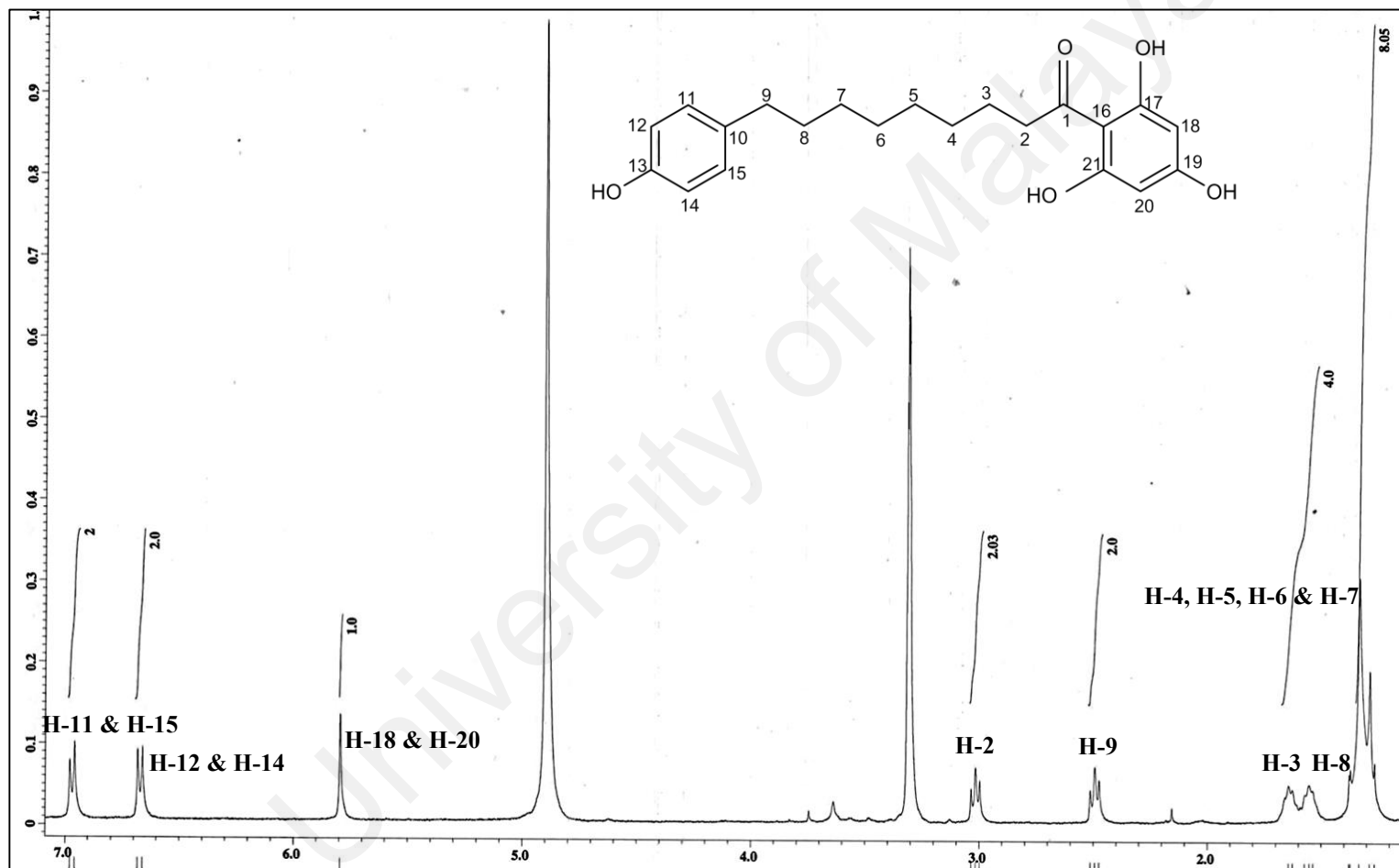
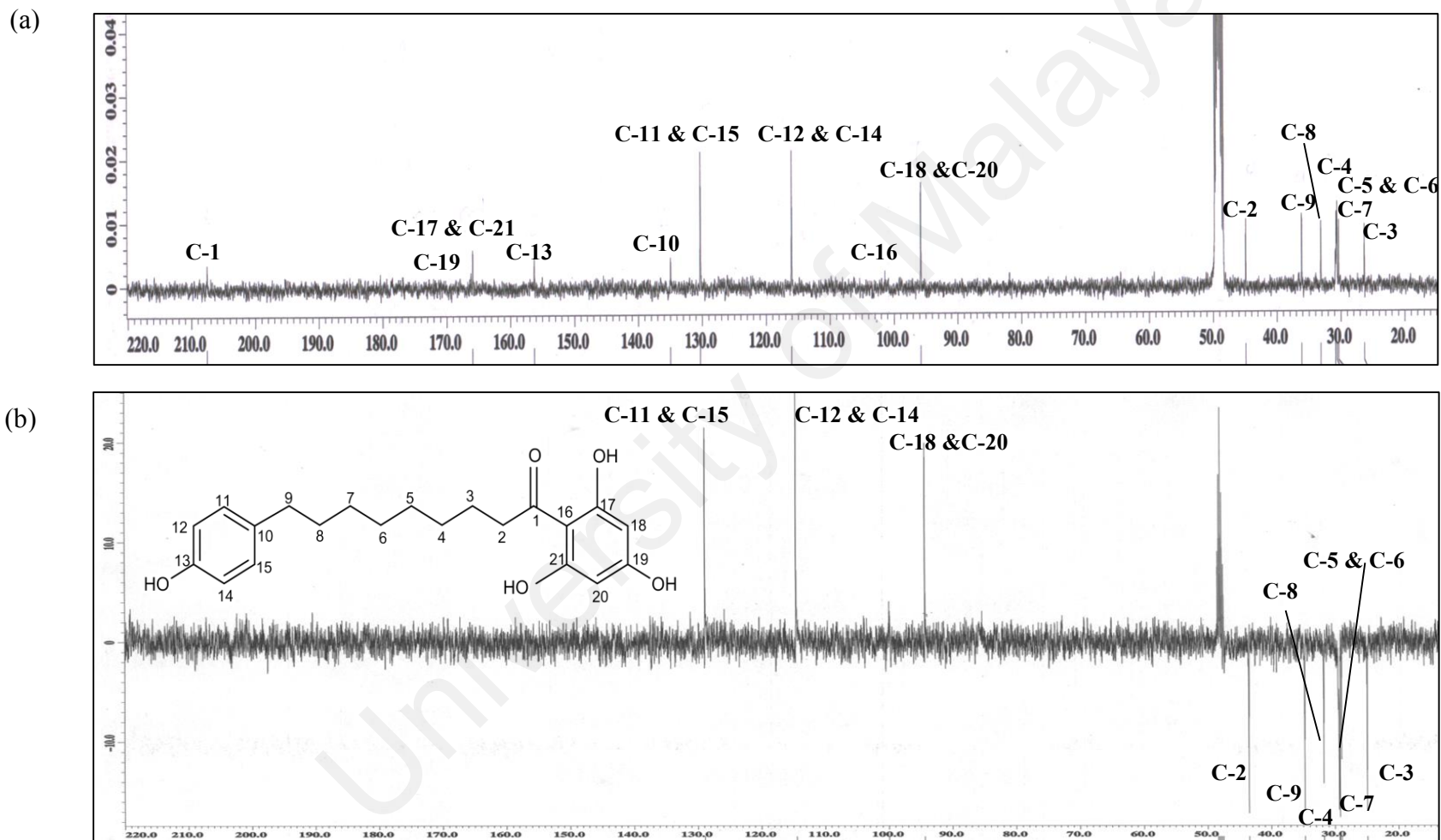


Figure 3.28: ¹H NMR spectrum of compound 72



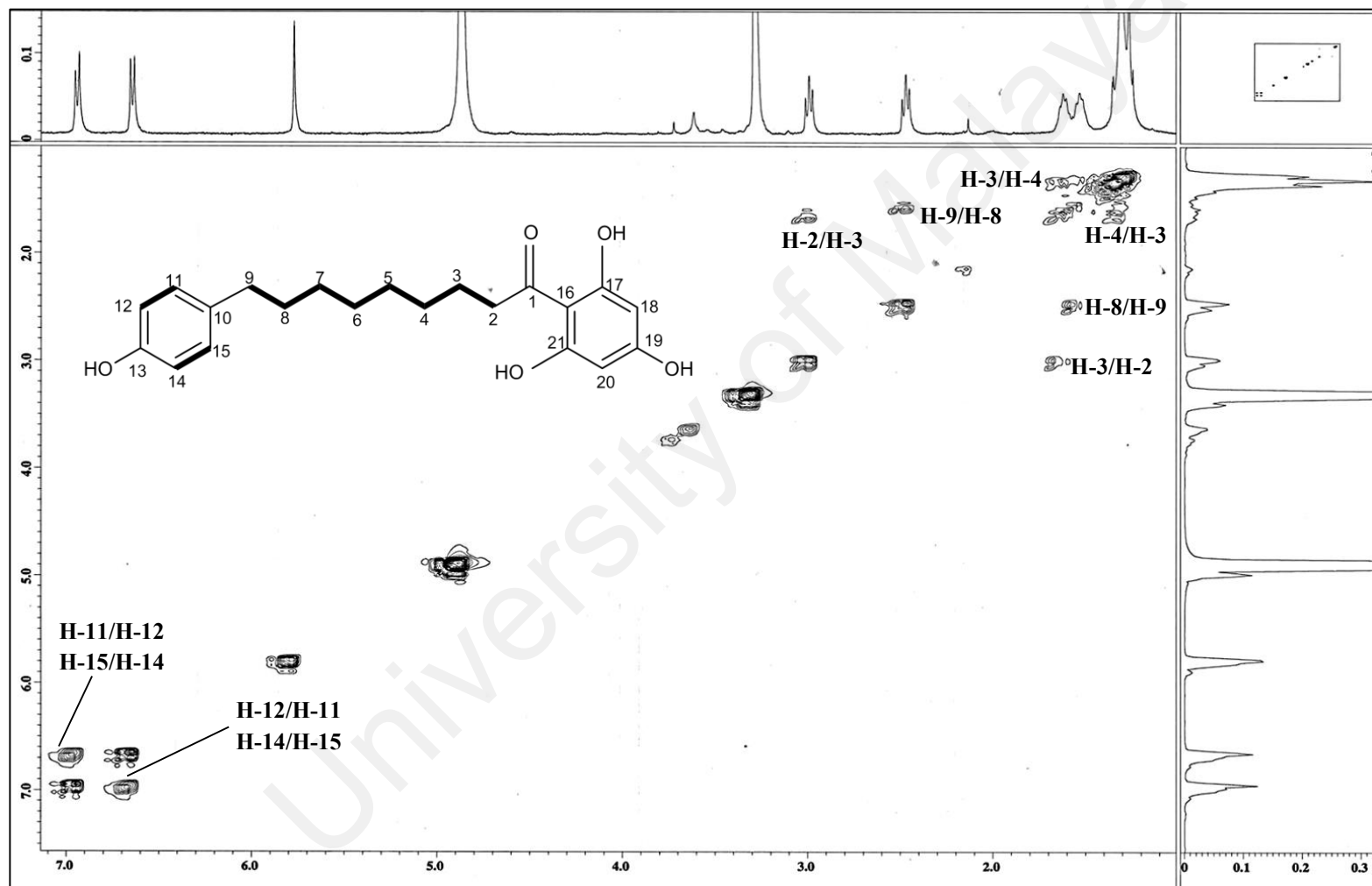


Figure 3.30: Selected COSY correlations of compound 72

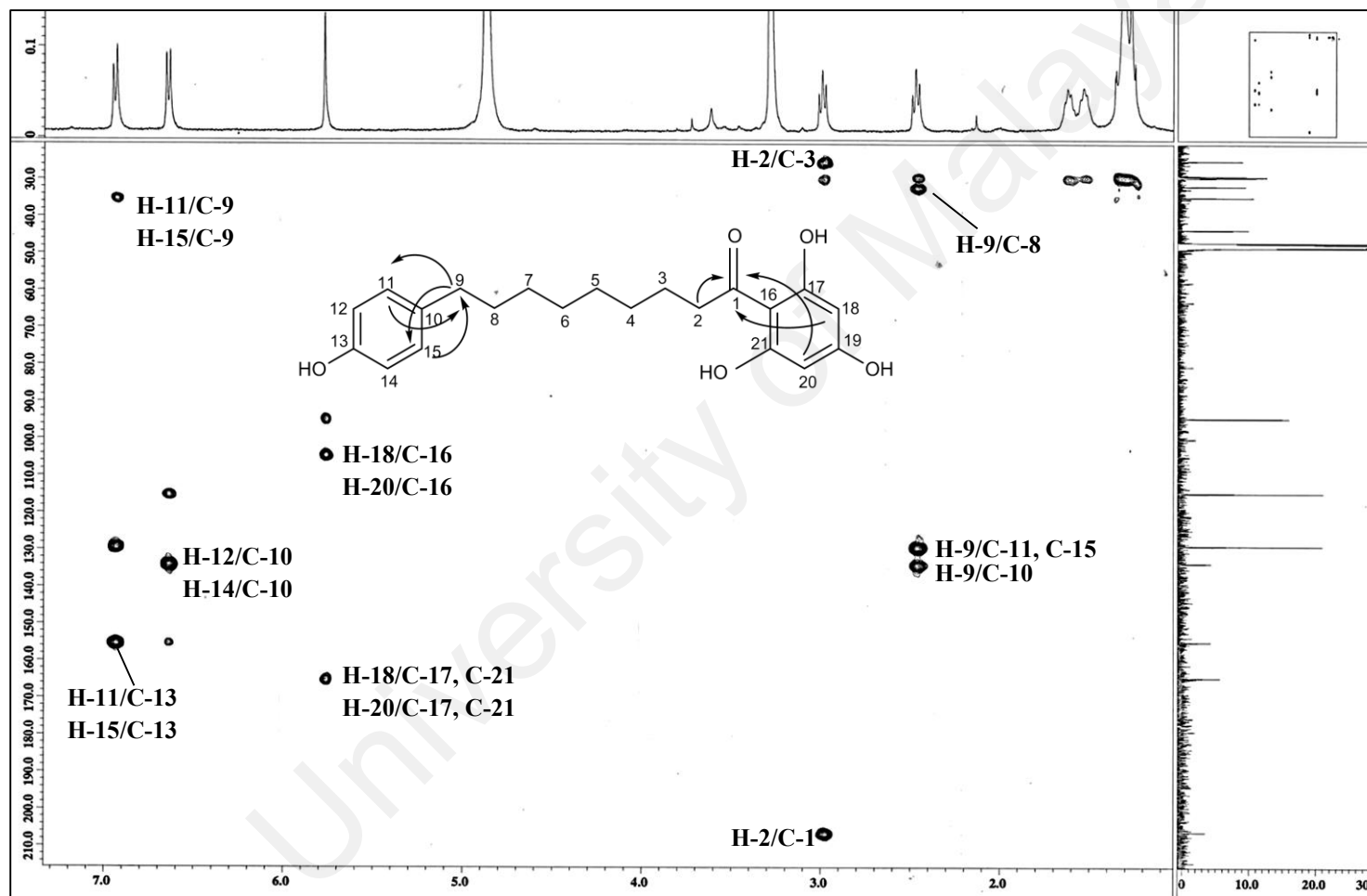
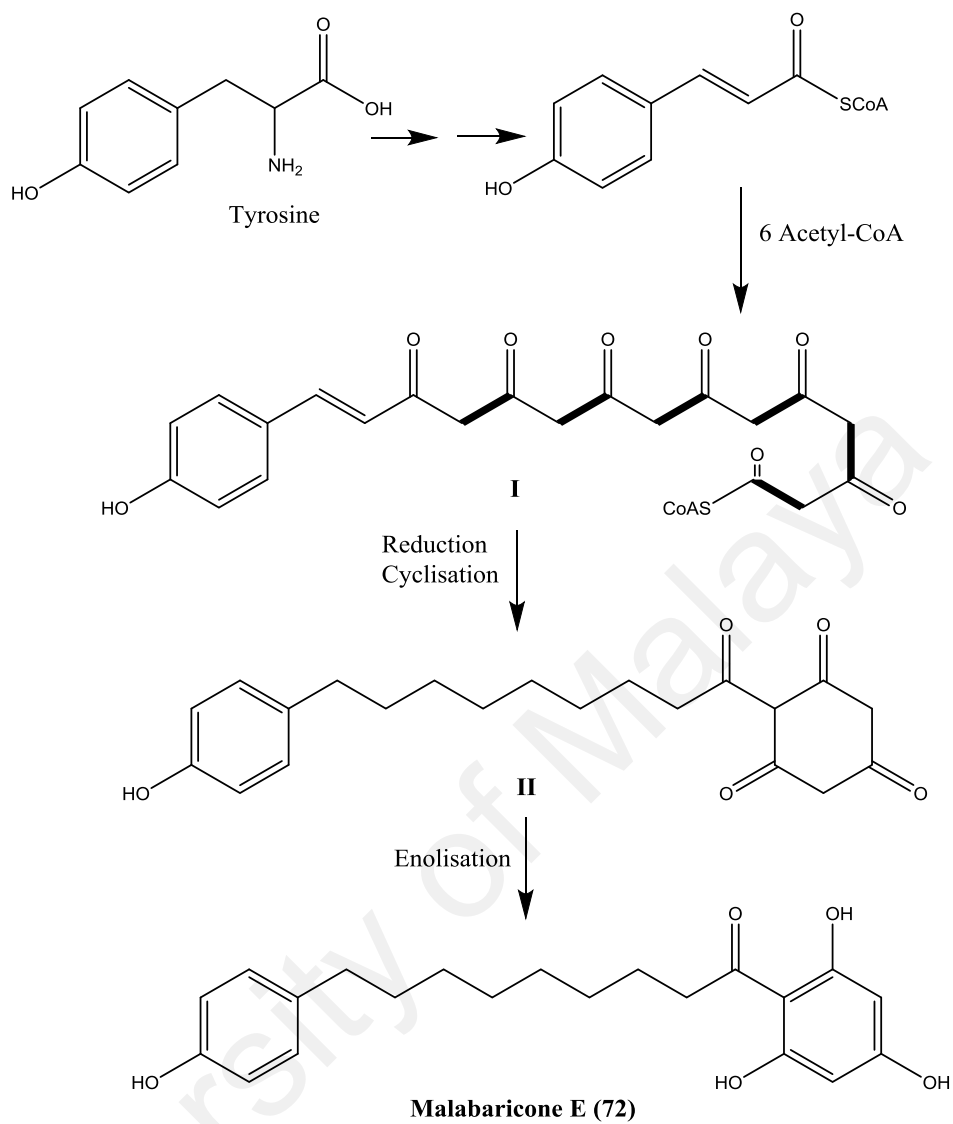


Figure 3.32: Selected HMBC correlations of compound 72



Scheme 3.1: Proposed biosynthetic pathway for the formation of compound **72**

(Abdul Wahab et al., 2016)

3.1.5 Compound 4: Maingayone A

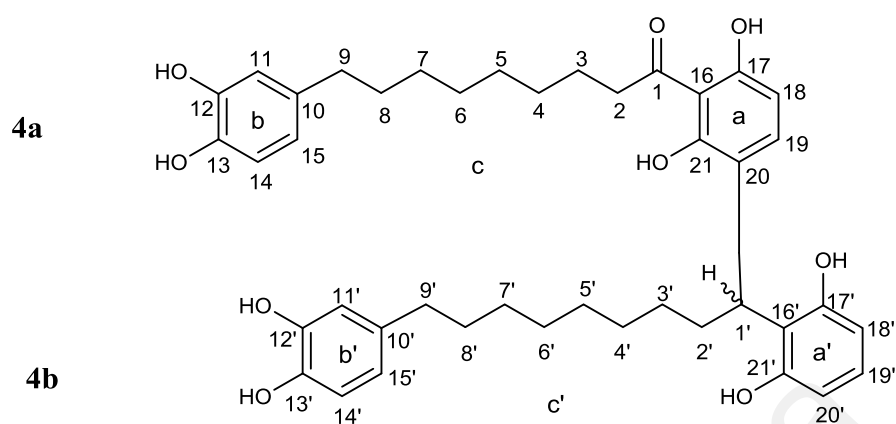


Figure 3.33: Structure of compound **4**

Compound **4** (Figure 3.33) was isolated as an optically active brown amorphous powder, $[\alpha]_D -2.4^\circ$ (c 1.25, MeOH). Its positive LCMS-IT-TOF (Figure 3.34) analysis which exhibited a pseudo-molecular ion $[M + H]^+$ at m/z 701.3627 (calcd. for $C_{42}H_{53}O_9$ 701.3684) and its ^{13}C NMR spectrum (Table 3.5, Figure 3.35a) were in agreement with the molecular formula of $C_{42}H_{52}O_9$, corresponding with 17 degrees of unsaturation. The IR spectrum (Figure 3.36) revealed absorption bands at ν_{max} 3401, 2928, 2855, 1701, 1606 and 1516 cm^{-1} , consistent with the presence of hydroxyl groups, methylene groups, a conjugated carbonyl group and aromatic rings in the molecule. The high molecular mass and considering the fact that dimeric acylphenols have been characterized in the genus *Myristica*, it was reasonable to postulate the possibility of compound **4** being such a compound. The paired signals in the ^{13}C NMR spectrum suggested that the dimer was not symmetrical in nature. Therefore, the structure of compound **4** was proposed to be constructed from two closely related acylphenol moieties ascribed as partial structures **4a** and **4b**. This was evident from the combined analysis of the ^{13}C NMR (Table 3.5, Figure 3.35a) and DEPT-135 (Figure 3.35b) spectra which displayed the presence of 24 aromatic

carbons (4 aromatic rings), 16 methylene carbons (two *n*-octyl chains), 1 carbonyl carbon and a methine carbon.

The ^1H NMR (Table 3.5, Figure 3.37) and COSY NMR (Figure 3.38) spectra of compound **4** depicted spin systems for four substituted aromatic rings; a 1, 2, 3, 4-tetrasubstituted ring (ring a) [δ_{H} 7.58 (*d*, $J=8.0$ Hz, H-19; δ_{C} 137.6, C-19) and δ_{H} 6.29 (*d*, $J=8.0$ Hz, H-18; δ_{C} 107.5, C-18)], a 1, 2, 3-symmetrically trisubstituted ring (ring a') [δ_{H} 6.80 (*t*, $J=8.0$ Hz, H-19'; δ_{C} 128.1, C-19') and δ_{H} 6.29 (*d*, $J=8.0$ Hz, H-18' & H-20'; δ_{C} 108.8, C-18' & C-20')] along with two 1, 3, 4-trisubstituted rings (rings b and b') [δ_{H} 6.47 (*dd*, $J=8.0, 1.8$ Hz, H-15; δ_{C} 120.8, C-15), δ_{H} 6.45 (*dd*, $J=8.0, 1.8$ Hz, H-15'; δ_{C} 120.8, C-15'), δ_{H} 6.60 (*d*, $J=1.8$ Hz, H-11; δ_{C} 116.6, C-11), δ_{H} 6.59 (*d*, $J=1.8$ Hz, H-11'; δ_{C} 116.6, C-11'), δ_{H} 6.66 (*d*, $J=8.0$ Hz, H-14; δ_{C} 116.3, C-14) and δ_{H} 6.64 (*d*, $J=8.0$ Hz, H-14'; δ_{C} 116.3, C-14')]. The signals in the upfield region were assigned to the 16 methylene groups which were distributed into two *n*-octyl chains (chains c and c'). The carbon resonances at δ_{C} 210.2 (C-1), δ_{C} 146.1 (C-12), δ_{C} 144.1 (C-13), δ_{C} 160.7 (C-17) and δ_{C} 160.8 (C-21) for partial structure **4a** and at δ_{C} 146.1 (C-12'), δ_{C} 144.1 (C-13') and δ_{C} 157.7 (C-17' & C-21') for partial structure **4b**, implied that they were oxygenated. The foregoing evidence suggested that partial structures **4a** and **4b** were respectively derived from compound **3** (malabaricone C) (Table 3.3, Figures 3.20 & 3.21a).

The connectivity between both these partial structures however has yet to be determined. The DEPT 135 spectrum (Figure 3.35b) of compound **4** disclosed a quaternary aromatic carbon at δ_{C} 123.9 (C-20) and a sp^3 methine carbon at δ_{C} 35.0 (C-1'). Hence, one could postulate that partial structures **4a** and **4b** were linked via positions 20 and 1', respectively. The H-1'/C-19, C-20, C-21 and H-19/C-1' heteronuclear correlations as

inferred from the HMBC experiment unambiguously confirmed that the inter-acylphenol linkage in compound **4** was between C-20 of partial structure **4a** and C-1' of partial structure **4b** (Figure 3.39). Partial structures **4a** and **4b** were identified as 20-substituted malabaricone C and 1'-substituted malabaricone C, respectively.

The complete assignments of the ^1H NMR and ^{13}C NMR spectroscopic data of compound **4** were achieved with the aid of the COSY, HMBC and HSQC experiments (Figures 3.38-3.40) and from the systematic analysis of the spectra of closely-related dimeric acylphenols. It was observed that the spectroscopic data of compound **4** were in excellent agreement with those reported for maingayone A (Pham et al., 2000). Therefore, compound **4** was identified as maingayone A.

Table 3.5: ^1H NMR and ^{13}C NMR spectroscopic assignments of compound **4** in methanol- d_4

Position	δ_{H} (ppm)		δ_{C} (ppm)	
	Experimental	Literature (Pham et al., 2000)	Experimental	Literature (Pham et al., 2000)
1	-	-	210.2	210.0
2	3.09 (<i>t</i> , $J = 8.0$ Hz)	3.08 (<i>t</i> , $J = 8.0$ Hz)	45.9	45.6
3	1.64 (<i>m</i>)	1.50 (<i>m</i>)	26.0	25.6
4	1.28 ^a (<i>brs</i>)	1.30 (<i>m</i>)	30.8 ^b	30.1
5	1.28 ^a (<i>brs</i>)	1.30 (<i>m</i>)	30.7 ^b	30.1
6	1.28 ^a (<i>brs</i>)	1.30 (<i>m</i>)	30.7 ^b	30.3
7	1.28 ^a (<i>brs</i>)	1.30 (<i>m</i>)	30.4 ^b	30.3
8	1.52 (<i>m</i>)	1.50 (<i>m</i>)	33.1	32.6
9	2.44 (<i>t</i> , $J = 8.0$ Hz)	2.42 (<i>t</i> , $J = 8.0$ Hz)	36.4	36.0
10	-	-	136.0	135.8
11	6.60 (<i>d</i> , $J = 1.8$ Hz)	6.59 (<i>d</i> , $J = 2.0$ Hz)	116.6	116.4
12	-	-	146.1	145.5
13	-	-	144.1	143.5
14	6.66 (<i>d</i> , $J = 8.0$ Hz)	6.64 (<i>d</i> , $J = 8.0$ Hz)	116.3	116.1
15	6.47 (<i>dd</i> , $J = 8.0, 1.8$ Hz)	6.45 (<i>dd</i> , $J = 8.0, 2.0$ Hz)	120.8	120.6
16	-	-	111.2	110.8
17	-	-	160.7	160.2
18	6.29 (<i>d</i> , $J = 8.0$ Hz)	6.30 (<i>d</i> , $J = 8.0$ Hz)	107.5	107.8
19	7.58 (<i>d</i> , $J = 8.0$ Hz)	7.57 (<i>d</i> , $J = 8.0$ Hz)	137.6	137.4
20	-	-	123.9	123.3
21	-	-	160.8	160.4
1'	4.55 (<i>dd</i> , $J = 9.1, 6.9$ Hz)	4.54 (<i>dd</i> , $J = 9.1, 6.8$ Hz)	35.0	34.7
2'	2.04, 2.41 (<i>m</i>)	2.04, 2.41 (<i>m</i>)	32.5	32.1
3'	1.28 ^a (<i>brs</i>)	1.50 (<i>m</i>)	29.6	29.3
4'	1.28 ^a (<i>brs</i>)	1.30 (<i>m</i>)	30.8 ^b	30.1
5'	1.28 ^a (<i>brs</i>)	1.30 (<i>m</i>)	30.7 ^b	30.1
6'	1.28 ^a (<i>brs</i>)	1.30 (<i>m</i>)	30.7 ^b	30.3
7'	1.28 ^a (<i>brs</i>)	1.30 (<i>m</i>)	30.4 ^b	30.3
8'	1.52 (<i>m</i>)	1.50 (<i>m</i>)	33.1	32.6
9'	2.40 (<i>t</i> , $J = 8.0$ Hz)	2.40 (<i>t</i> , $J = 8.0$ Hz)	36.4	36.0
10'	-	-	135.9	135.8
11'	6.59 (<i>d</i> , $J = 1.8$ Hz)	6.59 (<i>d</i> , $J = 2.0$ Hz)	116.6	116.4
12'	-	-	146.1	145.5
13'	-	-	144.1	143.5
14'	6.64 (<i>d</i> , $J = 8.0$ Hz)	6.63 (<i>d</i> , $J = 8.0$ Hz)	116.3	116.1
15'	6.45 (<i>dd</i> , $J = 8.0, 1.8$ Hz)	6.43 (<i>dd</i> , $J = 8.0, 2.0$ Hz)	120.8	120.6
16'	-	-	118.3	118.0
17'	-	-	157.7	157.1
18'	6.29 (<i>d</i> , $J = 8.0$ Hz)	6.28 (<i>d</i> , $J = 8.0$ Hz)	108.8	108.7
19'	6.80 (<i>t</i> , $J = 8.0$ Hz)	6.79 (<i>t</i> , $J = 8.0$ Hz)	128.1	127.9
20'	6.29 (<i>d</i> , $J = 8.0$ Hz)	6.28 (<i>d</i> , $J = 8.0$ Hz)	108.8	108.7
21'	-	-	157.7	157.1

^a Overlapping signals

^b Chemical shifts interchangeable

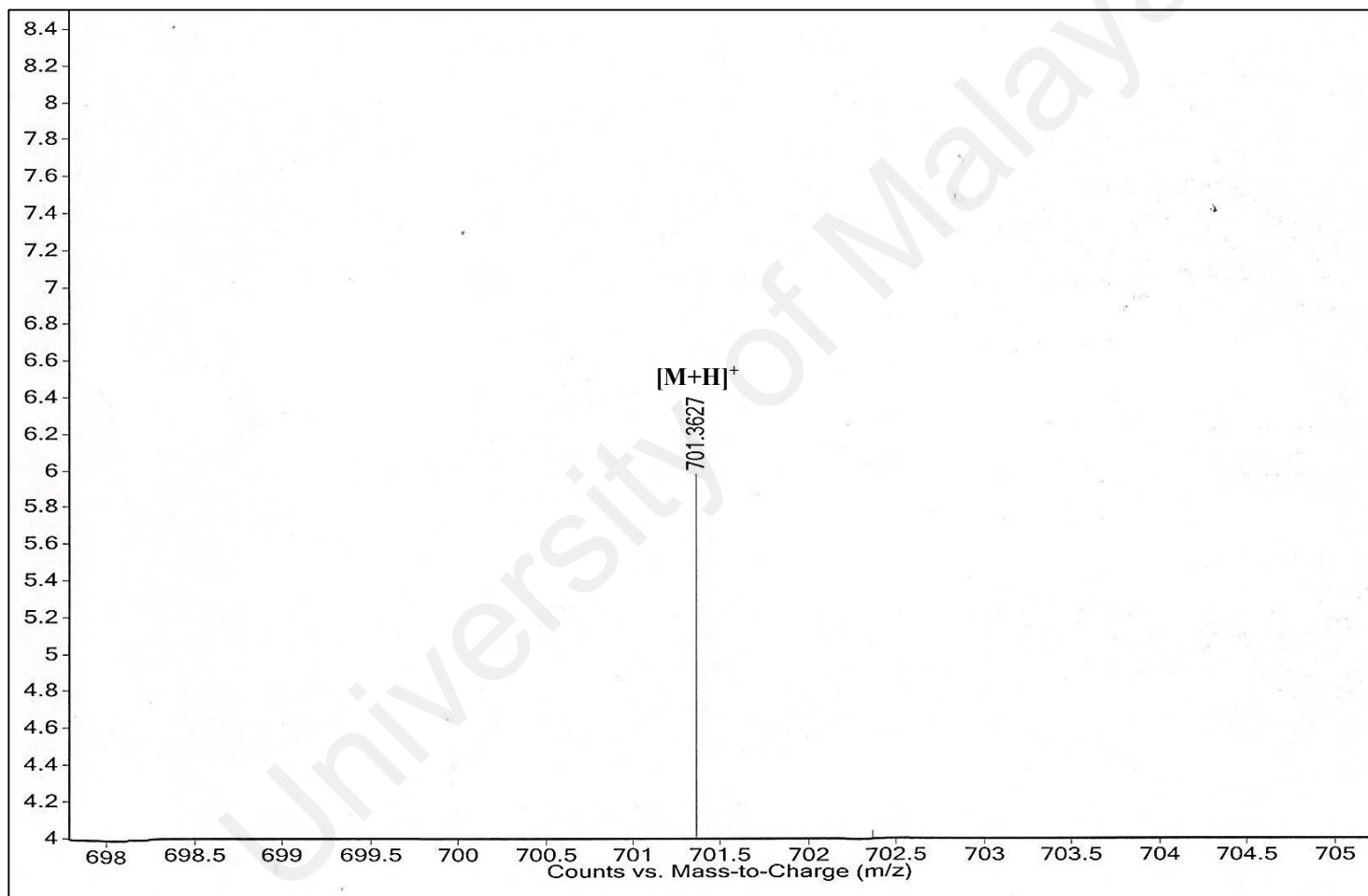


Figure 3.34: Mass spectrum of compound 4

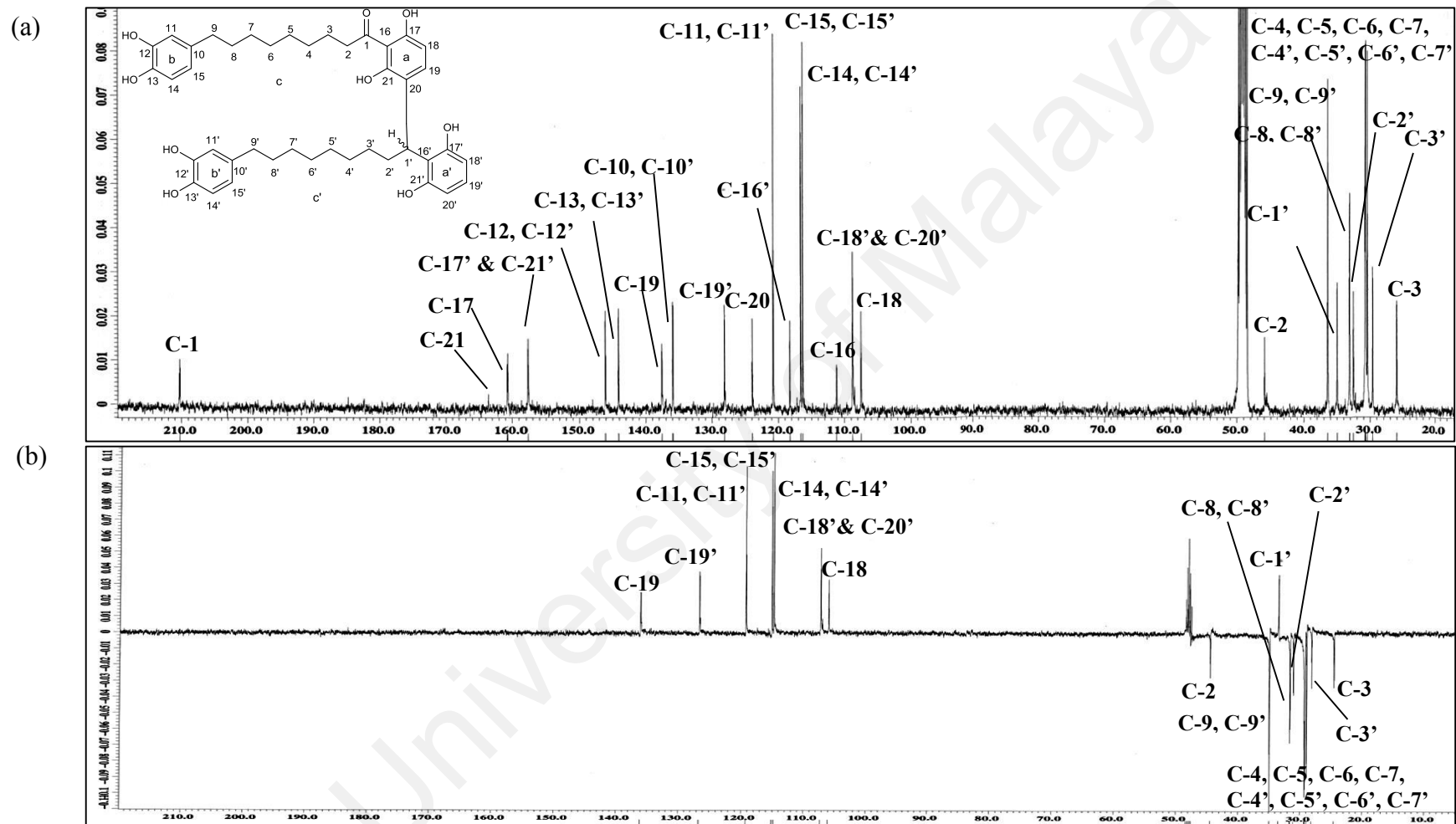


Figure 3.35: ^{13}C NMR (a) and DEPT-135 (b) spectra of compound 4

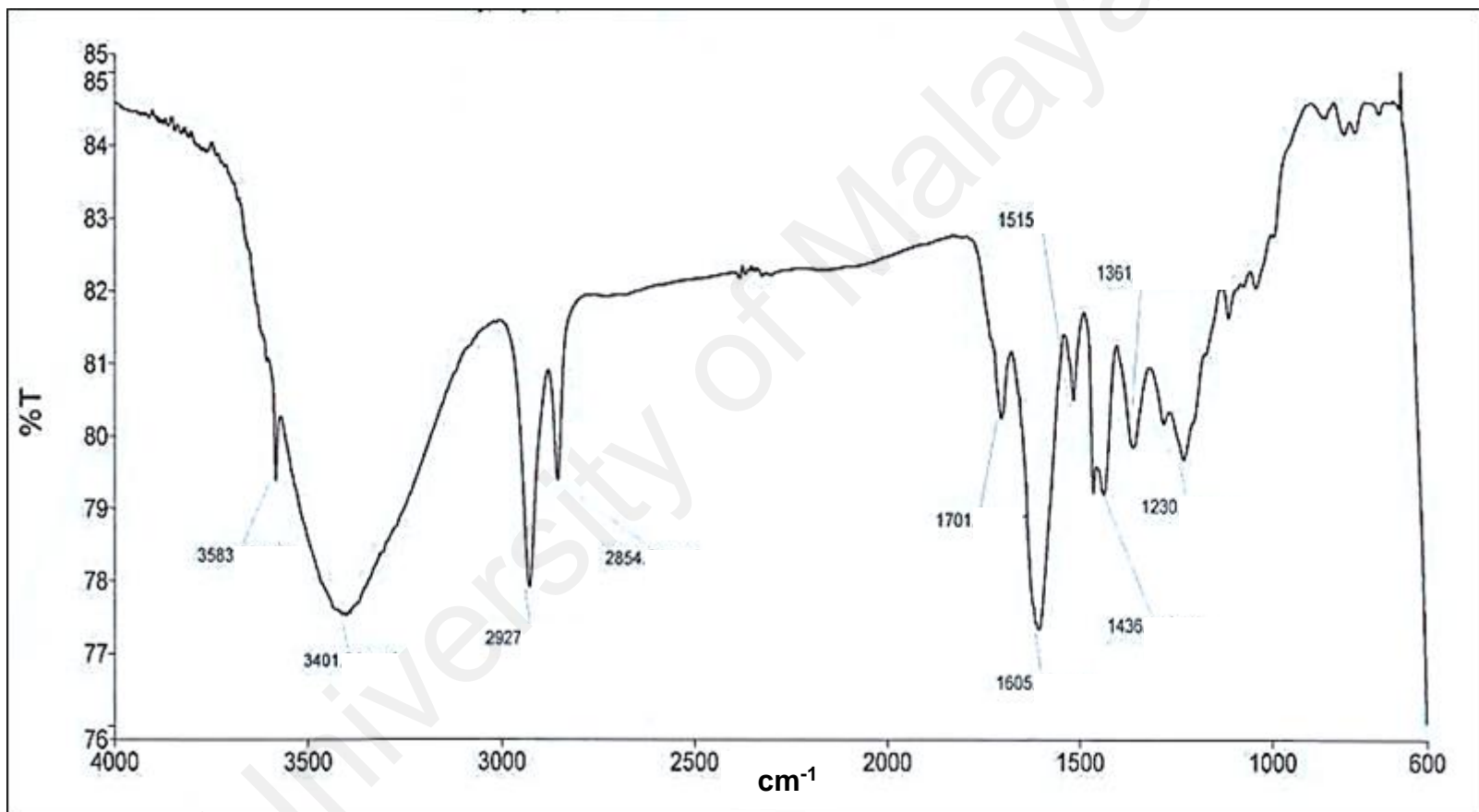


Figure 3.36: IR spectrum of compound 4

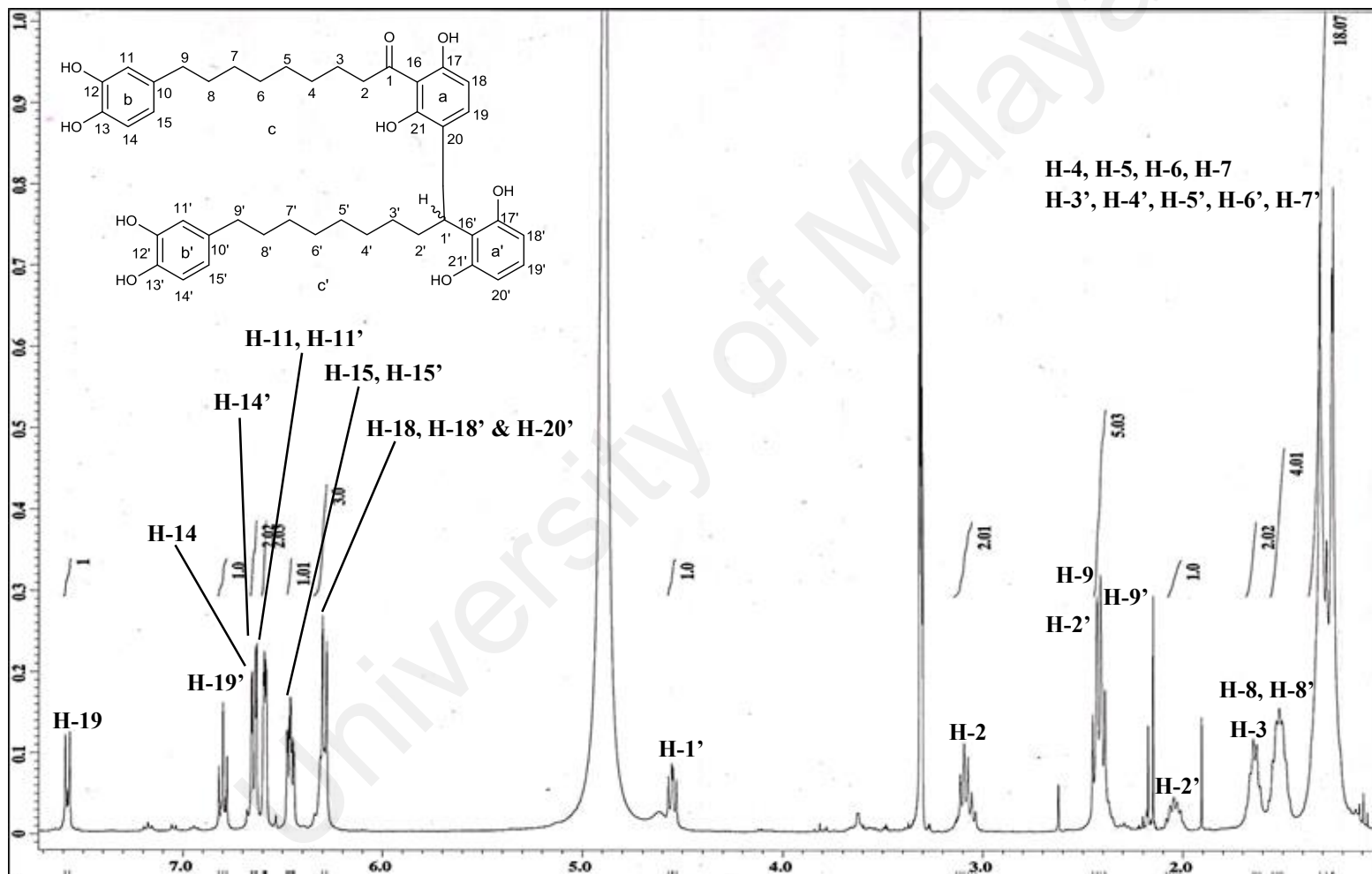


Figure 3.37: ¹H NMR spectrum of compound 4

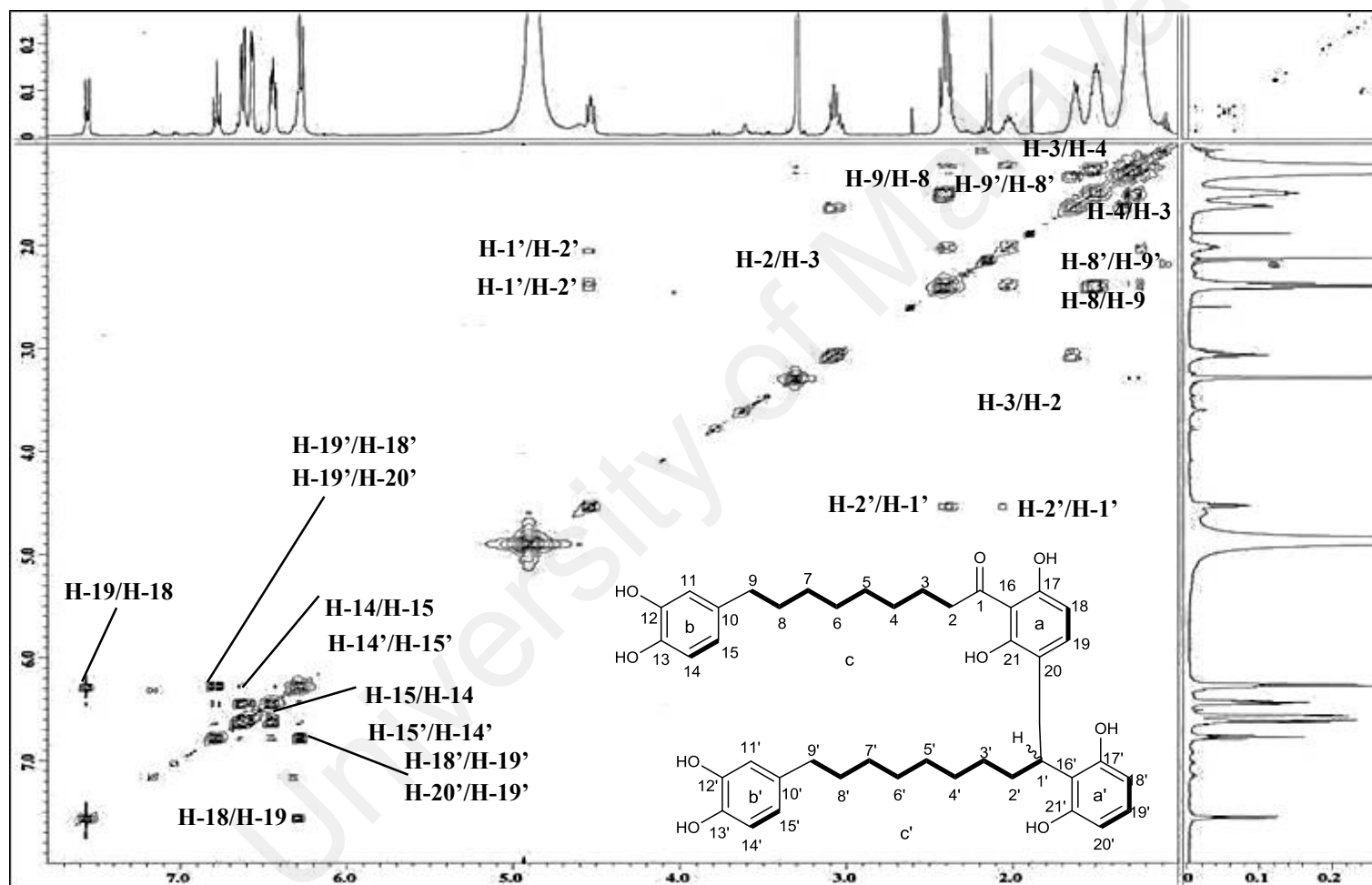


Figure 3.38: Selected COSY correlations of compound 4

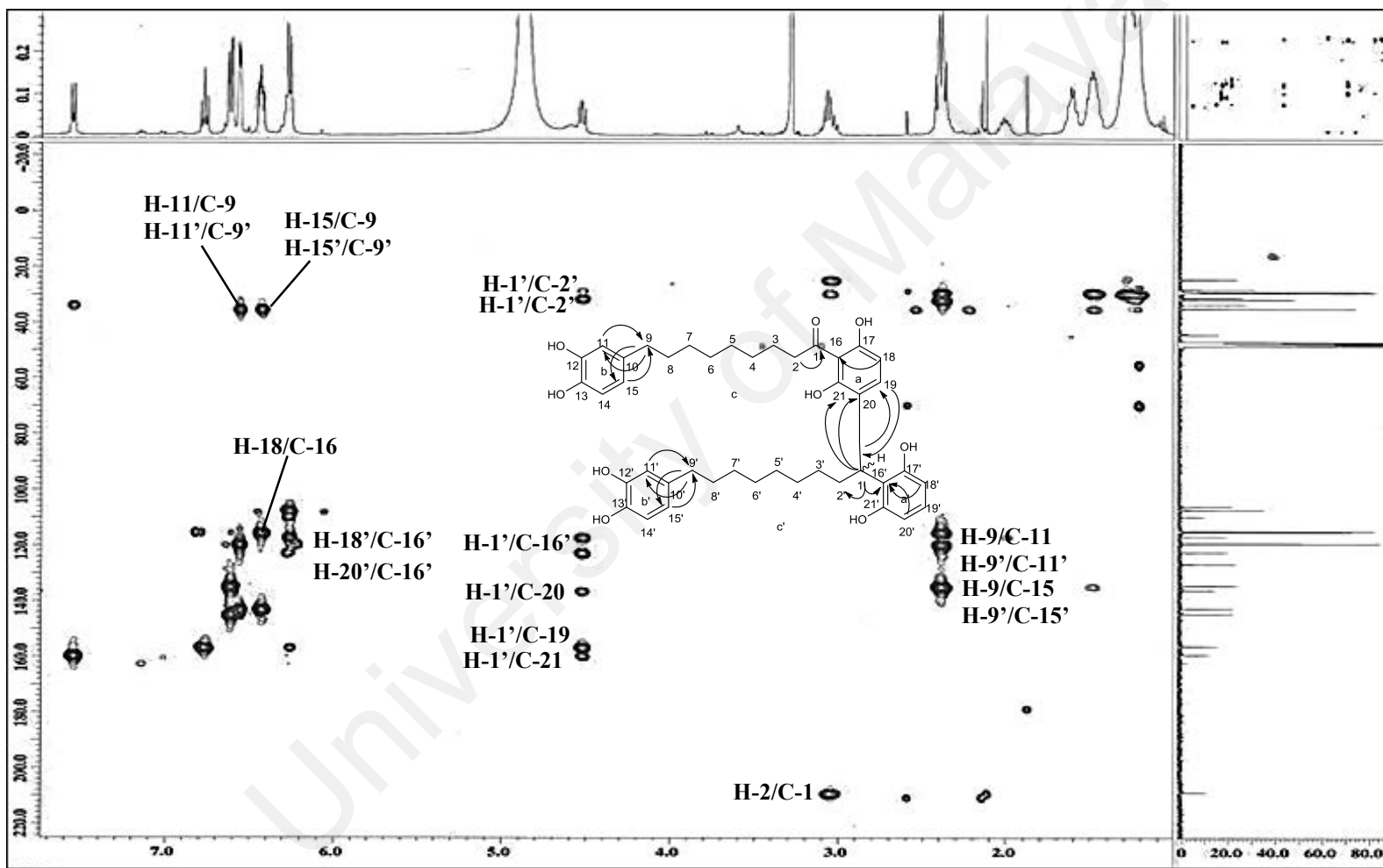


Figure 3.39: Selected HMBC correlations of compound 4

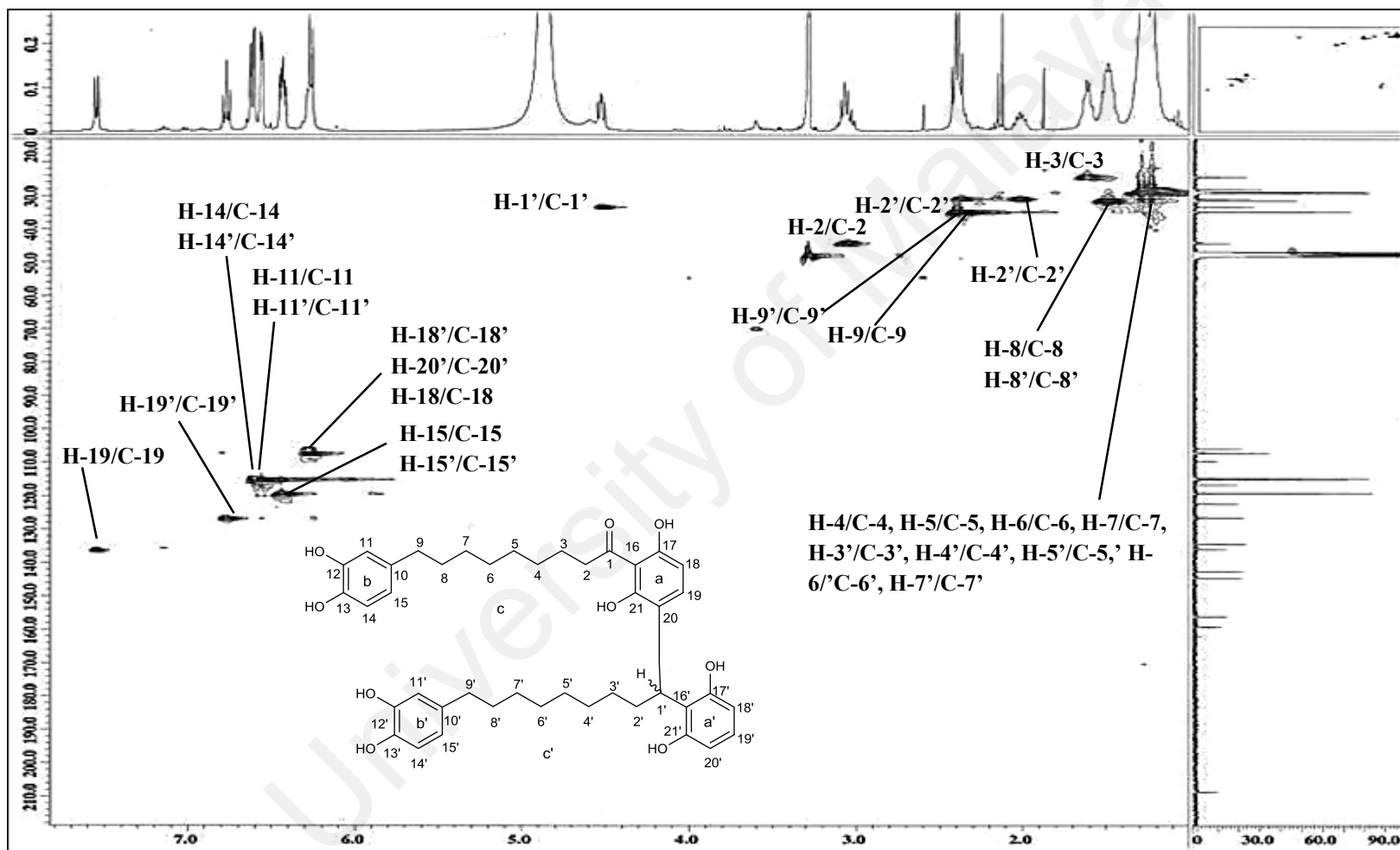


Figure 3.40: HSQC correlations of compound 4

3.1.6 Compound 5: Maingayone B

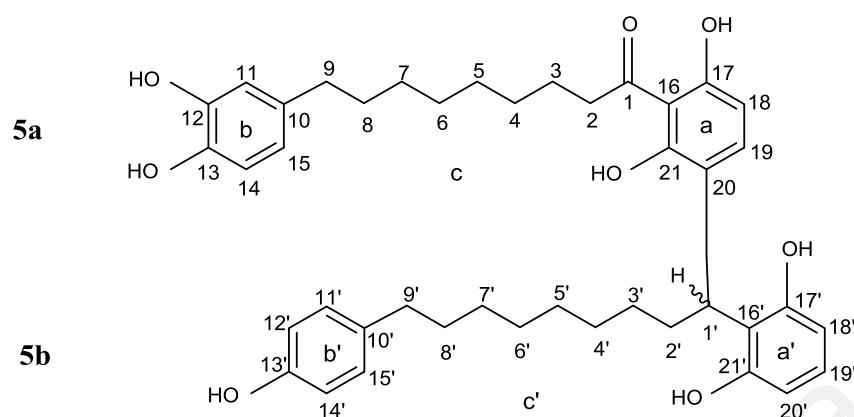


Figure 3.41: Structure of compound 5

Compound 5 (Figure 3.41), isolated as an optically active brown amorphous powder, $[\alpha]_D^{25} +0.8^\circ$ (c 1.25, MeOH), was assigned the molecular formula of $C_{42}H_{52}O_8$ with 17 degrees of unsaturation as deduced from its positive LCMS-IT-TOF analysis (Figure 3.42) $\{[M + Na]^+, m/z 707.3538$ (calcd. for $C_{42}H_{52}O_8Na$ 707.3554) $\}$. Though it has the same degrees of unsaturation as compound 4, nevertheless, its molecule lacked an oxygen atom.

The close similarities between the IR (Figure 3.43), 1H NMR (Table 3.6, Figure 3.44) and ^{13}C NMR (Table 3.6, Figure 3.45a) spectroscopic data of compounds 4 and 5 suggested that they were structurally related to each other. Therefore, compound 5 was also a non-symmetrical dimeric acylphenol constructed from two different acylphenols (partial structures 5a and 5b) as inferred from the two sets of signals displayed in the ^{13}C NMR spectrum (Table 3.6, Figure 3.45a). The 1H NMR and ^{13}C NMR spectroscopic data of partial structure 5a were superimposable with those of partial structure 4a, thus, establishing its structure as 20-substituted malabaricone C. Partial structure 5b on the other hand differed slightly from partial structure 4b. Its ring b' was a 1, 4-disubstituted aromatic ring instead of a 1, 3, 4-trisubstituted aromatic ring as was ascribed for partial structure 4b. The H-11'/H-12' and H-14'/H-15' homonuclear couplings (Figure 3.46)

provide full support for the above mentioned spin system of ring b'. The rather upfield value of the C-12' resonance at δ_c 116.1 when compared to the resonance of the corresponding atom (δ_c 146.1) in partial structure **4b** (Table 3.5) verified that C-12' was not substituted. Hence, it was obvious that partial structure **5b** was derived from malabaricone B and therefore, was identified as 1'-substituted malabaricone B. The inter-acylphenol linkage within compound **5** was established based on the similar manner as was carried out for compound **4** (Figure 3.47).

The complete assignments of the ^1H NMR and ^{13}C NMR spectroscopic data of compound **5** were achieved with the aid of the COSY, HSQC and HMBC experiments (Figures 3.46-3.48) and from the systematic analysis of the spectra of closely-related dimeric acylphenols. It was observed that the spectroscopic data of compound **5** were in excellent agreement with those reported for maingayone B (Maia et al., 2008). Hence, compound **5** was characterized as maingayone B.

Table 3.6: ^1H NMR and ^{13}C NMR spectroscopic assignments of compound **5** in methanol- d_4

Position	δ_{H} (ppm)		δ_{C} (ppm)	
	Experimental	Literature (Maia et al., 2008)	Experimental	Literature (Maia et al., 2008)
1	-	-	210.3	210.5
2	3.09 (<i>t</i> , $J = 8.0$ Hz)	3.09 (<i>t</i> , $J = 7.3$ Hz)	45.9	45.5
3	1.64 (<i>m</i>)	1.64 – 1.67 (<i>m</i>)	26.0	26.0
4	1.32 ^a (<i>brs</i>)	1.06 – 1.35 (<i>m</i>)	30.9 ^b	30.3 - 30.6
5	1.32 ^a (<i>brs</i>)	1.06 – 1.35 (<i>m</i>)	30.7 ^b	30.3 - 30.6
6	1.32 ^a (<i>brs</i>)	1.06 – 1.35 (<i>m</i>)	30.7 ^b	30.3 - 30.6
7	1.32 ^a (<i>brs</i>)	1.06 – 1.35 (<i>m</i>)	30.4 ^b	30.3 - 30.6
8	1.52 (<i>m</i>)	1.51 (<i>m</i>)	33.2	33.0
9	2.41 (<i>t</i> , $J = 8.0$ Hz)	2.42 (<i>t</i> , $J = 8.0$ Hz)	36.4	36.4
10	-	-	136.0	136.1
11	6.58 (<i>d</i> , $J = 2.0$ Hz)	6.60 (<i>d</i> , $J = 2.0$ Hz)	116.6	116.7
12	-	-	146.1	146.1
13	-	-	144.3	144.2
14	6.63 (<i>d</i> , $J = 8.0$ Hz)	6.65 (<i>d</i> , $J = 8.0$ Hz)	116.3	116.4
15	6.45 (<i>dd</i> , $J = 8.0, 2.0$ Hz)	6.46 (<i>dd</i> , $J = 8.0, 2.0$ Hz)	120.8	120.8
16	-	-	111.1	111.4
17	-	-	160.7	160.6
18	6.29 (<i>d</i> , $J = 8.0$ Hz)	6.31 (<i>d</i> , $J = 8.5$ Hz)	107.5	107.7
19	7.58 (<i>d</i> , $J = 8.0$ Hz)	7.59 (<i>d</i> , $J = 8.5$ Hz)	137.6	137.6
20	-	-	123.9	124.0
21	-	-	160.8	160.7
1'	4.55 (<i>t</i> , $J = 8.0$ Hz)	4.55 (<i>t</i> , $J = 8.0$ Hz)	35.0	35.1
2'	2.03, 2.39 (<i>m</i>)	2.07 - 2.39 (<i>m</i>)	32.6	32.6
3'	1.26 (<i>m</i>)	1.23 (<i>m</i>)	29.6	29.6
4'	1.32 ^a (<i>brs</i>)	1.06 - 1.35 (<i>m</i>)	30.9 ^b	30.3 - 30.6
5'	1.32 ^a (<i>brs</i>)	1.06 - 1.35 (<i>m</i>)	30.7 ^b	30.3 - 30.6
6'	1.32 ^a (<i>brs</i>)	1.06 - 1.35 (<i>m</i>)	30.7 ^b	30.3 - 30.6
7'	1.32 ^a (<i>brs</i>)	1.06 - 1.35 (<i>m</i>)	30.4 ^b	30.3 - 30.6
8'	1.52 (<i>m</i>)	1.54 (<i>m</i>)	33.2	33.1
9'	2.48 (<i>t</i> , $J = 8.0$ Hz)	2.49 (<i>t</i> , $J = 7.0$ Hz)	36.2	36.2
10'	-	-	135.1	135.1
11'	6.95 (<i>d</i> , $J = 8.0$ Hz)	6.96 (<i>m</i>)	130.2	130.3
12'	6.67 (<i>d</i> , $J = 8.0$ Hz)	6.68 (<i>m</i>)	116.1	116.2
13'	-	-	156.3	156.4
14'	6.67 (<i>d</i> , $J = 8.0$ Hz)	6.68 (<i>m</i>)	116.1	116.2
15'	6.95 (<i>d</i> , $J = 8.0$ Hz)	6.96 (<i>m</i>)	130.2	130.3
16'	-	-	118.0	118.5
17'	-	-	157.7	157.7
18'	6.29 (<i>d</i> , $J = 8.0$ Hz)	6.30 (<i>d</i> , $J = 8.1$ Hz)	108.8	108.9
19'	6.80 (<i>t</i> , $J = 8.0$ Hz)	6.79 (<i>t</i> , $J = 8.1$ Hz)	128.1	128.1
20'	6.29 (<i>d</i> , $J = 8.0$ Hz)	6.30 (<i>d</i> , $J = 8.1$ Hz)	108.8	108.9
21'	-	-	157.7	157.7

^a Overlapping signals

^b Chemical shifts interchangeable

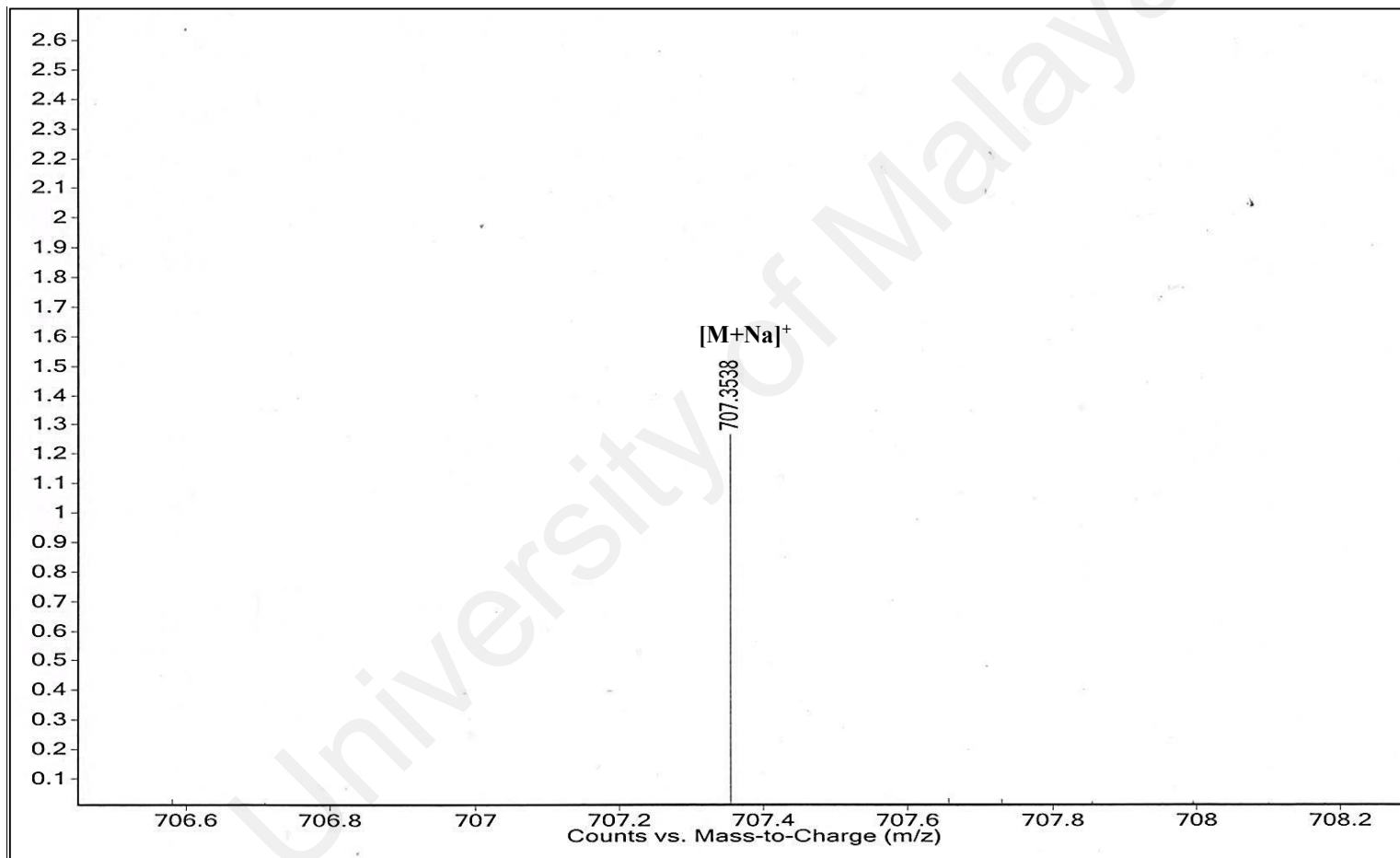


Figure 3.42: Mass spectrum of compound 5

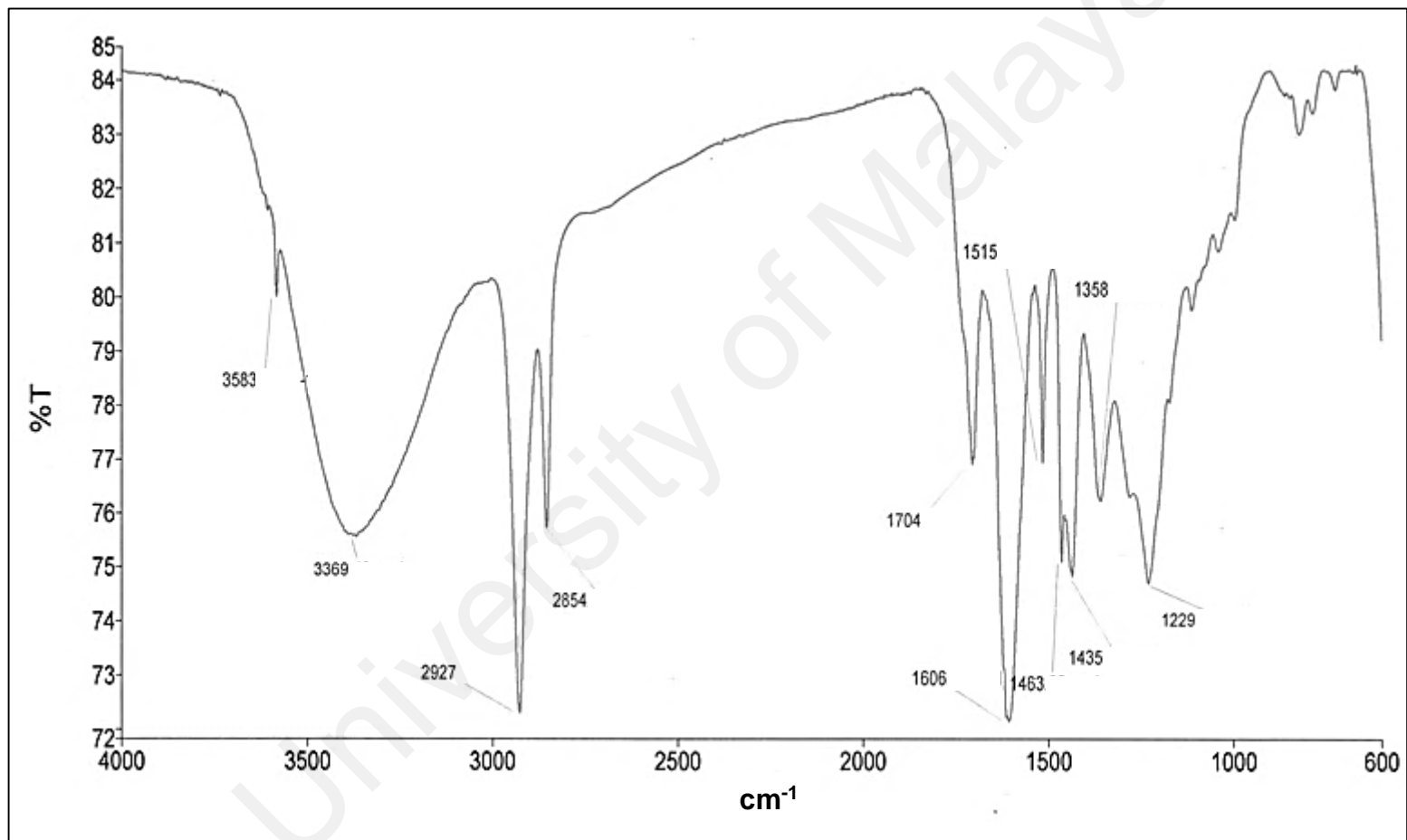


Figure 3.43: IR spectrum of compound 5

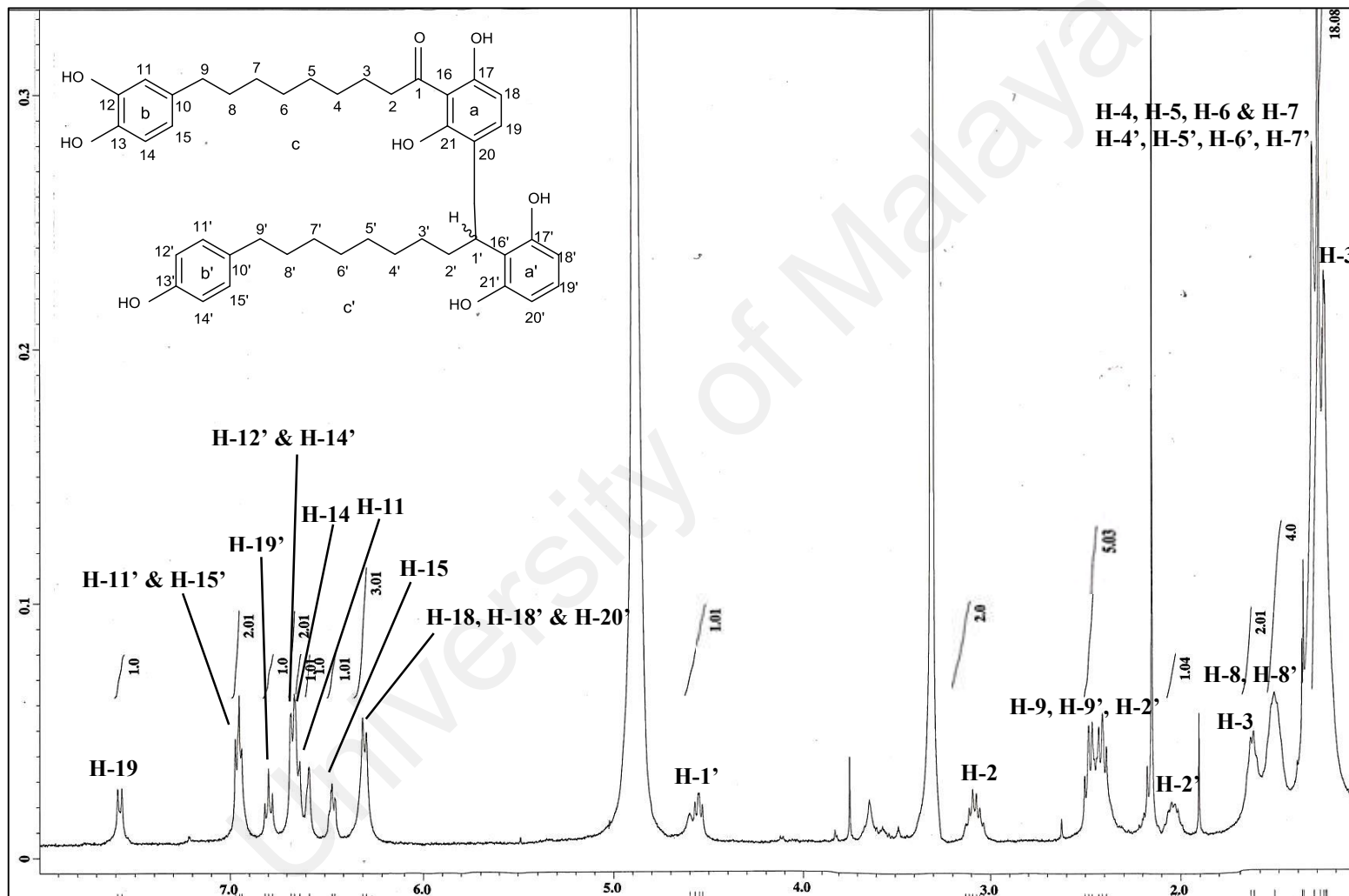


Figure 3.44: ¹H NMR spectrum of compound 5

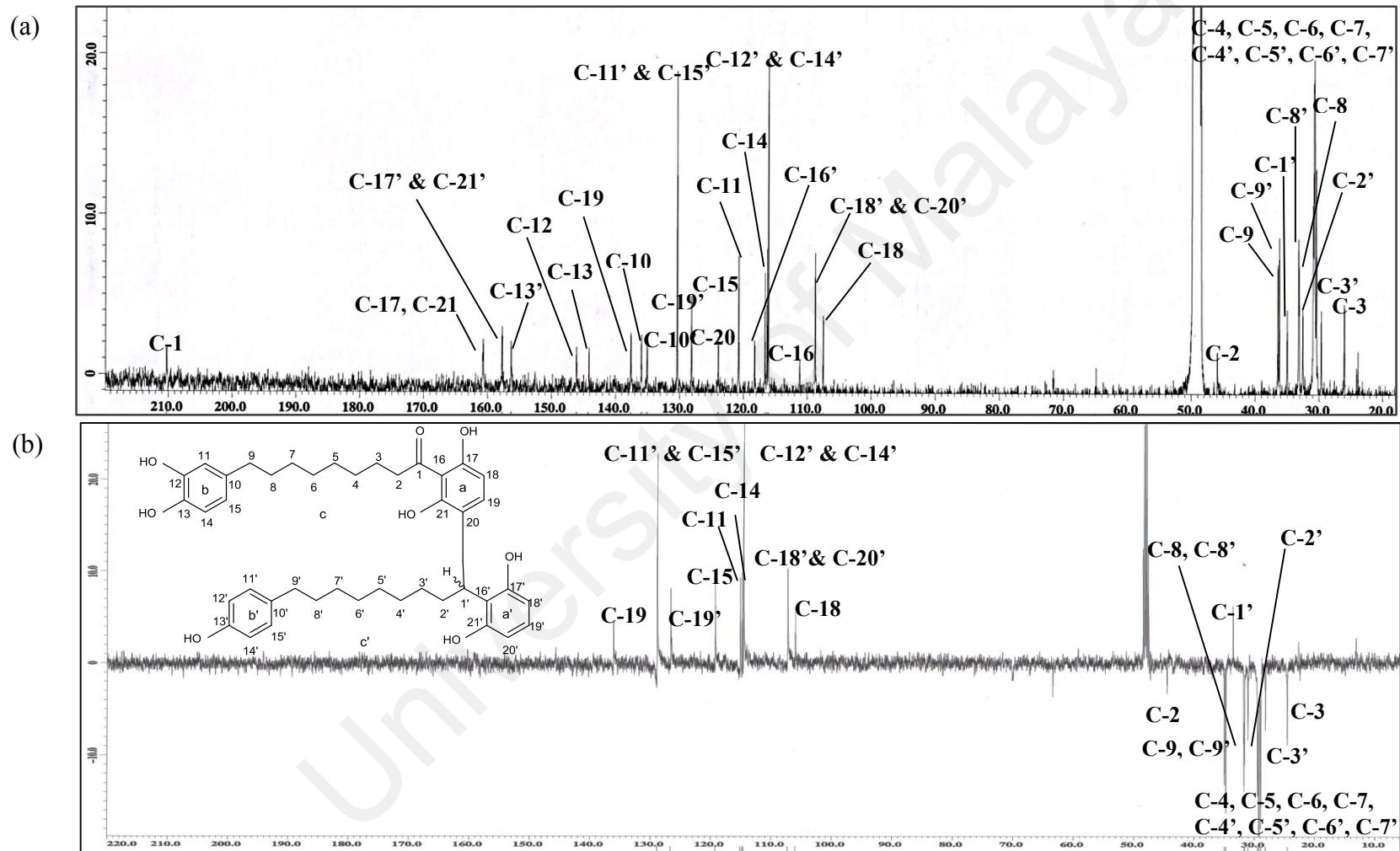


Figure 3.45: (a) ¹³C NMR and (b) DEPT 135 spectra of compound 5

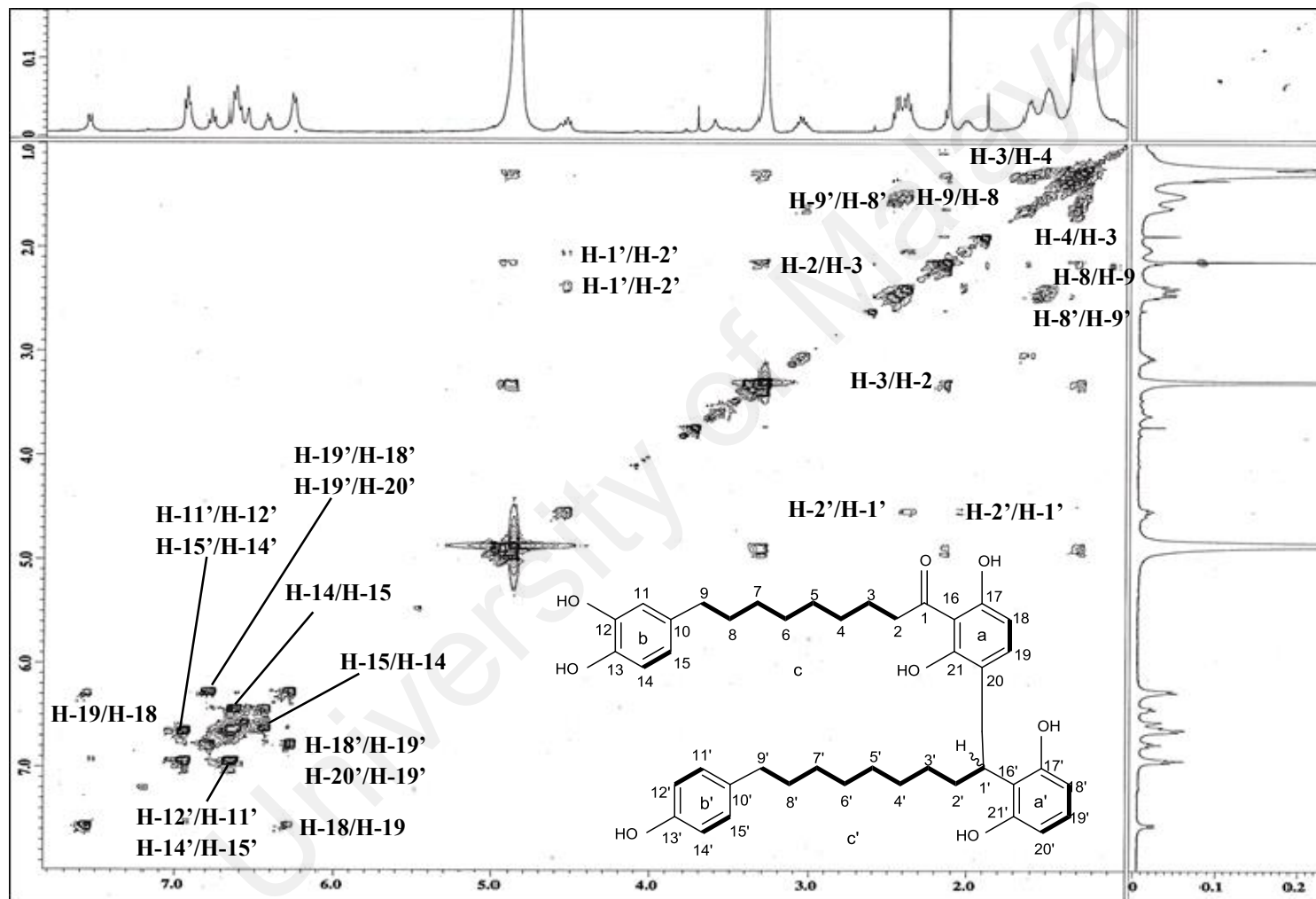


Figure 3.46: Selected COSY correlations of compound 5

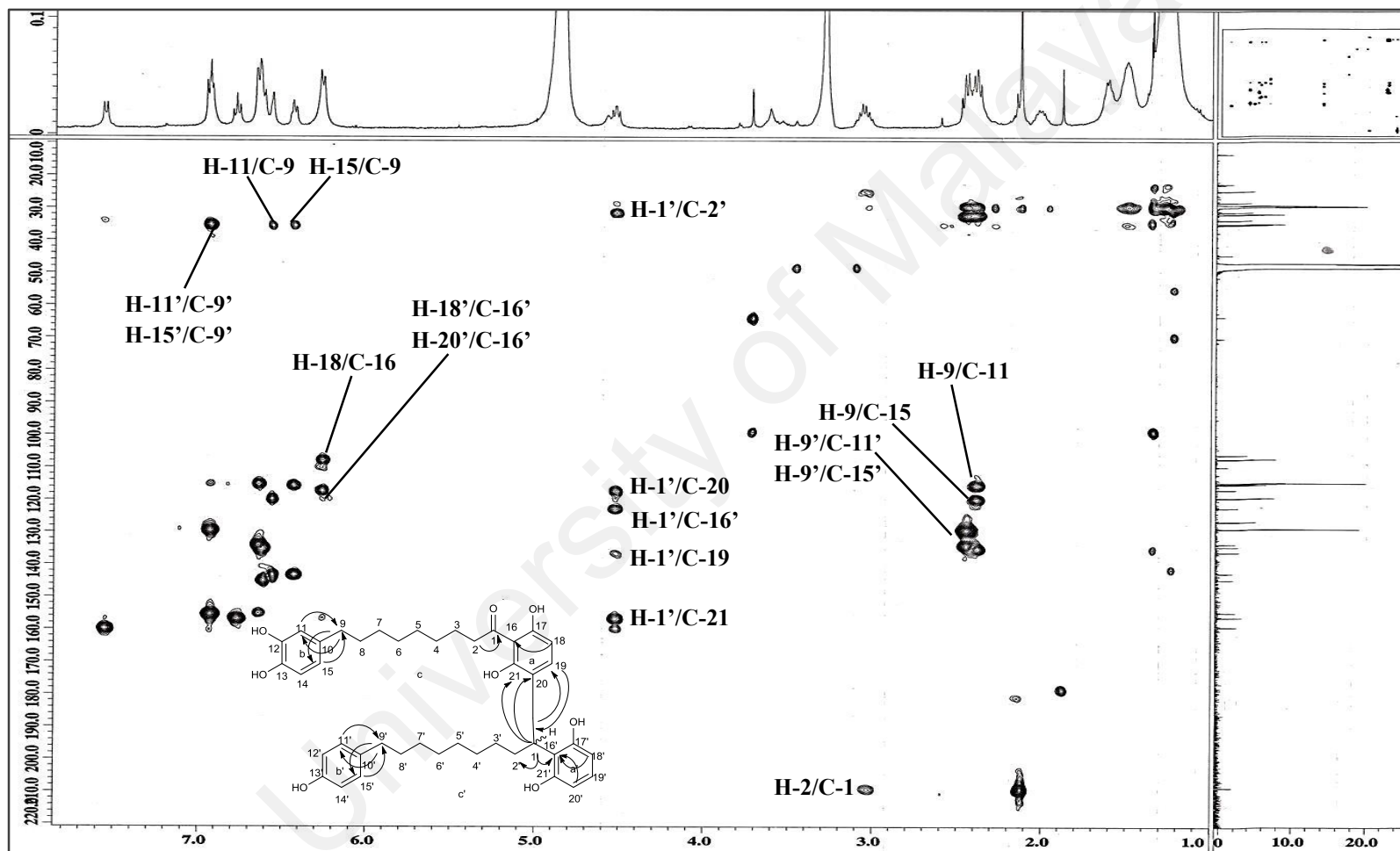


Figure 3.47: Selected HMBC correlations of compound 5

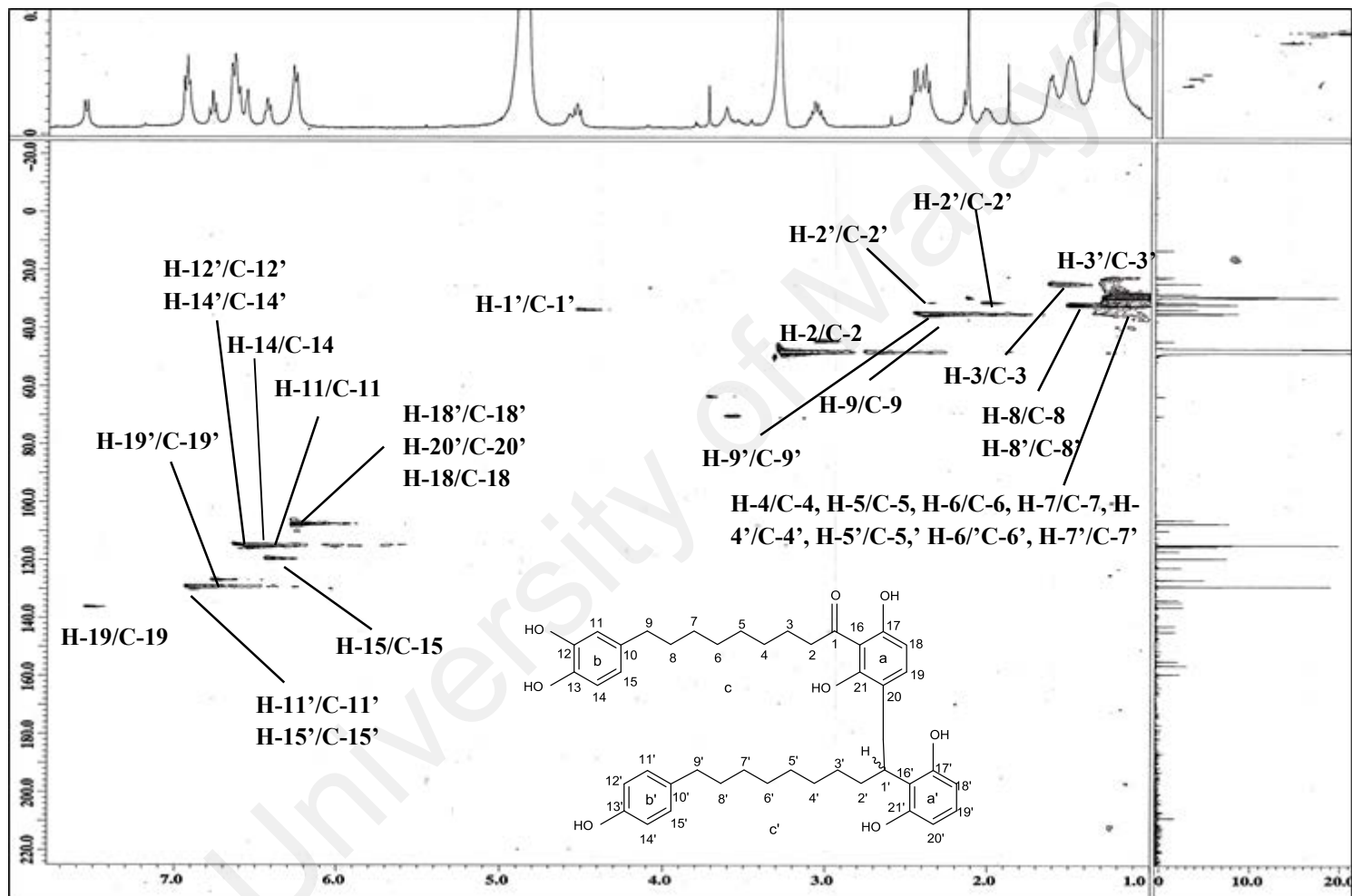


Figure 3.48: HSQC correlations of compound 5

3.1.7 Compound 69: Maingayic acid B

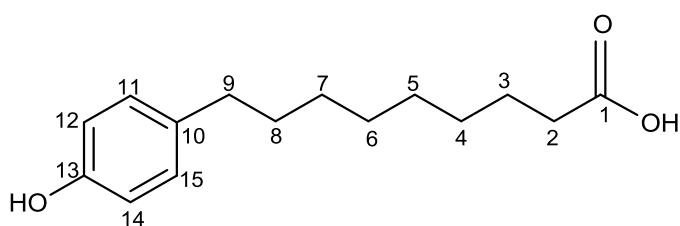


Figure 3.49: Structure of compound **69**

Compound **69** (Figure 3.49) was isolated as an optically inactive light yellow amorphous powder. A molecular formula of $C_{15}H_{22}O_3$ was proposed as deduced from the positive LCMS-IT-TOF (Figure 3.50) analysis $\{[M + Na]^+, m/z 273.1451$ (calcd. for $C_{15}H_{22}O_3Na$ 273.1461) $\}$ and ^{13}C NMR spectrum (Table 3.7, Figure 3.51a), consistent with 5 degrees of unsaturation. The strong absorption band at ν_{max} 1709 cm^{-1} in the IR spectrum (Figure 3.52) and the carbon resonance at δ_C 178.0 (Table 3.7, Figure 3.51a) suggested the possibility of compound **69** being a carboxylic acid. The IR spectrum (Figure 3.52) also revealed absorption bands due to hydroxyl groups (ν_{max} 3369 cm^{-1}), methylene groups (ν_{max} 2927 and 2854 cm^{-1}) and aromatic rings (ν_{max} 1515 and 1455 cm^{-1}) which were present in the molecule (Pham et al., 2000).

Analysis of the 1D and 2D NMR spectroscopic data (Table 3.7, Figures 3.51, 3.53-3.56) indicated that compound **69** comprised three substructures; a 4-hydroxyphenyl moiety [δ_H 6.97 ($J = 8.0$ Hz, H-11 & H-15; δ_C 130.4, C-11 & C-15) and δ_H 6.68 ($J = 8.0$ Hz, H-12 & H-14; δ_C 116.1, C-12 & C-14)], an *n*-octyl chain and a carboxylic acid functional group. The following HMBC crosspeaks; H-2/C-1, H-9/C-10, C-11, C-15, H-11/C-9 and H-15/C-9 confirmed the connectivities between these three substructures (Figure 3.54).

The complete assignments of the ^1H NMR and ^{13}C NMR spectroscopic data of compound **69** were achieved with the aid of the COSY, HSQC and HMBC experiments (Figures 3.54-3.56). All of the above mentioned NMR spectroscopic data of compound **69** revealed a striking resemblance to those of maingayic acid B. Comparison of the spectroscopic data of compound **69** with those reported in the literature confirmed that compound **69** was maingayic acid B (Pham et al. 2000).

Table 3.7: ^1H NMR and ^{13}C NMR spectroscopic assignments of compound **69** in methanol- d_4

Position	δ_{H} (ppm)		δ_{C} (ppm)	
	Experimental	Literature (Pham et al., 2000)	Experimental	Literature (Pham et al., 2000)
1	-	-	178.0	177.8
2	2.27 (<i>t</i> , $J = 8.0$ Hz)	2.26 (<i>t</i> , $J = 7.5$ Hz)	35.2	35.0
3	1.57 (<i>brt</i> , $J = 8.0$ Hz)	1.56 (<i>m</i>)	26.3	26.0
4	1.32 ^a (<i>brs</i>)	1.26 (<i>brs</i>)	30.4 ^b	30.2
5	1.32 ^a (<i>brs</i>)	1.26 (<i>brs</i>)	30.4 ^b	30.2
6	1.32 ^a (<i>brs</i>)	1.26 (<i>brs</i>)	30.5 ^b	30.3
7	1.32 ^a (<i>brs</i>)	1.26 (<i>brs</i>)	30.6 ^b	30.4
8	1.57 (<i>brt</i> , $J = 8.0$ Hz)	1.56 (<i>m</i>)	33.2	32.9
9	2.49 (<i>t</i> , $J = 8.0$ Hz)	2.47 (<i>t</i> , $J = 7.6$ Hz)	36.2	36.0
10	-	-	135.0	134.8
11	6.97 (<i>d</i> , $J = 8.0$ Hz)	6.95 (<i>d</i> , $J = 8.3$ Hz)	130.4	130.2
12	6.68 (<i>d</i> , $J = 8.0$ Hz)	6.68 (<i>d</i> , $J = 8.3$ Hz)	116.1	116.0
13	-	-	156.4	156.1
14	6.68 (<i>d</i> , $J = 8.0$ Hz)	6.68 (<i>d</i> , $J = 8.3$ Hz)	116.1	116.0
15	6.97 (<i>d</i> , $J = 8.0$ Hz)	6.95 (<i>d</i> , $J = 8.3$ Hz)	130.4	130.2

^a Overlapping signals

^b Chemical shifts are interchangeable

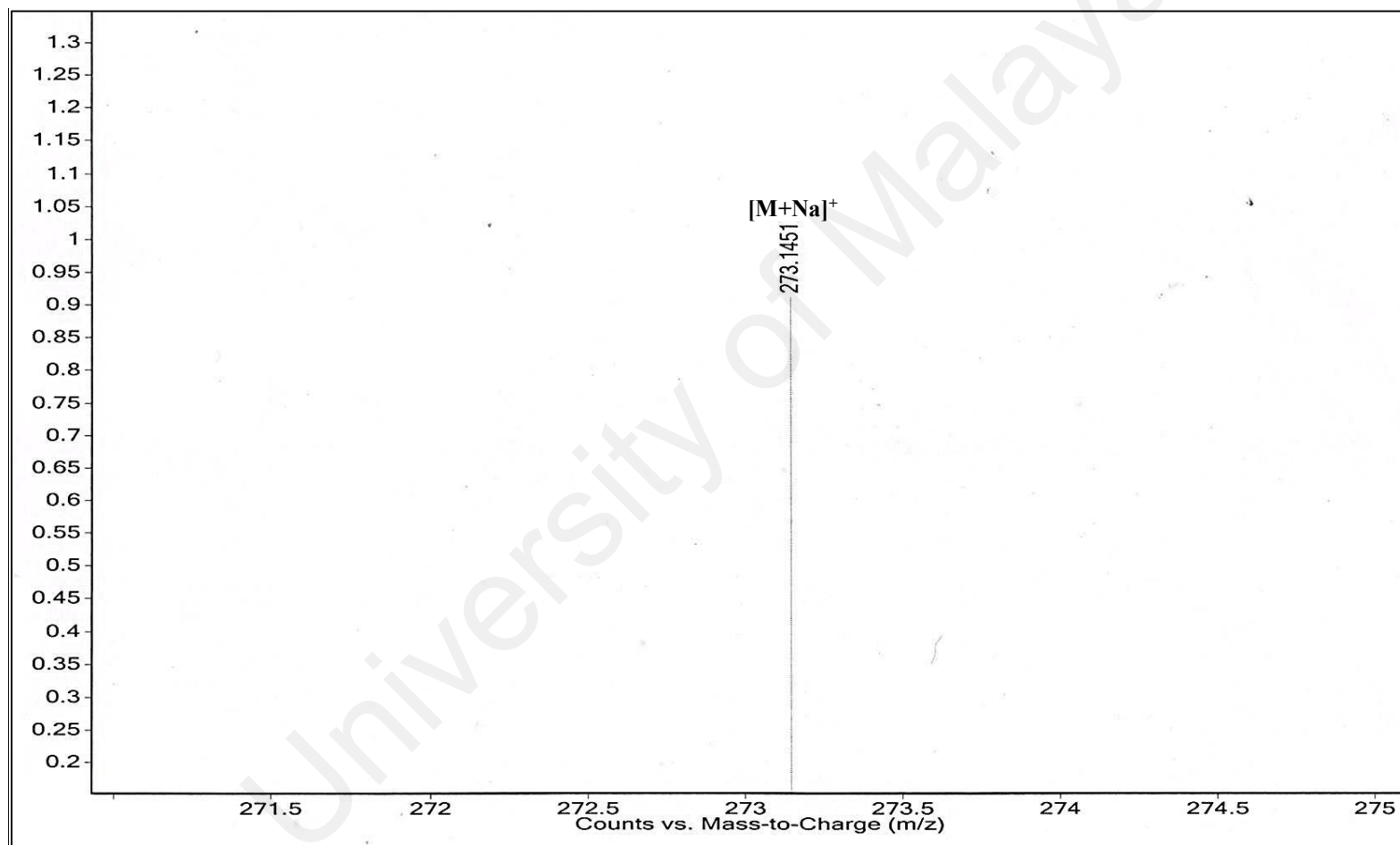


Figure 3.50: Mass spectrum of compound **69**

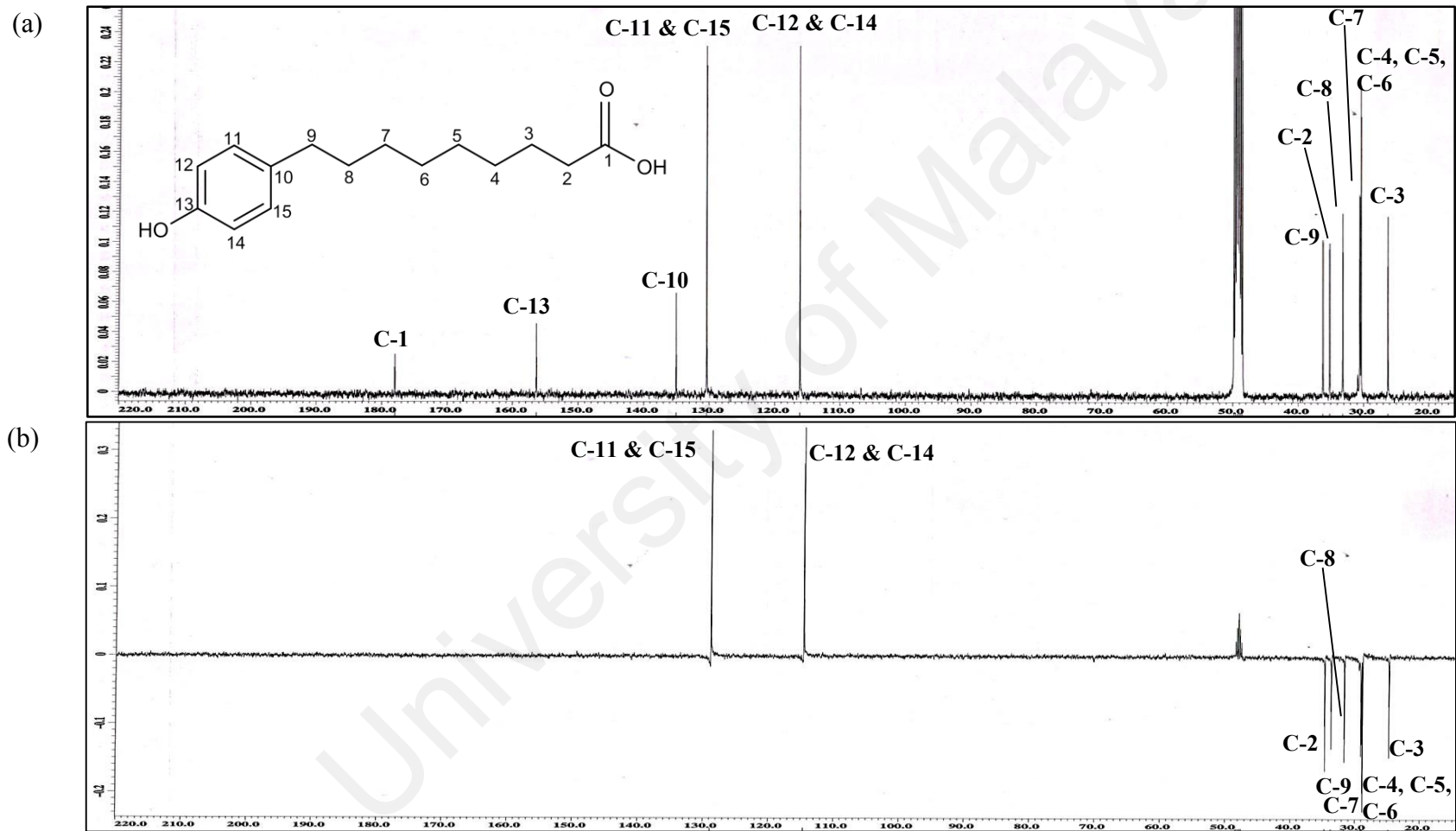


Figure 3.51: ^{13}C NMR (a) and DEPT-135 (b) spectra of compound **69**

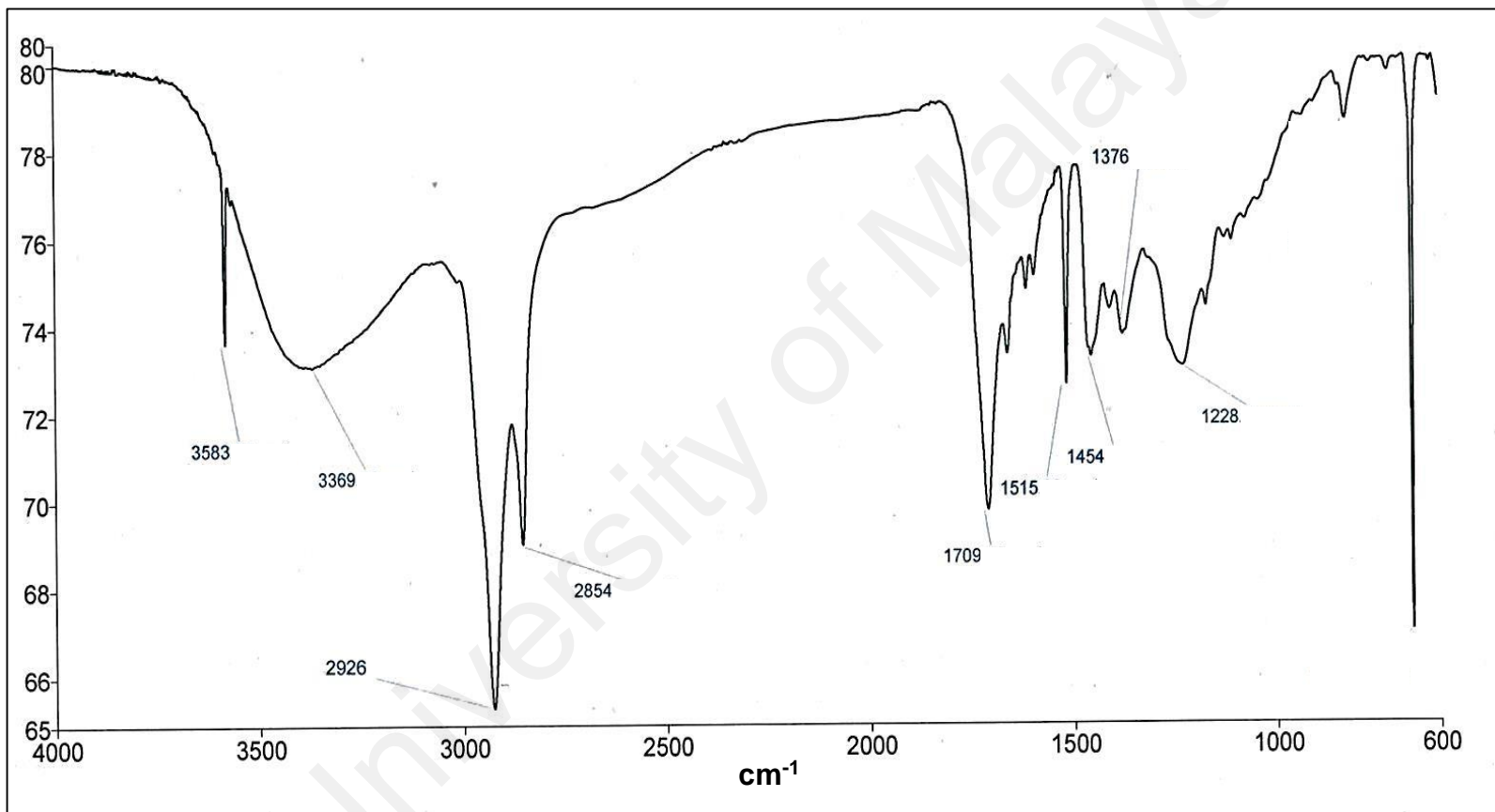


Figure 3.52: IR spectrum of compound 69

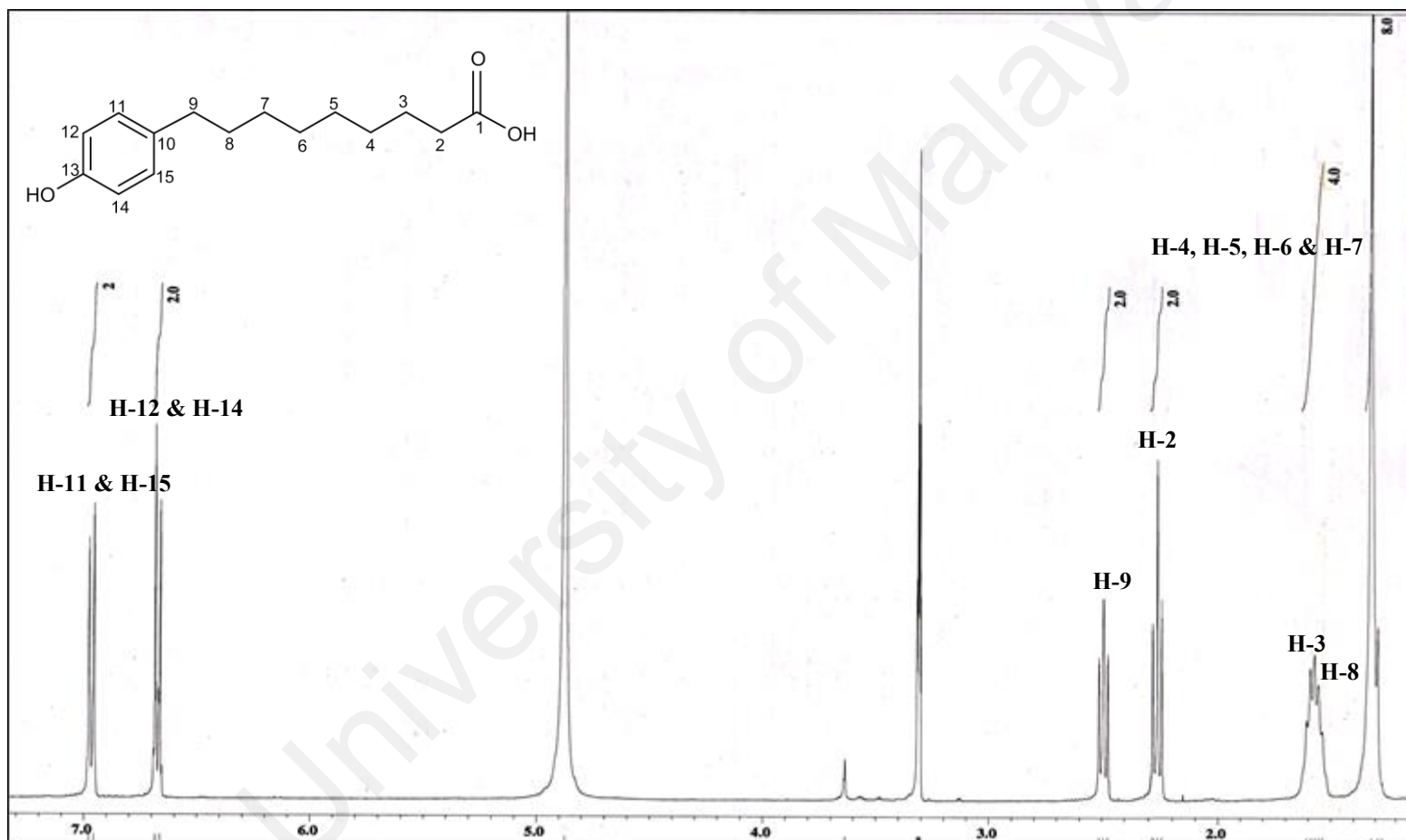


Figure 3.53: ¹H NMR spectrum of compound 69

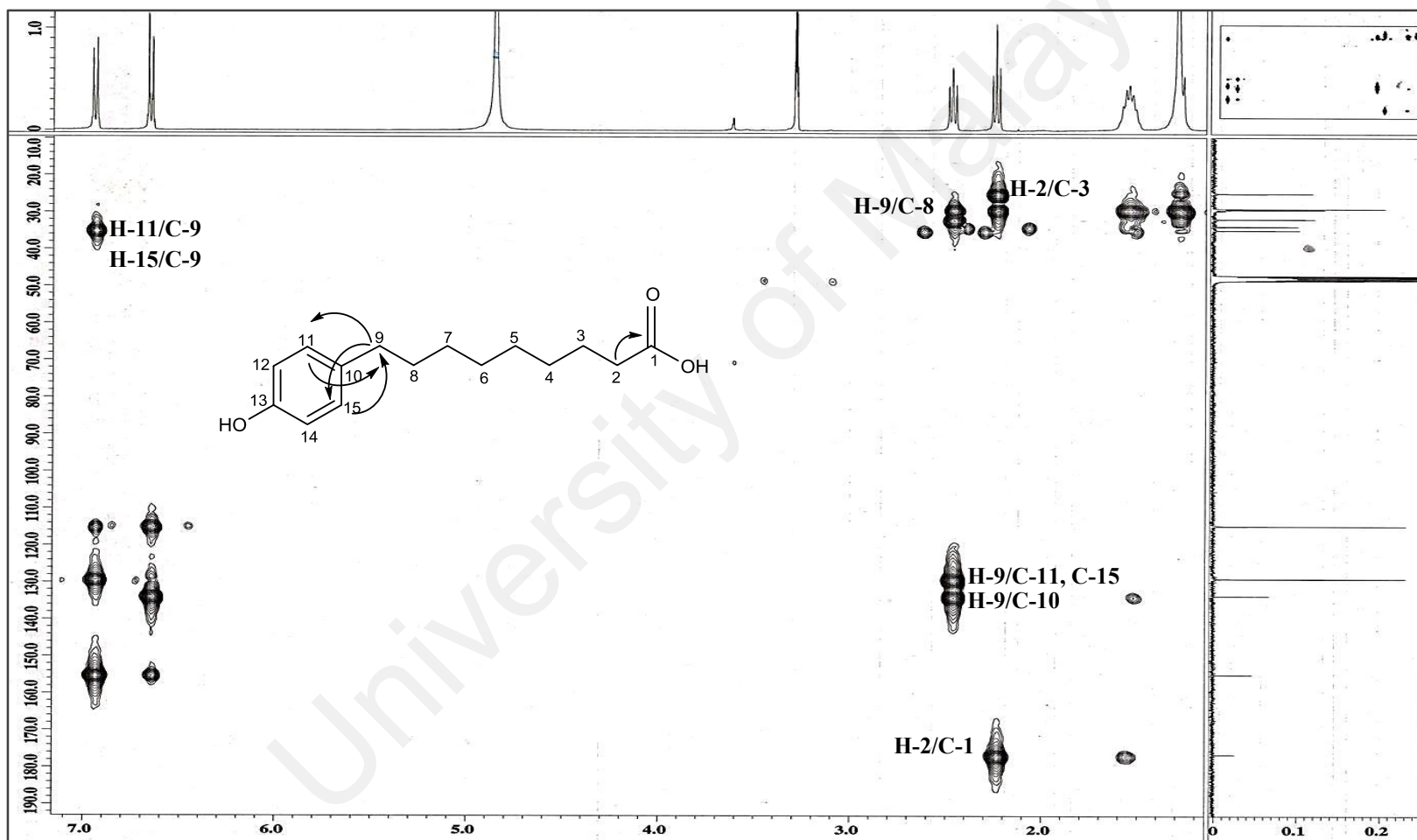


Figure 3.54: Selected HMBC correlations of compound 69

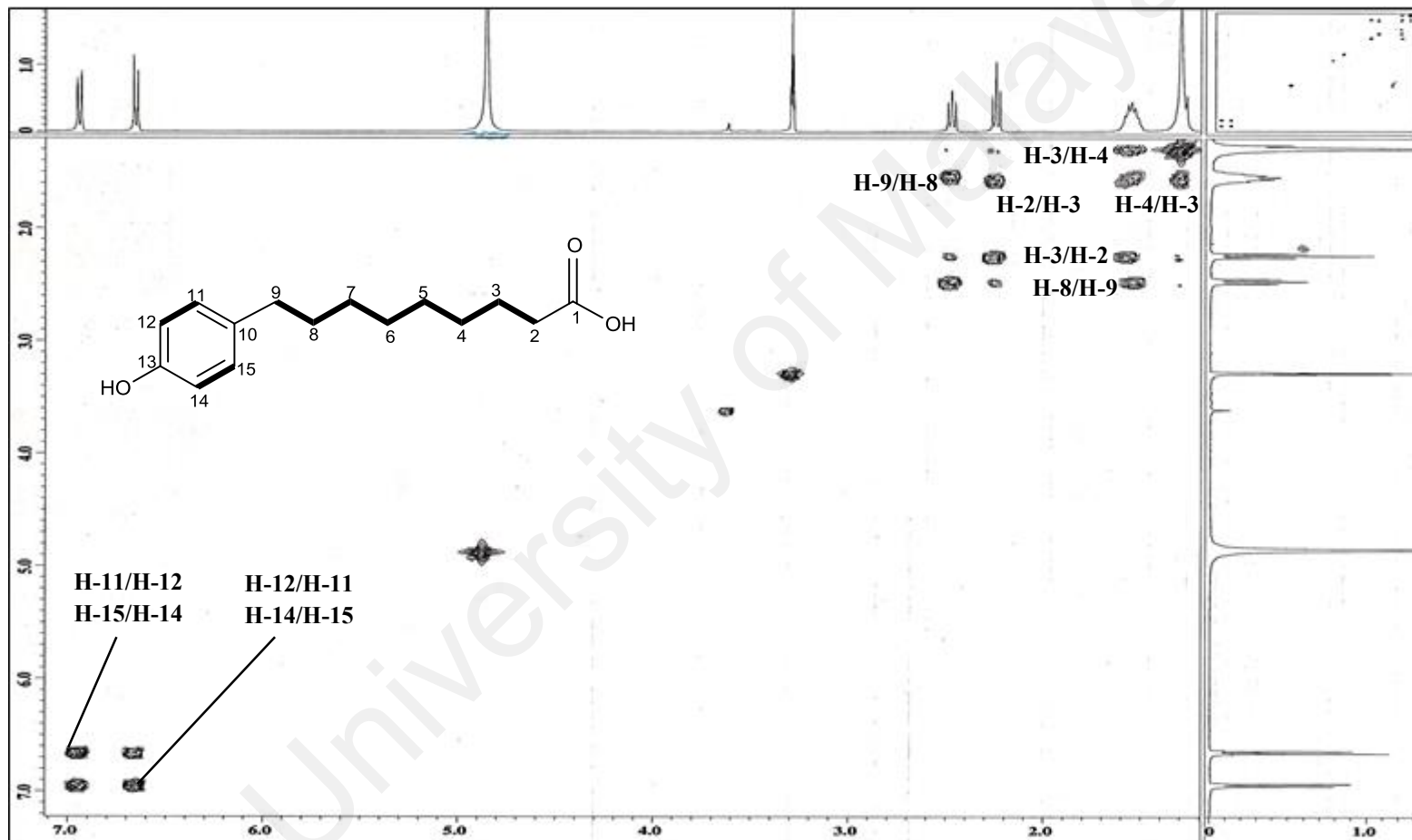


Figure 3.55: Selected COSY correlations of compound **69**

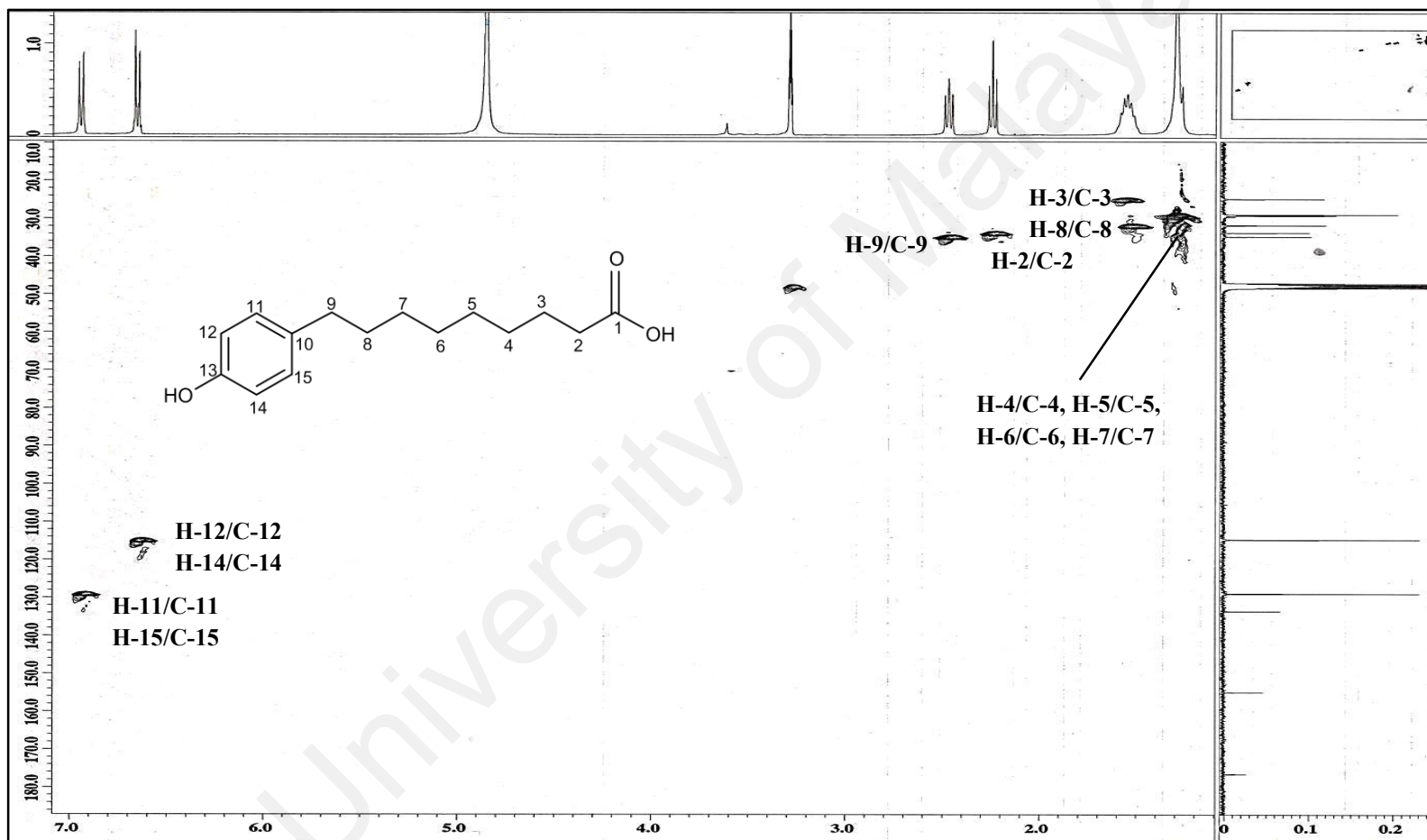


Figure 3.56: HSQC correlations of compound 69

3.2 Comparison between the secondary metabolites isolated from the fruits of *M. cinnamomea* in the current and previous investigations

A previous investigation of the fruits carried out by Sawadjoon and his co-workers (Sawadjoon et al., 2002) revealed high contents of atropisomeric flavans; myristinins A-F (**22-27**). They did not detect the acylphenols and dimeric acylphenols (**1-5** and **72**) isolated in this study. These marked differences in the phytochemical composition as determined by Sawadjoon and his co-workers from that of the present study could mainly be attributed to the source of collection of the plant material. The plant material used for the current study was collected from Johor, the southern part of Malaysia while that of the previous investigation was collected from Thailand, the northern border of Malaysia. Apart from geographical location, other factors such as vegetative stage, growing season of the plant under investigation, soil content and maturity of the plant species upon time of harvest could have given rise to these differences as well (Sari et al, 2006).

3.3 Cholinesterase inhibitory activities

Initial AChE and BChE inhibitory activities of compounds **1-5**, **69** and **72** were assayed at 100 µg/mL. Except for compound **69**, the remaining compounds (**1-5** and **72**) exhibited more than 75 % and 69 % inhibition towards the AChE and BChE, respectively. Subsequently, compounds **1-5** and **72** were further evaluated in order to determine their respective IC₅₀ values. The IC₅₀ values and selectivity indices of compounds **1-5** and **72** along with the reference standard, physostigmine are given in Table 3.8. Compounds **1** (IC₅₀ = 1.31 ± 0.17 µM), **2** (IC₅₀ = 1.84 ± 0.19 µM), **3** (IC₅₀ = 1.94 ± 0.27 µM) and **72** (IC₅₀ = 6.44 ± 0.85 µM), actively inhibited the AChE with compound **1** being the most potent among the four. As for the BChE, it was strongly inhibited by compounds **2** (IC₅₀

= $1.76 \pm 0.21 \mu\text{M}$), **3** ($\text{IC}_{50} = 2.80 \pm 0.49 \mu\text{M}$) and **72** ($\text{IC}_{50} = 6.65 \pm 0.13 \mu\text{M}$) with the former being a more effective inhibitor compared to the latter two. In contrary, compounds **4** and **5** were moderate AChE and BChE inhibitors with IC_{50} values ranging between 10.51 ± 2.07 - $30.67 \pm 8.14 \mu\text{M}$ (Abdul Wahab et al., 2016).

A closer look at the structures of compounds **1-5**, **69** and **72** provided further insight as to how the activities of these acylphenols (compounds **1-3** and **72**) and dimeric acylphenols (compounds **4** and **5**) might have been influenced by the chemical groups in their respective structures. The AChE inhibiting potential of compounds **1-3** may have decreased with the increase in the number of hydroxyl groups in their ring b (Figure 3.57). The lower AChE inhibiting potential of compound **72** upon comparison to compound **2** could have resulted from the additional hydroxyl group in its ring a (Figure 3.57). When the activities of compounds **1-3** and **72** were compared to that of compound **69**, the inactivity of compound **69** led to the assumption that the presence of two aromatic rings was a prerequisite for the AChE inhibitory activity. The dimeric acylphenols (compounds **4** and **5**) were weaker AChE inhibitors as compared to their monomers (compounds **2** and **3**) which they were constructed from. Therefore, one could postulate that dimerization which in turn resulted in the bulkiness of compounds **4** and **5** could have contributed to the decrease in their activity which was in agreement with the findings of Maia et al, 2008. However, the greater activity of compound **4** in comparison to compound **5** could have been due to the fact that the former bore two hydroxyl groups in its ring b' unlike the latter whose ring b' only bore a single hydroxyl group. In the case of the BChE inhibition studies, the presence of two aromatic rings was also essential for the inhibition of this enzyme. Among the acylphenols; compounds **1-3** and **72**, compound **1** showed the weakest activity ($\text{IC}_{50} = 39.21 \pm 3.46 \mu\text{M}$), which could have been due to the absence of the hydroxyl group in its ring b unlike compounds **2**, **3** and **72** which bore one or two

hydroxyl groups in their ring b. Similarly, compound **4** was a slightly more effective BChE inhibitor compared to compound **5** as its ring b' was more highly oxygenated (Abdul Wahab et al., 2016).

With regard to the selectivity of the compounds, it is interesting to note that compounds **2-4** and **72** were dual inhibitors, with almost equal inhibitory action against the AChE and BChE. Compound **1** like physostigmine was an AChE selective inhibitor. In contrary, compound **5** was a BChE inhibitor (Abdul Wahab et al., 2016). Dual inhibitors play an important role in the treatment of AD. As AD progresses, acetylcholine (ACh) regulation may become increasingly dependent on the BChE and dual inhibitors may provide more sustained efficacy than the AChE-selective agents (Ballard, 2002). In addition, new findings show that both AChE and BChE are involved in the breakdown of ACh in the brain and dual inhibition of these enzymes may increase the efficacy of treatment and broaden the indications (Giacobini, 2004; Tan, 2014).

Table 3.8: Cholinesterase inhibition activities of compounds **1-5**, **69**, **72** and physostigmine (Abdul Wahab et al., 2016)

Compounds	Percentage Inhibition at 100 $\mu\text{g/mL}^{\text{a}}$		IC_{50} (μM) ^a		Selectivity Index	
	AChE	BChE	AChE	BChE	AChE ^b	BChE ^c
1	97.42 \pm 2.09	69.55 \pm 6.31	1.31 \pm 0.17	39.21 \pm 3.46	32.95	0.04
2	95.86 \pm 0.64	87.35 \pm 8.58	1.84 \pm 0.19	1.76 \pm 0.21	0.96	1.05
3	97.09 \pm 3.00	94.13 \pm 1.40	1.94 \pm 0.27	2.80 \pm 0.49	1.44	0.69
72	99.39 \pm 0.37	86.85 \pm 1.42	6.44 \pm 0.85	6.65 \pm 0.13	1.03	0.97
4	75.39 \pm 0.67	81.11 \pm 3.07	12.66 \pm 1.48	10.51 \pm 2.07	0.83	1.20
5	91.48 \pm 1.17	86.74 \pm 1.46	30.67 \pm 8.14	12.52 \pm 2.86	0.41	2.45
69	45.13 \pm 9.23	48.96 \pm 1.61	-	-	-	-
Physostigmine	-	-	0.08 \pm 0.02	0.22 \pm 0.02	2.75	0.36

^a Data presented as Mean \pm SD (n = 3)

^b Selectivity for AChE is defined as IC_{50} (BChE)/ IC_{50} (AChE)

^c Selectivity for BChE is defined as IC_{50} (AChE)/ IC_{50} (BChE)

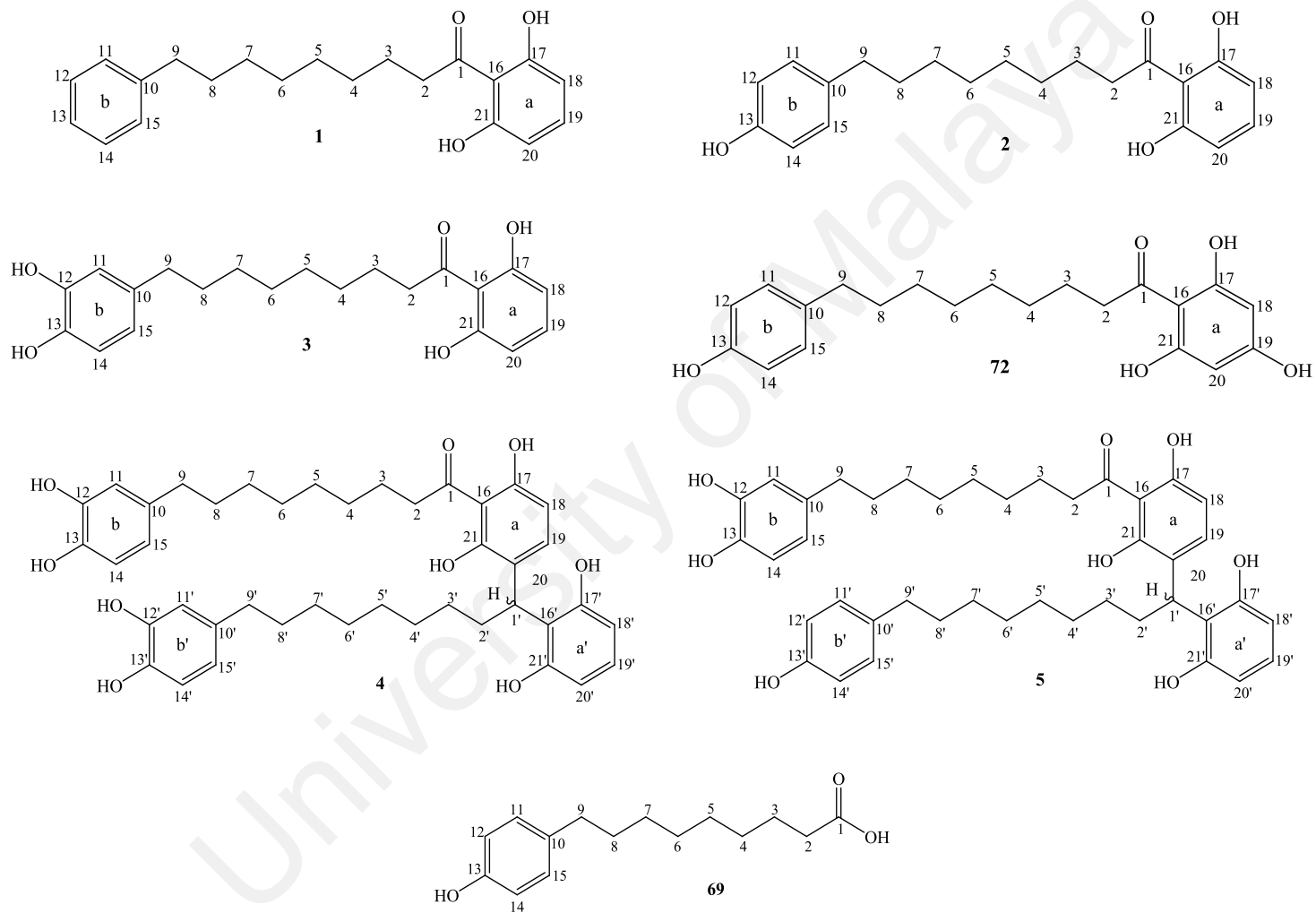


Figure 3.57: Structures of compounds 1-5, 69 and 72

Cholinesterase inhibition kinetics were determined for the dual inhibitors; compounds **2** and **3**, which showed significant interactions with both the AChE and BChE. As illustrated in the Lineweaver-Burk plot analyses (Figure 3.58), compounds **2** and **3** both displayed mixed-mode inhibition against the AChE and BChE as indicated by their data lines which either intersected in the first (for inhibition of the BChE) or second (for inhibition of the AChE) quadrants (Abdul Wahab et al., 2016; Khaw et al., 2014). This type of inhibitor is able to bind to the active site of the enzyme as well as at different sites of the enzyme (allosteric site) due to the allosteric effect (Khaw et al., 2014). The inhibition constants, K_{iAChE} and K_{iBChE} , which were derived from the secondary plots (Figure 3.59) of compounds **2** (4.33 μ M and 0.56 μ M, respectively) and **3** (5.86 μ M and 11.46 μ M, respectively), inferred that compound **2** had a higher affinity to both enzymes in particular to the BChE rather than compound **3** (Abdul Wahab et al., 2016). A smaller value of the inhibition constant indicates a stronger inhibition (Majouli et al., 2016).

Since compounds **2** and **3** were active dual inhibitors towards the AChE and the BChE, molecular docking studies were performed in order to understand the binding interactions between the two active compounds with both the enzymes. For the AChE, the aromatic rings a of both the active compounds were involved in hydrophobic interactions with His 440 from the catalytic triad. In addition, hydrogen bonds were formed between the hydroxyl group at C-21 for both compounds (Figure 3.57) with Ser 200 from the catalytic triad as well as Gly 118 and Gly 119 from the oxyanion hole (Figure 3.60). The catalytic triad is the active site of the enzyme where acetylcholine is hydrolyzed into choline and acetate while the oxyanion hole provides hydrogen bond donors that stabilises the tetrahedral transition state of the substrate. Hydrophobic interaction was observed between the aromatic ring b of compound **2** (Figure 3.57) with Asp 72 from the peripheral anionic site (PAS) while the hydroxyl group at C-12 of compound **3** (Figure 3.57) formed

hydrogen bonding with Asp 72 from the PAS (Figure 3.60). The PAS is located at the entrance of the active site gorge of both the AChE and BChE. The binding of the acetylcholine to the PAS is the first step in the catalytic pathway and allosteric modulations. The PAS is known to be involved in accelerating non-cholinergic functions such as cell adhesion, neurite outgrowth and amyloid β deposition in AD (Johnson and Moore, 2006). Hence, amyloid β deposition can be reduced or prevented with the presence of the PAS blocker (Inestrosa et al., 1996). Since compounds **2** and **3** were involved in the binding interaction with Asp 72; an essential component of the PAS in the AChE (Masson et al., 1996), it can be proposed that the potency of both compounds in inhibiting the cholinesterase activity started through the blocking at the PAS before the inhibition of the binding of the substrate at the active site. Since compounds **2** and **3** both had binding interactions with the active site (catalytic triad) and the allosteric site (PAS and oxyanion hole) of the AChE, the finding was in agreement with the mode of inhibition of both compounds; mixed-mode inhibition (Abdul Wahab et al., 2016).

For the BChE, hydrogen bond interactions were observed between both compounds with the enzyme. The hydroxyl group at C-17 and the carbonyl group at C-1 (Figure 3.57) formed hydrogen bonds with Ser 198 from the catalytic triad (Figure 3.61). Besides, hydrogen bonds were also formed between the carbonyl group at C-1 with Gly 116 and Gly 117 from the oxyanion hole (Figure 3.61). The only difference in the binding interactions of compounds **2** and **3** with the BChE was that the hydroxyl group at C-12 of compound **3** (Figure 3.57) formed a hydrogen bond with His 438 from the catalytic site while the aromatic ring b of compound **2** (Figure 3.57) underwent hydrophobic interaction with Tyr 332 from the peripheral anionic site. It can be suggested that the binding of compound **2** to the PAS of the BChE played an important role in inhibiting the binding of the substrate which in turn gave rise to its lower IC_{50} value (1.76 μ M) of the

cholinesterase inhibitory activity compared to compound **3** (IC_{50} value: 2.80 μ M). In addition, the finding was also in agreement with the mode of inhibition for both compounds; mixed-mode inhibition, whereby both compounds were able to bind to the active site (catalytic triad) and the allosteric site (PAS and oxyanion hole) of the BChE (Abdul Wahab et al., 2016).

For physostigmine (Figure 3.62), its ring c formed hydrophobic interactions with Gly 118 from the oxyanion hole and Trp 84 from the choline binding site (CBS) of the AChE. The methyl group at C-6 also formed hydrophobic interaction with Trp 84 and the oxygen atom of the ester group at C-9 formed hydrogen bond with Ser 122 of the AChE (Figure 3.60). Besides, at the CBS of the BChE, the methyl group at C-6 of physostigmine formed hydrophobic interaction with Trp 82. Hydrogen bonds were observed between the ester group at C-9 of physostigmine with Ser 198 and His 438 from the catalytic triad. In addition, the ketone group at C-13 of physostigmine formed a hydrogen bond with Ser 198 from catalytic triad. Hydrogen bonds were formed between Gly 117 and Ala 199 of the oxyanion hole of the BChE with the ketone group at C-13 of physostigmine (Figure 3.61). The binding interaction data for compounds **2**, **3** and physostigmine with the amino acid residues of *TcAChE* and *hBChE* are summarized in Table 3.9 (Abdul Wahab et al., 2016).

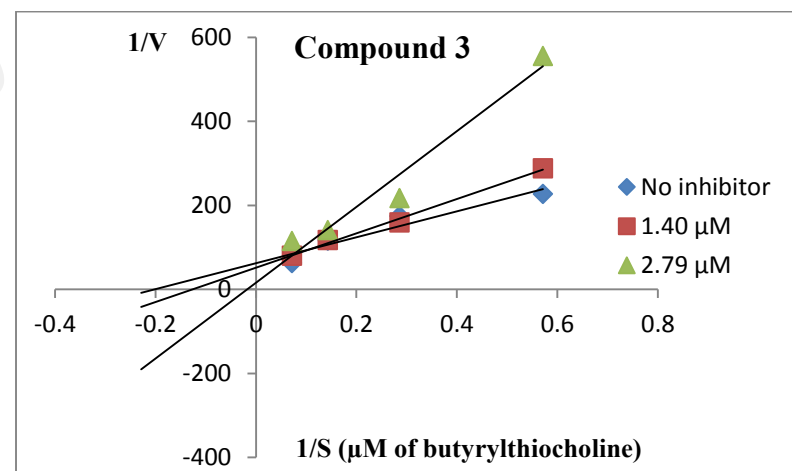
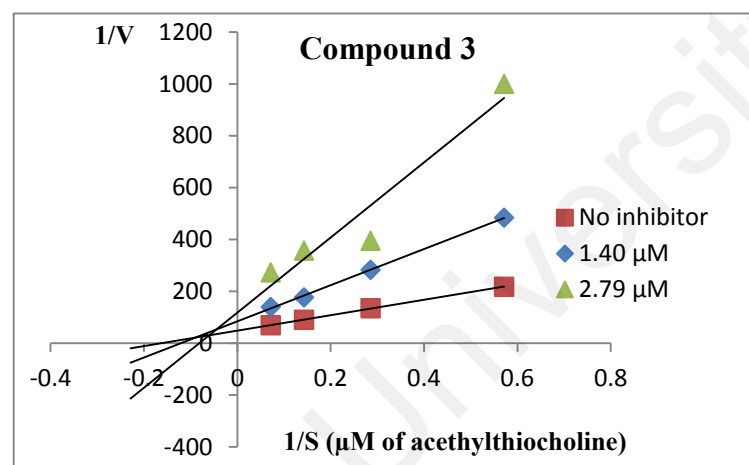
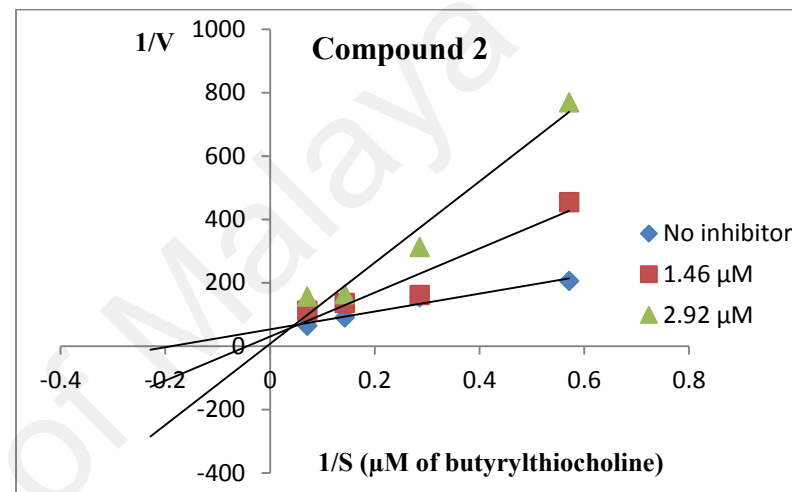
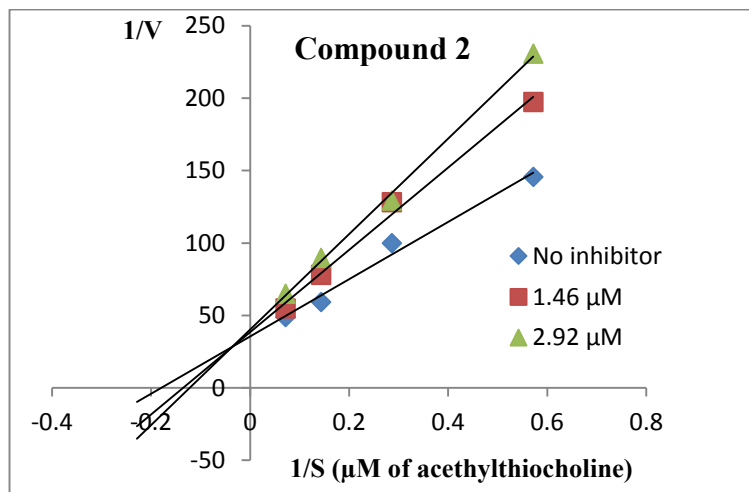


Figure 3.58: Lineweaver-Burk plots of cholinesterase inhibition activities of compounds 2 and 3 (Abdul Wahab et al., 2016)

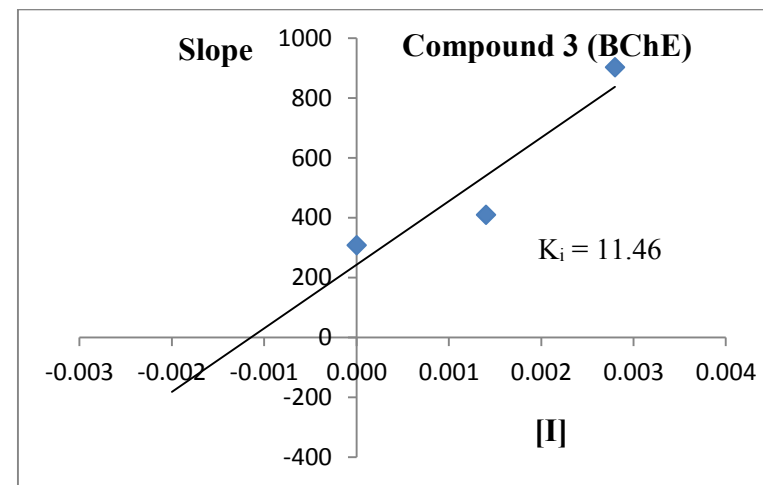
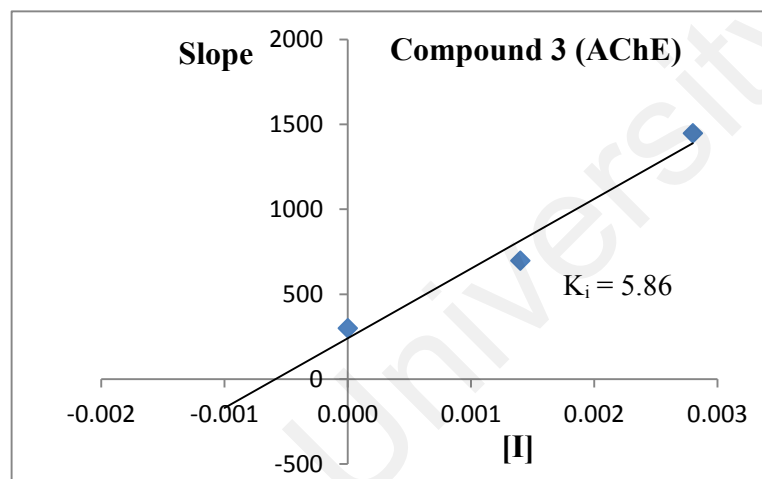
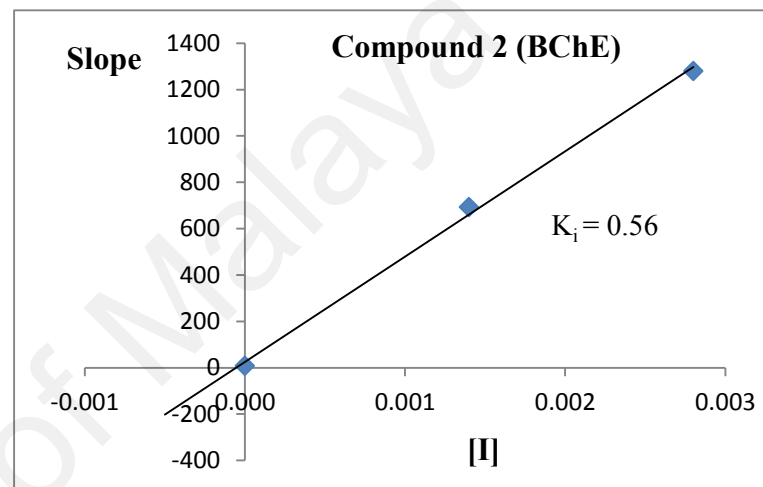
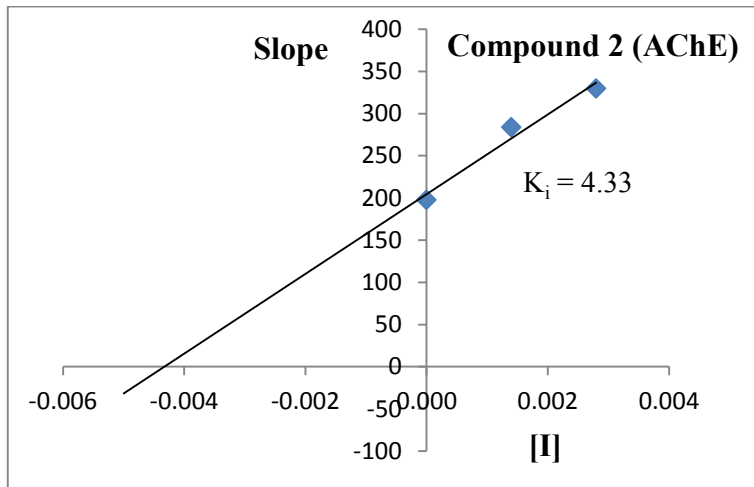


Figure 3.59: Secondary plot of Lineweaver-Burk plots of compounds 2 and 3 (Abdul Wahab et al., 2016)

Table 3.9: Binding interaction data for compounds **2**, **3** and physostigmine with amino acid residues of *TcAChE* and *hBChE* (Abdul Wahab et al., 2016)

Ligand/Compound	Enzyme	Binding Energy (kcal)	Interacting site	Residue	Type of Interaction	Distance (Å)	Ligand Interacting
Malabaricone B (3)	<i>TcAChE</i>	-13.32	Catalytic triad	Ser 200	Hydrogen	2.26	Hydroxyl group at C-21
				His 440	Hydrophobic	-	Aromatic ring a
			Oxyanion hole	Gly 118	Hydrogen	1.97	Hydroxyl group at C-21`
				Gly 119	Hydrogen	2.12	
	Peripheral anionic	Asp 72	Hydrophobic	-	Aromatic ring b		
	<i>hBChE</i>	-12.82	Catalytic triad	Ser 198	Hydrogen	2.99	Hydroxyl group at C-17
					Hydrogen	2.71	Carbonyl group at C-1
			Oxyanion hole	Gly 116	Hydrogen	2.29	Carbonyl group at C-1
				Gly 117	Hydrogen	2.12	
			Peripheral anionic	Tyr 332	Hydrophobic	-	Aromatic ring b
Malabaricone C (4)			<i>TcAChE</i>	-13.27	Catalytic triad	Ser 200	Hydrogen
	His 440	Hydrophobic				-	Aromatic ring a
	Oxyanion hole	Gly 118			Hydrogen	2.26	Hydroxyl group at C-21
		Gly 119			Hydrogen	2.07	
	Peripheral anionic	Asp 72	Hydrogen	3.05	Hydroxyl group at C-12		
	<i>hBChE</i>	-12.30	Catalytic triad	Ser 198	Hydrogen	2.65	Hydroxyl group at C-17
					Hydrogen	2.76	Carbonyl group at C-1
			Oxyanion hole	His 438	Hydrogen	3.11	Hydroxyl group at C-12
				Gly 116	Hydrogen	2.14	Carbonyl group at C-1
				Gly 117	Hydrogen	2.13	

Physostigmine	<i>TcAChE</i>	-9.78	Oxyanion hole	Gly 118	Hydrophobic	-	Aromatic ring C
			Choline binding site	Trp 84	Hydrophobic	-	Aromatic ring C
			Wall of gorge	Ser 122	Hydrogen	2.29	Methyl group at C-6 Ester group at C-9
	<i>hBChE</i>	-9.65	Choline binding site	Trp 82	Hydrophobic	-	Methyl group at C-6
			Catalytic triad	Ser 198	Hydrogen	2.91	Ester group at C-9
						2.64	Ketone group at C-13
				His 438	Hydrogen	2.48	Ester group at C-9
			Oxyanion hole	Gly 117	Hydrogen	2.01	Ketone group at C-13
				Ala 199	Hydrogen	2.33	

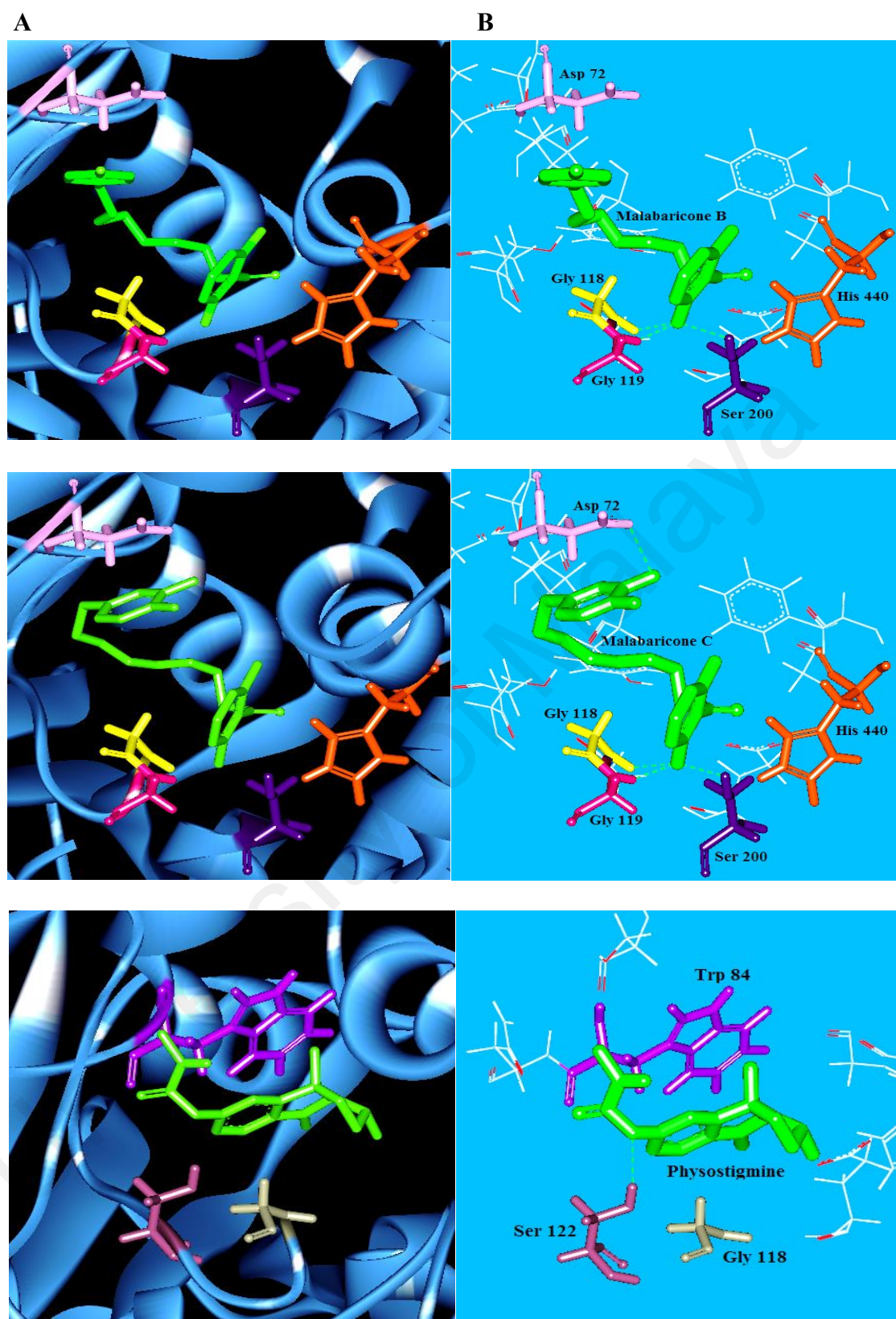


Figure 3.60: (A) View of compounds **2** (up), **3** (middle) and physostigmine at the binding site of AChE (protein structures are represented by solid ribbon format). (B) Simplified view of compounds **2** (up), **3** (middle) and physostigmine interacting with the surrounding amino acid residues which are shown in stick format. The hydrogen bond interaction of the ligands (compounds) with the amino acid residues are shown in green dotted lines (Abdul Wahab et al., 2016)

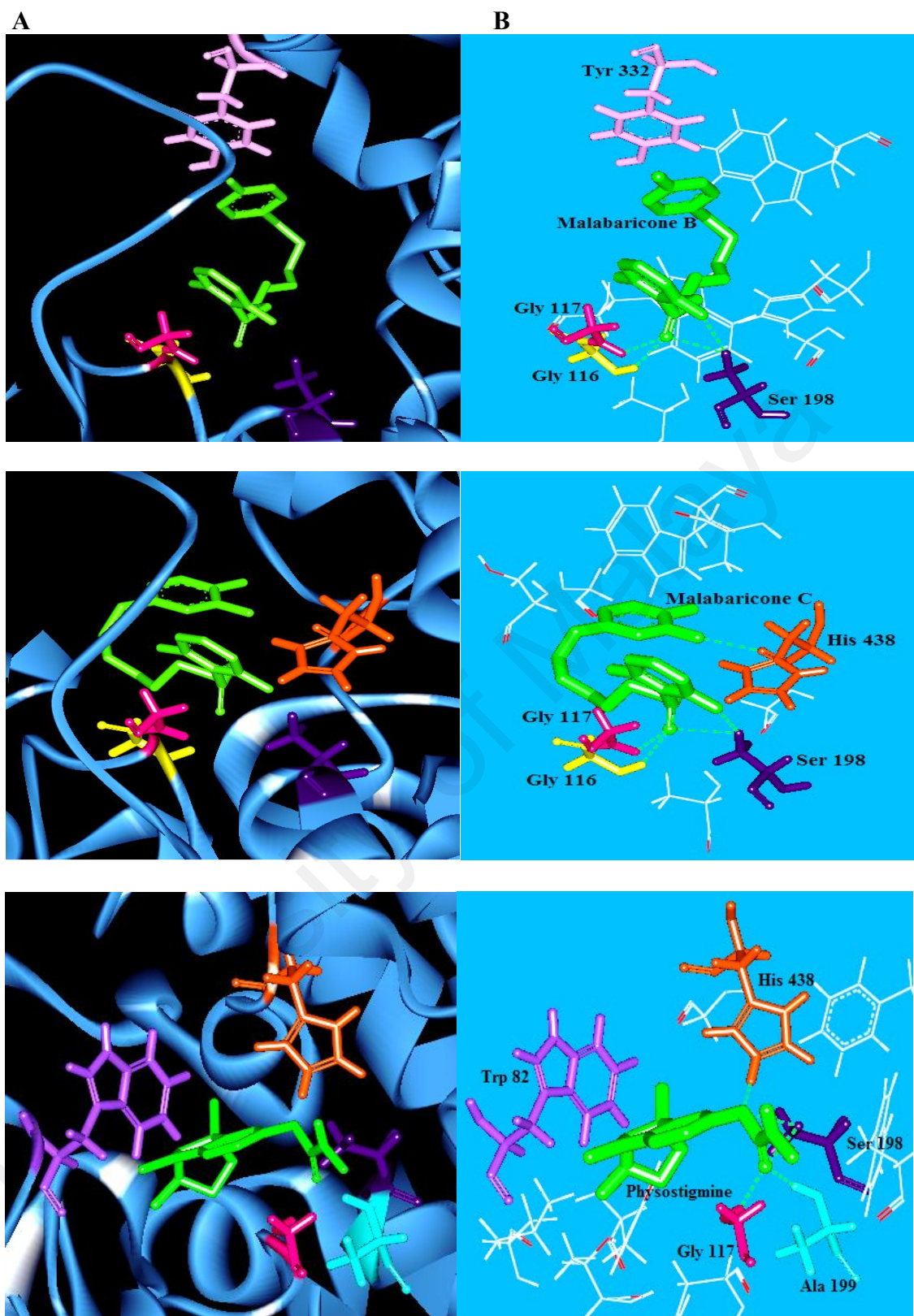


Figure 3.61: (A) View of compounds **2** (up), **3** (middle) and physostigmine at the binding site of BChE (protein structures are represented by solid ribbon format). (B) Simplified view of compounds **2** (up), **3** (middle) and physostigmine interacting with the surrounding amino acid residues which are shown in stick format. The hydrogen bond interaction of the ligands (compounds) with the amino acid residues are shown in green dotted lines (Abdul Wahab et al., 2016)

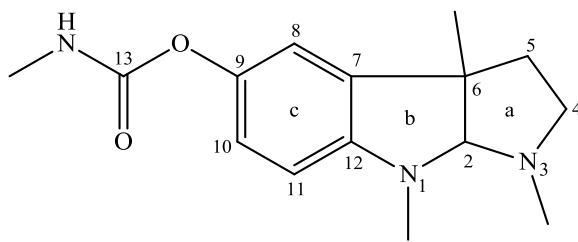


Figure 3.62: Structure of physostigmine (reference standard)

University of Malaya

CHAPTER 4

CONCLUSION

The ethyl acetate extract of the dried fruits of *M. cinnamomea* at 100 µg/mL was found to inhibit the acetylcholinesterase (AChE) (95.93 ± 7.86 %) and butyrylcholinesterase (BChE) (70.00 ± 13.17 %) enzymes. The extract was subjected to repeated column chromatography over silica gel or Sephadex LH-20 and preparative TLC to yield seven compounds (**1-5**, **69** and **72**) among which compound **72** was identified to be a new acylphenol, malabaricone E. Compounds **1-5** and **69** were characterized as the known malabaricones A-C (**1-3**), maingayones A and B (**4** and **5**) and maingayic acid B (**69**). Their structures were elucidated on the basis of 1D and 2D NMR techniques and LCMS-IT-TOF analysis.

The AChE and BChE inhibiting potentials of compounds **1-5**, **69** and **72** were evaluated with the intention of identifying the compound(s) which could be responsible in giving rise to the respective activities. Kinetic and molecular docking studies were carried out on the compound(s) which actively inhibited each enzyme in order to determine their mode of inhibition (competitive, non-competitive or mixed-type) and to investigate the site at which the active compound(s) bind to the enzymes.

In summary, compounds **2** and **3** were dual mixed-mode inhibitors as they each actively inhibited the AChE and BChE with low IC_{50} values in the range of 1.76 ± 0.21 - 2.80 ± 0.49 µM. Compound **2** however was found to have a higher affinity towards both enzymes. Molecular docking simulation revealed that compounds **2** and **3** interacted with the peripheral anionic site (PAS), the catalytic triad and the oxyanion hole of the AChE.

As for the BChE, compound **2** also interacted with the PAS, the catalytic triad and the oxyanion hole while compound **3** only interacted with the catalytic triad and the oxyanion hole. Therefore, both of the above mentioned acylphenols are promising candidates in the search for natural drugs which can be employed to cure diseases related to neurodegenerative disorders, in particular in the treatment of AD.

The moderate to strong cholinesterase inhibitory activities of all of the acylphenols and dimeric acylphenols isolated in the present study provided scientific evidence for the possible usage of the fruits of *M. cinnamomea* as a natural remedy especially as memory enhancers like the fruits of its closely related species, *M. fragrans* (nutmeg).

University of Malaya

CHAPTER 5

MATERIALS AND EXPERIMENTAL

5.1 Plant Material

M. cinnamomea was collected from Hutan Simpan Labis, Segamat, Johor in 2003. The plant was identified by Mr. Teo Leong Eng and a voucher specimen (KL 5043) was deposited in the herbarium of the Department of Chemistry, Faculty of Science, University of Malaya, Kuala Lumpur.

5.2 Chemicals and Reagents

1. *Acetone (Chemolab, Malaysia)
2. *Dichloromethane (Chemolab, Malaysia)
3. *Ethyl Acetate (Chemolab, Malaysia)
4. *Methanol (Chemolab, Malaysia)
5. Methanol AR grade (Chemolab, Malaysia)
6. Methanol spectroscopy grade (Merck, Germany)
7. Methanol- d_4 , with 99.8 atom % D (Merck, Germany)
8. Sephadex LH-20 (Sigma-Aldrich, USA)
9. Silica Gel 60 for column chromatography, (0.040-0.063 mm) (230-400 mesh ASTM)
(Merck, Germany)

10. TLC Aluminium Sheets, Silica Gel 60 F₂₅₄, 20 cm x 20 cm (Merck, Germany)
11. Silica Gel 60 F₂₅₄, pre-coated glass plates 20 cm x 20 cm x 0.5 mm (Merck, Germany)
12. Celite (Merck, Germany)
13. Ferric Chloride, FeCl₃.6H₂O (Merck, Germany)
14. 5, 5'-Dithiobis (2-nitrobenzoic acid) (Sigma-Aldrich, USA)
15. Physostigmine (Sigma-Aldrich, USA)
16. Sodium Dihydrogen Phosphate Anhydrous AR (Sigma-Aldrich, USA)
17. Disodium Dihydrogen Phosphate Anhydrous AR (Sigma-Aldrich, USA)
18. Butyrylcholinesterase from Equine Serum (Sigma-Aldrich, USA)
19. S-Butyrylthiocholine Chloride (Sigma-Aldrich, USA)
20. Acetylcholinesterase (Sigma-Aldrich, USA)
21. Acetylthiocholine Iodide (Sigma-Aldrich, USA)

* Solvents were distilled prior to use

5.2.1 Preparation of Detecting Reagent

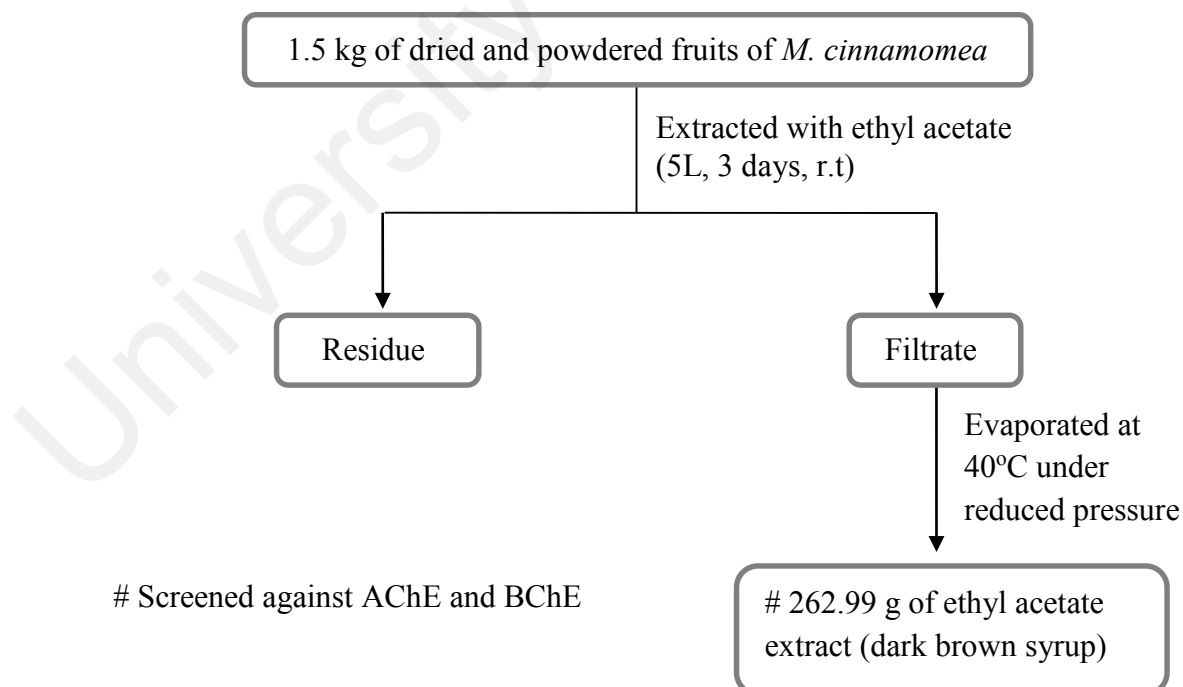
1% Ferric chloride

1 g of ferric chloride was dissolved in 100 mL of methanol. Developed TLC aluminium sheets were dipped into the reagent following which an immediate change in colour will indicate the presence of phenolic compounds.

5.3 Isolation and Purification of the Secondary Metabolites from the Fruits of *M. cinnamomea*

5.3.1 Extraction Procedure

Dried and powdered fruits (1.5 kg) of *M. cinnamomea* were soaked in ethyl acetate (5 L) at room temperature for three days and then filtered. The resulting filtrate was evaporated to dryness under reduced pressure to afford 262.99 g of dark brown syrup.



Scheme 5.1: Extraction procedure of the fruits of *M. cinnamomea*

5.3.2 Separation Techniques

5.3.2.1 Thin Layer Chromatography (TLC)

Preliminary investigation of the chromatographic separation of the crude ethyl acetate extract was carried out using TLC aluminium sheets (7 cm x 1 cm). Different solvent systems were employed to identify the system which could achieve the best separation for the ethyl acetate extract. The selected solvent systems were later utilized in its column chromatographic separation to isolate the pure compounds. Developed TLC sheets were visualized using an UV lamp (365 nm) and dipped in 1 % FeCl₃ to aid visualization, as described in Section 5.2.1.

5.3.2.2 Column Chromatography (CC)

Column chromatography using silica gel or Sephadex LH-20 was employed for the isolation and purification of compounds. When silica gel was used as the adsorbent, elution was carried out using either isocratic or gradient solvent systems. However, in the case of Sephadex LH-20, methanol was used instead. Eluates were collected in 20 mL fractions and the composition of each fraction was monitored by TLC. Fractions with the similar TLC profiles were pooled together, and the solvents were evaporated off. Repeated purification using the same techniques was carried out until a pure compound was obtained.

5.3.2.3 Preparative Thin Layer Chromatography (Prep-TLC)

This method was only employed for the final purification of the compounds which could not be achieved through column chromatography. Each silica gel plate (20 cm x 20 cm x 0.5 mm) was loaded with 20 mg of sample in a narrow band. The plates were placed in a

large covered glass chamber (30 cm x 30 cm x 10 cm), developed with a suitable isocratic solvent system and visualized as described in Section 5.3.2.1. The location of a compound on the plate was marked, and the adsorbent in the marked region was scrapped off and placed into a conical flask and extracted repeatedly (8 x 20 mL) with acetone. The compound was recovered upon evaporation of the acetone.

5.3.3 Isolation and Purification of Compounds 1-5, 69 and 72 from the Ethyl

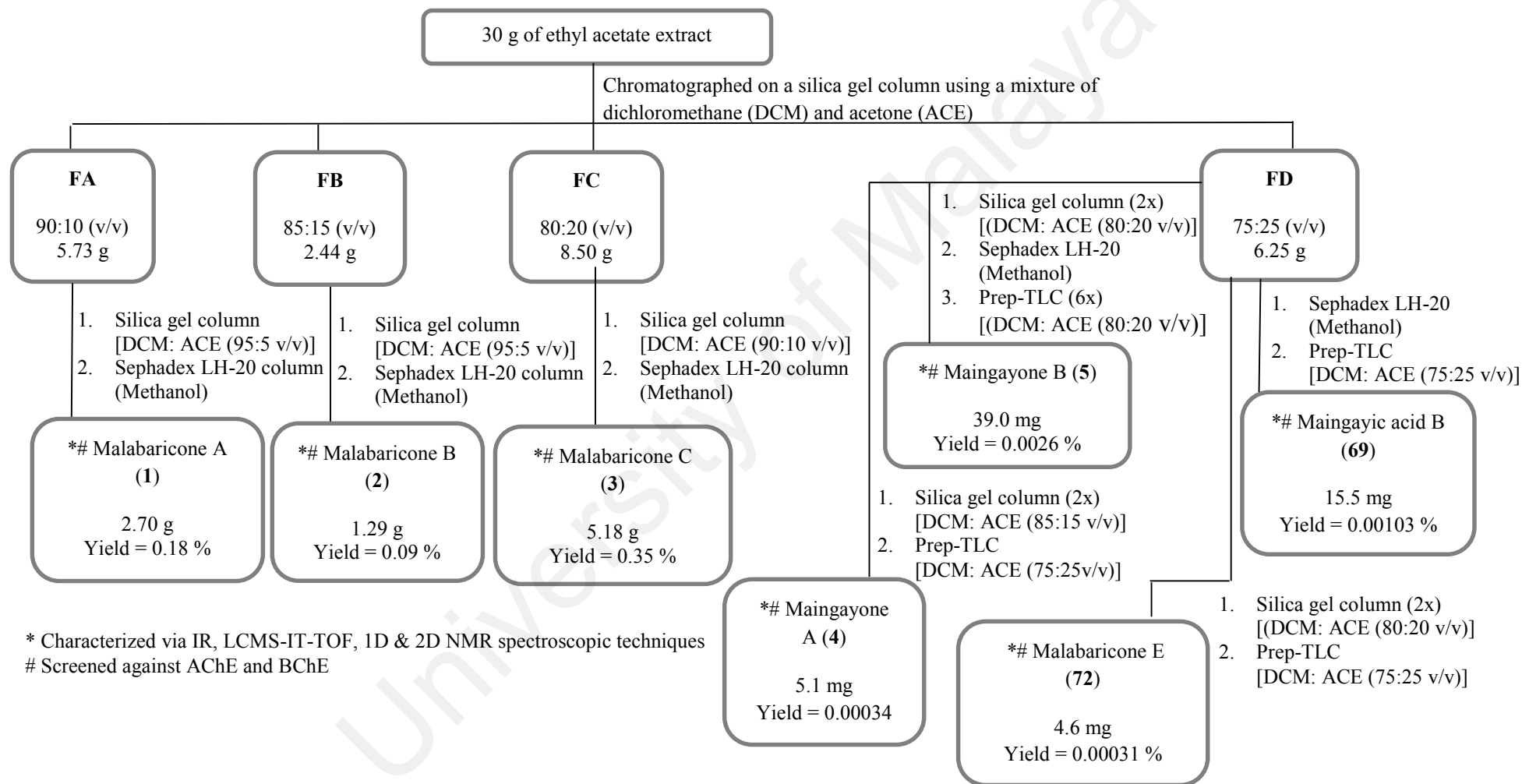
Acetate Extract

The ethyl acetate extract (30 g) was chromatographed on a silica gel column (625 g, 7.2 cm x 63 cm). Elution was carried out using mixtures of dichloromethane : acetone in proportions of 90:10 (v/v, 3 L), 85:15 (v/v, 5 L), 80:20 (v/v, 5 L), 75:25 (v/v, 3 L), 70:30 (v/v, 3 L) and 60:40 (v/v, 3 L) sequentially to afford fractions FA (5.73 g), FB (2.44 g), FC (8.50 g), FD (6.25 g), FE (3.35 g) and FF (3.10 g), respectively. FA was fractionated on a silica gel column (180 g, 2.5 cm x 72 cm) eluted using dichloromethane (2 L) to afford sub-fraction FA 1 (3.24 g), following which FA 1 was rechromatographed over a Sephadex LH-20 column (25 g) using methanol (1 L) as the eluent to afford **1 (2.70 g)**. Compound **1** gave a single grayish black spot with 1% FeCl₃ on TLC [100% dichloromethane, R_f = 0.50; dichloromethane : ethyl acetate (95:5 v/v), R_f = 0.73; dichloromethane : methanol (98:2 v/v), R_f = 0.73]. FB was subjected to column chromatography over 60 g of silica gel (2.5 cm x 64 cm) with an isocratic solvent system of dichloromethane : acetone (95:5 v/v, 1 L) to provide sub-fraction FB 1 (1.86 g). FB 1 was further separated by passing it through a Sephadex LH-20 column (25 g) with methanol (500 mL) to yield **2 (1.29 g)**. Compound **2** gave a single grayish black spot with 1% FeCl₃ on TLC [dichloromethane : acetone (95:5 v/v), R_f = 0.50; dichloromethane : ethyl acetate (90:10 v/v), R_f = 0.58; dichloromethane : methanol (95:5 v/v), R_f = 0.49]. Column chromatography of FC over silica gel (270 g, 5 cm x 72 cm) to afford sub-fraction

FC 1 (6.50 g) was achieved using dichloromethane : acetone (90:10 v/v, 1 L). Next, the purification of FC 1 to provide **3 (5.18 g)** was carried out over a Sephadex LH-20 column (25 g) using methanol (1 L) as the eluting solvent. Compound **3** gave a single grayish black spot with 1% FeCl₃ on TLC [dichloromethane : acetone (90:10 v/v), R_f = 0.73; dichloromethane : ethyl acetate (80:20 v/v), R_f = 0.36; dichloromethane : methanol (95:5 v/v), R_f = 0.33]. Column chromatography of FD over silica gel (180 g, 2.5 cm x 72 cm) with successive elution using dichloromethane : acetone in ratios of (85:15 v/v, 300 mL) and (80:20 v/v, 500 mL) afforded sub-fractions FD 1 (3.14 g) and FD 2 (1.25 g), respectively. FD 1 was rechromatographed over a silica gel column (120 g, 2.5 cm x 72 cm) with an isocratic solvent system of dichloromethane : acetone (80:20 v/v, 1.5 L) to give sub-fractions FD 1.1 (0.09 g), FD 1.2 (0.08 g) and FD 1.3 (1.05 g). FD 1.1 was next fractionated on a silica gel column (25 g, 2 cm x 58 cm) with dichloromethane : acetone (80:20 v/v, 1 L) as the eluent to provide sub-fraction FD 1.1.1 (0.03 g) following which it was then purified by prep-TLC using dichloromethane : acetone [75:25 v/v] to afford **4 (5.1 mg)**. Compound **4** gave a single grayish black spot with 1% FeCl₃ on TLC [dichloromethane : acetone (75:25 v/v), R_f = 0.73; dichloromethane : methanol (95:5 v/v), R_f = 0.27]. FD 1.2 was purified over a Sephadex LH-20 column (25 g) using methanol (500 mL) as the eluent to afford sub-fraction FD 1.2.1 (0.02 g) which was later further purified via repetitive prep-TLC with dichloromethane : acetone [75:25 v/v] to yield compound **72 (4.6 mg)**. Compound **72** gave a single grayish black spot with 1% FeCl₃ on TLC [dichloromethane : acetone (75:25 v/v), R_f = 0.50; dichloromethane : ethyl acetate (70:30 v/v), R_f = 0.35; dichloromethane : methanol (95:5 v/v), R_f = 0.27]. FD 1.3 was further fractionated by passing it through a 30 g silica gel column (2 cm x 58 cm), eluting with dichloromethane : acetone (80:20 v/v, 500 mL) to obtain sub-fraction FD 1.3.1 (0.05 g). Final purification to yield compound **5 (39.0 mg)** was achieved via prep-TLC of FD 1.3.1 using the same solvent system. Compound **5** gave a single grayish black spot with

1% FeCl₃ on TLC [dichloromethane : acetone (80:20 v/v), R_f = 0.64; dichloromethane : methanol (95:5 v/v), R_f = 0.27]. FD 2 was subjected over a Sephadex LH-20 column (25 g) and chromatographed using methanol (500 mL) as the eluent to yield sub-fraction FD 2.1 (0.04 g) which was further purified via prep-TLC [dichloromethane : acetone (75:25 v/v)] to obtain compound **69 (15.5 mg)**, which gave a single grayish black spot with 1% FeCl₃ on TLC [dichloromethane : acetone (75:25 v/v), R_f = 0.50; dichloromethane : ethyl acetate (85:15 v/v), R_f = 0.38; dichloromethane : methanol (95:5 v/v), R_f = 0.45].

University of Malaya



Scheme 5.2: Isolation and purification of compounds from the ethyl acetate extract of the fruits of *M. cinnamomea*

5.4 Characterization of Compounds 1-5, 69 and 72

The structures of the isolated compounds were elucidated on the basis of IR, NMR, LCMS-IT-TOF and UV spectroscopic techniques.

5.4.1 Infrared Spectroscopy (IR)

IR spectra were recorded using a Perkin-Elmer System 400 FT-IR Spectrometer. Spectra were obtained using a sodium chloride (NaCl) window. The range of measurement was from 4000 to 600 cm^{-1} .

5.4.2 Nuclear Magnetic Resonance Spectroscopy (NMR)

NMR spectra were acquired using a JOEL ECA 400 MHz Spectrometer operated at 400 MHz for ^1H NMR and 100 MHz for ^{13}C NMR. The samples were dissolved in deuterated methanol (CD_3OD) in 180 mm x 5 mm NMR tubes. The 1D (^1H , ^{13}C and DEPT 135) and 2D (COSY, HSQC and HMBC) NMR experiments were carried out at room temperature. Standard JOEL pulse programmes were used.

5.4.3 Liquid Chromatography Mass Spectrometry-Ion Trap-Time of Flight (LCMS-IT-TOF)

The high resolution mass spectra were obtained using an Agilent 6530 Accurate-Mass Q-TOF LC/MS system, with a SPD-M20A diode array detector coupled to an IT-TOF mass spectrometer.

5.4.4 Ultra-Violet Spectroscopy (UV)

UV spectra were recorded using a Jasco V530 UV-Vis Spectrophotometer. The stock solutions were prepared by dissolving 0.1 mg of each compound in 10 mL of spectroscopy grade methanol.

5.4.5 Optical Rotation

The specific optical rotation, $[\alpha]_D$, of compounds **4** and **5** were measured at room temperature (28°C) using a Jasco DIP-370 digital polarimeter equipped with a Sodium lamp (589 nm). A cell with a path length of 10 cm was used for each measurement. Measurements were recorded in 10 mL of spectroscopy grade methanol.

5.5 Cholinesterase Inhibitory Assay

Cholinesterase inhibitory activity of the test samples was determined by Ellman's microplate assay with modification (Ellman et al., 1961). Briefly, for the AChE inhibitory assay, 140 μ L of 0.1 M sodium phosphate buffer (pH 8) was initially added to each well of a 96-well microplate followed by 20 μ L of the test sample (in 10% methanol) and 20 μ L of 0.09 unit/mL AChE. After pre-incubation at room temperature, 10 μ L of 10 mM DTNB was added into each well followed by 10 μ L of 14 mM acetylthiocholine iodide as the substrate. The absorbance of the colored end product was measured using a microplate reader (Tecan Sunrise, Austria) at 412 nm, 30 minutes after the initiation of the enzymatic reaction. For the BChE inhibitory assay, the same procedure as described above was employed with the only difference being in the enzyme and substrate used, which were BChE from equine serum and S-butyrylthiocholine chloride, respectively. Known inhibitor, physostigmine was used as the reference standard. The test samples and reference standard were prepared in methanol. The concentration of methanol in the final reaction mixture was 10%. At this concentration, methanol had no inhibitory effect on both the AChE and BChE (Obregon et al., 2005). The absorbance of the test samples were corrected by subtracting the absorbance of their respective blank (test samples in methanol with substrate and DTNB, but without enzyme). A set of ten concentrations was used to estimate the 50% inhibitory concentration (IC_{50}) (Khaw et al., 2014). Each test

was conducted in triplicates. Percentage of inhibition was calculated using the following formula:

Percentage of inhibition:

$$= \frac{\text{Absorbance of control} - \text{Absorbance of sample}}{\text{Absorbance of control}} \times 100\%$$

5.6 Enzyme Kinetics and Mode of Inhibition

Lineweaver–Burk plot and the secondary plot of the Lineweaver-Burk plot analyses were carried out to determine the mode of enzyme inhibition and enzyme kinetics of the compound(s) which strongly inhibited both the AChE and BChE. The enzyme inhibition kinetics was carried out in the absence and the presence of the test samples (0, 1.53, 3.07 µg/mL) at various concentrations of the substrates (14, 7, 3.5, 1.75 mM). The inhibition constant (K_i) was derived from the secondary plot of the Lineweaver–Burk plot.

5.7 Molecular Docking

Briefly, molecular docking of the active inhibitors were carried out using Autodock 3.0.5 and AutoDockTools (ADT) (Morris et al., 1998). The three dimensional crystal structures of the AChE from *Torpedo californica* (PDB ID: 1W6R) (Greenblatt et al., 2004) and the BChE from *Homo sapiens* (PDB ID: 2WIJ) (Carletti et al., 2009) were retrieved from the Protein Data Bank. Both proteins were edited using ADT to remove all of the water molecules and hydrogen atoms were added. For the ligands, the two dimensional structure of the compounds were built using Hyperchem 8 and subjected to energy minimization with a convergence criterion of 0.05 kcal/(molÅ). Non-polar hydrogens and lone pairs were then merged and each atom was assigned with Gasteiger partial charges. A grid box was generated at the center of the active site gorge with 60×60×60 points and a spacing of 0.375 Å. One hundred independent dockings were carried out for each docking

experiment with a population size of 150 and 2,500,000 energy evaluations. The best conformation with the lowest docked energy in the most populated cluster was selected. The conformations from the docking experiments were analyzed and visualized using Accelrys Discovery Studio 2.5 (Accelrys Inc., San Diego, CA, USA).

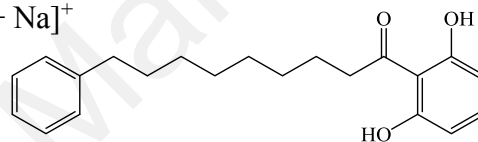
5.8 Physical Data of the Isolated Compounds

Malabaricone A (1)

Physical appearance: pale yellow amorphous powder

Mass (m/z): 327.1953 $[M + H]^+$, 349.1774 $[M + Na]^+$

Molecular formula: $C_{21}H_{26}O_3$



UV λ_{max} (MeOH) nm (log ϵ): 342 (3.07), 269 (3.67) and 214 (3.78)

IR ν_{max} (cm^{-1}): 3583, 3271, 2920, 2851, 1714, 1589 and 1511

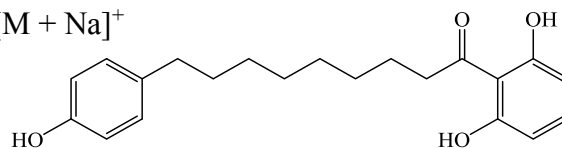
NMR: Refer to Table 3.1 and Figures 3.3, 3.5-3.8

Malabaricone B (2)

Physical appearance: yellow amorphous powder

Mass (m/z): 343.1898 $[M + H]^+$, 365.1717 $[M + Na]^+$

Molecular formula: $C_{21}H_{26}O_4$



UV λ_{max} (MeOH) nm (log ϵ): 341 (2.83), 270 (3.46) and 206 (3.56)

IR ν_{max} (cm^{-1}): 3584, 3339, 2927, 2854, 1708, 1596 and 1514

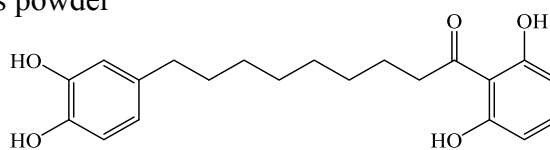
NMR: Refer to Table 3.2 and Figures 3.12-3.16

Malabaricone C (3)

Physical appearance: yellow amorphous powder

Mass (m/z): 343.1898 $[M + H]^+$

Molecular formula: $C_{21}H_{26}O_5$



UV λ_{max} (MeOH) nm (log ϵ): 338 (2.80), 269 (3.36), 222 (3.50) and 204 (3.70)

IR ν_{max} (cm^{-1}): 3583, 3343, 2927, 2854, 1714, 1589 and 1516

NMR: Refer to Table 3.3 and Figures 3.20-3.24

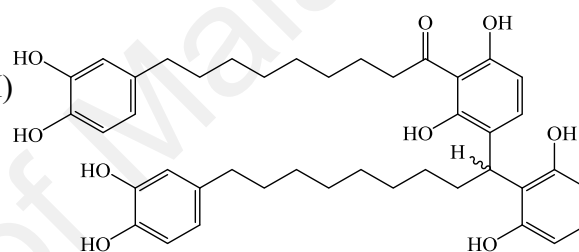
Maingayone A (4)

Physical appearance: yellow powder

Optical rotation, $[\alpha]_D -2.4^\circ$ (c 1.25, MeOH)

Mass (m/z): 701.3624 $[M + H]^+$

Molecular formula: $C_{42}H_{52}O_9$



UV λ_{max} (MeOH) nm (log ϵ): 275 (3.74) and 206 (4.18)

IR ν_{max} (cm^{-1}): 3584, 3401, 2928, 2855, 1701, 1605 and 1516

NMR: Refer to Table 3.5 and Figures 3.35, 3.37-3.40

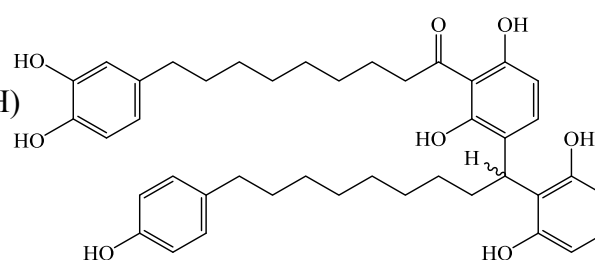
Maingayone B (5)

Physical appearance: yellow powder

Optical rotation, $[\alpha]_D +0.8^\circ$ (c 1.25, MeOH)

Mass (m/z): 707.3525 $[M + Na]^+$

Molecular formula: $C_{42}H_{52}O_8$



UV λ_{max} (MeOH) nm (log ϵ): 471 (3.13), 351 (3.57), 274 (4.15) and 233 (4.16)

IR ν_{max} (cm^{-1}): 3584, 3369, 2928, 2855, 1704, 1607 and 1515

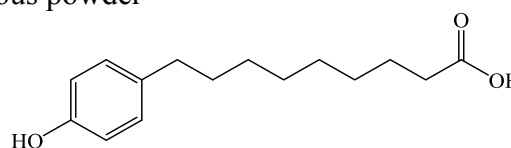
NMR: Refer to Table 3.6 and Figures 3.44-3.48

Maingayic acid B (69)

Physical appearance: light yellow amorphous powder

Mass (m/z): 251.1582 $[M + H]^+$

Molecular formula: $C_{15}H_{22}O_3$



UV λ_{max} (MeOH) nm (log ϵ): 443 (1.06), 348 (1.72), 279 (3.15), 224 (3.75) and 203 (3.68)

IR ν_{max} (cm^{-1}): 3583, 3369, 2927, 2854, 1515 and 1455

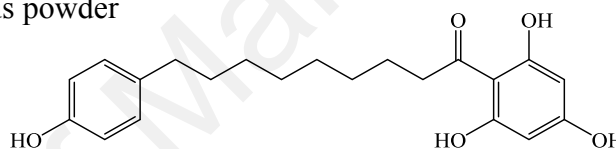
NMR: Refer to Table 3.7 and Figures 3.51, 3.53-3.56

Malabaricone E (72)

Physical appearance: yellow amorphous powder

Mass (m/z): 381.1675 $[M + Na]^+$

Molecular formula: $C_{21}H_{26}O_5$



UV λ_{max} (MeOH) nm (log ϵ): 341 (2.83), 270 (3.46), 224 (3.67)

IR ν_{max} (cm^{-1}): 3583, 3272, 2924, 2853, 1611 and 1515

NMR: Refer to Table 3.4 and Figures 3.28-3.32

REFERENCES

- Abdul Wahab, S. M., Sivasothy, Y., Liew, S. Y., Litaudon, M., Mohamad, J. & Awang, K. (2016). Natural Cholinesterase Inhibitors from *Myristica cinnamomea* King. *Bioorganic & Medicinal Chemistry Letters*, 26, 3785-3792.
- Adjene, J. O. & Igbigbi, P. S. (2010). Effect of Chronic Consumption of Nutmeg on the Stomach of Adult Wistar Rats. *Fooyin Journal of Health Sciences*, 2(2), 62-65.
- Awang, K., Chan, G., Litaudon, M., Ismail, N. H., Martin, M. & Gueritte, F. (2010). 4-Phenylcoumarins from *Mesua elegans* with acetylcholinesterase inhibitory activity. *Bioorganic & Medicinal Chemistry*, 18(22), 7873-7877.
- Ballard, C. G. (2002). Advances in the treatment of Alzheimer's disease: benefits of dual cholinesterase inhibition. *European Neurology*, 47(1), 64-70.
- Bandara Herath, H. M. T., & Anoma Priyadarshani, A. M. (1996). Two lignans and an aryl alkanone from *Myristica dactyloides*. *Phytochemistry*, 42(5), 1439-1442.
- Bandera Herath, H. M. T., & Anoma Priyadarshini, A. M. (1997). Lignans from *Myristica dactyloides*. *Phytochemistry*, 44(4), 699-703.
- Barceloux, D. G. (2009). Nutmeg (*Myristica fragrans* Houtt.). *Disease-a-Month*, 55(6), 373-379.
- Beaman, J. H. (2002). Flora Malesiana Series I: Seed Plants. Volume 14-2000. Myristicaceae, W. J. J. O. de Wilde, P. F. Stevens. *Kew Bulletin*, 57(1), 251-253.
- Boada, M., Tárraga, L., Hernández, I., Valero, S., Alegret, M., Ruiz, A. & Becker, J. T. (2014). Design of a comprehensive Alzheimer's disease clinic and research center in Spain to meet critical patient and family needs. *Alzheimer's & Dementia*, 10(3), 409-415.
- Burnham, Veronica L., & Thornton, J. E. (2015). Luteinizing hormone as a key player in the cognitive decline of Alzheimer's disease. *Hormones and Behavior*, 76, 48-56.
- Calliste, C. A., Kozlowski, D., Duroux, J. L., Champavier, Y., Chulia, A. J. & Trouillas, P. (2010). A new antioxidant from wild nutmeg. *Food Chemistry*, 118(3), 489-496.

Cao, G. Y., Yang, X. W., Xu, W. & Li, F. (2013). New inhibitors of nitric oxide production from the seeds of *Myristica fragrans*. *Food and Chemical Toxicology*, 62, 167-171.

Cao, G. Y., Xu, W., Yang, X. W., Gonzalez, F. J. & Li, F. (2015). New neolignans from the seeds of *Myristica fragrans* that inhibit nitric oxide production. *Food Chemistry*, 173, 231-237.

Carletti, E., Aurbek, N., Gillon, E., Loiodice, M., Nicolet, Y., Fontecilla Camps, J.C., Masson, P., Thiermann, H., Nachon, F. & Worek, F. (2009). Structure-activity analysis of aging and reactivation of human butyrylcholinesterase inhibited by analogues of tabun. *Biochemical Journal* 421, 97-106.

Chong, Y. M., Yin, W. F., Ho, C. Y., Mustafa, M. R., Hadi, A. H. A., Awang, K. & Chan, G. (2011). Malabaricone C from *Myristica cinnamomea* Exhibits Anti-Quorum Sensing Activity. *Journal of Natural Products*, 74(10), 2261-2264.

Cuong, T. D., Hung, T. M., Na, M., Ha, D. T., Kim, J. C., Lee, D. & Min, B. S. (2011). Inhibitory effect on NO production of phenolic compounds from *Myristica fragrans*. *Bioorganic & Medicinal Chemistry Letters*, 21(22), 6884-6887.

Doyle, J.A., Manchester, S.R. & Sauquet, H. (2008). A seed related to Myristicaceae in the Early Eocene of Southern England. *Syst. Botany*, 33(4): 636–646.

Ebrahimabadi, A. H., Ebrahimabadi, E. H., Djafari-Bidgoli, Z., Kashi, F. J., Mazoochi, A. & Batooli, H. (2010). Composition and antioxidant and antimicrobial activity of the essential oil and extracts of *Stachys inflata* Benth from Iran. *Food Chemistry*, 119(2), 452-458.

Ellman, G.L., Courtney, D., Anddres, K. D. V. & Featherstone, R. M. (1961). A new and rapid colometric determination of acetylcholinesterase activity. *Biochem Pharmacol* 7, 88-95.

Filleur, F., Pouget, C., Allais, D. P., Kaouadji, M. & Chulia, A. J. (2002). Lignans and Neolignans from *Myristica Argentea* Warb. *Natural Product Letters*, 16(1), 1-7.

Fort, D. M., Ubillas, R. P., Mendez, C. D., Jolad, S. D., Inman, W. D. & Carney, J. R. (2000). Novel Antihyperglycemic Terpenoid-Quinones from *Pycnanthus angolensis*. *J. Org. Chem*, 65, 6534-6539.

Giacobini, E. (2004). Cholinesterase inhibitors: new roles and therapeutic alternatives. *Pharmacological Research*, 50(4), 433-440.

Greenblatt, H.M., Guillou, C., Guénard, D., Argaman, A., Botti, S., Badet, B., Thal, C., Silman, I. & Sussman, J.L. (2004). The Complex of a Bivalent Derivative of Galanthamine with Torpedo Acetylcholinesterase Displays Drastic Deformation of the Active-Site Gorge: Implications for Structure-Based Drug Design. *Journal of the American Chemical Society* 126, 15405-15411.

Gurib-Fakim, A. (2006). Medicinal plants: Traditions of yesterday and drugs of tomorrow. *Molecular Aspects of Medicine*, 27(1), 1-93.

Hazalin, Mohamad Nor, N. A., Ramasamy, K., Lim, S. M., Cole, A. L. J. & Abdul Majeed, A. B. (2012). Induction of apoptosis against cancer cell lines by four ascomycetes (endophytes) from Malaysian rainforest. *Phytomedicine*, 19(7), 609-617.

Herath, H. M. T. B., Priyadarshani, A. M. A. & Jamie, J. (1998). Dactyloidin, a New Diaryl Nonanoid from *Myristica Dactyloides*. *Natural Product Letters*, 12(2), 91-95.

Herath, H. M. T. B. & Padmasiri, W. (1999). Demethyldactyloidin and Other Constituents in *Myristica Ceylanica*. *Natural Product Letters*, 14(2), 141-146.

Inestrosa, N. C., Alvarez, A., Pérez, C. A., Moreno, R. D., Vicente, M., Linker, C., Casanueva, O. I., Soto, C. & Garrido, J. (1996). Acetylcholinesterase Accelerates Assembly of Amyloid- β -Peptides into Alzheimer's Fibrils: Possible Role of the Peripheral Site of the Enzyme. *Neuron* 16, 881-891.

Janovec, J. P., & García, R. (2004). TROPICAL FORESTS Myristicaceae A2 - Burley, Jeffery *Encyclopedia of Forest Sciences* (pp. 1762-1767). Oxford: Elsevier.

Johnson, G. & Moore, S.W. (2006). The Peripheral Anionic Site of Acetylcholinesterase: Structure, Functions and Potential Role in Rational Drug Design. *Current Pharmaceutical Design* 12, 217-225.

Juan C. M. V. (2000). Distribution of flavonoids in the Myristicaceae. *Phytochemistry*, 55(6), 505-511.

Kang, J. W., Min, B. S. & Lee, J. H. (2013). Anti-platelet activity of erythro-(7S,8R)-7-acetoxy-3,4,3',5'-tetramethoxy-8-O-4'-neolignan from *Myristica fragrans*. *Phytotherapy Research: PTR*, 27(11), 1694-1699.

Khaw, K. Y., Choi, S. B., Tan, S. C., Wahab, H. A., Chan, K. L. & Murugaiyah, V. (2014). Prenylated xanthenes from mangosteen as promising cholinesterase inhibitors and their molecular docking studies. *Phytomedicine*, 21(11), 1303-1309.

Kuo, Y. H., Lin, S. T. & Wu, R. E. (1989). Three New Lignans from the Nutmeg of *Myristica cagayanesis*. *CHEMICAL & PHARMACEUTICAL BULLETIN*, 37(9), 2310-2312.

Liang, J., Kulasiri, D., & Samarasinghe, S. (2015). Ca²⁺ dysregulation in the endoplasmic reticulum related to Alzheimer's disease: A review on experimental progress and computational modeling. *Biosystems*, 134, 1-15.

Logue, M. W., Schu, M., Vardarajan, B. N., Farrell, J., Bennett, D. A., Buxbaum, J. D., Byrd, G. S., Taner, N. E., Evans, D., Foroud, T., Goate, A., Graff-Radford, N. R., Kamboh, M. I., Kukull, W. A. & Manly, J.J. (2014). Two rare *AKAP9* variants are associated with Alzheimer's disease in African Americans. *Alzheimer's & Dementia*, 10(6), 609-618.

Maia, A., Schmitz-Afonso, I., Martin, M. T., Awang, K., Laprévote, O., Guéritte, F. & Litaudon, M. (2008). Acylphenols from *Myristica crassa* as New Acetylcholinesterase Inhibitors. *Planta Med*, 74(12), 1457-1462.

Maity, B., Banerjee, D., Bandyopadhyay, S. K. & Chattopadhyay, S. (2009). Regulation of arginase/nitric oxide synthesis axis via cytokine balance contributes to the healing action of malabaricone B against indomethacin-induced gastric ulceration in mice. *International Immunopharmacology*, 9(4), 491-498.

Maity, B., Yadav, S. K., Patro, B. S., Tyagi, M., Bandyopadhyay, S. K. & Chattopadhyay, S. (2012). Molecular mechanism of the anti-inflammatory activity of a natural diarylnonanoid, malabaricone C. *Free Radical Biology and Medicine*, 52(9), 1680-1691.

Majouli, K., Besbes Hlila, M., Hamdi, A., Flamini, G., Ben Jannet, H. & Kenani, A. (2016). Antioxidant activity and α -glucosidase inhibition by essential oils from *Hertia cheirifolia* (L.). *Industrial Crops and Products*, 82, 23-28.

Masson, P., Froment, M. T., Bartels, C. F. & Lockridge, O. (1996). Asp70 in the Peripheral Anionic Site of Human Butyrylcholinesterase. *European Journal of Biochemistry* 235, 36-48.

Min, B., Cuong, T. D., Hung, T. M., Min, B., Shin, B. & Woo, M. (2011). *Bulletin of the Korean Chemical Society*, 32(11), 4059-4062.

Morris, G. M., Goodsell, D. S., Halliday, R. S., Huey, R., Hart, W. E., Belew, R. K. & Olson, A. J. (1998). Automated docking using a Lamarckian genetic algorithm and an empirical binding free energy function. *Journal of Computational Chemistry* 19, 1639-1662.

Nguyen, P. H., Le, T. V. T., Kang, H. W., Chae, J., Kim, S. K., Kwon, K. & Oh, W. K. (2010). AMP-activated protein kinase (AMPK) activators from *Myristica fragrans* (nutmeg) and their anti-obesity effect. *Bioorganic & Medicinal Chemistry Letters*, 20(14), 4128-4131.

Obregon, A., Schetinger, M. R., Correa, M. M., Morsch, V. M., Da Silva, J. E. & Martins, M. A. (2005). Effects per se of organic solvents in the cerebral acetylcholinesterase of rats. *Neurochem. Res.*, 30, 379-384.

Pham, V. C., Jossang, A., Sévenet, T. & Bodo, B. (2000). Cytotoxic Acylphenols from *Myristica maingayi*. *Tetrahedron*, 56(12), 1707-1713.

Pham, V. C., Jossang, A., Sévenet, T. & Bodo, B. (2002). Novel cytotoxic acylphenol dimers of *Myristica gigantea*; enzymatic synthesis of giganteones A and B. *Tetrahedron*, 58(28), 5709-5714.

Puri, V., Wang, X., Vardigan, J. D., Kuduk, Scott, D., & Uslaner, J. M. (2015). The selective positive allosteric M1 muscarinic receptor modulator PQCA attenuates learning and memory deficits in the Tg2576 Alzheimer's disease mouse model. *Behavioural Brain Research*, 287, 96-99.

- Rahmani, M. (2003). *Chemical Diversity of Malaysian Flora: Potential Source of Rich Therapeutic Chemicals*. Bahagian Komunikasi Korporat, Universiti Putra Malaysia.
- Sari, M., Biondi, D. M., Kaabeche, M., Mandalari, G., D'Arrigo, M. & Bisignano, G. (2006). Chemical composition, antimicrobial and antioxidant activities of the essential oil of several populations of Algerian *Origanum glandulosum* Desf. *Flavour and Fragrance Journal*, 21 (6), 890-898.
- Sartorelli, P., Young, M. C. M. & Kato, M. J. (1998). Antifungal lignans from the arils of *Viola oleifera*. *Phytochemistry*, 47(6), 1003-1006.
- Sawadjoon, S., Kittakoop, P., Kirtikara, K., Vichai, V., Tanticharoen, M. & Thebtaranonth, Y. (2002). Atropisomeric Myristinins: Selective COX-2 Inhibitors and Antifungal Agents from *Myristica cinnamomea*. *J. Org. Chem.*, 67(16), 5470-5475.
- Seidemann, J. (2005). *World Spice Plants: Economic Usage, Botany Taxonomy*. Springer-Verlag Berlin Heidelberg.
- Silva, D. H. S., Pereira, F. C., Zanoni, M. V. B. & Yoshida, M. (2001). Lipophyllic antioxidants from *Iryanthera juruensis* fruits. *Phytochemistry*, 57(3), 437-442.
- Sivasothy, Y., Loo, K. Y., Leong, K. H., Litaudon, M. & Awang, K. (2016a). A potent alpha-glucosidase inhibitor from *Myristica cinnamomea* King. *Phytochemistry*, 122, 265-269.
- Sivasothy, Y., Krishnan, T., Chan, G., Abdul Wahab, S. M., Othman, M. A., Litaudon, M. & Awang, K. (2016b). Quorum Sensing Inhibitory Activity of Giganteone A from *Myristica cinnamomea* King against *Escherichia coli* Biosensors. *Molecules*, 21, 391.
- Subclass MAGNOLIIDAE Takhtajan 1966. (2012) *Medicinal Plants of the Asia-Pacific* (pp. 1-74): WORLD SCIENTIFIC.
- Tan, W. N., Khairuddean, M., Wong, K. C., Khaw, K. Y. & Vikneswaran, M. (2014). New cholinesterase inhibitors from *Garcinia atroviridis*. *Fitoterapia*, 97, 261-267.
- Tran, L. & Ha-Duong, T. (2015). Exploring the Alzheimer amyloid- β peptide conformational ensemble: A review of molecular dynamics approaches. *Peptides*, 69, 86-91.

Van Gils, C. & Cox, P. A. (1994). Ethnobotany of nutmeg in the Spice Islands. *Journal of Ethnopharmacology*, 42(2), 117-124.

Victor, K., Eric, C. N., Pierre, M., Kirk, M., Philip G. H. & Augustin E. N. (2011) Antimicrobial activities of the CH₂Cl₂-CH₃OH (1 : 1) extracts and compounds from the roots and fruits of *Pycnanthus angolensis* (Myristicaceae). *Natural Product Research*, 25(4), 432-443.

Zahir, A., Jossang, A., Bodo, B., Hadi, H. A., Schaller, H. & Sevenet, T. (1993). Knerachelins A and B, antibacterial phenylacylphenols from *Knema furfuraceae*. *Journal of Natural Products*, 56, 1634-1637.

Zhang, Y., Zhang, J. J., Kang, W. Y. & Yan, W. Y. (2014). Advances of chemical constituents and pharmacological activities of *Myristica* genus. *Zhongguo Zhong Yao Za Zhi*, 39(13), 2438-2449.

University of Malaya

APPENDICES

PUBLISHED MANUSCRIPT

1. **Siti Mariam Abdul Wahab**, Yasodha Sivasothy, Liew Sook Yee, Marc Litaudon, Jamaludin Mohamad and Khalijah Awang. Natural Cholinesterase inhibitors from *Myristica cinnamomea* King. *Bioorganic & Medicinal Chemistry Letters*. 2016, doi: <http://dx.doi.org/10.1016/j.bmcl.2016.05.046>.
2. Yasodha Sivasothy, Thiba Krishnan, Kok Gan Chan, **Siti Mariam Abdul Wahab**, Muhamad Aqmal Othman, Marc Litaudon and Khalijah Awang. Quorum Sensing Inhibitory Activity of Giganteone A from *Myristica cinnamomea* King against *Escherichia coli* Biosensors. *Molecules*, 2016, 21, 391.

PATENT FILED

Quorum Sensing Inhibitory Activity of Giganteone A from *Myristica cinnamomea* King against *Escherichia coli* Biosensors (UM-PT02-PK01/UPTK/PATEN/PINDAAN/03).

CONFERENCES

1. **Oral Presentation:** Chemical Constituents from the Fruits of *Myristica cinnamomea* King.
International Postgraduate Conference on Science and Mathematics 2015 at Sultan Idris Education University. October 10-11, 2015, Perak, Malaysia.
2. **Poster Presentation:** Acylphenols Isolated from the Fruits of *Myristica cinnamomea* King.
Annual Colloquim on Drug Development from Natural Products 2015 at University of Malaya. August 12, 2015, Kuala Lumpur, Malaysia.

Accepted Manuscript

Natural Cholinesterase Inhibitors from *Myristica cinnamomea* King

Siti Mariam Abdul Wahab, Yasodha Sivasothy, Liew Sook Yee, Marc Litaudon, Jamaludin bin Mohamad, Khalijah Awang

PII: S0960-894X(16)30531-5

DOI: <http://dx.doi.org/10.1016/j.bmcl.2016.05.06>

Reference: BMCL 23905

To appear in: *Bioorganic & Medicinal Chemistry Letters*

Received Date: 1 March 2016

Revised Date: 12 May 2016

Accepted Date: 16 May 2016



Please cite this article as: Wahab, S.M.A., Sivasothy, Y., Yee, L.S., Litaudon, M., Mohamad, J.b., Awang, K., Natural Cholinesterase Inhibitors from *Myristica cinnamomea* King, *Bioorganic & Medicinal Chemistry Letters* (2016), doi: <http://dx.doi.org/10.1016/j.bmcl.2016.05.046>

This is a PDF file of an unedited manuscript that has been accepted for publication. As a service to our customers we are providing this early version of the manuscript. The manuscript will undergo copyediting, typesetting, and review of the resulting proof before it is published in its final form. Please note that during the production process errors may be discovered which could affect the content, and all legal disclaimers that apply to the journal pertain.

Natural Cholinesterase Inhibitors from *Myristica cinnamomea* King

Siti Mariam Abdul Wahab^a, Yasodha Sivasothy^a, Liew Sook Yee^{a,b}, Marc Litaudon^c, Jamaludin bin Mohamad^d, Khalijah Awang^{a,b*}

^a *Department of Chemistry, Faculty of Science, University of Malaya, 50603, Kuala Lumpur, Malaysia*

^b *Centre for Natural Products and Drug Research (CENAR), University of Malaya, 50603, Kuala Lumpur, Malaysia*

^c *Institut de Chimie des Substances Naturelles, Centre National de la Recherche Scientifique, 91198 Gif-sur-Yvette, Cedex, France*

^d *Institute of Biological Sciences, Faculty of Science, University of Malaya, 50603, Kuala Lumpur, Malaysia*

*Corresponding author: Tel.: +60379674064; Fax: +60379674193; Email address: khalijah@um.edu.my

Abstract

A new acylphenol, malabaricone E (**1**) together with the known malabaricones A-C (**2-4**), maingayones A and B (**5** and **6**) and maingayic acid B (**7**) were isolated from the ethyl acetate extract of the fruits of *Myristica cinnamomea* King. Their structures were determined by 1D and 2D NMR techniques and LCMS-IT-TOF analysis. Compounds **3** (1.84 ± 0.19 and 1.76 ± 0.21 μM , respectively) and **4** (1.94 ± 0.27 and 2.80 ± 0.49 μM , respectively) were identified as dual inhibitors, with almost equal acetylcholinesterase (AChE) and butyrylcholinesterase (BChE) enzymes inhibiting potentials. The Lineweaver-Burk plots of compounds **3** and **4** indicated that they were mixed-mode inhibitors. Based on the molecular docking studies, compounds **3** and **4** interacted with the peripheral anionic site (PAS), the catalytic triad and the oxyanion hole of the AChE. As for the BChE, while compound **3** interacted with the PAS, the catalytic triad and the oxyanion hole, compound **4** only interacted with the catalytic triad and the oxyanion hole.

Keywords: *Myristica cinnamomea* King; Myristicaceae; Acylphenols, Dimeric acylphenols, Malabaricone E, Acetylcholinesterase enzyme, Butyrylcholinesterase enzyme

Alzheimer's disease (AD) is an incurable neurodegenerative disorder which exhibits progressive brain disorder that slowly destroys the memory and thinking skills, leading to difficulties in carrying out the simplest tasks including language problems, recognition and capacity to perform gestures.^{1, 2} AD is affecting millions of people worldwide and the prevalence is increasing as the population ages.³ However, till now, there is still a great lack

of clinical treatment for those who suffer from this disease.⁴ Currently, cholinesterase enzyme (ChE) inhibition represents the most efficacious treatment approach for AD.⁵ There are two types of ChE which have been characterized in the vertebrate tissues; acetylcholinesterase and butyrylcholinesterase enzymes (AChE and BChE).⁵

Myristica cinnamomea King (Myristicaceae), commonly known as cinnamon nutmeg, is distributed in the Malayan Peninsula, Singapore, Borneo and Philippines. Locally, it is referred to as 'pala bukit'. *M. cinnamomea* is a tree 15 m in height and 45 cm in diameter. Its outer bark is dark brown, rugose with fine grid cracks while the inner bark is pale brown. The leaves are oblong to oblanceolate, bright green above and pale silvery brown below. The fruit is yellow and globose to broadly globular-oblong. Its seeds are red and used as spices.⁶ A previous phytochemical study of the dichloromethane extract of the fruits yielded six flavans; myristinins A-F, which were identified as anti-fungal agents and COX-2 inhibitors.⁷ The methanol extract of the bark on the other hand afforded malabaricone C, an anti-quorum sensing agent.⁸ Recently, our group has identified two α -glucosidase inhibitors; giganteone D (IC₅₀ 5.05 μ M) and cinnamomeone A (IC₅₀ 358.80 μ M) from the hexane extract of its bark.⁹

M. cinnamomea is closely related to *M. fragrans* Houtt. (nutmeg) and since the secondary metabolites of *M. fragrans* are memory enhancers, there is a strong possibility that based on this evidence the secondary metabolites of *M. cinnamomea* could inhibit the AChE and BChE which in turn could prevent AD.^{10, 11} The genus *Myristica* is a rich source of acylphenols.¹² The significant AChE inhibitory activity of the acylphenols isolated from *M. crassa* with low IC₅₀ values in the range between 9.4 \pm 1.6 - 11.7 \pm 2.5 μ M made it worthy to investigate the fruits of *M. cinnamomea* in search of potential AD inhibitors.¹² Preliminary screening proved that the ethyl acetate extract (at 100 μ g/ml) of the fruits of *M. cinnamomea* was a potential inhibitor of the AChE (95.93 \pm 7.86 %) and BChE (70.00 \pm 13.17 %). Therefore, the extract was subjected to further investigation with the intention of identifying the compound(s) which were responsible in giving rise to the strong AChE and BChE inhibitory activities. Kinetic studies were subsequently carried out on the compound(s) which actively inhibited the AChE and BChE in order to determine their mode of inhibition. Following this, molecular docking studies were conducted to investigate the site at which the active compound(s) bind to the enzymes.

The ethyl acetate extract of the dried fruits of *M. cinnamomea* was subjected to repeated silica gel column chromatography and preparative TLC to yield seven compounds (1-7) among which compound 1 was identified to be a new acylphenol. Compounds 2-7 were characterized as malabaricones A-C (2-4), maingayones A and B (5-6) and maingayic acid B (7) upon comparison of their spectroscopic data with those reported in the literature (Figure 1).^{12, 13} Compounds 2-4 were the major metabolites in the fruits while the remaining compounds were obtained in smaller amounts (Supplementary Data S1).

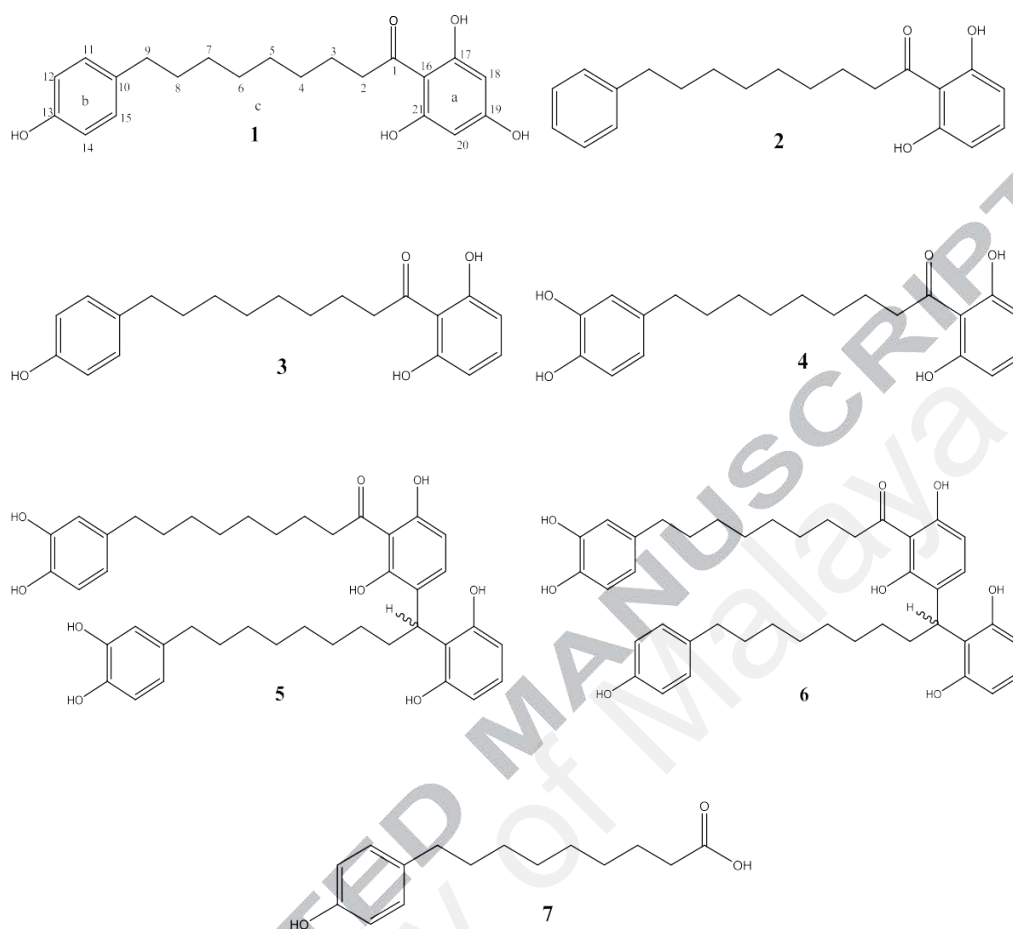


Figure 1: Structures of compounds **1-7**

Compound **1**¹⁴ was isolated as an optically inactive pale yellow amorphous powder. The positive LCMS-IT-TOF which exhibited a pseudo-molecular ion $[M + Na]^+$ at m/z 381.1675 (calcd. for $C_{21}H_{26}O_5Na$ 381.1672) enabled us to propose a molecular formula of $C_{21}H_{26}O_5$, consistent with 9 degrees of unsaturation. The IR spectrum revealed absorption bands due to hydroxyl (ν_{max} 3272 cm^{-1}), methylene (ν_{max} 2924 and 2852 cm^{-1}), conjugated carbonyl (ν_{max} 1642 cm^{-1}) and aromatic (ν_{max} 1515 and 1455 cm^{-1}) functional groups in the molecule.¹² The combined analysis of the ^{13}C NMR (Table 1) and DEPT-135 spectra confirmed the presence of 21 carbon signals comprising 1 carbonyl, 12 aromatic and 8 methylene carbons.

Analysis of the 1H NMR spectrum (Table 1) indicated that ring a was a 1, 2, 3, 5- tetrasubstituted symmetrical aromatic ring with a two proton system forming a singlet at δ_H 5.80 (H-18 & H-20; δ_C 95.8, C-18 & C-20). The 1H NMR and COSY spectra (Figure 2) also exhibited the typical spin system for a 1, 4-disubstituted aromatic ring (ring b) with the characteristic AA'BB' doublets at δ_H 6.97 ($J = 8.0$ Hz, H-11 & H-15; δ_C 130.3, C-11 & C-15) and δ_H 6.67 ($J = 8.0$ Hz, H-12 & H-14; δ_C 116.1, C-12 & C-14). The four quaternary aromatic carbons at δ_C 156.3 (C-13), δ_C 166.5 (C-19) and δ_C 165.9 (C-17 & C-21) suggested that they were oxygenated.¹⁵ The absence of the H-18/H-19 and H-19/H-20 homonuclear

couplings (Figure 2) in addition to the large downfield shift in the carbon resonance of C-19 (δ_C 166.5) upon comparison to the corresponding atom in compounds **2-4** (δ_C 136.9, 137.0, 137.0, respectively), led to the assumption that C-19 was oxygenated.

Table 1: ^1H NMR and ^{13}C NMR spectroscopic assignments of compound **1** in methanol- d_4 (^1H : 400 MHz; ^{13}C : 100 MHz; δ in ppm)

Position	δ_{H} (ppm)	δ_{C} (ppm)
1	-	207.6
2	3.02 (<i>t</i> , $J = 8.0$ Hz)	44.9
3	1.64 (<i>p</i> , $J = 8.0$ Hz)	26.3
4	1.33 ^a (<i>brs</i>)	30.9 ^b
5	1.33 ^a (<i>brs</i>)	30.6 ^b
6	1.33 ^a (<i>brs</i>)	30.6 ^b
7	1.33 ^a (<i>brs</i>)	30.4 ^b
8	1.55 (<i>brt</i> , $J = 8.0$ Hz)	33.2
9	2.50 (<i>t</i> , $J = 8.0$ Hz)	36.2
10	-	135.0
11	6.97 (<i>d</i> , $J = 8.0$ Hz)	130.3
12	6.67 (<i>d</i> , $J = 8.0$ Hz)	116.1
13	-	156.3
14	6.67 (<i>d</i> , $J = 8.0$ Hz)	116.1
15	6.97 (<i>d</i> , $J = 8.0$ Hz)	130.3
16	-	105.0
17	-	165.9
18	5.80 (<i>s</i>)	95.8
19	-	166.5
20	5.80 (<i>s</i>)	95.8
21	-	165.9

^a Overlapping signals

^b Chemical shifts are interchangeable

The signals in the upfield region of the ^1H NMR and ^{13}C NMR spectra of compound **1** were those of the *n*-octyl chain. The chemical shift of the methylene protons at δ_{H} 3.02 (*t*, $J = 8.0$ Hz, H-2; δ_{C} 44.9, C-2) suggested that they were vicinal to the carbonyl carbon at δ_{C} 207.6 (C-1).^{11, 14} The HMBC cross peaks between C-1 with the methylene protons of H-2 and H-3 and with those of the aromatic protons of H-18 and H-20 (4J W-coupling) unambiguously linked one side of the *n*-octyl chain to C-16 (δ_{C} 105.0) of ring a (Figure 2).¹⁵ The H-9/C-10, C-11, C-15, H-11/C-9 and H-15/C-9 heteronuclear correlations confirmed the connectivity of the other end of the *n*-octyl chain to C-10 (δ_{C} 135.0) of ring b (Figure 2). Thus, based on the above spectroscopic data, the structure of compound **1** was established as 1-(2, 4, 6-trihydroxyphenyl)-9-(4-hydroxyphenyl)-nonanone or trivially named as malabaricone E.

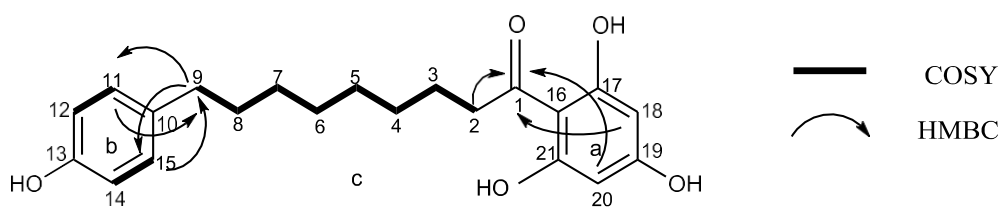
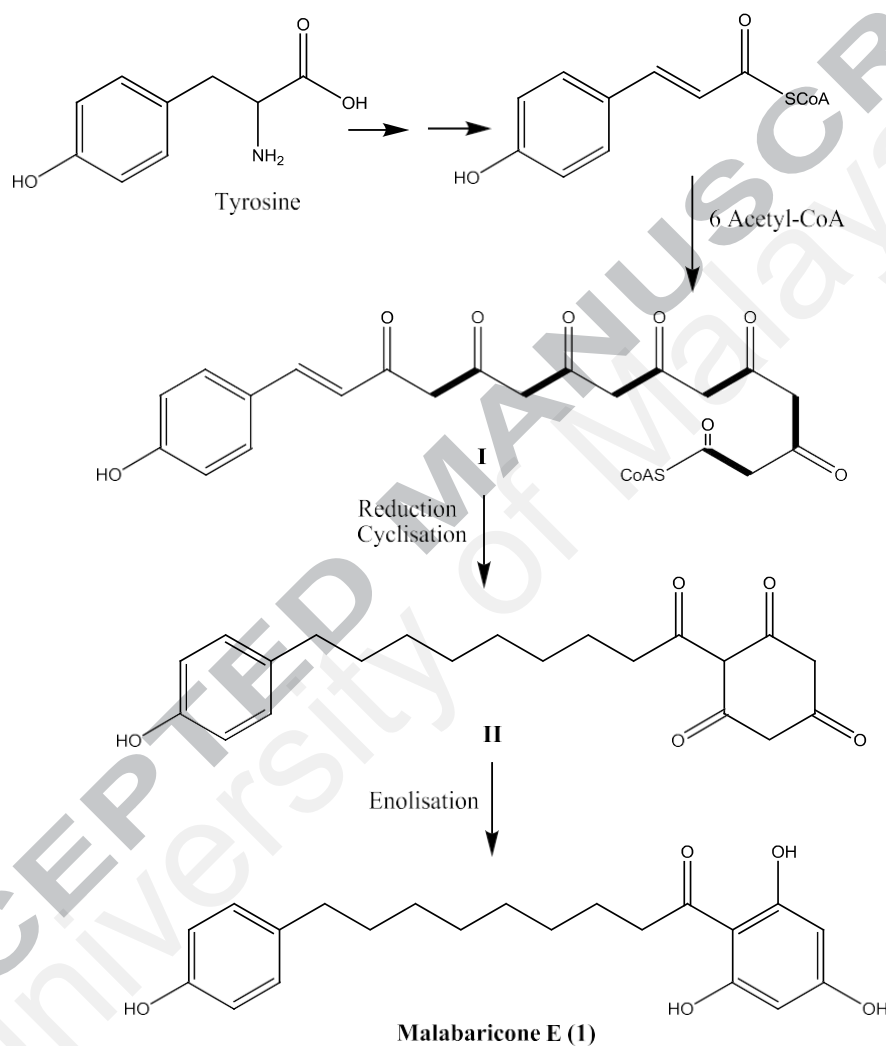


Figure 2: Selected COSY and H MBC correlations for compound 1

University of Malaya

The biosynthetic pathway for the formation of malabaricone E (**1**) presumably resulted from the elongation of a cinnamoyl type precursor, originating from a molecule of tyrosine by six acetate (malonate) units to form **I**. Reduction of the first three acetate units and the cyclisation of the last three acetate units of **I** into a triketonic cyclohexane ring according to the phloroglucinol type cyclisation generated **II** following which the enolisation of the ketones in the aromatic ring led to the formation of malabaricone E (Scheme 1).¹²



Scheme 1: Proposed biosynthetic pathway for the formation of compound **1**

Initial AChE and BChE inhibitory activities of compounds **1-7** were assayed at 100 µg/ml. Except for compound **7**, the remaining compounds (**1-6**) exhibited more than 75 % and 69 % inhibition towards the AChE and BChE, respectively. Subsequently, compounds **1-6** were further evaluated in order to determine their respective IC₅₀ values (Supplementary Data S2). The IC₅₀ values and selectivity indices of compounds **1-6** along with the reference standard, physostigmine are given in Table 2. Compounds **1** (IC₅₀ = 6.44 ± 0.85 µM), **2** (IC₅₀ = 1.31 ± 0.17 µM), **3** (IC₅₀ = 1.84 ± 0.19 µM) and **4** (IC₅₀ = 1.94 ± 0.27 µM) actively inhibited the AChE with compound **2** being the most potent among the four. As for the BChE, it was strongly inhibited by compounds **3** (IC₅₀ = 1.76 ± 0.21 µM), **4** (IC₅₀ = 2.80 ± 0.49 µM) and **1** (IC₅₀ = 6.65 ± 0.13 µM) with the former being a more effective inhibitor compared to the latter two. In contrary, compounds **5** and **6** were moderate AChE and BChE inhibitors with IC₅₀ values ranging between 10.51 ± 2.07 -30.67 ± 8.14 µM.

A closer look at the structures of compounds **1-7** provided further insight as to how the activities of these acylphenols (compounds **1-4**) and dimeric acylphenols (compounds **5** and **6**) might be influenced by the chemical groups in their respective structures (Supplementary Data S3). The AChE inhibiting potential of compounds **2-4** may have decreased with the increase in the number of hydroxyl groups in their ring b (Supplementary Data S3). The lower AChE inhibiting potential of compound **1** upon comparison to compound **3** could have resulted from the additional hydroxyl group in its ring a. When the activities of compounds **1-4** were compared to that of compound **7**, the inactivity of compound **7** led to the assumption that the presence of two aromatic rings was a prerequisite for the AChE inhibitory activity. The dimeric acylphenols (compounds **5** and **6**) were weaker AChE inhibitors as compared to their monomers (compounds **3** and **4**) which they were constructed from. Therefore, one could postulate that dimerization which in turn results in the bulkiness of compounds **5** and **6** could have contributed to the decrease in their activity which was in agreement with the findings of Maia et al, 2008. However, the greater activity of compound **5** in comparison to compound **6** could have been due to the fact that the former bore two hydroxyl groups in its ring b' unlike the latter whose ring b' only bore a single hydroxyl group (Supplementary Data S3). In the case of the BChE inhibition studies, the presence of two aromatic rings was also essential for the inhibition of this enzyme. Besides, among the monomers; compounds **1-4**, compound **2** showed the weakest activity (IC₅₀ = 39.21 ± 3.46 µM), which could have been due to the absence of the hydroxyl group in its ring b compared to compounds **1**, **3** and **4** which bore one or two hydroxyl groups in their ring b.

With regard to the selectivity of the compounds (Table 2), it is interesting to note that compounds **1**, **3**, **4** and **5** were dual inhibitors, with almost equal inhibitory action against the AChE and BChE. Compound **2** like physostigmine was an AChE selective inhibitor. In contrary, compound **6** was a BChE inhibitor. Dual inhibitors play an important role in the treatment of AD. As AD progresses, acetylcholine (ACh) regulation may become increasingly dependent on BChE and dual inhibitors may provide more sustained efficacy than AChE-selective agents.¹⁶ In addition, new findings show that both AChE and BChE are involved in the breakdown of ACh in the brain and dual inhibition of these enzymes may increase the efficacy of treatment and broaden the indications.^{17, 18}

Table 2: Cholinesterase inhibition activities of compounds 1-7 and physostigmine

Compound	Percentage Inhibition at 100 $\mu\text{g/ml}^{\text{a}}$		IC_{50} (μM) ^a		Selectivity Index	
	AChE	BChE	AChE	BChE	AChE ^b	BChE ^c
1	99.39 \pm 0.37	86.85 \pm 1.42	6.44 \pm 0.85	6.65 \pm 0.13	1.03	0.97
2	97.42 \pm 2.09	69.55 \pm 6.31	1.31 \pm 0.17	39.21 \pm 3.46	32.95	0.04
3	95.86 \pm 0.64	87.35 \pm 8.58	1.84 \pm 0.19	1.76 \pm 0.21	0.96	1.05
4	97.09 \pm 3.00	94.13 \pm 1.40	1.94 \pm 0.27	2.80 \pm 0.49	1.44	0.69
5	75.39 \pm 0.67	81.11 \pm 3.07	12.66 \pm 1.48	10.51 \pm 2.07	0.83	1.20
6	91.48 \pm 1.17	86.74 \pm 1.46	30.67 \pm 8.14	12.52 \pm 2.86	0.41	2.45
7	45.13 \pm 9.23	48.96 \pm 1.61	-	-	-	-
Physostigmine	-	-	0.08 \pm 0.02	0.22 \pm 0.02	2.75	0.36

^a Data presented as Mean \pm SD (n = 3)

^b Selectivity for AChE is defined as IC_{50} (BChE)/ IC_{50} (AChE)

^c Selectivity for BChE is defined as IC_{50} (AChE)/ IC_{50} (BChE)

Cholinesterase inhibition kinetics were determined for the dual inhibitors; compounds **3** and **4**, which showed significant interactions with both the AChE and BChE. As illustrated in the Lineweaver-Burk plot analyses (Figure 3), compounds **3** and **4** both displayed mixed-mode inhibition against the AChE and BChE as indicated by their data lines which either intersected in the first (for inhibition of the BChE) or second (for inhibition of the AChE) quadrants.¹⁹ This type of inhibitor is able to bind to the active site of the enzyme as well as at different sites of the enzyme (allosteric site) due to the allosteric effect.¹⁹ The inhibition constants, K_{iAChE} and K_{iBChE} , were derived from the secondary plots (Figure 4) for compounds **3** (4.33 μ M and 0.56 μ M, respectively) and **4** (5.86 μ M and 11.46 μ M, respectively), inferring that compound **3** has a higher affinity to both enzymes in particular to the BChE rather than compound **4**. A smaller value of the inhibition constant indicates a stronger inhibition.²⁰

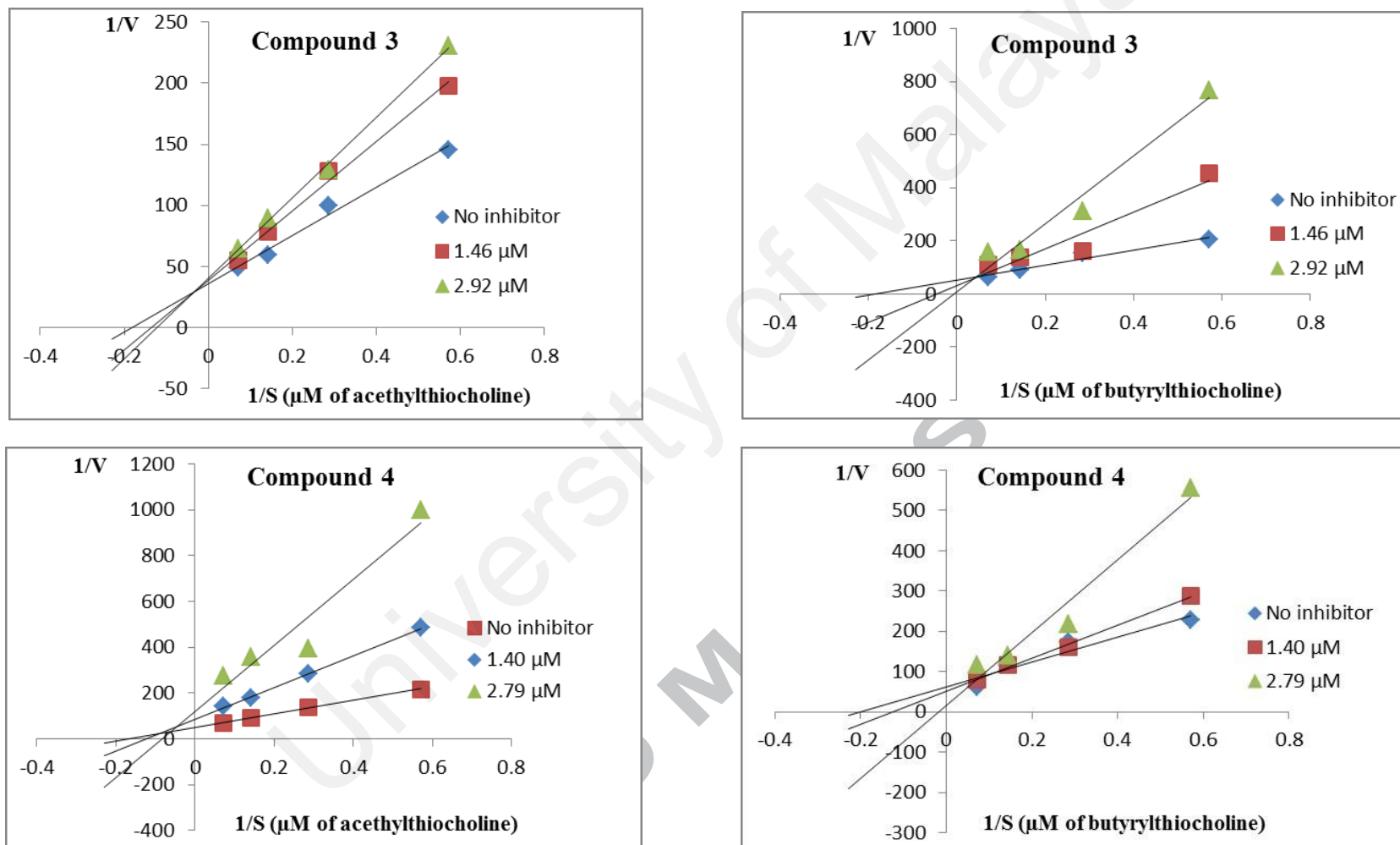


Figure 3: Lineweaver-Burk plots of cholinesterase inhibition activities of compounds 3 and 4

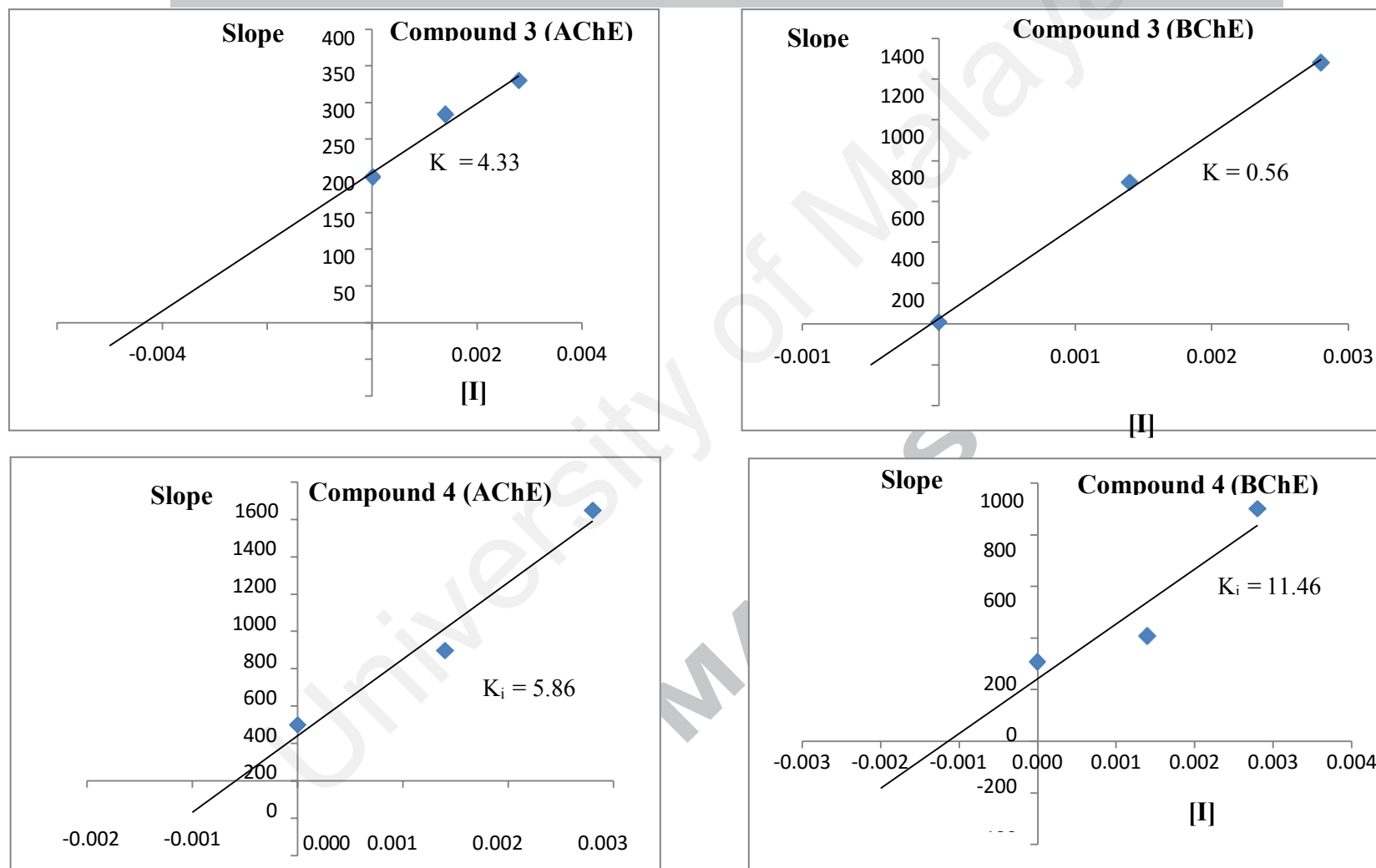


Figure 4: Secondary plot of Lineweaver-Burk plots of compounds 3 and 4

Since compounds **3** and **4** were active dual inhibitors towards the AChE and the BChE, molecular docking studies were performed in order to understand the binding interactions between the two active compounds with both the enzymes. For the AChE, the aromatic rings of both the active compounds were involved in hydrophobic interactions with His 440 from the catalytic triad. In addition, hydrogen bonds were formed between the hydroxyl group at C-17 for both compounds with Ser 200 from the catalytic triad as well as Gly 116 and Gly 119 from the oxyanion hole (Figure 5). The catalytic triad is the active site of the enzyme where acetylcholine is hydrolyzed into choline and acetate while the oxyanion hole provides hydrogen bond donors that stabilises the tetrahedral transition state of the substrate.²¹ Hydrophobic interaction was observed between the aromatic ring b of compound **3** with Asp 72 from the peripheral anionic site (PAS) while the hydroxyl group at C-12 of compound **4** formed hydrogen bonding with Asp 72 from the PAS (Figure 5). The PAS is located at the entrance of the active site gorge of both the AChE and BChE. The binding of the acetylcholine to the PAS is the first step in catalytic pathway and allosteric modulations. The PAS is known to be involved in accelerating non-cholinergic functions such as cell adhesion, neurite outgrowth and amyloid β deposition in AD.²¹ Hence, amyloid β deposition can be reduced or prevented with the presence of the PAS blocker.²² Since compounds **3** and **4** were involved in the binding interaction with Asp 70; an essential component of the PAS in the AChE, it can be proposed that the potency of both compounds in inhibiting the cholinesterase activity started through the blocking at the PAS before the inhibition of the binding of the substrate at the active site.²³ Since compounds **3** and **4** both had binding interaction with the active site (catalytic triad) and the allosteric site (PAS and oxyanion hole) of the AChE, the finding was in agreement with the mode of inhibition of both compounds; mixed-mode inhibition.

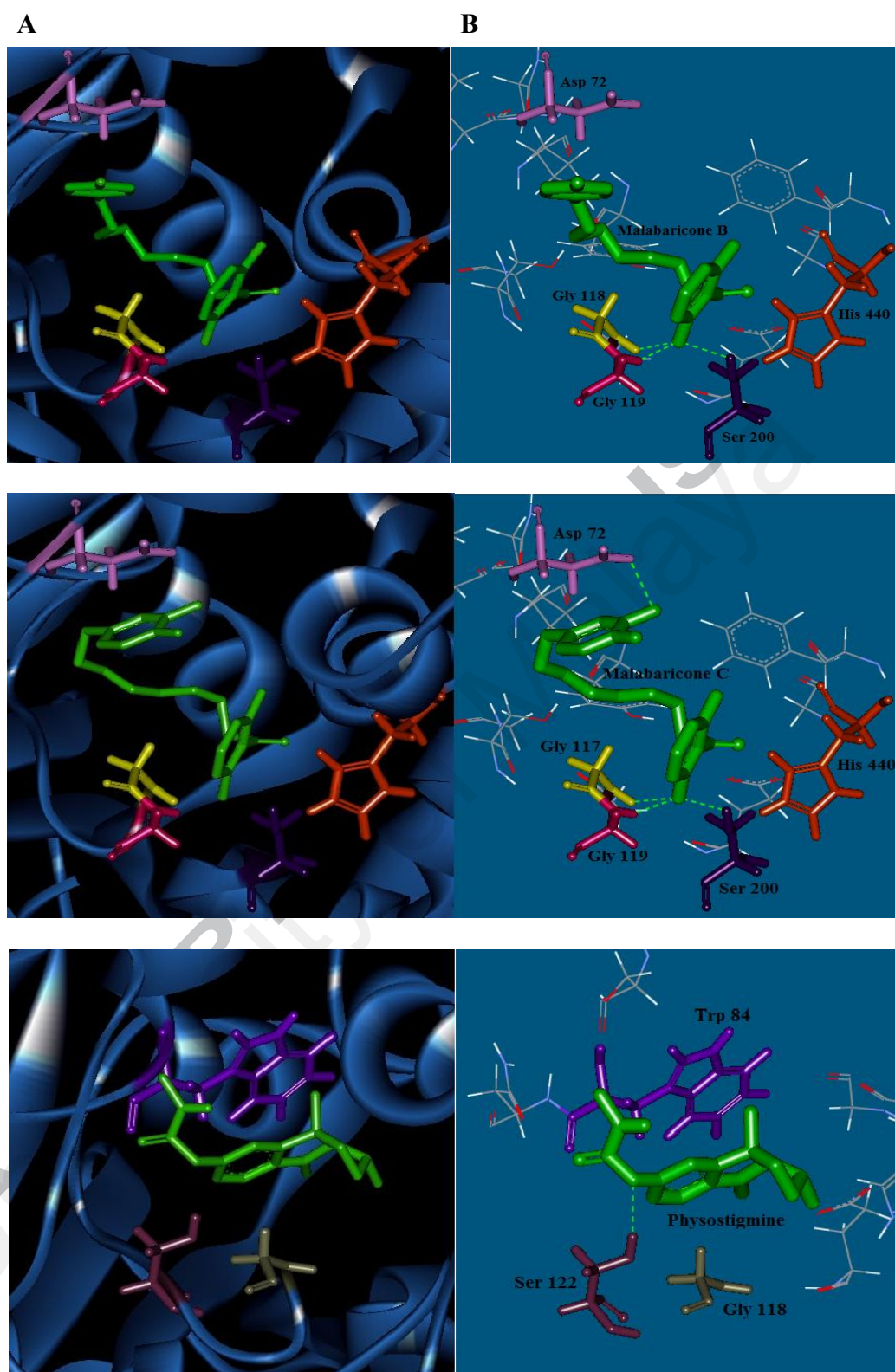


Figure 5: (A) View of compounds **3** (up), **4** (middle) and physostigmine at the binding site of AChE (protein structures are represented by solid ribbon format). (B) Simplified view of compounds **3** (up), **4** (middle) and physostigmine interacting with surrounding amino acid residues which are shown in stick format. The hydrogen bond interaction of the ligands (compounds) with amino acid residues are shown in green dotted lines.

For the BChE, hydrogen bond interactions were observed between both compounds with the enzyme. The hydroxyl group at C-17 and the carbonyl group at C-1 formed hydrogen bonds with Ser 198 from the catalytic triad (Figure 6). Besides, hydrogen bonds were also formed between the carbonyl group at C-1 with Gly 116 and Gly 117 from the oxyanion hole (Figure 6). The only difference in the binding interaction of compounds **3** and **4** with the BChE was that the hydroxyl group at C-12 of compound **4** formed a hydrogen bond with His 438 from the catalytic site while the aromatic ring b of compound **3** underwent hydrophobic interaction with Tyr 332 from peripheral anionic site. It can be suggested that the binding of compound **3** to the PAS of the BChE played an important role in inhibiting the binding of the substrate which in turn gave rise to its lower IC_{50} value (1.76 μ M) of the cholinesterase inhibitory activity compared to compound **4** (IC_{50} value: 2.80 μ M). In addition, the finding was also in agreement with the mode of inhibition for both compounds; mixed-mode inhibition, whereby both compounds were able to bind to the active site (catalytic triad) and the allosteric site (PAS and oxyanion hole) of the BChE.

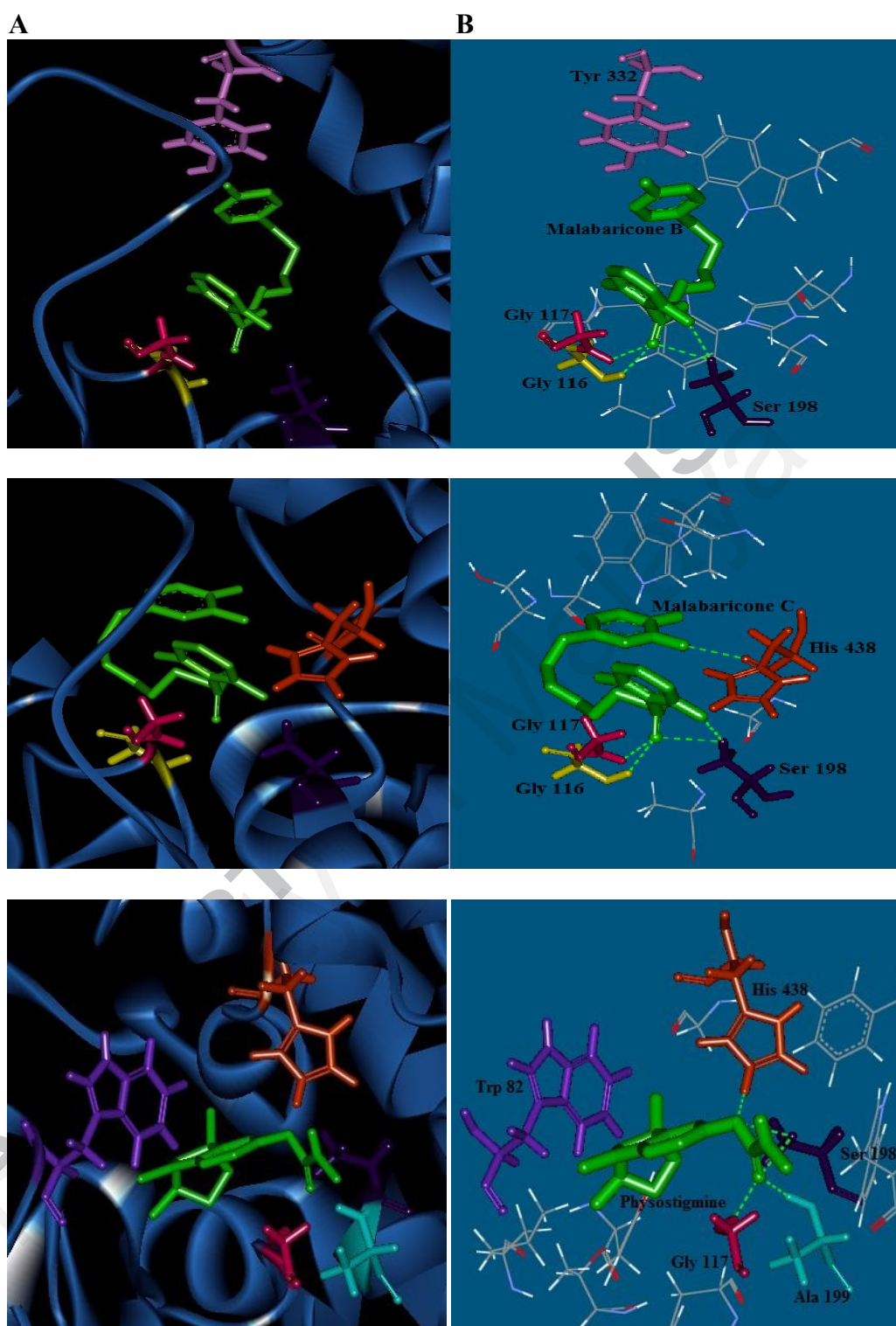


Figure 6: (A) View of compounds **3** (up), **4** (middle) and physostigmine at the binding site of BChE (protein structures are represented by solid ribbon format). (B) Simplified view of compounds **3** (up), **4** (middle) and physostigmine interacting with surrounding amino acid residues which are shown in stick format. The hydrogen bond interaction of the ligands (compounds) with amino acid residues are shown in green dotted lines.

For physostigmine (Figure 7), its ring c formed hydrophobic interaction with Gly 118 from the oxyanion hole and Trp 84 from the choline binding site (CBS) of the AChE. The methyl group at C-6 also formed hydrophobic interaction with Trp 84 and the oxygen atom of the ester group at C-9 formed hydrogen bond with Ser 122 of the AChE (Figure 5). Besides, at the CBS of the BChE, the methyl group at C-6 of physostigmine formed hydrophobic interaction with Trp 82. Hydrogen bonds were observed between the ester group at C-9 of physostigmine and Ser 198 and His 438 from the catalytic triad. In addition, the ketone group at C-13 of physostigmine formed a hydrogen bond with Ser 198 from catalytic triad. Hydrogen bonds were formed between Gly 117 and Ala 199 of the oxyanion hole of the BChE with the ketone group at C-13 of physostigmine (Figure 6). The binding interaction data for compounds **3**, **4** and physostigmine with the amino acid residues of *TcAChE* and *hBChE* are summarized in Table 3.

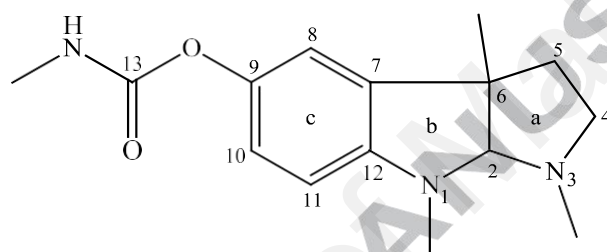


Figure 7: Structure of physostigmine (reference standard)

ACCEPTED MANUSCRIPT

Table 3: Binding interaction data for compounds **3**, **4** and physostigmine with amino acid residues of *TcAChE* and *hBChE*

Ligand/Compound	Enzyme	Binding Energy (kcal)	Interacting site	Residue	Type of Interaction	Distance (Å)	Ligand Interacting
Malabaricone B (3)	<i>TcAChE</i>	-13.32	Catalytic triad	Ser 200	Hydrogen	2.26	Hydroxyl group at C-17
				His 440	Hydrophobic	-	Aromatic ring a
			Oxyanion hole	Gly 118	Hydrogen	1.97	Hydroxyl group at C-17
				Gly 119	Hydrogen	2.12	
			Peripheral anionic	Asp 72	Hydrophobic	-	Aromatic ring b
	<i>hBChE</i>	-12.82	Catalytic triad	Ser 198	Hydrogen	2.99	Hydroxyl group at C-17
					Hydrogen	2.71	Carbonyl group at C-1
			Oxyanion hole	Gly 116	Hydrogen	2.29	Carbonyl group at C-1
				Gly 117	Hydrogen	2.12	
			Peripheral	Tyr 332	Hydrophobic	-	Aromatic ring b
Malabaricone C (4)	<i>TcAChE</i>	-13.27	Catalytic triad	Ser 200	Hydrogen	2.05	Hydroxyl group at C-17
				His 440	Hydrophobic	-	Aromatic ring a
			Oxyanion hole	Gly 118	Hydrogen	2.26	Hydroxyl group at C-17
				Gly 119	Hydrogen	2.07	
			Peripheral	Asp 72	Hydrogen	3.05	Hydroxyl group at C-12
	<i>hBChE</i>	-12.30	Catalytic triad	Ser 198	Hydrogen	2.65	Hydroxyl group at C-17
						2.76	Carbonyl group at C-1
				His 438	Hydrogen	3.11	Hydroxyl group at C-12
			Oxyanion hole	Gly 118	Hydrogen	2.14	Carbonyl group at C-1
				Gly 119	Hydrogen	2.13	

ACCEPTED MANUSCRIPT

Physostigmine	<i>TcAChE</i>	-9.78	Oxyanion hole	Gly 118	Hydrophobic	-	Aromatic ring C
			Choline binding site	Trp 84	Hydrophobic	-	Aromatic ring C
			Wall of gorge	Ser 122	Hydrogen	2.29	Methyl group at C-6 Ester group at C-9
	<i>hBChE</i>	-9.65	Choline binding site	Trp 82	Hydrophobic	-	Methyl group at C-6
			Catalytic triad	Ser 198	Hydrogen	2.91 2.64	Ester group at C-9 Ketone group at C-13
				His 438	Hydrogen	2.48	Ester group at C-9
			Oxyanion hole	Gly 117	Hydrogen	2.01	Ketone group at C-13
				Ala 199	Hydrogen	2.33	

In summary, compounds **3** and **4** were dual mixed-mode inhibitors as they each actively inhibited the AChE and BChE with low IC₅₀ values in the range of 1.76 ± 0.21-2.80 ± 0.49 μM. Compound **3** however was found to have a higher affinity towards both enzymes. Molecular docking simulation revealed that compounds **3** and **4** interacted with the peripheral anionic site (PAS), the catalytic triad and the oxyanion hole of the AChE. For the BChE, compound **3** also interacted with the PAS, the catalytic triad and the oxyanion hole while compound **4** only interacted with the catalytic triad and the oxyanion hole. Therefore, both the above mentioned acylphenols are promising candidates in the search for natural drugs which can be employed to cure diseases related to neurodegenerative disorder, in particular in the treatment of AD.

The moderate to strong cholinesterase inhibitory activities of all of the acylphenols and dimeric acylphenols isolated in the present study provided scientific evidence for the possible usage of the fruits of *M. cinnamomea* as traditional medicine especially as memory enhancers like the fruits of its closely related species *M. fragrans* (nutmeg).

Acknowledgement

The authors acknowledge the University of Malaya Research Grant RP001-2012A/B and the Centre National de la Recherche Scientifique (CNRS) grant (57-02-03-1007) which have made this work possible. The results from this work are a collaborative effort of the Phytolab- IFM NatProLab (UM-CNRS). The authors would also like to acknowledge Mr. Abdulwali Ablat for his valuable guidance and assistance in conducting the cholinesterase enzymes inhibition assay.

References

1. Puri, V., Wang, X., Vardigan, J. D., Kuduk, S. D., & Uslander, J. M. *Behavioural Brain Research*. **2015**, *287*, 96-99.
2. Liang, J., Kulasiri, D., & Samarasinghe, S. *Biosystems*. **2015**, *134*, 1-15.
3. Boada, M., Tárraga, L., Hernández, I., Valero, S., Alegret, M., Ruiz, A., Becker, J. T. *Alzheimer's & Dementia*. **2014**, *10*(3), 409-415.
4. Burnham, V. L., & Thornton, J. E. *Hormones and Behavior*. **2015**, *76*, 48-56.
5. Awang, K., Chan, G., Litaudon, M., Ismail, N. H., Martin, M.-T., & Gueritte, F. *Bioorganic & Medicinal Chemistry*. **2010**, *18*(22), 7873-7877.
6. Seidemann, J. *World Spice Plants: Economic Usage, Botany, Taxonomy*. Springer- Verlag Berlin Heidelberg, **2005**.
7. Sawadjoon, S., Kittakoo, P., Kirtikara, K., Vichai, V., Tanticharoen, M., & Thebtaranonth, Y. *J. Org. Chem.* **2002**, *67*(16), 5470-5475.
8. Chong, Y. M., Yin, W. F., Ho, C. Y., Mustafa, M. R., Hadi, A. H. A., Awang, K., Chan, K.-G. *J. Nat. Prod.* **2011**, *74*(10), 2261-2264.
9. Sivasothy, Y., Loo, K. Y., Leong, K. H., Litaudon, M., & Awang, K. *Phytochemistry*. **2016**, *122*, 265-269.
10. Cao, G.-Y., Yang, X.-W., Xu, W., & Li, F. *Food and Chemical Toxicology*. **2013**, *62*, 167-171.

11. Cuong, T. D., Hung, T. M., Han, H. Y., Roh, H. S., Seok, J., Lee, J. K., Jeong, J. Y., Choi, J. S., Kim, J. A., Min, B. S. *Natural Product Communications*. **2014**, 9(4), 499- 502.
12. Pham, V. C., Jossang, A., Sevenet, T., & Bodo, B. *Tetrahedron*. **2002**, 56(12), 1707- 1713.
13. Maia, A., Schmitz-Afonso, I., Martin, M.-T., Awang, K., Laprevote, O., Gueritte, F., & Litaudon, M. *Planta Med.* **2008**, 74(12), 1457-1462.
14. Light yellow amorphous powder, UV λ_{\max} (MeOH) nm (log ϵ): 341 (2.83), 270 (3.46), 224 (3.67); IR ν_{\max} (NaCl) cm^{-1} : 3272, 2924, 2852, 1642, 1515, 1455, 1244; LCMS- IT-TOF m/z : 381.1675 [M + Na]⁺ (calcd. for C₂₁H₂₆O₅Na, 381.1672). For ¹H and ¹³C NMR spectroscopic data; see Table 1.
15. Pham, V. C., Jossang, A., Sevenet, T., & Bodo, B. *Tetrahedron*. **2002**, 58(28), 5709- 5714.
16. Ballard, C. G. *European Neurology*. **2002**, 47(1), 64-70.
17. Giacobini, E. *Pharmacological Research*. **2004**, 50(4), 433-440.
18. Tan, W.-N., Khairuddean, M., Wong, K.-C., Khaw, K.-Y., & Vikneswaran, M. *Fitoterapia*. **2014**, 97, 261-267.
19. Khaw, K. Y., Choi, S. B., Tan, S. C., Wahab, H. A., Chan, K. L., & Murugaiyah, V. *Phytomedicine*. **2014**, 21(11), 1303-1309.
20. Majouli, K., Besbes Hlila, M., Hamdi, A., Flamini, G., Ben Jannet, H., & Kenani, A. *Industrial Crops and Products*. **2016**, 82, 23-28.
21. Johnson, G., Moore, S.W. *Current Pharmaceutical Design*. **2006**, 12, 217-225.
22. Inestrosa, N.C., Alvarez, A., Pérez, C.A., Moreno, R.D., Vicente, M., Linker, C., Casanueva, O.I., Soto, C., Garrido, J. *Neuron*. **1996**, 16, 881-891.
23. Masson, P., Froment, M.-T., Bartels, C.F., Lockridge, O. *European Journal of Biochemistry*. **1996**, 235, 36-48.

Quorum Sensing Inhibitory Activity of Giganteone A from *Myristica cinnamomea* King against *Escherichia coli* Biosensors

Yasodha Sivasothy ^{1,†}, Thiba Krishnan ^{2,†}, Kok-Gan Chan ^{2,†}, Siti Mariam Abdul Wahab ^{1,†}, Muhamad Aqmal Othman ^{1,†}, Marc Litaudon ^{3,†} and Khalijah Awang ^{1,*,†}

¹ Department of Chemistry, Faculty of Science, University of Malaya, Kuala Lumpur 50603, Malaysia; yasodhasivasothy@gmail.com (Y.S.); maryamabdwahab@gmail.com (S.M.A.W.); qmalxez44@gmail.com (M.A.O.)

² Division of Genetics and Molecular Biology, Institute of Biological Sciences, Faculty of Science, University of Malaya, Kuala Lumpur 50603, Malaysia; thibavengdes@yahoo.com (T.K.); kokgan@um.edu.my (K.-G.C.)

³ Institut de Chimie des Substances Naturelles, Centre National de la Recherche Scientifique, 91198 Gif-sur-Yvette, Cedex, France; marc.LITAUDON@cnrs.fr

* Correspondence: khalijah@um.edu.my; Tel.: +60-379-674-064; Fax: +60-379-674-193

† These authors contributed equally to this work.

Academic Editor: Derek J. McPhee

Received: 26 January 2016 ; Accepted: 15 March 2016 ; Published: 21 March 2016

Abstract: Malabaricones A–C (**1–3**) and giganteone A (**4**) were isolated from the bark of *Myristica cinnamomea* King. Their structures were elucidated and characterized by means of NMR and MS spectral analyses. These isolates were evaluated for their anti-quorum sensing activity using quorum sensing biosensors, namely *Escherichia coli* [pSB401] and *Escherichia coli* [pSB1075], whereby the potential of giganteone A (**4**) as a suitable anti-quorum sensing agent was demonstrated.

Keywords: *Myristica cinnamomea* King; Myristicaceae; acylphenols; dimeric acylphenols; anti-quorum sensing activity

1. Introduction

The increasing incidence of multi-drug resistant bacteria has prompted the search for potent, novel antibacterial drugs or complementary agents against resistant pathogens with new targets or novel mechanisms [1]. Quorum sensing is one such target mechanism. It is a cell-cell communication system used by most Gram-negative bacteria [2]. In quorum sensing (QS), bacteria use chemical signaling molecules commonly known as auto-inducers to track changes in cell population density. By monitoring the changes in the concentration of the auto-inducers, QS regulates gene expression especially virulence factor production in pathogenic bacteria [3]. Therefore, the disruption of QS is considered as an alternative for antibiotic treatment. New QS inhibitory compounds are known to constitute a new group of antimicrobial agents with applications in many fields such as medicine and agriculture [4,5].

Plants have been used for centuries in traditional medicine due to their diverse secondary metabolites. Plants grow in environments with high bacterial densities and have developed an evolutionary co-existence with QS inhibitory compounds or QS mimic compounds which reduce the pathogenic capability of bacteria [1,2]. Due to their diverse chemical repertoire, the anti-virulence properties of medicinal plants and their constituents are attracting attention since plants are able to interfere with bacterial communication process thereby disrupting associated cellular mechanisms of functions [1,2].

Myristica cinnamomea King (Myristicaceae), commonly known as cinnamon nutmeg, is distributed in the Malayan Peninsula, Singapore, Borneo and Philippines. Locally, it is referred to as “pala bukit” [6]. *M. cinnamomea* is a tree 15 m in height and 45 cm in diameter. Its outer bark is dark brown, rugose with fine grid cracks, while the inner bark is pale brown. The leaves are oblong to oblanceolate, bright green above and pale silvery brown below. The fruit is yellow and globose to broadly globular-oblong. Its seeds are red and used as spices [6]. Recently, we isolated two new α -glucosidase inhibitors from the hexane extract of the bark; giganteone D (IC_{50} 5.05 μ M) and cinnamomeone A (IC_{50} 358.80 μ M) [7]. In a previous study of ours, we identified malabaricone C isolated from the methanol extract of the bark to possess anti-QS activity against *Pseudomonas aeruginosa* PAO1 [8]. In the current work however, we decided to increase the amount of plant material and reinvestigate its chemical constituents in search of new acylphenols and dimeric acylphenols with anti-QS properties against *Escherichia coli* biosensors.

2. Results and Discussion

The ethyl acetate soluble fraction of the acetone extract of the dried bark of *M. cinnamomea* was subjected to repeated silica gel column chromatography to yield four known acylphenols and dimeric acylphenols 1–4. They were identified as malabaricone A (1), malabaricone B (2), malabaricone C (3) and giganteone A (4) (Figure 1) upon comparison of their spectroscopic data with those reported in the literature [9,10] and were further assessed for their anti-QS activity against *E. coli* QS biosensors. The 1H -NMR and ^{13}C -NMR spectra of compounds 1–4 are depicted in Figures 2–5.

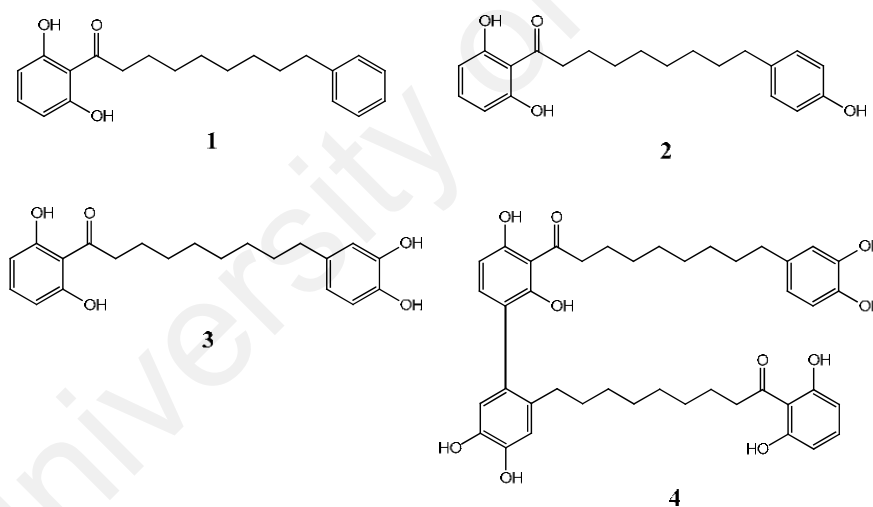


Figure 1. Structures of compounds 1–4.

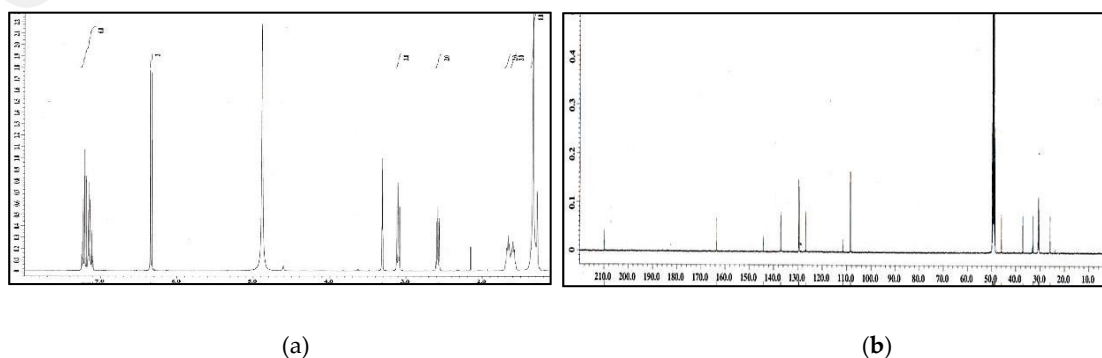
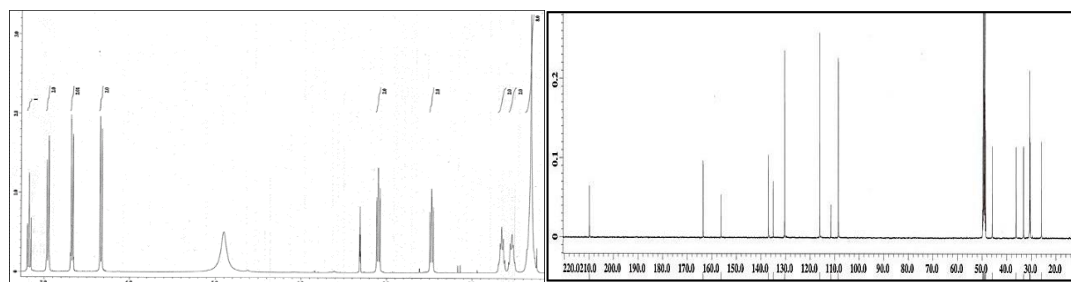
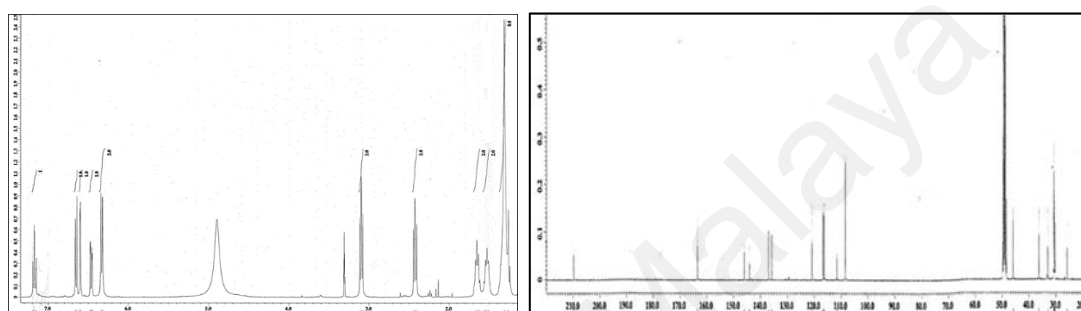


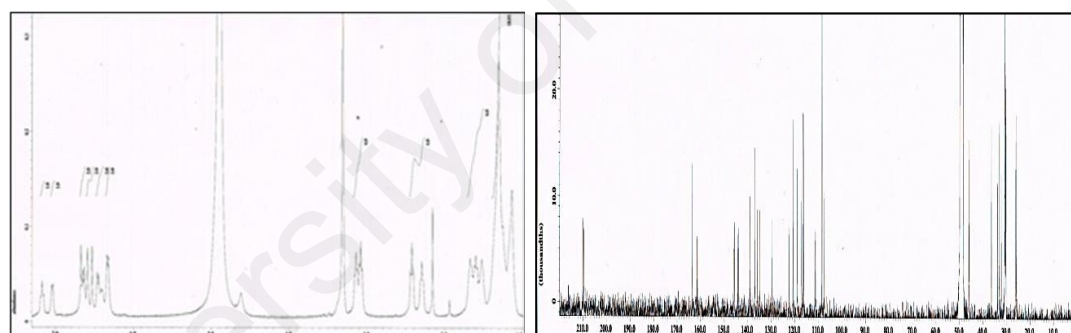
Figure 2. 1H -NMR (a) and ^{13}C -NMR (b) spectra of compound 1.



(a) (b)
Figure 3. ^1H -NMR (a) and ^{13}C -NMR (b) spectra of compound 2.



(a) (b)
Figure 4. ^1H -NMR (a) and ^{13}C -NMR (b) spectra of compound 3.



(a) (b)
Figure 5. ^1H -NMR (a) and ^{13}C -NMR (b) spectra of compound 4.

In the present study, compounds 1–4 were tested for possible anti-QS properties using *E. coli* [pSB401] and *E. coli* [pSB1075] as QS biosensors. These biosensor strains respond to the QS signaling molecules *N*-acylhomoserine lactones by producing bioluminescence preferentially to the presence of exogenous AHLs from six to eight carbons in length (for strain *E. coli* [pSB401]) or AHLs with acyl chains of 10–14 carbons in length (for strain *E. coli* [pSB1075]). Therefore, the reduction in bioluminescence compared to the control showed the presence of anti-QS effect. As a prerequisite, we have verified that the compounds did not show bactericidal effect on all biosensor cells (Figure 6a,b). Under the present experimental conditions, increasing concentrations of compound 4 showed significant inhibition of the bioluminescence produced by both *E. coli* [pSB401] (from increasing the concentration of 95 $\mu\text{g}/\text{mL}$ to 380 $\mu\text{g}/\text{mL}$) and *E. coli* [pSB1075] (from increasing concentration of 285 $\mu\text{g}/\text{mL}$ to 380 $\mu\text{g}/\text{mL}$) (Figures 7 and 8). DMSO (solvent) did not show any antimicrobial effects in the performed bioassays when applied at different concentrations. However, malabaricone A (1), malabaricone B (2) and malabaricone C (3) showed no significant bioluminescence inhibition. Thus, the current study indicates the promising anti-QS activity for both short and long chain AHL QS

systems. A similar study has shown that compound 3 isolated from the methanol extract of the bark of *M. cinnamomea* also exhibited anti-QS activity [8]. Besides that, other compounds including *trans*-cinnamaldehyde [11], polyhydroxyanthraquinones [12] and furanones [13] have been reported as QS inhibitors in recent studies.

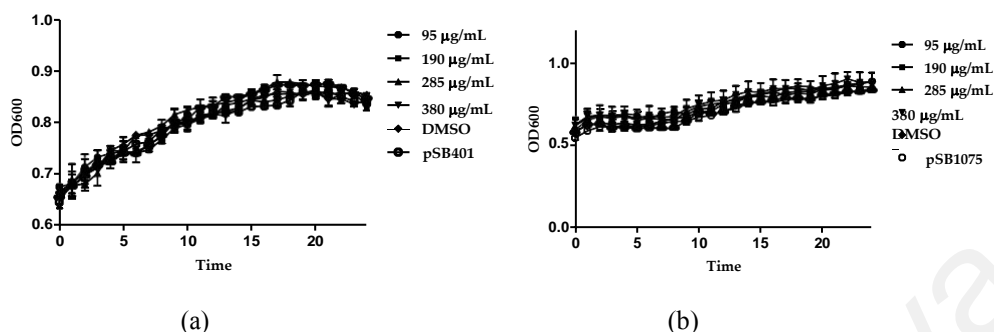


Figure 6. Growth effect of giganteone A with increasing concentration from 95 µg/mL (circle), 190 µg/mL (square), 285 µg/mL (triangle) to 380 µg/mL (inverted triangle) while DMSO (diamond) on (a) *E. coli* [pSB401] and (b) *E. coli* [pSB1075], respectively served as control (circle with hole). Data were analyzed by one-way analysis of variance with $p < 0.05$ being significant.

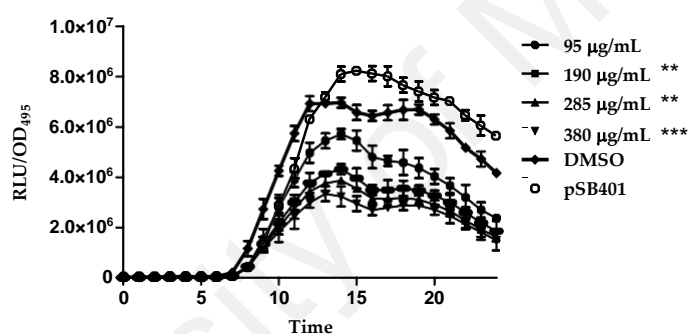


Figure 7. Bioluminescence expression of *E. coli* [pSB401] by giganteone A with increasing concentration from 95 µg/mL (circle), 190 µg/mL (square), 285 µg/mL (triangle) to 380 µg/mL (inverted triangle) while DMSO (diamond) and *E. coli* [pSB401] supplemented with C6-HSL, respectively served as control (circle with hole) was included. The data were presented as RLU/OD to account for any differences in growth. Data were analyzed by one-way analysis of variance with $p < 0.05$ being significant. “**” means the value is very significant while “***” means the value is extremely significant.

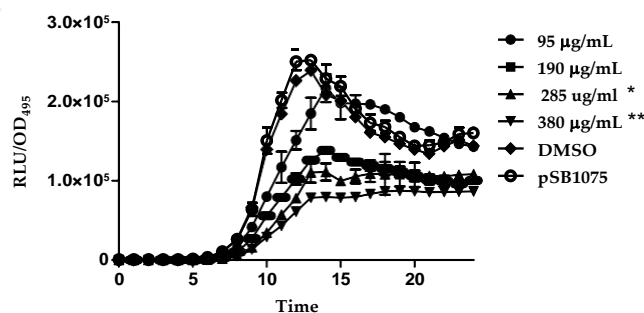


Figure 8. Bioluminescence expression of *E. coli* [pSB1075] by giganteone A with increasing concentration 95 µg/mL (circle), 190 µg/mL (square), 285 µg/mL (triangle) to 380 µg/mL (inverted triangle) while DMSO (diamond) as control were included. The data were presented as RLU/OD to account for any differences in growth. Data were analyzed by one-way analysis of variance with $p < 0.05$ being significant. “*” means the value is significant while “**” means the value is very significant.

3. Materials and Methods

3.1. General Procedures

Analytical TLC was carried out on 60 F₂₅₄ silica gel plates (absorbent thickness: 0.25 mm, Merck, Darmstadt, Germany). Column chromatography was performed using silica gel (Merck 230–400 mesh, ASTM). IR spectra were recorded using a Perkin-Elmer Spectrum 400 FT-IR Spectrometer (Perkin Elmer, Waltham, MA, USA). NMR spectra were acquired in CD₃OD (Merck) using a JEOL ECA 400 MHz NMR spectrometer (JEOL, Tokyo, Japan). The LCMS-IT-TOF spectra were obtained on a UFLC Shimadzu Liquid Chromatograph with a SPD-M20A diode array detector coupled to an IT-TOF mass spectrometer (Shimadzu, Kyoto, Japan). UV spectra were recorded using a Shimadzu 1650 PC UV-Vis Spectrophotometer (Shimadzu). All solvents were of analytical grade and were distilled prior to use.

3.2. Plant Material

M. cinnamomea was collected from Johor in 2003. The plant was identified by Mr. Teo Leong Eng and its voucher specimen (KL 5043) has been deposited with the University of Malaya herbarium.

3.3. Extraction and Isolation

Dried powdered bark (2.0 kg) of *M. cinnamomea* was extracted twice with hexane (10.0 L,) followed by acetone (15.0 L) at room temperature, affording 8.40 g and 242.56 g of extracts, respectively. The acetone extract was re-extracted twice with ethyl acetate (2.0 L) at room temperature to yield 58 g of extract. 26 g of the ethyl acetate extract was chromatographed over a silica gel column (650 g, 7.2 cm × 63 cm) eluting with dichloromethane gradually enriched with ethyl acetate (0%–100%) to provide 12 main fractions (MC 1 to MC 12). Fraction MC 2 (8.50 g; eluted with dichloromethane:ethyl acetate [80:20 v/v]) was further purified via silica gel column chromatography (210 g, 4.0 cm × 50 cm) with dichloromethane:ethyl acetate (95:5 v/v, 0.5 L) as the eluent which led to the isolation of **1** (4.80 g) and **2** (1.54 g). Fractions MC 3 and MC 4 (9.3 g, which eluted with dichloromethane:ethyl acetate [80:20 v/v]) were combined and re-chromatographed over silica gel (230 g, 4.0 cm × 50 cm) with 1.5 L of the same solvent system to afford **3** (3.43 g). Column chromatography (25 g, 2.5 cm × 30 cm) of fraction MC 5 (0.93 g; eluted with dichloromethane:ethyl acetate [60:40 v/v]) using an isocratic solvent system of dichloromethane:ethyl acetate (75:25 v/v, 0.5 L) provided sub-fractions MC 5-1 (0.01 g), MC 5-2 (0.10 g) and MC 5-3 (0.55 g). Final purification to yield **4** (127.8 mg) was achieved via column chromatography (25 g, 2.5 cm × 30 cm) of sub-fraction MC 5-3 with dichloromethane:acetone (80:20 v/v, 0.4 L) as the eluent. The purified compounds; malabaricone A (**1**), malabaricone B (**2**), malabaricone C (**3**) and giganteone A (**4**), were dissolved in 20% v/v DMSO and stored at ~20 °C prior to use.

3.4. Biosensors and Growth Conditions

Biosensors used in this study are listed in Table 1. The strains were routinely cultured at 37 °C in Luria Bertani (LB) broth (1% w/v peptone, 0.5% w/v yeast extract, 0.5% w/v NaCl, per 100 mL distilled water) with shaking (220 rpm) and supplemented with tetracycline (20 µg/mL) [14].

Table 1. List of biosensors used.

Biosensors	Description	Source
<i>Escherichia coli</i> [pSB401]	<i>luxRluxI</i> (<i>Photobacterium fischeri</i> [ATCC 7744]): <i>luxCDABE</i> (<i>Photobacterium luminescens</i> [ATCC 29999]) fusion; pACYC184-derived, TetR, AHL biosensor producing bioluminescence in respond to short chain AHL <i>lasRlasI</i> (<i>P. aeruginosa</i> PAO1); <i>luxCDABE</i> (<i>P. luminescens</i> [ATCC 29999]) fusion in pUC18 AmpR, AHL biosensor	[15]
<i>Escherichia coli</i> [pSB1075]	producing bioluminescence in respond to long chainAHL	[15]

University of Malaya

3.5. Quantification of Bioluminescence for Anti-QS Assay

Bioluminescence production was quantified using a Tecan Infinite M200Pro microplate reader (Tecan Group Ltd., Mannedorf, Switzerland). Briefly, an overnight culture of *E. coli* biosensor cells was diluted using LB Broth to an OD₆₀₀ of 0.1. Next, 0.2 mL of *E. coli* biosensor cells and giganteone A were added into the well of a Greiner 96-well microtitre plate with increasing concentrations from 95 µg/mL to 380 µg/mL. This step was repeated for all of the other compounds. For *E. coli* [pSB401] and *E. coli* [pSB1075], *N*-hexanoyl-L-homoserine lactone (C6-HSL, 0.2 µg/mL) and *N*-(3-oxo-dodecanoyl)-L-homoserine lactone (3-oxo-C12-HSL, 0.2 µg/mL) were supplemented, respectively. The bioluminescence and OD₄₉₅ were determined every 30 min for 24 h at 37 °C by the microplate reader. The production of bioluminescence is given as the relative light units (RLU) per unit of optical density at 495 nm, which accounted for the influence of increased growth on the total bioluminescence [16]. Reduction of bioluminescence in *E. coli* [pSB401] and *E. coli* [pSB1075] suggested anti-QS properties. Biosensor cells treated with DMSO alone were used as the negative control. Experiments were performed in triplicates and repeated three times [17,18].

3.6. Statistical Analysis

All results represent the average of three independent experiments. The data were presented as mean ± standard deviation (SD) and analyzed by one-way analysis of variance (ANOVA) and Student's *t*-test. The *p* < 0.05 was considered as significant, calculated using the GraphPad Prism Version 5 (GraphPad Software Inc., San Diego, CA, USA).

4. Conclusions

In summary, giganteone A (**4**) can be considered a QS inhibitor against *E. coli* biosensors.

Acknowledgments: The authors acknowledge the University of Malaya for providing the University Research Grant RP001-2012, the High Impact Research Grants UM.C/625/1/HIR/MOHE/SC/37 Grant No. H-21001-F000037, UM.C/625/1/HIR/MOHE/CHAN/01 Grant No. A-000001-50001 UM.C/625/1/HIR/MOHE/CHAN/14/1, Grant No.H-50001-A000027 which have made this work possible.

Author Contributions: K.A. and K.G.C. conceived and designed the experiments; Y.S., T.K., S.M.A.W. and M.A.O. performed the experiments; Y.S. and T.K. analyzed the data; K.A., K.G.C. and M.L. contributed reagents and materials; Y.S., T.K., K.A. and K.G.C. wrote the paper.

Conflicts of Interest: Authors declare no conflict of interest.

References

1. Aliyu, A.B.; Koorbanally, N.A.; Moodley, B.; Singh, P.; Chenia, H.Y. Quorum sensing inhibitory potential and molecular docking studies of sesquiterpene lactones from *Vernonia blumeoides*. *Phytochemistry* **2016**. [CrossRef] [PubMed]
2. Sheng, J.Y.; Chen, T.T.; Tan, X.J.; Chen, T.; Jia, A.Q. The quorum-sensing inhibiting effects of stilbenoids and their potential structure-activity relationship. *Bioorg. Med. Chem. Lett.* **2015**, *25*, 5217–5220. [CrossRef] [PubMed]
3. Swem, L.R.; Swem, D.L.; O'Loughlin, C.T.; Gatmaitan, R.; Zhao, B.; Ulrich, S.M.; Bassler, B.L. A quorum-sensing antagonist targets both membrane-bound and cytoplasmic receptors and controls bacterial pathogenicity. *Mol. Cell* **2009**, *352*, 143–153. [CrossRef] [PubMed]
4. Hentzer, M.; Givskov, M. Pharmacological inhibition of quorum sensing for the treatment of chronic bacterial infections. *J. Clin. Investig.* **2003**, *112*, 1300–1307. [CrossRef] [PubMed]
5. Hong, K.W.; Koh, C.L.; Sam, C.K.; Yin, W.F.; Chan, K.G. Quorum quenching revisited—from signal decays to signaling confusion. *Sensors* **2012**, *12*, 4661–4696. [CrossRef] [PubMed]
6. Seidemann, J. *World Spice Plants: Economic Usage, Botany, Taxonomy*; Springer-Verlag: Berlin/Heidelberg, Germany, 2005.
7. Sivasothy, Y.; Loo, K.Y.; Leong, K.H.; Litaudon, M.; Awang, K. A potent alpha-glucosidase inhibitor from *Myristica cinnamomea* King. *Phytochemistry* **2016**, *122*, 265–269. [CrossRef] [PubMed]

8. Chong, Y.M.; Yin, W.F.; Ho, C.Y.; Mustafa, M.R.; Hadi, A.H.A.; Awang, K.; Narrima, P.; Koh, C.L.; Appelton, D.R.; Chan, K.G. Malabaricone C from *Myristica cinnamomea* exhibits anti-quorum sensing activity. *J. Nat. Prod.* **2011**, *74*, 2261–2264. [[CrossRef](#)] [[PubMed](#)]
9. Pham, V.C.; Jossang, A.; Sevenet, T.; Bodo, B. Cytotoxic acylphenols from *Myristica maingayi*. *Tetrahedron* **2000**, *56*, 1707–1713. [[CrossRef](#)]
10. Pham, V.C.; Jossang, A.; Sevenet, T.; Bodo, B. Novel cytotoxic acylphenol dimers of *Myristica gigantea*; enzymatic synthesis of giganteones A and B. *Tetrahedron* **2002**, *58*, 5709–5714. [[CrossRef](#)]
11. Chang, C.Y.; Krishnan, T.; Wang, H.; Chen, Y.; Yin, W.F.; Chong, Y.M.; Chan, K.G. Non-antibiotic quorum sensing inhibitors acting against *N*-acyl homoserine lactone synthase as druggable target. *Sci. Rep.* **2014**, *4*. [[CrossRef](#)] [[PubMed](#)]
12. Figueroa, M.; Jarmusch, A.K.; Raja, H.A.; El-Elimat, T.; Kavanaugh, J.S.; Horswill, A.R.; Oberlies, N.H. Polyhydroxyanthraquinones as quorum sensing inhibitors from the guttates of *Penicillium restrictum* and their analysis by desorption electrospray ionization mass spectrometry. *J. Nat. Prod.* **2014**, *77*, 1351–1358. [[CrossRef](#)] [[PubMed](#)]
13. Hentzer, M.; Riedel, K.; Rasmussen, T.B.; Heydorn, A.; Andersen, J.B.; Parsek, M.R.; Givskov, M. Inhibition of quorum sensing in *Pseudomonas aeruginosa* biofilm bacteria by a halogenated furanone compound. *Microbiology* **2002**, *148*, 87–102. [[CrossRef](#)] [[PubMed](#)]
14. Tan, L.Y.; Yin, W.F.; Chan, K.G. *Piper nigrum*, *Piper betle* and *Gnetum gnemon* – Natural food source with anti-quorum sensing properties. *Sensors* **2013**, *13*, 3975–3985. [[CrossRef](#)] [[PubMed](#)]
15. Winson, M.K.; Swift, S.; Fish, L.; Throup, J.P.; Jorgensen, F.; Chhabra, S.R.; Stewart, G.S. Construction and analysis of luxCDABE-based plasmid sensors for investigating *N*-acylhomoserine lactone-mediated quorum sensing. *FEMS Microbiol. Lett.* **1998**, *163*, 185–192. [[CrossRef](#)] [[PubMed](#)]
16. Winzer, K.; Falconer, C.; Garber, N.C.; Diggie, S.P.; Camara, M.; Williams, P. The *Pseudomonas aeruginosa* lectins PA-IL and PA-IIL are controlled by quorum sensing and by RpoS. *J. Bacteriol.* **2000**, *182*, 6401–6411. [[CrossRef](#)] [[PubMed](#)]
17. Krishnan, T.; Yin, W.F.; Chan, K.G. Inhibition of quorum sensing-controlled virulence factor production in *Pseudomonas aeruginosa* PAO1 by Ayurveda spice clove (*Syzygium aromaticum*) bud extract. *Sensors* **2012**, *12*, 4016–4030. [[CrossRef](#)] [[PubMed](#)]
18. Priya, K.; Yin, W.F.; Chan, K.G. Anti-quorum sensing activity of the Chinese traditional herb, *Phyllanthus amarus*. *Sensors* **2013**, *13*, 14558–14569. [[CrossRef](#)] [[PubMed](#)]

Sample Availability: Samples of the compounds are not available from the authors.



© 2016 by the authors; licensee MDPI, Basel, Switzerland. This article is an open access article distributed under the terms and conditions of the Creative Commons by Attribution (CC-BY) license (<http://creativecommons.org/licenses/by/4.0/>).

**THE UNIVERSITY OF MALAYA TECHNOLOGY/INVENTION
DISCLOSURE FORM**

To : The Vice Chancellor, University of Malaya

Through : Head, Department of Institute of Biological Sciences,
Faculty of Science

1. TITLE OF TECHNOLOGY/INVENTION/PRODUCTS

Quorum Sensing Inhibitory Activity of Giganteone A against Escherichia coli biosensors from Myristica cinnamomea King

2. INVESTIGATOR(S)/INVENTOR(S)

No	Name of Member(s)	Role	Address
1.	Dr. Chan Kok Gan 03 – 79675162 (Office) 03-79674509 (Fax) kokgan@um.edu.my	Project Leader	Institute of Biological Sciences, Faculty of Science, UM 50603 W.Persekutuan Kuala Lumpur
2.	Thiba A/PKrishnan	Member	ISB (Genetics and Molecular Biology), Faculty of Science, UM 50603 W.Persekutuan Kuala Lumpur
3.	Muhammad Aqmal Othman	Member	Department of Chemistry, Faculty of Science, UM 50603 W.Persekutuan Kuala Lumpur
4.	Siti Mariam Abdul Wahab	Member	Department of Chemistry, Faculty of Science, UM 50603 W.Persekutuan Kuala Lumpur

5.	Profesor Dr. Khalijah Binti Awang 03- 79674064 (Office) Khalijah@u.edu.my	Member	Department of Chemistry Faculty of Science, UM 50603 W.Persekutuan Kuala Lumpur
6.	Yasodha Sivasothy	Member	Department of Chemistry Faculty of Science, UM 50603 W.Persekutuan Kuala Lumpur

3. **SPONSOR(S)**

Indicate Project Grant No. or Name of Sponsor, MOU/Agreement, whichever is applicable.

Project Grant No : A000001-50001; H-21001-F000037,

If technology/invention is not a result of a funded Research Project or an Agreement, please indicate University resources/facilities used

This is a UM funded project.

4. **DESCRIPTION OF TECHNOLOGY/INVENTION**

Information given in this section may be transmitted to companies for evaluation. Confidential information should be given in a separate attachment marked "STRICTLY CONFIDENTIAL".

Description (include diagrams where relevant)

5. **Indicated possible commercial applications of your technology/invention.**

Pharmaceutical companies.

6. **Indicate the area of your technology.**

Medical chemistry, pharmaceutical.

7. **List organizations that may have interest in this technology/invention. If contact has already been made, please provide information on status of discussions.**

8. Name organizations (public or private/local or overseas) presently working in a similar area and are likely to be technology suppliers.

No	Name of company	Contact person	Tel/Fax
-			

9. Provide six keywords related to your technology/invention.

- (a) Date of conception of invention. Has the date been documented. If so, where?

Myristica cinnamomea King, Myristicaceae, acylphenols, dimeric acylphenols, anti-quorum sensing activity

10. If disclosure is related to an application to file a patent, please complete this section.

Dates of conception and public disclosure (Accurate information is essential as it may affect the possibility of obtaining patent rights. Please submit the patent documents/publications which have relevance to your application.) References/comments : Please include names of periodicals and journals.

- (a) Date of conception of invention. Has the date been documented. If so, where?

We conceived this idea in 2011, and we have not disclosed it to anyone in any form including publication. This has not been anticipated before.

- (b) First publication containing sufficient description to enable a person skilled in this field to understand and make or use the invention (to include thesis and the date submitted).

No.

- (c) First public oral disclosure of invention sufficient to enable a person skilled in this field to understand and make or use the invention.

No.

- (d) If unpublished and undisclosed, provide the anticipated publication or oral disclosure date and any submission made for potential publication.

We plan to submit for publication in June 2015.

11. Was there a previous patent application made by you/your co-inventors in the same area? If yes, please state name of invention and date of application.

No

12. Has the invention been produce or put to practice? If yes, please give details.

No

13. Has a patent search been conducted for the purpose of preparing this application? Yes/No. If yes, what is the result of the search? (Please submit patent documents/publications relevant to your application)

No

14. Are there already patents granted in similar fields or related process? Yes/No. Please name a few that you have knowledge of or referred to. (Please submit the patent documents publications which have relevance to your application).

No

15. Name at least two other staff members (who are not the investigators/inventors who are knowledgeable in this fields.

No	Name of Staff	Department	Tel/Fax
1.	Profesor Madya Dr. Ng Ching Ching	Institut Sains Biologi, Fakulti Sains	Office: 03-79675872 Fax: 03-79675908
2.	Profesor Saad Tayyab	Institut Sains Biologi, Fakulti Sains	Office: 03-79677118 Fax: 03-79674178

I/We hereby declare that all statements made and information given are true and correct.

(1) **Name of Principal Investigator/Inventor** : DR. CHAN KOK GAN

I/C No : 720222145201

Date : 17/05/2015

Status Declaration : **Approve**

(2) **Name of Co-Investigator/Co-Inventor** : PROF. DR. KHALIJAH BINTI AWANG

I/C No : 640922107118

Date : 17/05/2015

Status Declaration : **Approve**

Certificate of Participation

This Certificate is presented to
SITI MARIAM ABDUL WAHAB
(PRESENTER)

The 3rd International Postgraduate Conference on Science and Mathematics 2015

Science and Mathematics
Empower Innovative Generation

Convention Hall, E-Learning Building,
Sultan Idris Education University
October 10th - 11th, 2015



Associate Professor Dr. Zulkifley Mohamed
Dean, Faculty of Science and Mathematics



IPCSM'15

CENAR



Centre for Natural Product Research and Drug Discovery
University of Malaya

Certificate of Appreciation

is hereby granted to

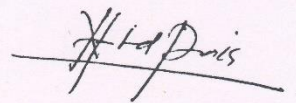
Siti Mariam Abdul Wahab

for poster presentation in the
*Annual Colloquium on
Drug Development from Natural Products*

12th August 2015

at

University of Malaya, Kuala Lumpur.

A handwritten signature in black ink, appearing to read "H. Rais".

Prof. Dr. Mohd Rais bin Mustaffa
Director of CENAR